E-Proceedings
of
The 5th International Conference on Highway Engineering 2024

"Future-Proofing Roads for Asia and Beyond"

4 - 6 September 2024
Bangkok International Trade & Exhibition Centre (BITEC)
Bangkok, Thailand

Organised by
Department of Highways
and
Roads Association of Thailand

Edited by
Ponlathep Lertworawanich, Ph.D.
Auckpath Sawangsuriya, Ph.D.
Harutus Phoban, Ph.D.

Published by
Department of Highways
Ministry of Transport

E-Proceedings

of

The 5th International Conference on Highway Engineering 2024

“Future-Proofing Roads for Asia and Beyond“

4 - 6 September 2024
Bangkok International Trade & Exhibition Centre (BITEC)
Bangkok, Thailand

Organised by
Department of Highways
and
Roads Association of Thailand

Edited by
Ponlathep Lertworawanich, Ph.D.
Auckpath Sawangsuriya, Ph.D.
Harutus Phoban, Ph.D.

Published by
Department of Highways
Ministry of Transport

Published by the Department of Highways, Ministry of Transport
2/486 Si Ayutthaya Road,
Thung Phaya Thai, Ratchathewi,
Bangkok, 10400, Thailand.

ISBN (e-book) 978-616-7754-87-1

Preface

This E-proceedings contains papers from the **International Conference on Highway Engineering 2024 (iCHE2024)** with the theme of **"Future-Proofing Roads for Asia and Beyond"**, held in Bangkok, Thailand, on September 4-6, 2024. This conference is the 5th International Conference on Highway Engineering in this conference series which serves as the platform for national and global leaders, policy-makers, industry professionals, specialists, research scholars, and academia to attend and exchange knowledge, experience, and insights on roads and road transport in these following topics: (a) efficient, inclusive, and safe road management, (b) smart mobility, digital technology, and innovation for roads, and (c) sustainability and resilience of road networks.

This E-proceedings includes a collection of papers from three main tracks of the iCHE2024. **Track A** involves efficient, inclusive, and safe road management. 37 papers were collected in this track. These papers described a wide range of road administrator tasks from planning for effective road networks to managing road infrastructure and transportation system for promoting economic growth and social development as well as improving the lives of citizens across the country. In addition, they also covered road safety management, which is essential towards achieving social equity in accessibility in rural areas.

Track B is associated with smart mobility, digital technology, and innovation for roads. 12 papers were collected in this track. These papers summarized mobility on roads, which was a crucial aspect of modern society, enabling people to access essential services, to engage in economic activities, and to connect with others. The papers addressed the application of new technologies and digital transformation concept in road transport, which optimized the road network operations and enhance the intelligent transportation system. In addition, they also discussed the implementation of emerging technologies and innovations that could help supporting road agencies during the design, construction, operation, and maintenance of roads.

Track C involves sustainability and resilience of road networks. 16 papers were collected in this track. These papers described sustainable and resilient road infrastructure and networks to ensure the serviceability and reliability of road transportation systems. The papers also demonstrated that an increasingly significant global impact of climate change and natural hazards such as floods, landslides, and earthquakes had a devastating impact on road networks, disrupted transportation, and caused significant economic and social harm. The papers presented the resilience of road networks, the development of robust disaster management plans, the investment in resilient infrastructure to mitigate the impact of these events as well as the ongoing monitoring and adaptation to changing conditions. In addition, they also discussed about the decarbonization efforts e.g. the use of low-carbon materials and the adoption of sustainable construction practices, making transportation systems more resilient to the impacts of climate change, and reducing the carbon footprint of road construction and maintenance.

The Editors,

Ponlathep Lertworawanich, Ph.D., Department of Highways
Auckpath Sawangsuriya, Ph.D., Department of Highways
Harutus Phoban, Ph.D., Department of Highways

Acknowledgments

Thanks are due to the authors, reviewers, technical committees, scientific committees, and chairman of iCHE2024 without whom this publication would not be possible.

iCHE2024 Chairman

Dr. Piyapong Jiwattanakulpaisarn
Deputy Director-General for Engineering, Department of Highways

iCHE2024 Scientific Committees

Prof. Dr. Agachai Sumalee, Chulalongkorn School of Integrated Innovation, Thailand
Prof. Dr. Kasem Choocharukul, Chulalongkorn University, Thailand
Prof. Dr. Kunnawee Kanitpong, A sian Institute of Technology, Thailand
Assoc. Prof. Dr. Sorawit Narupiti, Chulalongkorn University, Thailand
Prof. Dr. Saksith Chalermpong, Chulalongkorn University, Thailand
Prof. Dr. Vilas Nitivattananon, Asian Institute of Technology, Thailand
Prof. Dr. Somnuk Tangtermsirikul, Sirindhorn International Institute of Technology, Thailand
Dr. Ponlathep Lertworawanich, Department of Highways, Thailand
Dr. Auckpath Sawangsuriya, Department of Highways, Thailand
Dr. Sumet Ongkittikul, Thailand Development Research Institute (TDRI), Thailand
Prof. Dr. Hiroaki Nishiuchi, Kochi University of Technology, Japan
Dr. John Calvin Milton, Washington State Department of Transportation, United States
Mr. Christos S. Xenophontos, Rhode Island Department of Transportation, United States
Ms. Caroline Evans, PIARC Strategic Theme 1 Coordinator, Australia

iCHE2024 Technical Committees

Attasit Sawatparnich	Advisor
Ponlathep Lertworawanich	Chairman
Jakraphob Watcharamonthian	Member
Auckpath Sawangsuriya	Member
Songrit Chayanan	Member
Tunwin Svasdisant	Member
Sukit Yindeesuk	Member
Gridsana Pensomboon	Member
Patthanapong Tongsuk	Member
Poranic Jitareekul	Member
Chairat Supachawarote	Member
Jutha Sunitsakul	Member
Bhanitiz Aursudkij	Member
Pattharin Sarutipand	Member
Apivat Jotisankasa	Member
Wasin Rujikietgumjorn	Member
Puttipan Seraneeprakarn	Member
Pichanan Aursudkij	Member
Kavalin Wangsiripaisal	Member
Rajwanlop Kumpoopong	Member
Harit Prasertsin	Member
Waritz Rattanasiriphan	Member
Harutus Phoban	Member and Secretary
Warit Chookate	Member and Assistant Secretary
Siwakorn Dumduang	Member and Assistant Secretary
Patra Sukmoung	Member and Assistant Secretary
Nattapong Nusrikaew	Member and Assistant Secretary
Wuttichai Amornprasitpol	Member and Assistant Secretary
Punnawat Siripatthiti	Member and Assistant Secretary

Acknowledgments

Local Reviewers

Ackchai Sirikijpanichkul
Agachai Sumalee
Ampol Karoonsoontawong
Apichai Issariyanukula
Apivat Jotisankasa
Arkhom Termpittayapaisith
Auckpath Sawangsuriya
Boonchai Sangpetngam
Chaiyut Charoenphon
Chakrapan Tuakta
Chutipong Paraphantakul
Dussadee Satirasetthavee
Harit Prasertsin
Jetthawee Mark
Jittichai Rudjanakanoknad
Jumrus Pitaksringkarn
Kasem Choocharukul
Kazuya Tomiyama
Kerkritt Sriroongvikrai
Kriangkrai Pattanapakdee
Kunnawee Kanitpong
Ladda Tanwanichkul
Manop Kaewmoracharoen
Monchai Chumintarajak
Muanmas Wichiensin
Nongnuch Poolsawad
Nopadon Kronprasert
Noppakun Boongrapue
Nuksit Noomwongs
Pakpoom Limtong
Paramet Luathep
Parinya Sanguansat
Pasan Kulvanit
Pattara Kiatisevi
Peeranut Jeammaneeporn
Peerapol Sittivijan
Piya Chotickai
Pongsun Bunditsakulchai
Ponlathep Lertworawanich
Pornpote Nusen
Puttipan Seraneeprakarn
Rapee Tangsongsuwan
Rattaphol Pueboobpaphan
Rosalind Amornpitakpun
Sarawut Jansuwan
Saroch Boonsiripant
Siradech Surit
Sittinun Tongbai
Sivach Kaewcharoen
Somnuk Tangtermsirikul
Songpol Charuvisit
Songrit Chayanan
Sruangsaeng Chaikasetsin
Sukit Yindeesuk
Suladda Subsin
Tanakorn Chaiyarungyos
Teerapong Panboonyuen
Teerapun Phumrattanaprapin
Thaned Satiennam
Thapat Silalertruksa
Thavatchai Tayjasanant
Treerapot Siripirote
Tunwin Svasdisant
Usanee Raha
Warit Wipulanusat
Waritz Rattanasiriphan
Wasin Rujikietgumjorn
Watchara Sattayaprasert
Wichuda Satiennam
Winai Raksuntorn
Wirat Chinnan
Withit Pansuk

Table of Contents

Track A-2

Efficient, Inclusive and Safe Road Management

Data-Driven Decision-Making Protocol for Road Friction Improvement: Correlating International Friction Index with Accident Rates in Blackspots

Peerapong Jitsangiam[1,*], Kritsanaphong Chaikla[2] and Nopadon Kronprasert[3]
Weerachai Wongweeranimit[4], Nuntawat Lersinghanart[5], Theeraruk Maneenart[6]

[1] Department of Civil Engineering, Chiang Mai University, Chiang Mai, Thailand, peerapong@eng.cmu.ac.th
[2] Chiang Mai University Advanced Railway Civil and Foundation Engineering Center (CMU-RailCFC), Chiang Mai University, Chiang Mai, Thailand, ckritsanaphong@gmail.com
[3] Department of Civil Engineering, Chiang Mai University, Chiang Mai, Thailand, nopkron@eng.cmu.ac.th
[4] Transportation Institute, Chulalongkorn University, Bangkok, Thailand, Weerachai.W@chula.ac.th
[5] Transportation Institute, Chulalongkorn University, Bangkok, Thailand, Nuntawat.l@chula.ac.th
[6] Infra Corporation, Bangkok, Thailand, Theeraruk.m@infra-corp.co

ABSTRACT

This study investigates the relationship between road friction, quantified by the International Friction Index (IFI), and accident rates in identified blackspots to establish a decision-making framework for initiating road friction improvement interventions. The proposed framework aims to enable road authorities to initiate improvement projects based on empirical data rather than relying solely on time-based routine maintenance practices. Road friction improvement projects are typically initiated based on routine maintenance schedules or observations of accident rates at specific sites. Two years of accident data and corresponding road friction values, including geospatial information, were collected to address this. Subsequently, an algorithm was developed to identify blackspots and analyze the correlation between accident rates and IFI values within these areas. This analysis facilitated the determination of investigatory and intervention thresholds based on the IFI and accident rate, serving as the fundamental components of the decision-making protocol. The findings of this study provide valuable insights for prioritizing road friction improvement efforts and optimizing resource allocation to enhance road safety effectively.

Keywords: International Friction Index, Blackspot, Geospatial Information, Decision-Making Protocol, Road Friction improvement Intervention

1. INTRODUCTION (Times New Roman 12 pt)

Skid resistance plays an important role in road safety. Inadequate skid resistance can lead to a major accident. Especially on wet road surfaces, skid resistance decreases significantly by 40%—50% compared to dry road surfaces (Watanabe et al., 2023). Moyer (1959), Rizenbergs et al. (1973), Ivey et al. (1992), and Henry (2000) found that crash rates decrease when the friction between the tires and road surface increases.

Previous studies agreed that skid resistance affects accident rates. However, they did not recommend the managerial aspects of improving road skid resistance interventions. The accident-prone location, or blackspot, is key to identifying the level of skid resistance involved in accidents.

The Bureau of Highway Safety, Department of Highways (DOH), Ministry of Transport, Thai Royal Government defined a blackspot as a location with accident rates of 3 – 6 times/3 years within a 100 m radius of locations of interest such as intersections, bridges, and curves.

Since there is no definition of skid blackspot and intervention level of skid improvement, this study created an algorithm to manipulate road and accident data to establish the decision-making framework for road network management. The International Friction Index (IFI) is adopted to represent skid resistance value.

2. METHODOLOGY

This study proposed a decision–making framework for initiating road friction improvement intervention based on empirical evidence with the assistance of data science applications. The framework establishment had five phases: Phase 1: Road Data Collection of The Road, Phase 2: Road Accident Data Collection and Cleansing, Phase 3: Data Merging and Cleansing, Phase 4: Accident Cluster Formation, and Phase 5: Data Analysis.

2.1 Phase 1: Road Data Collection

In this phase, the vehicles were equipped with a fixed slip T-10, laser profiler, and camera (Figure 1). Before field measurement, the T-10 and laser profiler were tested and calibrated against the reference set of DOH by the Paired T-test statistical method within a 95% confidence interval. The field data point was collected every 10 m. Moreover, the operating vehicles maintained their speed at approximately 60 km/h. Every point contained information including GPS coordinates, speed limit, coefficient of friction, speed-at-reading, and Mean Profile Depth (MPD).

At this phase, The IFI (PIARC,1995) can be calculated by following Equation (1), (2), and (3);

$$S_p = a + (b \times Tx) \quad (1)$$

$$FR60 = FRS \times \exp\left[\frac{S-60}{S_p}\right] \quad (2)$$

$$F60 = A + (B \times FR60) + (C \times Tx) \quad (3)$$

Where; S_p = Calculated Speed Number for IFI (km/h)
Tx = Measured Mean Profile Depth (mm.)
a, b = Calibration Constants for Laser Profiler (a = 14.2, b = 89.7)
S = Slip Speed (km/h)
FRS = Measured Coefficient of Friction
FR60 = Friction Level at 60 km/h

F60 = IFI Friction Level at 60 km/h

A, B, C = Calibration Constants for T-10
(A = 0.08209, B = 0.9104, C = 0)

Speed limit was also included in this study because speed is one of many factors that can cause accidents. The speed-at-readings and MPD values were deleted from the field data points to minimize the processing time during analysis. Moreover, the coefficient-of-friction values were substituted by IFI values. Therefore, the modified field data points consist of GPS coordinates and IFI values.

(a) T- 10

(b) Laser Profiler

Figure 1 Field Measuring Equipment

2.2 Phase 2: Road Accident Data Collection

The road accident data was retrieved from the Highway Accident Information Management System (HAIMS) hosted by DOH from 2019 to 2021. The HAIMS provided in-depth information on each accident point, including accident type, GPS location, pavement type, pavement condition, road alignment, and casualties. Five accident types were presumably considered as an accident due to lack of skid resistance consisting of 1) rear-end collision with vehicles heading one direction, 2) lane-changing or side-to-side collision with vehicles heading one direction, 3) collision with on-path permanent objects, 4) run-off path on straight, and 5) run-off path on a curve.

2.3 Phase 3: Data Merging and Cleansing

The algorithm was created to merge modified field data points to an accident point and clean an unmerged accident point. During the merging process, the algorithm was programmed to match an accident point to the nearest modified field data point and use it as a reference point to trace the previous ten modified field data points. For the IFI value at the accident point establishment, the IFI values of 11 modified field data points (reference point and ten traced points) were averaged and then used to represent the IFI value at the accident point. The cleansing process commenced after the verification of the merging process had been completed. The cleansing process minimizes the processing duration by eliminating the unmerged accident points and modified field data points (Figure 2).

Therefore, at the end of this phase, each accident point consists of accident type, GPS location, pavement type, pavement condition, road alignment, casualties, and representing IFI value.

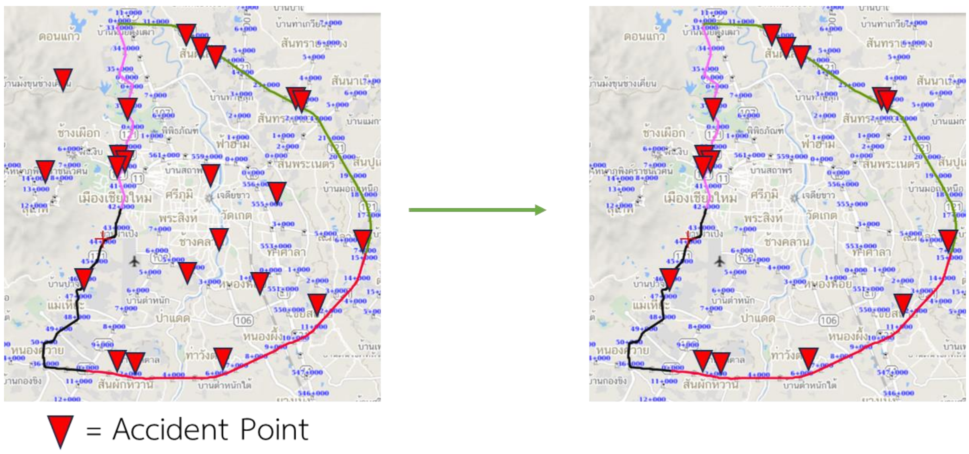

Figure 2 The illustration of a cleansing process

2.4 Phase 4: Accident Cluster Formation

The identification of accident-prone locations or blackspots was assisted by the algorithm, which was programmed to create a circle with a radius of 100 m around every accident point (Figure 3a). The cluster was formed by the overlapping circles of accident points intercepted in a circle with a radius of 100 m. (Figure 3b). Once the clusters were formed, the representing IFI values of accident points in each cluster were averaged and used as an IFI value of the cluster. At the end of this phase, each cluster consists of the accident rate in the cluster, IFI value, GPS location at the centermost accident point in a cluster, accident type, pavement type, pavement condition, road alignment, and casualties (Figure 3c).

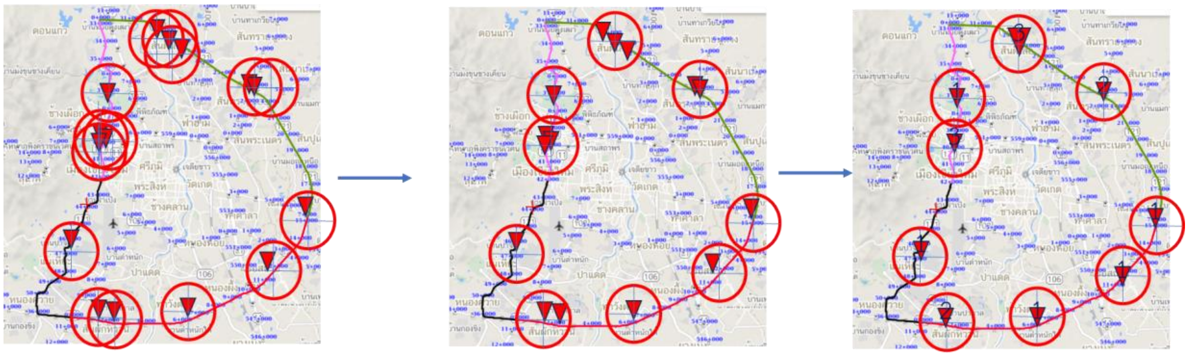

(a) (b) (c)

Figure 3 The illustration of the Accident Cluster Formation process

2.5 Phase 5: Data Analysis

The previous 4 phases prepared the data for the analysis. At this stage, the quality data, e.g., pavement type and pavement condition, can be related to quantity data, e.g., IFI value and accident rate. Thus, the study was classified into 19 cases by the quality data attached to each accident point in a cluster (Table 1). As a result, for individual cases, each blackspot or cluster can establish the relationship plot between accident rate and IFI value.

Table 1 The 19 cases of study

Case No.		1	2	3	4	5	6	7	8	9	10	11	12	13	14	15	16	17	18	19
Speed Limits	90*	•	•	•	•	•	•	•	•	•										•
	120**	•	•	•	•	•	•	•	•	•	•	•	•	•	•	•	•	•	•	
Pavement Condition	Dry	•	•	•	•	•	•				•	•	•	•	•	•				•
	Wet	•	•	•				•	•	•	•	•	•				•	•	•	•
Pavement Alignment	Straight	•	•		•	•		•	•		•	•		•	•		•	•		•
	Curve	•		•	•		•	•		•	•		•	•		•	•		•	•

* Speed limit at 90 km/h or below

** Speed limit at 120 km/h

3. RESULT AND DISCUSSION

The DOH is responsible for constructing and maintaining Thailand's road network for more than 65,000 km. This study covered 5,492.26 km. or approximately 8.45% of the total road length, under the responsibility of DOH. The field road data was collected from the paved road with asphaltic concrete (AC) for 4,433.51 km. and concrete (CC) for 1058.75 km. The accident points retrieved from HAIMS were in the three years. However, the accident points from 2019 were not matched with any field data points. Consequently, there were only accident points from 2020 to 2021 (2 years) in the analysis.

3.1 Quadrant Analysis

In phase 5 of data analysis, case 1, for instance, the upper right corner of the plotting area was clear and noticeable, which could be interpreted that, at a certain level of IFI value (0.35), the accident rate was limited, as shown in Figure 4. From the IFI values of 0 to 0.35, the accident rate ranged from 1 to 10 accidents/blackspot/2 years. On the other hand, for IFI values more than 0.35, the accident rate did not exceed five accidents/blackspot/2 years. Hence, the plotting area could be divided into four quadrants by drawing the blue vertical and horizontal lines through the center coordinates (0.35,5). It might require a high maintenance cost to keep the IFI value above 0.35. In lowering the cost, the IFI value should be less than 0.35 but not too low. Therefore, the 80th percentile is the optimal IFI value.

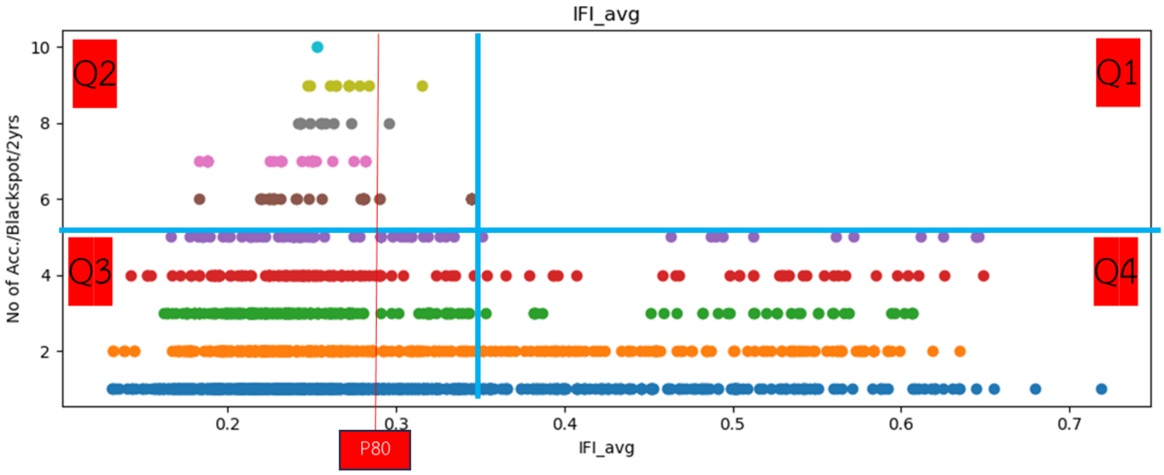

Figure 4 The relationship plot of accident rate and IFI value (Case 1)

Nevertheless, as mentioned earlier, the process applied to all 19 cases could be biased and time-consuming. The algorithm was developed to eliminate these advantages, as shown in Figure 5. The algorithm's output is shown in Table 2.

```python
import numpy as np

# 1. Find the Q2 and Q3 for IFI
q2_ifi = result_df['IFI_avg'].quantile(0.25)  # 25th percentile is Q1
q3_ifi = result_df['IFI_avg'].quantile(0.75)  # 75th percentile is Q3

# 2. Filter the data for IFI values that lie in the range [Q2, Q3]
filtered_ifi_data = result_df[(result_df['IFI_avg'] >= q2_ifi) & (result_df['IFI_avg'] <= q3_ifi)]['IFI_avg']

# 3. Calculate the desired percentiles
percentiles = [0.50, 0.60, 0.70, 0.80, 0.90, 1.00]  # These represent 50% up to 100%
percentile_values = np.percentile(filtered_ifi_data, [p*100 for p in percentiles])

# Print results
for p, val in zip(percentiles, percentile_values):
    print(f"Percentile {int(p*100)}%: {val}")
```

Figure 5 The Algorithm of Quadrant Analysis

Table 2 The output of The Algorithm of Quadrant Analysis

Case No.		**1**	**2**	**3**	**4**	**5**	**6**	**7**	**8**	**9**	**10**	**11**	**12**	**13**	**14**	**15**	**16**	**17**	**18**	**19**
Center Coordinate	**X** (IFI Value)	0.35	0.35	0.40	0.35	0.34	0.35	0.32	0.32	0.39	0.33	0.32	0.28	0.32	0.32	0.28	0.32	0.32	0.24	0.35
	Y (Acc/BS/2yrs)	5	5	2	5	5	2	3	3	3	4	5	1	4	4	1	1	1	1	5
80th Percentile		0.29	0.29	0.33	0.301	0.30	0.33	0.27	0.26	0.33	0.26	0.26	0.28	0.27	0.27	0.28	0.26	0.26	0.23	0.29

3.2 9-Square Protocol

The 9-Square protocol was developed to establish a decision-making framework for initiating road friction improvement interventions by considering the maximum and minimum values of IFIs and accident rates from the output of Quadrant Analysis. The maximum and minimum values of IFI at the 80th percentile were 0.33 and 0.23, respectively. As well as, the maximum and minimum values of accident rates were 5 and 1 accidents/blackspot/2 years, respectively. The two vertical and two horizontal lines were drawn, dividing the plotted area into nine squares, as shown in Figure 6.

The visualization of the 9-Square protocol could be interpreted into two matters. The first matter was the threshold levels of intervention in road friction maintenance. The threshold levels were divided into investigatory and intervention levels, as shown in Table 3. According to the Bureau of Materials, Analysis, and Inspection, DOH, there was in-house research called "Analysis of Skid Resistance of Road Surfaces". The investigatory Level of IFI was 0.32 which agreed with this study.

The second matter was the decision-making framework. The 9-Square protocol allows operators, such as civil engineers, surveyors, and any involved parties, to assess the road skid resistance condition. Nevertheless, if the IFI value is unavailable, the operators can still decide about the road skid resistance condition. As shown in Figure 6, each of the nine squares has different action guidelines when a location of interest falls into a square. The urgency of action escalates from following up to Requiring immediate improvement and considering other safety measurements throughout all nine squares, as shown in Table 4.

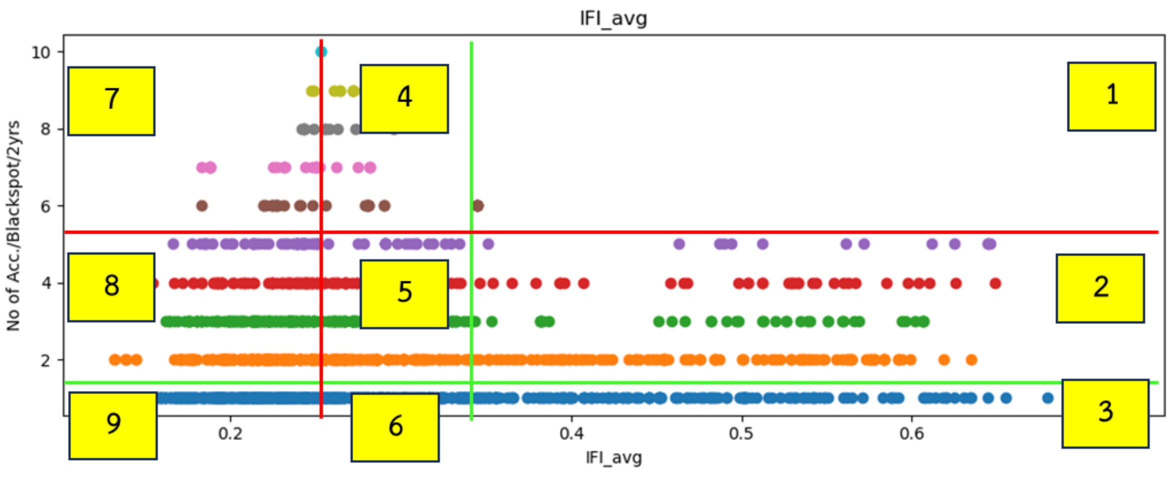

Figure 6 The 9-Square Protocol

Table 3 The Threshold Levels of Road Friction Improvement Intervention

	Investigatory Level	**Intervention Level**
IFI	0.33	0.23
Acc.No./BS/2yrs	1	5

Table 4 Guidelines of Actions of 9-Square protocol

Square No.	**Actions**
1	Follow-up
2	Follow-up and consider other safety measurements
3	Follow-up and consider other safety measurements
4	Require immediate improvement and consider other safety measurements.
5	Consider improvement and other safety measurements.
6	Consider improvement and other safety measurements.
7	Require immediate improvement
8	Require immediate improvement
9	Require improvement

4. CONCLUSIONS

The field and road accident data underwent a series of data science techniques to develop a decision-making framework called the "9-Square protocol." The protocol allows operators to assess the road skid resistance conditions and to act accordingly to the performance of the road surface itself. The action could range from following up to requiring immediate improvement and considering other safety measurements.

5. ACKNOWLEDGMENTS

The authors thank the Department of Highway (DOH), Thailand, for supporting this project.

6. REFERENCES

Henry, J.J. (2000). EVALUATION OF PAVEMENT FRICTION CHARACTERISTICS. NCHRP Synthesis of Highway Practice.

Ivey, D. L., Griffin III, L. I., Lock, J. R., & Bullard, D. L. (1992). Texas Skid Initiated Accident Reduction Program. Final Report (No. TX-92/910-1F).

Moyer, R.A. (1959). A review of the variables effecting pavement slipperiness. First International Skid Prevention Conference Proceedings, Part 2, pp. 411-433.

PIARC (1995). International PIARC experiment to compare and harmonize texture and skid resistance measurements, Technical committee on surface characteristics. Paris.

Rizenbergs, R. L., Burchett, J. L., & Napier, C. T. (1973). Accidents on rural interstate and parkway roads and their relation to pavement friction.

Watanabe, A., Kageyama, I., Kuriyagawa, Y., Haraguchi, T., Kaneko, T., & Nishio, M. (2023). Study on the Influence of Environmental Conditions on Road Friction Characteristics. Lubricants, 11(7), NA. https://link.gale.com/apps/doc/A759189171/AONE?u=anon~ea19ce21&sid=sitemap&xid=c37c844b

Operational Analysis of Lane-specific Speed Variations on Multilane Highways

Moe Sandi Zaw[1,*], Nopadon Kronprasert[2], Pongthep Pisetsit[3]

[1]Department of Civil Engineering, Faculty of Engineering, Chiang Mai University, emmamoe1523@gmail.com
[2]Department of Civil Engineering, Faculty of Engineering, Chiang Mai University, nopkron@eng.cmu.ac.th
[3]Department of Civil Engineering, Faculty of Engineering, Chiang Mai University, pongthep.pisetsit@gmail.com

ABSTRACT

The phenomenon of varying speeds among lanes on roadways has long been recognized as a critical factor influencing traffic flow efficiency and safety; understanding the consequences of speed differences is crucial for informing successful traffic management strategies and infrastructure design. However, lane-specific desired speeds present challenges for traffic management authorities in effectively balancing the needs of diverse road users while maintaining optimal traffic flow and ensuring road safety. This study aims to investigate the dynamics of lane-specific speed variations and their impact on overall roadway performance by utilizing calibrated and validated microscopic traffic simulation. The result indicates how speed differences between lanes influence overall traffic flow patterns, including lane utilization, lane-changing behavior, and the formation of traffic patterns. In addition, the drivers in faster lanes attempt to overtake slower vehicles by changing lanes frequently, and higher-speed lanes experience increased crash rates due to faster-moving traffic, while slower lanes are prone to rear-end collisions or unsafe passing maneuvers as drivers attempt to overtake slower vehicles. It is necessary to implement strategies to encourage drivers to use lanes that align with their desired speeds, optimizing lane utilization. Enhanced comprehension of the impacts of speed variations across lanes can lead to improved roadway safety and the development of traffic management strategies.

Keywords: Lane-specific speed variation, Traffic operations, Microscopic traffic simulation, Lane utilization, Lane-change behavior

1. INTRODUCTION

Multilane highways serve as the backbone of modern transportation systems, facilitating the efficient movement of people and goods across vast distances. These vital arteries of commerce and connectivity are essential to social engagement, economic growth, and the general well-being of society. Currently in Thailand, there has been a new ministerial regulation specifying speed limits according to traffic lanes and increasing the maximum speed limit for cars on divided highways from not exceeding 90 km/h to not exceeding 120 km/h. This regulation applies to high-standard highways with four or more lanes, setting the maximum speed limit for the rightmost lane at no more than 120 km/h but not less than 100 km/h. The speed limit for the leftmost lane is set at no more than 80 km/h, and the speed limit for the middle lane is set at no more than 100 km/h as shown in Figure 1. However, the establishment of different speed limits for different traffic lanes and the increase of the speed limit to 120 km/h on highways in Thailand have been contentious regarding their impact on traffic efficiency and the safety of road users.

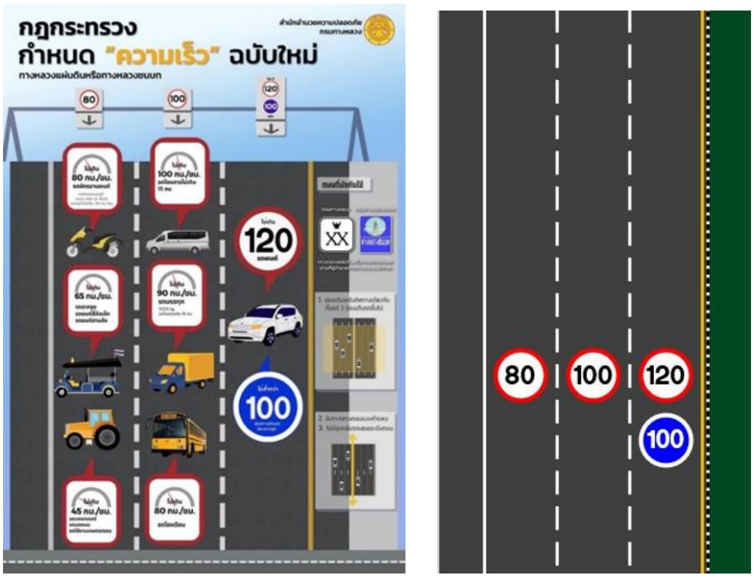

Figure 1 A Ministerial Regulation on Lane-Specific Speed Limits
(Department of Highways, 2021)

The multilane highways allow for higher traffic volumes and faster travel speeds by providing more lanes for vehicles to move in parallel, thereby reducing traffic congestion and enhancing overall traffic flow efficiency. However, maintaining the efficient traffic flow on multilane highways constitutes a significant challenge for highway engineers and planners. Vehicles in different lanes frequently travel at significantly different speeds, disrupting the smooth flow of traffic and creating inefficiencies. These result in a range of issues such as decreased capacity, increased congestion, and heightened safety risks.

Several studies have explored speed variations on multilane highways. Lane speed variations affect highway capacity by influencing lane changes and overtaking maneuvers. When slower vehicles occupy faster lanes, bottlenecks may arise, decreasing overall throughput. Conversely, maintaining consistent speeds across lanes facilitates smoother traffic flow, optimizing capacity. Drivers in faster lanes weave and change lanes frequently to overtake slower vehicles, increasing the risk of accidents due to the higher speeds.

This study investigates lane-specific speed variations on multilane highways using a combined approach: real-world data collection and calibrated microscopic traffic simulation models. The study evaluates the impact of lane-specific speed variations on vehicle speeds, lane utilization, lane-changing behaviors, and possible traffic conflicts. This research on lane-specific speed variations has the potential to significantly improve traffic flow efficiency, and ultimately, enhance safety for all users of multilane highways.

2. LITERATURE REVIEW

Various studies have modeled lane-specific speed variations. The speed in each lane can influence the capacity and efficiency of the highway by affecting lane changes and overtaking maneuvers. The number of lane changes depends on traffic volume as well as the number of lanes provided for a direction of travel (Srikanth et al., 2020). The strong correlation observed between vehicle speeds and lane-change frequency suggests that as vehicles accelerate, drivers are more inclined to switch lanes, either to maintain their desired speed or to pass slower vehicles. This relationship highlights the influence of traffic density on lane-changing behavior within a weaving section, indicating that the volume of vehicles on the road affects both the frequency and intensity of lane-change (Jin, 2010). Lane-specific speed variations on multilane highways are influenced by factors such as lane position, traffic volume, and driver characteristics (Alomari et al., 2021; Shi & Liu, 2019). Furthermore, speed violations by heavy vehicles can also impact the speed of each lane. If heavy vehicles exceed speed limits, it can lead to unsafe conditions and disruptions in traffic flow, affecting the speed of other vehicles in the same lane and adjacent lanes (Kuşkapan et al., 2021).

Laval & Daganzo (2006) employed a hybrid approach, the number of lane changes is directly proportional to the speed differences between lanes. Liu et al. (2022) focused on analyzing lane-changing behavior when there is a following vehicle in the adjacent lane, examining drivers' lane-changing characteristics under various relative speed conditions. The compliance rate of drivers with the differentiated per-lane speed limits had specific impacts on traffic safety indexes. The compliance rate of slow vehicles entering the inner lane influenced the incident rate of the dangerous overtaking vehicles on the right-left (Liu & Shi, 2018). Lane choice becomes a strategic decision for drivers, influenced by their desired speed, perceived traffic flow, and potential delays.

Frequent lane-changing, often associated with aggressive driving, poses substantial safety risks. Inappropriate lane change behavior contributes to rear-end collisions, sideswipe collisions, and angle collisions (Liu & Shi, 2018). The speed limit plays a significant role in the occurrence of lane-change crashes, with higher speed limits correlating with a higher likelihood of such crashes (Shawky, 2020). The study considers different relative speeds between vehicles during lane changes, which is crucial for accurate risk assessment. The greater variation in speeds within a lane, especially when traffic volume is high, leads to a higher risk of crashes (Choudhary et al., 2018). A significant relative speed difference between the subject vehicle and following vehicles during lane changes can lead to an increased risk of rear-end and side-swipe collisions.

Microsimulation of traffic plays a pivotal role in urban transportation and roadway strategizing. It helps bridge the gap between model predictions and real-world observations (Espejel-Garcia et al., 2017). It allows for the modification of speed distributions in individual road sections, mimicking how drivers respond to changes in posted speed limits, and allows for a more accurate representation of real-world traffic conditions (Srikanth et al., 2017). This can simulate the movement of individual vehicles and analyze factors like speed, density, and delays.

In Thailand, previous studies on lane-specific speed variations on multilane highways have focused on specific aspects such as motorcycle lane configurations or the relationship between mean average speeds and accident frequency (Burlacu & Rogers, 2019; Mama & Taneerananon, 2016; Sutheerakul et al., 2024). Nonetheless, there is a gap in thorough investigations that consider all the factors affecting speed fluctuations across various lanes. This research is essential for informing evidence-based decision-making and implementing effective strategies to improve highway safety and efficiency in Thailand.

3. MATERIAL AND METHODS

In this study, a multilane highway segment of Highway No. 32 was selected as a case study area. Traffic data were collected both before and after the implementation of lane-specific speed limits to compare the speeding behavior. Due to the challenges associated with collecting lane change data in real-time traffic conditions, a simulation model was utilized. Lane change behavior data from test vehicles were collected to ensure accurate calibration and validation of the simulation model. Traffic simulation models were developed for both uniform and lane-specific speed limits to evaluate vehicle lane changes and safety measures.

3.1 Study Area

The case study of a segment of Highway No. 32 between KM 4+100 and KM 50+000 features 4 traffic lanes, each with a width of 3.5 meters, and 2.5-meter shoulder with. Additionally, median barriers are separating the lanes, and there are no U-turn points. The design hourly volume in this segment is approximately 2,500 vehicles per hour, with trucks accounting for 10% of the total volume. Figure 2 shows the lane-specific speed limits on multilane highway segments.

Figure 2. An example of lane-specific speed limits on multilane highway segments.

3.2 Data Collection

Field data were collected on a selected highway segment using CCTV video recording. Data were gathered for a week period before (March 2021) and after (May 2021) the announcement of lane-specific speed limits, which was announced on the 1st April 2021. The collected field data include traffic data by lane (i.e. traffic volume, speed, traffic composition) and car following model data by lane (i.e. headway, lane utilization rates). A detailed summary of the field data is presented in Table 1.

Table 1 Field Data and Parameters used in simulation models.

Parameters	Approach	
	Before Implementation	After Impelementation
Field data		
Traffic volume (PCU/day)	55,244	57,320
Traffic composition (%)	MC 2% / PC 44% /LT 31% / HT 23%	MC 2% / PC 41% /LT 32% / HT 25%
Average speed (kph) (Left to Right lane)	62.3 / 82.7 / 84.2 / 105.0	70.9 / 86.4 / 88.6 / 110.0
Average headway (s) (Left to Right lane)	5.4 / 4.3 / 4.1 / 3.3	5.5 / 4.6 / 4.5 / 3.8
Lane utilization (%) (Left to Right lane)	12% / 20% / 40% / 28%	11% / 24% / 32% / 33%
Microscopic Traffic Simulation		
Parameters for car following model	Wiedemann 99 (default)	
Surrogate Safety Assessment Model		
Time to collision (sec)	1.5 sec	
Post Encroachment Time (sec)	5 sec	
Conflicting speed (kph)	> 30 kph	
Rear-end threshold angle (θ)	<30°	
Lane-change threshold angle	$30° \le \theta° \le 85°$	

3.3 Model Development

The research utilized PTV Vissim software to develop microscopic traffic simulation models to assess the lane change behavior and safety impacts of lane-specific speed limit enforcement measures. Two simulation scenarios were created as depicted in Figure 3.

- A model represents a roadway segment with uniform speed limits across all lanes, set at 90 kilometers per hour. The average speeds for each lane, based on field data, are 62.3, 82.7, 84.2, and 105.0 kph, from left to right, respectively.
- The model was calibrated using parameters such as average speed, traffic volume, and headway from each lane.
- A model representing the same roadway segment with lane-specific speed limit enforcement. The lane-specific speed limits were defined as follows:
    - Inner lane (Lane 1, the rightmost): Not exceeding 120 km/h and not less than 100 km/h.
    - Middle lanes (Lane 2 and Lane 3): Not exceeding 100 km/h.
    - Outer lane (Lane 4, the leftmost): Not exceeding 80 km/h.

The simulation models for both cases of the studied roadway segment have a length of 5 kilometers and consist of 4 traffic lanes without any access points. The traffic volume is set between 2,500 and 3,500 vehicles per hour per direction, with 10% of them being commercial vehicles. The speed range for passenger cars is between 40 and 140 km/h, while for trucks, it is between 40 and 120 km/h. These parameters align with the data collected from the field.

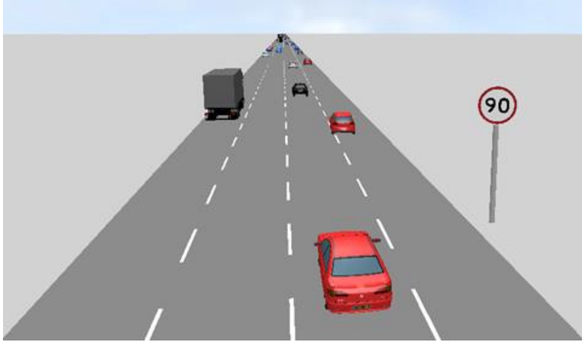

(a) Uniform speed limit

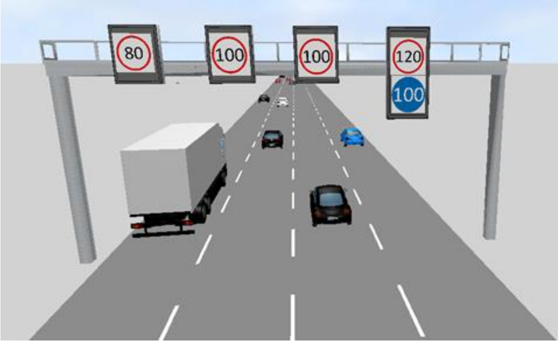

(b) Lane-specific speed limit

Figure 3 Simulation models for two scenarios of speed limit settings

4. RESULTS

This research compares the impact of different per-lane speed limit regulations. It will compare the situation under uniform and lane-specific speed limit enforcement. The results of this study are divided into three parts: comparison of vehicle speed, lane change behavior, and surrogate safety.

4.1 Analysis of Speed Behavior

The analysis of speed behavior on the highway from field data revealed that the uniform per-lane speed limit and the lane-specific speed limit, resulted in an increasing trend in speed behavior. The statistical values of vehicle speeds are presented in Table 2. The average speed increased from 83.7 to 89.2 km/h, and the 85th percentile speed increased from 98.0 to 101.2 km/h. However, there was a greater clustering of vehicle speeds close to each other. The standard deviation of speed decreased from 12.2 to 11.8 km/h. The coefficient of variation of speed was lower than the uniform speed limit.

When considering each lane separately, significant increases were observed in both the average speed and the 85th percentile speed of vehicles in each lane. The cumulative frequency distribution of vehicle speeds in each lane is depicted in Figure 4.

- In Lane 1, the average speed increased from 105.0 to 110.0 km/h, and the 85th percentile speed increased from 117.1 to 119.8 km/h.
- In Lane 2, the average speed increased from 84.2 to 88.6 km/h, and the 85th percentile speed increased from 103.3 to 105.7 km/h.
- In Lane 3, the average speed increased from 82.7 to 86.4 km/h, and the 85th percentile speed increased from 95.5 to 97.8 km/h.
- In Lane 4, the average speed increased from 62.3 to 70.9 km/h, and the 85th percentile speed increased from 76.2 to 81.7 km/h.

Table 2. Comparison of speed data between uniform and lane-specific speed limits.

Traffic Lane	Uniform Speed Limit (Before)				Lane-specific Speed Limit (After)			
	$\bar{x}$	Confidence interval*	S.D.	CV	$\bar{x}$	Confidence interval*	S.D.	CV
Passenger Cars								
Inner (Lane 1)	105	81.8-128.2	11.8	0.112	110	89.9-130.0	10.2	0.093
Middle (Lane 2)	91	69.7-112.3	10.8	0.119	94	73.3-114.7	10.6	0.113
Middle (Lane 3)	84	62.2-105.8	13.1	0.156	85	62.9-107.1	11.2	0.133
Outer (Lane 4)	63	39.2-86.7	12.1	0.192	67	41.4-92.5	13.0	0.193
Trucks								
Inner (Lane 1)	98	73.6-112.4	12.5	0.128	67	41.4-92.5	13.0	0.194
Middle (Lane 2)	81	62.2-99.8	9.6	0.118	85	62.9-107.1	11.2	0.132
Middle (Lane 3)	72	55.7-88.3	8.3	0.115	94	73.3-114.7	10.6	0.113
Outer (Lane 4)	59	43.4-74.6	7.6	0.129	110	89.9-130.0	10.2	0.093

* 95% confidence level

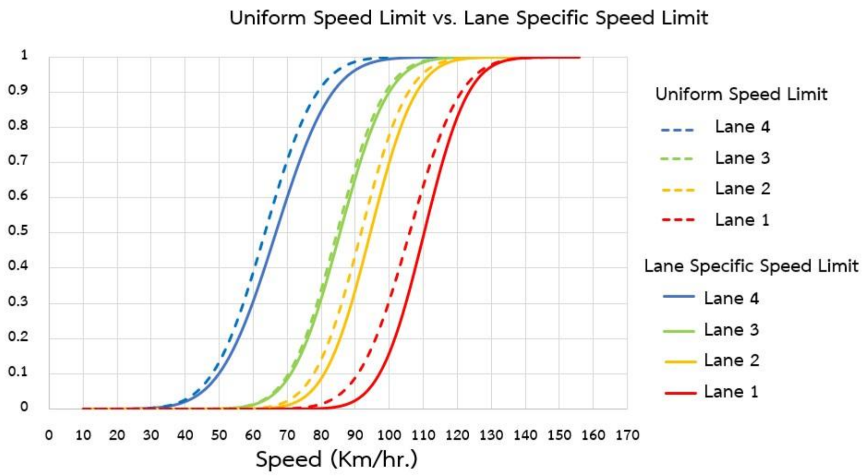

Figure 4. Cumulative frequency distribution of vehicle speeds by lane.

4.2 Analysis of Lane-Changing Behavior

The analysis of lane-changing behavior found that the per-lane speed limit and the increase in speed limit to 120 km/h resulted in the reduction of lane-change behavior. Under the uniform speed limit, most vehicles changed lanes at least 1-2 times (approximately 25% each), but under the lane-specific speed limit, most vehicles (approximately 45%) did not change lanes at all (0.4 times) throughout the route, as shown in Figure 5. The lane-changing rate decreased from 2.2 times per vehicle for the uniform speed limit to 1.0 time per vehicle for the lane-specific speed limit.

Moreover, when considering vehicles that did change lanes, the direction of lane changes became more orderly after the implementation of the per-lane speed limit. The proportion of vehicles changing lanes to the right was higher than those changing lanes to the left, whereas, before the implementation, the proportion of vehicles changing lanes to both the left and right was nearly equal, as shown in Figure 6. This reduction in random lane-changing behavior suggests a decrease in risky driving behaviors.

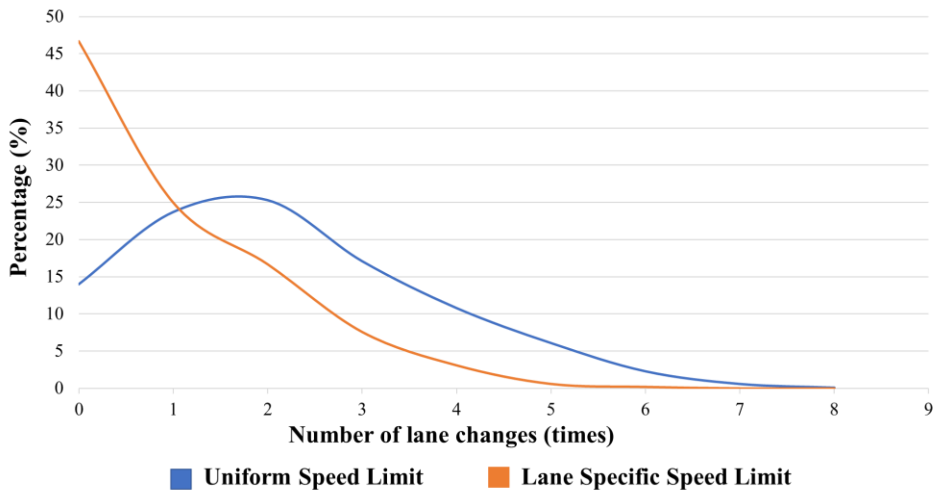

Figure 5. Frequency distribution of the number of times vehicles change lanes

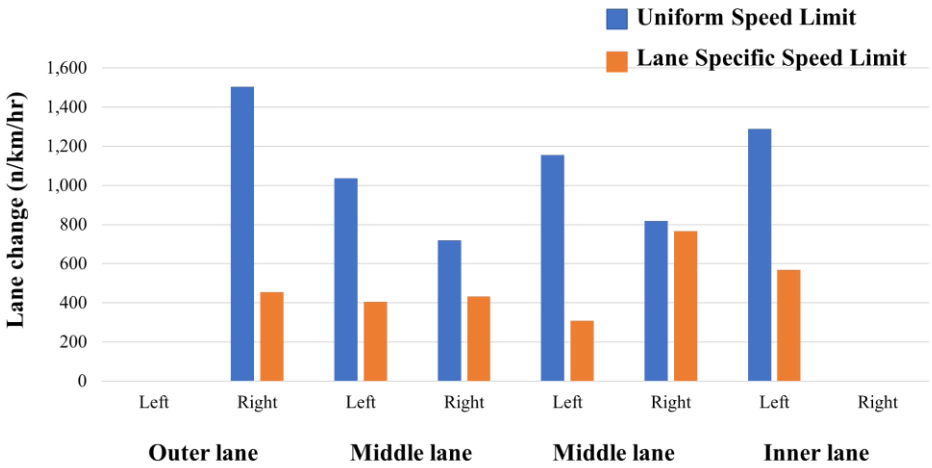

Figure 6. Frequency of vehicles changing lanes, separated by traffic lanes. (change to the left, right)

4.3 Surrogate Safety Assessment

A surrogate safety assessment model was employed to record the number of potential conflicts by conflict type (e.g., rear-end and lane-change conflicts) on a 5-kilometer, six-lane highway. Models were developed for scenarios with uniform and lane-specific speed limits, analyzing traffic volumes ranging from low to high (500 to 1,500 vehicles per hour per lane). The results of the comparison between uniform and lane-specific speed limit scenarios are presented below:

- At low volume (500 veh/h/ln), no conflicts occurred in either scenario.
- At medium volume (1,000 veh/h/ln), the number of rear-end conflicts decreased from 22 to 14, and lane-change conflicts decreased from 3 to 0 conflict.
- At high volume (1,500 veh/h/ln), the number of rear-end conflicts decreased from 44 to 30, and lane-change conflicts decreased from 15 to 10 conflicts.

5. CONCLUSIONS

This study examined the efficiency of implementing lane-specific speed limits and increasing the speed limit to 120 km/h using microscopic traffic simulation models. Two scenarios were developed: a uniform speed limit of 90 km/h across all lanes, and the lane-specific speed limits for each lane set at 120, 100, 100, and 80 km/h, respectively. The analysis of speed behavior showed that there was a tendency for higher speeds. The average speed and the 85th percentile speed increased by 3.3% and 6.6%, respectively. Additionally, vehicles tended to travel at more uniform speeds, as indicated by a 3.3% decrease in the standard deviation of vehicle speeds.

The analysis of lane-changing behavior found that the lane-specific speed limits result in a reduction in lane-changing behavior. The number and rate of lane changes decreased from 2.2 times per vehicle to 1.0 time per vehicle, a reduction of 54.5%. However, this research was conducted under the assumption that the highway's physical characteristics remain consistent (design consistency), with no interchanges or U-turns throughout the route, and that vehicle drivers comply with the specified lane speed limits. Consequently, the observed speed behavior aligns with the designated speed limits.

For future research, it is recommended to further develop models to reflect actual usage conditions more accurately. For example, studying speed usage along the entire route and considering the impact of interchanges, which could potentially reduce speeds, would provide a more comprehensive understanding.

6. ACKNOWLEDGMENTS

The authors would like to express special thanks to the Department of Highways for their invaluable support and assistance throughout the research process.

7. REFERENCES

Alomari, A., Al-Omari, B., Al-Adwan, M., & Sandt, A. (2021). Investigating and modeling speed variability on multilane highways. *Advances in Transportation Studies*, *LIV*, 5-16.

Burlacu, A., & Rogers, L. (2019). *Speed Variation Analysis -A Case Study for Thailand's Roads*.

Choudhary, P., Imprialou, M., Velaga, N. R., & Choudhary, A. (2018). Impacts of speed variations on freeway crashes by severity and vehicle type. *Accident Analysis & Prevention*, *121*, 213-222. https://doi.org/https://doi.org/10.1016/j.aap.2018.09.015

Jin, W.-L. (2010). A kinematic wave theory of lane-changing traffic flow. *Transportation Research Part B: Methodological*, *44*(8), 1001-1021. https://doi.org/10.1016/j.trb.2009.12.014

Kuşkapan, E., Çodur, M. Y., & Atalay, A. (2021). Speed violation analysis of heavy vehicles on highways using spatial analysis and machine learning algorithms. *Accident Analysis & Prevention*, *155*, 106098. https://doi.org/https://doi.org/10.1016/j.aap.2021.106098

Laval, J. A., & Daganzo, C. F. (2006). Lane-changing in traffic streams. *Transportation Research Part B: Methodological*, *40*(3), 251-264. https://doi.org/https://doi.org/10.1016/j.trb.2005.04.003

Liu, M., & Shi, J. (2018). Exploring the Impact of Differentiated Per-Lane Speed Limits on Traffic Safety of Freeways with Considering the Compliance Rate. *Journal of Advanced Transportation*, *2018*, 8368294. https://doi.org/10.1155/2018/8368294

Mama, S., & Taneerananon, P. (2016). Effective Motorcycle Lane Configuration Thailand: A Case Study of Southern Thailand. *Engineering Journal*, *20*, 113-121. https://doi.org/10.4186/ej.2016.20.3.113

Shawky, M. (2020). Factors affecting lane change crashes. *IATSS Research*, *44*(2), 155-161. https://doi.org/https://doi.org/10.1016/j.iatssr.2019.12.002

Shi, J., & Liu, M. (2019). Impacts of differentiated per-lane speed limit on lane changing behaviour: A driving simulator-based study. *Transportation Research Part F: Traffic Psychology and Behaviour*, *60*, 93-104. https://doi.org/https://doi.org/10.1016/j.trf.2018.10.018

Srikanth, S., Mehar, A., & Praveen, K. (2017). Simulation of traffic flow to analyze lane changes on multi-lane highways. *European Transport - Trasporti Europei*, *48*. https://doi.org/10.3311/PPtr.10150

Sutheerakul, C., Kronprasert, N., Satiennam, W., & Zaw, M. (2024). Classification of Roadway Context and Target Speed for Multilane Highways in Thailand Using Fuzzy Expert System. *Sustainability*, *16*, 3865. https://doi.org/10.3390/su16093865

AI-Driven Road Infrastructure Monitoring and Maintenance: A Case Study of Rasta.ai's Model for Road Defect Detection

Rahul Andhale[1], Ameya Joshi[2], N.R Kale[3]

Rahul Andhale, 903, Gera's Imperium Rise, Wipro Circle, Rajiv Gandhi Infotech Park, Phase-2, Hinjewadi, Pune, Maharashtra, India -411057
Email-rahul@aiunika.com

Abstract

Artificial intelligence (AI) presents substantial opportunities for streamlining road infrastructure monitoring and maintenance. This study looks at the use of AI to automate road inspections, emphasizing the early identification and evaluation of flaws including cracks, potholes, and surface deterioration. AI models are capable of real-time infrastructure problem detection by analyzing data from several sources and utilizing sophisticated computer vision and machine learning methods. The study includes an evaluation of the Rasta.ai AI model, which is capable of digitally tracking and identifying road conditions and was created by Ai Unika Technologies (P) Limited, India. Incorporating cutting-edge artificial intelligence, the Rasta.ai model detects defects before they become issues, allowing for targeted repairs and preventative maintenance. By continuously monitoring road infrastructure, this technique helps road authorities allocate resources effectively and maintain an up-to-date road inventory. Challenges including data quality, training models, and practical application are additionally addressed in this study. For road inspection results to be accurate and reliable, well-trained AI models and high-quality input data are necessary. By enabling preventive maintenance, integrating AI in road management reduces energy consumption and emissions, thereby becoming environmentally responsible. The study concludes with the effectiveness of the AI Model Developed by Rasta.ai for road maintenance and safety and operational efficiency. The study, therefore, highlights the scope of AI and its applicability for digital tracking at a much cheaper cost rather than costly NSV and traditional survey methods as a result, the integration of AI in road maintenance and management practices can lead to more resilient infrastructure and safer, more reliable road networks for drivers and pedestrians alike.

Keywords: AI road maintenance, Defect detection, Virtual road monitoring, Road inventory management

Introduction

Effective road condition monitoring and maintenance are essential to making transportation safety and infrastructure longevity. Traditional methods for identifying and addressing road issues include manual inspections and basic sensor-based assessments. However, the accuracy, coverage, and timeliness of these systems can create problems, which cause maintenance to be delayed and repair costs to rise. The limitations of these traditional methods highlight the need for more sophisticated and effective road infrastructure management technologies.

The emergence of artificial intelligence (AI) has created revolutionary prospects across multiple industries, including the monitoring of road infrastructure. AI-driven solutions, which make use of extensive datasets and complex machine learning techniques, have the potential to improve the accuracy and efficiency of road maintenance. With the use of these technologies, road conditions can be continuously monitored and analyzed in real-time, allowing for more proactive maintenance. Because artificial intelligence (AI) has the potential to greatly reduce human labour and minimize errors, it is especially important to integrate AI in this field to improve the overall quality of road maintenance.

Rasta.ai represents a pioneering effort in the application of AI for road infrastructure monitoring. This paper explores the road defect detection model developed by Rasta.ai, which uses deep learning algorithms and sophisticated image processing techniques to accurately identify a variety of road faults. The model continuously analyses road surfaces by using data from several sources, such as high-resolution cameras and sensors. Rasta.ai's automation of the defect detection process speeds up issue identification and produces comprehensive reports that help with prompt and efficient maintenance.

The Rasta.ai model case study demonstrates the substantial influence artificial intelligence (AI) can have on road maintenance plans. The results demonstrate the model's precision, effectiveness, and potential for broad use in the management of road infrastructure. In summary, the study highlights how artificial intelligence (AI) may revolutionize road condition monitoring and maintenance, opening the door to more dependable and secure transportation systems.

Objectives of the study

1. To highlight the scope of Artificial Intelligence and its applicability in Road condition monitoring
2. To explain the role of AI in the sustainability of Road operations and smoother transportation
3. To demonstrate Rasta.ai's AI model for effective maintenance and inventory management
4. To study the effectiveness of the AI model developed by Rasta.ai for Road maintenance

Importance of the Study

The study highlights the potential benefits of integrating Artificial Intelligence (AI) into road condition monitoring and maintenance. By employing AI, the research addresses key issues in infrastructure management, such as enhancing road safety through timely and accurate detection of road defects, which reduces accident risks. AI-driven maintenance planning allows for proactive repairs, optimizing resource allocation and reducing long-term maintenance costs. Moreover, efficient maintenance practices extend the lifespan of road infrastructure, minimizing the need for frequent, extensive repairs and lessening the associated environmental impact. The study demonstrates the working and efficiency of the Model developed by Rasta.ai for road condition monitoring using Artificial intelligence.

Scope of Artificial Intelligence and its applicability in Road Condition Monitoring

Artificial Intelligence (AI) is significantly transforming the field of road condition monitoring, offering innovative solutions that enhance efficiency, accuracy, and cost-effectiveness in road maintenance and safety operations. The following points highlight the scope and applicability of AI in Road condition monitoring:

1. *Predictive Maintenance:* AI enables predictive maintenance by analyzing data from sensors embedded in road infrastructure. These sensors monitor parameters such as vibrations and temperature, providing real-time data. AI algorithms predict potential road failures, allowing for timely interventions, reducing maintenance costs, and extending the lifespan of roads.
2. *Automated Defect Detection:* AI, particularly through computer vision and deep learning, automates the detection of road defects. High-resolution cameras capture images of road surfaces, which are then analyzed by AI to identify issues such as cracks and potholes. This method is faster, more accurate, and covers larger areas than traditional manual inspections.
3. *Real-time Monitoring and Reporting:* AI facilitates real-time monitoring by analyzing data from sources like satellite imagery, drones, and roadside cameras. This enables immediate detection of hazards and road deterioration, allowing for quick response and mitigation. AI systems also generate detailed reports and visualizations for road maintenance authorities.

4. *Traffic Management and Safety:* AI enhances traffic management and safety by integrating with IOT devices. Smart traffic systems monitor road conditions, traffic flow, and environmental factors. AI algorithms optimize traffic signals, reroute traffic in case of road damage, and predict accidents, improving overall road safety and traffic efficiency.
5. *Cost Efficiency and Resource Allocation:* AI in road condition monitoring leads to significant cost savings by reducing the need for extensive manual inspections and enabling targeted maintenance. Predictive maintenance helps in efficient resource allocation, ensuring maintenance efforts are focused where they are most needed, and optimizing budget utilization.
6. *Environmental Impact:* AI promotes sustainability in road maintenance by ensuring efficient use of materials and reducing the frequency of major repairs. Predictive maintenance maintains roads in good condition, lowering the environmental impact associated with extensive reconstruction activities. AI-driven traffic management also reduces vehicle emissions by minimizing congestion

Role of AI in Sustainability of Roads

This study seeks to delve into the pivotal role of Artificial Intelligence (AI) in ensuring the sustainability of road operations and promoting smoother transportation systems. By examining the application of AI technologies, particularly focusing on Rasta.ai's model for road defect detection, the research aims to elucidate how AI-driven approaches can contribute to the efficient management of road infrastructure. Through analysis and evaluation, the study aims to showcase how AI can facilitate proactive maintenance, timely interventions, and optimized resource allocation, thereby enhancing the overall sustainability and resilience of road networks. Additionally, the research intends to explore how AI-driven solutions can streamline transportation processes, minimize disruptions, and improve the overall flow of traffic, thereby promoting smoother and more reliable transportation systems.

Demonstration of Rasta AI Model

Rasta.ai presents a cutting-edge object detection model, specifically tailored to identify and categorize road assets and defects. Leveraging the latest advancements in deep learning, Rasta.ai aims to transform road maintenance and safety through precise and real-time detection of various road features and anomalies.

Key Features of Rasta.ai:

- *Advanced Detection Capabilities:* Rasta.ai demonstrates proficiency in detecting a diverse range of road assets such as traffic signs, lane markings, and barriers, along with identifying defects including potholes, cracks, and other surface irregularities.
- *High Accuracy:* Constructed on the YOLOv8 (You Only Look Once version 8) architecture, Rasta.ai guarantees high precision and recall rates, ensuring reliability for critical applications.
- *Real-Time Processing:* The model processes images in real-time, facilitating immediate detection and response, essential for applications such as autonomous driving and real-time road monitoring.
- *Scalability and Flexibility:* Rasta.ai can be deployed across various platforms, from edge devices with GPU capabilities to cloud-based infrastructures, offering versatility and scalability for different use cases.
- *User-Friendly Deployment:* With a straightforward and intuitive deployment process, users can seamlessly integrate Rasta.ai into existing systems and workflows without requiring extensive technical expertise.

Rasta.ai Model Structure:

The following steps are followed for the Rasta.ai model

1. *Data Collection:*
    - 360-degree Cameras: Mounted on vehicles to capture comprehensive road images and videos.
    - Sensors: Additional sensors like accelerometers and gyroscopes to detect vibrations and movements.
2. *Data Preprocessing:*
    - Image Enhancement: Improving image quality using techniques like noise reduction and contrast adjustment.
    - Frame Extraction: Extracting frames from video feeds for analysis.
    - Data Augmentation: Generating more training data through rotation, flipping, and scaling of images.
3. *Feature Extraction:*
    - Convolutional Neural Networks (CNNs): Used to extract features from images.
    - Edge Detection: Identifying edges and contours of potholes and road defects.

4. *Model Training:*
    - Deep Learning Models: Training models like YOLO (You Only Look Once), SSD (Single Shot MultiBox Detector), and Faster R-CNN (Region-based Convolutional Neural Networks) on labelled datasets.
    - Transfer Learning: Using pre-trained models to improve accuracy and reduce training time.
5. *Detection and Classification:*
    - Object Detection: Identifying and classifying potholes, cracks, and other road defects in real time
    - Severity Assessment: Analyzing the depth, width, and area of detected potholes to assess their severity.
6. *Post-Processing:*
    - Localization: Mapping the detected defects to specific GPS coordinates.
    - Reporting: Generating reports and alerts for road maintenance authorities.
7. *Visualization:*
    - Dashboard: Displaying detected potholes and road defects on a user-friendly interface.
    - 3D Reconstruction: Creating 3D models of road surfaces to visualize defects.
    - Continuous Learning: Feedback Loop: Continuously updating the model with new data to improve accuracy and performance.

Key components:
1. *Data Ingestion:*
    - Raw Data: Collects various data sources like maps, traffic data, points of interest (POIs), weather, road conditions, user data, etc.
    - Data Cleaning and Preprocessing: Cleanses and prepares data for further processing.
    - Data Storage: Stores processed data in a suitable database or data lake.

2. *Map and POI data:*
    - Map Data: Stores road networks, geographical information, elevation, etc.
    - POI Data: Contains information about points of interest (restaurants, hotels, attractions, etc.) with categories, ratings, and user reviews.
3. *User Profile and Preferences:*
    - User Data: Stores user information, preferences, travel history, and feedback.
    - Profile Generation: Creates user profiles based on collected data.

4. *AI Models:*
    - Route Planning Model: Determines optimal routes based on user preferences, traffic conditions, and road network data.
    - POI Recommendation Model: Suggests points of interest based on user preferences, location, and historical data.
    - Traffic Prediction Model: Predicts traffic conditions based on historical data, real-time traffic updates, and weather information.

- Natural Language Processing (NLP) Model: Understands and responds to user queries and commands.

5. *Route Optimization:*
    - Route Calculation: Calculates possible routes based on starting point, destination, and constraints.
    - Optimization: Optimizes routes considering factors like distance, time, fuel consumption, traffic, and user preferences.

6. *User Interface:*
    - Mobile App: Provides an interactive interface for users to plan and navigate routes.
    - Web Application: Offers similar functionalities for desktop users.
    - Feedback Loop: User Feedback: Collects user feedback on routes, recommendations, and overall experience.

Model Architecture:

YOLOv8 Overview: YOLOv8 is a state-of-the-art object detection model renowned for its speed and accuracy. It processes images in a single pass, making it highly efficient for real-time applications.

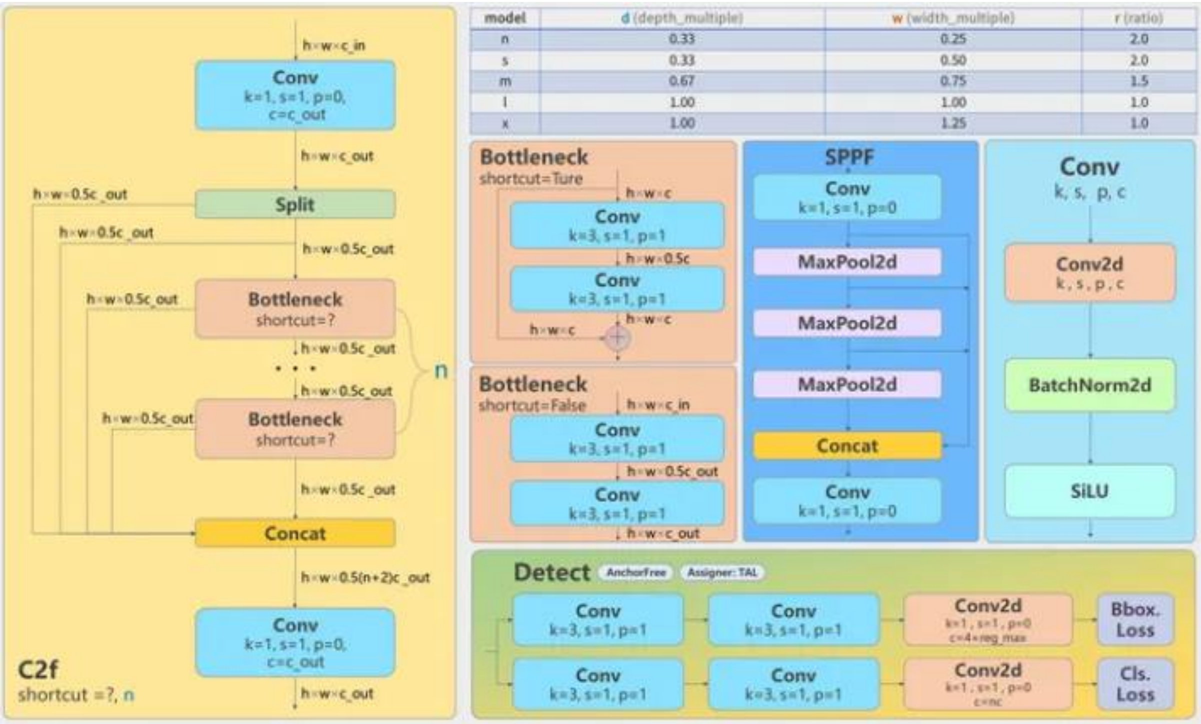

Figure 1 Model Architecture

Customizations for Rasta.ai: Specific modifications to YOLOv8 enhance its performance in detecting road assets and defects. These include tailored anchor boxes and fine-tuned hyperparameters.

Rationale for using YOLOv8

- *High Accuracy:* YOLOv8 exhibits a high rate of accuracy as measured by Microsoft COCO and Roboflow 100.
- *Developer-Convenience Features:* YOLOv8 offers user-friendly features, including an easy-to-use CLI and a well-structured Python package.
- *Community Support:* The extensive community surrounding YOLO and the growing community around YOLOv8 provide ample resources and support for users.
- YOLOv8 achieves robust accuracy on COCO, with the medium model (YOLOv8m) attaining a 50.2% mAP. It also performs well against Roboflow 100, demonstrating substantial improvements over YOLOv5. The model's developer-convenience features, such as an intuitive CLI and a seamless Python package, enhance the overall user experience. The vibrant community around YOLO ensures ample guidance and support for practical implementation.

Data Collection

Total samples used for training the model for 30 various classes (i.e. speedbreakers, streetlights) are 15,000 images respectively for each class, i.e. 4,50,000 images. The relevant data is collected through the following methods -

1. *360-Degree Cameras* - Vehicle-mounted and helmet-mounted (small and large) used to Capture high-resolution, panoramic images of road surfaces for detailed visual data
2. *LiDAR Sensors* - Emit laser pulses to capture precise road geometry and surface conditions. The main purpose was to measure distances and create 3D maps of road surfaces
3. *Environmental and Traffic Data APIs* - Open-source and paid APIs are used to collect real-time data on weather conditions and traffic patterns
4. *Mobile and IoT Sensors* - Collection of additional data from vehicles and smart devices for real-time insights
5. *Crowdsourced Data* – The data was used to gather user-reported information on road issues via mobile apps or online platforms
6. *Historical Data Integration* – To use past data for trend analysis and predictive modelling

Dataset Description

The dataset for training the Rasta.ai model comprises annotated images of various road assets and defects, with the following distribution:

StreetLamp	2,395 instances
Mandatory-sign	975 instances
Speedbreaker	896 instances
TrafficLight	823 instances
Manhole	699 instances
Cautionary-sign	613 instances
Minor-Pothole	586 instances
Roadpatch	583 instances
Left-Chevron	531 instances
Informatory-Sign	469 instances
Right-Chevron	457 instances
Major-Pothole	382 instances
Hotspot	245 instances

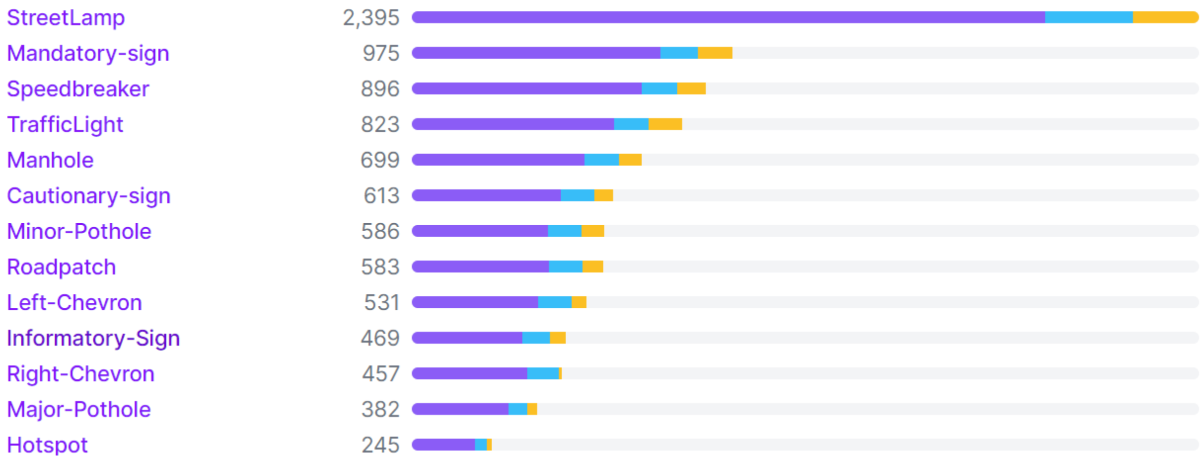

Figure 2 Dataset Description

This meticulously curated dataset ensures balanced representation, crucial for training an effective object detection model. Preprocessing steps, including resizing and augmentations, enhance the model's generalizability across different scenarios. The dataset is split into training, validation, and test sets for thorough model evaluation and fine-tuning.

Annotations and Augmentations

Image Annotation: The process involves labelling images to train machine learning models. Precise image annotation is critical as any errors are replicated by the model.

Augmentations: Techniques such as converting 15% of images to grayscale and adjusting saturation by ±25% are applied to improve model robustness and generalization.

Model Training

- *Training Parameters:* Key parameters include a learning rate of 0.001, batch size of 16, image size of 640, and 100 epochs. The model is trained using a stochastic gradient descent (SGD) optimizer.
- *Training Environment:* Conducted on a GPU-accelerated environment (Google Colab), significantly reducing training time. A custom YAML file is used to provide dataset information.

Inference

- The training results offer insights into the model's performance, with metrics like accuracy, precision, and recall. Visualizations such as confusion matrices and sample predictions highlight the model's strengths and weaknesses, guiding further training and adjustments for optimal real-world deployment.
- YOLOv8 can process various input sources for inference, including static images, video streams, and different data formats. Custom weights obtained from training replace the default model weights for making predictions, with results saved locally

Sample Detections:

Efficiency of Rasta.Ai Model and Diagrams

Training Results:

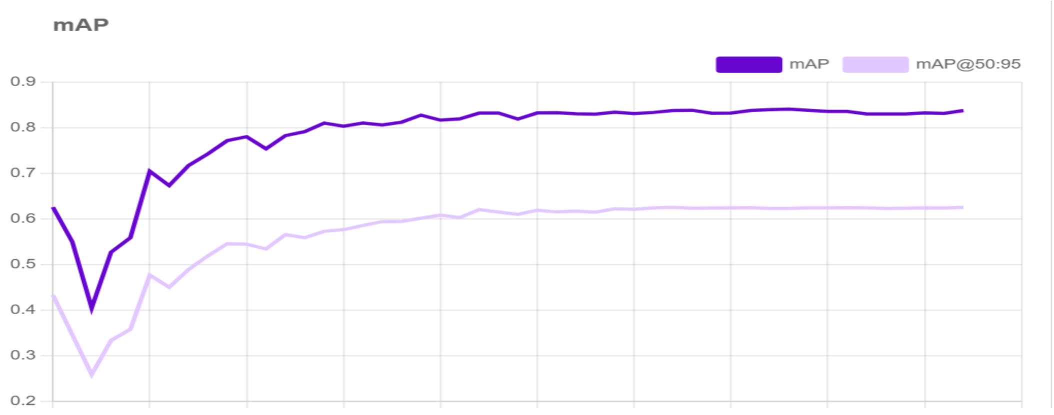

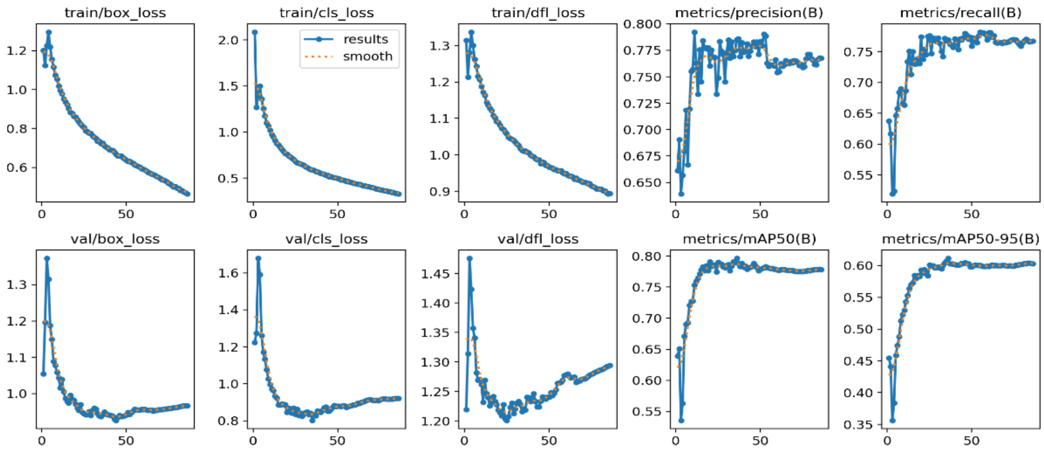

Figure 3 Model Results

- *Loss curves:* The first two rows (train/box_loss, train/cls loss, etc.) show the model's loss curves during training. The loss refers to how well the model's predictions differ from the ground truth. Lower loss indicates better performance.
- *Epochs:* The x-axis represents the number of epochs or iterations the model has been trained on.
- *Metrics:* The rows titled "metrics" show different metrics used to evaluate the model's performance. These include precision, recall, mAP50 (mean Average Precision at IoU=50), and mAP50-95 (mean Average Precision at IoU=0.5 to 0.95).
- Precision is a metric of how many relevant detections are returned by the model out of all the detections it generates.
- Recall is a metric of how many relevant objects are detected by the model out of all the relevant objects.
- IoU or Intersection over Union is a measure of how well a predicted bounding box overlaps with the ground truth bounding box.

The values in the table show the model's performance at every 50th epoch.

Overall, the image suggests that the model's performance is improving as the number of training epochs increases. This can be inferred from the general downward trend of the loss curves and the increasing values in the metrics table.

Performance Metrics

- *Precision, Recall, and F1 Score:* These metrics quantify the model's accuracy in detecting objects correctly.
- *Mean Average Precision (mAP):* A comprehensive metric that evaluates the model's performance across all classes and thresholds.

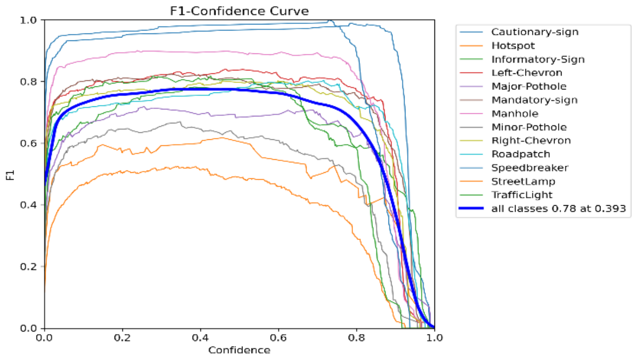

Figure 4 F1 Curve

- The F1 score is a way of measuring the accuracy of a model that considers both precision and recall. It's the harmonic mean of those two metrics. A higher F1 score indicates better overall performance.
- In the image, the x-axis represents the confidence threshold, and the y-axis represents the F1 score. The different lines in the graph correspond to different classes of objects that the model is trying to classify. For example, the blue line might represent the "Cautionary-sign" and the red line might represent the "Mandatory-sign".
- The steeper the curve for a particular class, the more confident the model is in its classifications for that class. Ideally, the curve would be highest at 1.0 confidence (i.e., the model is always perfectly confident when it's correct) and 0.0 at all other confidence levels (i.e., the model never makes mistakes).

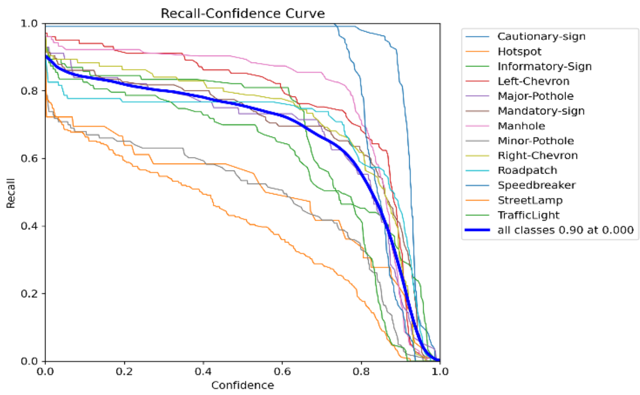

Fig 5 Recall-curve

- Recall: Recall is a metric of how many relevant objects are detected by the model out of all the relevant objects. In the context of this graph, it represents the proportion of correctly classified objects among all the objects the model said belonged to a certain class.
- In the image, the x-axis represents the confidence threshold, and the y-axis represents the recall. The different lines in the graph correspond to different classes of objects that the model is trying to classify. For example, the blue line might represent the "Cautionary-sign" and the red line might represent the "Mandatory-sign".
- The higher the curve for a particular class at a given confidence level, the better the model is at recalling (correctly classifying) all the objects of that class. Ideally, the curve would be at 1.0 for all confidence levels (i.e., the model correctly classifies all objects regardless of its confidence level).

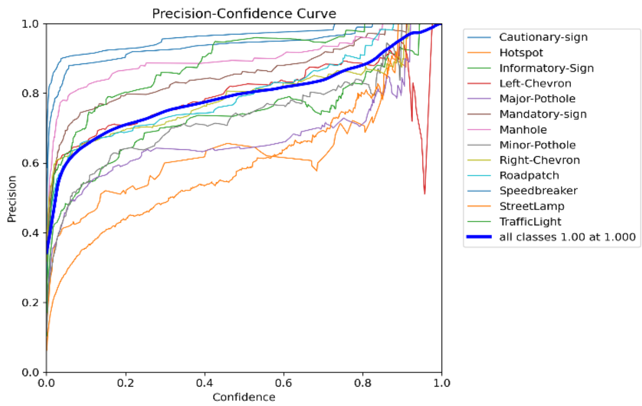

Fig 6 Precision-curve

- Precision is a metric of how many relevant detections are returned by the model out of all the detections it generates for a specific class. In simpler terms, it reflects how many of the things the model said belonged to a certain class were actually correct.
- In the image, the x-axis represents the confidence threshold, and the y-axis represents the precision. The different lines in the graph correspond to different classes of objects that the model is trying to classify. For example, the blue line might represent "Cautionary-sign" and the red line might represent "Mandatory-sign".

- The higher the curve for a particular class at a given confidence level, the better the model is at classifying only the relevant objects (i.e., avoiding false positives) with that confidence level. Ideally, the curve would be at 1.0 for all confidence levels (i.e., the model only predicts objects from a certain class when it's absolutely sure).

Key observations from the precision curve:

- The precision for all classes is 1.0 at a confidence of 1.0, which means that when the model is very confident in its predictions (confidence threshold = 1.0), all of its predictions are correct.
- As the confidence threshold decreases, the precision for most classes also decreases. This is because the model is considering lower-confidence predictions, which are more likely to be incorrect.
- The precision for some classes (e.g., "Cautionary-sign", "Informatory-Sign") seems to be consistently higher than for others (e.g., "Minor-Pothole", "StreetLamp"). This suggests that the model may be better at differentiating certain objects from the background than others.

Confusion matrix:

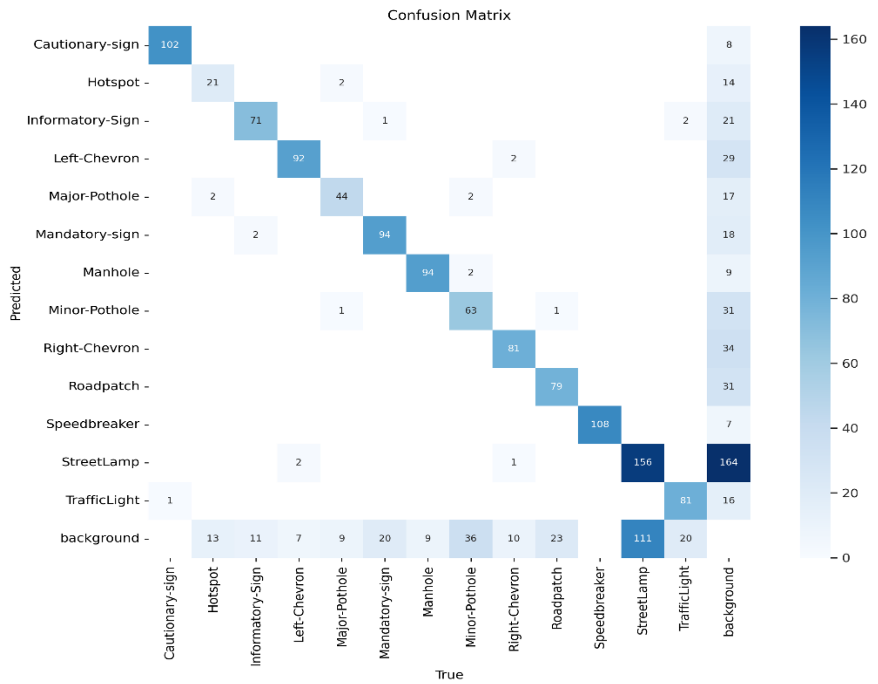

Figure 6 Confusion Matrix results

Confusion Matrix Elements

- True Positives (TP): Correctly detected objects.
- False Positives (FP): Incorrectly detected objects.
- True Negatives (TN): Correctly rejected non-objects.
- False Negatives (FN): Missed detections.

Limitations of the Model

1. *Limited sample size* – The AI model is based on the limited sample size of. To improve the accuracy of the model, additional sample feeding is required.
2. *Similarity in sample* – Samples are not collected from diverse regions and roads and therefore may create biased results.
3. *Data validation* – The crowdsourced data and data collected from various APIs are not validated for accuracy. Thus, a lack of data validation may question the results of the model.

Scope for Improvement

Basis the limitations of the AI model, following point summarizes the further improvement points:

1. *Enhance AI Capabilities* – Improvement in detection and forecasting with advanced deep learning is possible with additional and diverse samples feeding into the model
2. *Optimize Data Integration* – Development of better methods for combining diverse data sources to enhance the efficiency of the model
3. *Accelerate Real-Time Processing* – Implementation of edge computing for faster data analysis
4. *Upgrade User Interfaces* – Creation of innovative dashboards and apps for better data access to the users
5. *Ensure Scalability* – Maintenance of performance across different regions
6. *Validate Crowdsourced Data* – Implementation of methods to ensure data reliability
7. Cut Costs – Exploration of affordable technologies to streamline the overall operations
8. *Ensure Compliance* - Adherence to data privacy and road safety regulations with different extant legislation
9. *Refine Predictive Maintenance* – Improvement in accuracy of road maintenance forecasts over a period of time

Conclusion

Rasta.ai marks a significant advancement in the domain of road infrastructure monitoring and maintenance. Leveraging state-of-the-art deep learning methodologies, particularly the YOLOv8 architecture, Rasta.ai offers superior real-time detection and classification of road assets and defects, thereby enhancing road safety and maintenance efficiency. The model's advanced detection capabilities, coupled with high accuracy and real-time processing, facilitate precise identification of traffic signs, lane markings, barriers, and defects such as potholes and cracks. Its scalability and user-friendly deployment ensure seamless integration across various platforms, from edge devices to cloud infrastructures.

The meticulously curated dataset and effective data augmentation techniques ensure that Rasta.ai performs robustly across diverse scenarios. The rigorous training process, conducted in a GPU-accelerated environment, optimizes the model's performance. Performance metrics including precision, recall, F1 score, and mean Average Precision (mAP) underscore the model's efficacy. Detailed training results and inference capabilities provide comprehensive insights into its strengths and areas for enhancement.

In conclusion, Rasta.ai exemplifies the transformative potential of AI-driven solutions in road infrastructure monitoring and maintenance. It significantly contributes to safer and more efficient road management, while also supporting advancements in autonomous driving and smart city initiatives.

Bibliography

Li, J., Yao, Y., & Zhu, H. (2023, June 19). Automated road damage detection using UAV images and deep learning techniques [Abstract]. In IEEE Access (Vol. 11, pp. 62918-62931). Institute of Electrical and Electronics Engineers (IEEE). (from https://ieeexplore.ieee.org/document/10155434)

Meocci, M. (2024). A vibration-based methodology to monitor road surface: A process to overcome the speed effect. Sensors, 24(3), 925. https://doi.org/10.3390/s24030925

Ranyal, E., Sadhu, A., & Jain, K. (2022). Road condition monitoring using smart sensing and artificial intelligence: A review. Sensors [Internet], 22(8), 3044. (from https://www.mdpi.com/1424-8220/22/8/3044)

Zakeri, H., Nejad, F. M., & Fahimifar, A. (2017). Image Based Techniques for Crack Detection, Classification and Quantification in Asphalt Pavement: A Review. Archives of Computational Methods in Engineering, 24(4), 935-977. https://doi.org/10.1007/s11831-016-9194-z

Webliography

1. https://www.aiunika.com/
2. https://www.rasta-ai.com/
3. https://www.linkedin.com/pulse/ai-traffic-management-joshua-obwengi-nq55f
4. https://www.researchgate.net/publication/352177699_AI_Driven_Road_Maintenance
5. https://content.iospress.com/articles/journal-of-smart-cities-and-society/scs230001

A Study of Truck Drivers' Behavior for Determining Appropriate Truck Parking Spaces in Border Checkpoint Area.

Warakorn Bunyot[1,*], Supornchai Utainarumol

[1]Civil Engineering Department/King Mongkut's University of Technology North Bangkok,
+666-242-4261/S6501081856054@email.kmutnb.ac.th
[2]Associate Professor, Civil Engineering Department/ King Mongkut's University of Technology North Bangkok,
+662-555-2000 Ext. 8620-8624/ supornchai.u@eng.kmutnb.ac.th

ABSTRACT

From the study of Office of Transport and Traffic Policy and Planning in 2014 found that currently Thailand still shortage standard truck rest areas along the country's main freight corridors. To promote road safety, it is necessary to provide adequate truck parking facilities. Previous studies by FHWA in the USA developed a model to determine the appropriate number of truck parking spaces along the National Highway System. However, this model is not detailed enough to predict the demand for specific highway segments. Therefore, this study will focus on developing a model for truck parking demand along highway segments which is an open highway system adjacent to border checkpoint area, considering the behavior of truck drivers using rest areas and the impact of law enforcement in Thailand study on the section of Highway Route No.2 adjacent to the Thai-Lao border checkpoint area, Nong Khai Province. Using a questionnaire that collected personal preferences in choosing rest areas. Parking time for each activity. it was found that if not including extended rest. Parking to wait for Shipper/Receiver or Load/Unload will take the longest. Not driven by the needs of truck drivers. The average weekly driving time of the sample group was 64.89 hours, which is more than the legal limit. The short-haul to long-haul ratios of 0.1147/0.8853 When combined with the parameters obtained from field surveys using questionnaires entered into TPD, it was found that the demand for truck parking was 312 Spaces. Counting trucks parked in the field found that there were 349 spaces. As a result, the GEH value is 2.03. It indicates that the model's results are in good agreement with the field survey.

Keywords: Truck Driver Behavior, Truck Rest Area, Estimation of Truck Parking Spaces.

1. INTRODUCTION

Based on the data on domestic freight transport in 2022, it was found that road transport accounted for 79.48% of the total volume, primarily relying on trucks [1]. However, because truck transportation takes a long time to reach its destination, it leads to driver fatigue and results in accidents, causing damage to life and property [2]. Consequently, the Land Transport Act B.E. 2522 (1979), Section 103 bis, is now being enforced to prohibit truck drivers from driving continuously for more than 4 hours. In practice, however, Often, truck drivers are unable to find accessible rest areas along main freight corridors. This is because Thailand has yet to develop sufficient truck rest areas that can accommodate large vehicles along the country's main freight corridors [3]. As a result, most truck drivers are unable to take breaks as required by law.

To promote road safety, it is necessary to provide adequate truck parking facilities. A study conducted by the Federal Highway Administration (FHWA) in the USA developed a model to determine the appropriate number of truck parking spaces along the National Highway System. However, this model is not detailed enough to predict the demand for specific highway segments[4,5,6]. Additionally, previous studies in Thailand have focused on facilities designed to attract users to rest areas along concession highways and expressways, which are controlled access highways [7,8]. These findings may not be entirely suitable for application to open highway system.

Therefore, this study will focus on developing a model for truck parking demand along highway segments which is an open highway system adjacent to border checkpoint area, considering the behavior of truck drivers using rest areas and the impact of law enforcement in Thailand which not include pickup. Subsequently, the model's accuracy will be validated by comparing the projected truck parking demands with actual field data. This approach aims to create a more accurate model for future truck parking needs.

2. TRUCK PARKING DEMAND MODEL, TPD

The truck parking demand model was developed by Federal Highway Administration in 2002 for estimates truck parking demand for the highway segment rather than a single parking facility. The modeling framework starts by estimating truck-hours of travel using annual average daily traffic (AADT), the percentage of trucks, the length of the highway segment, and the speed limit or average truck speed. Number of parking hours required by drivers based on their travel hours, indirectly influenced by Federal HOS regulations. Higher parking time relative to driving time increases estimated parking demand. The model provides a peak-hour estimate of parking spaces needed for a highway segment. Short-haul drivers, who do not make overnight trips, require parking based on minutes

2.1. Model Development for National Assessment of Commercial Vehicle Parking

The research objective was to develop a truck parking demand model to estimate the extent and geographic distribution of truck rest parking supply and demand along the National Highway System.

The model parameters were derived from survey responses from over 2,000 drivers and field observations of parked trucks. 29 segments of highway in eight States representing four regions and ten corridors across the USA. The parking demand estimates produced by the model are highly variable at the segment level, but more accurate at the corridor level (Table 1). The variance at the segment level can be attributed to the fact that the model does not consider the geographic distribution of available truck parking spaces.

Table 1 Variable at the level.

Level	Accuracy	Accuracy (%)
Segment	±10 percent of observed parked trucks for 4 segments of the 29 segments	14%
	±20 percent of observed parked trucks for 11 segments of the 29 segments	38%
	±30 percent of observed parked trucks for 20 segments of the 29 segments	69%
Corridor	±8 percent of observed parked trucks for 6 corridors of the 10 corridors	60%
	±20 percent of observed parked trucks for 8 corridors of the 10 corridors	80%

(Federal Highway Administration, 2002)

The absolute errors in estimated demand at the segment, corridor, and regional level were 38, 12, and 3 percent, respectively. Because the model does not consider the geographic distribution of available truck parking spaces, it may not be suitable for evaluating specific highway segments or those with many intersections.

2.2. Law Enforcement Against Truck Drivers in Thailand

Truck drivers in Thailand It is necessary to perform duties under two parts of the law: the Land Transport Act, B.E. 2522, Section 103 bis, and under the labor law that allows drivers to work no more than 60 hours per week.

Both the laws that apply to truck drivers in both the USA and Thailand. There are some differences, such as in Table 2.

Table 2 Differences in laws that apply to truck drivers in the USA and Thailand

	Unites state of America	Thailand
Maximum Hours of Driving	11 Hours/day	12 Hours/day
Break	30 Minute / 8 Hours	30 Minute / 4 Hours
Extended Rest	24 Hours / Week	10 Hours / day

3. METHODS

A study of truck drivers' behavior for determining appropriate truck parking spaces involves several steps. Firstly, the study area is defined. A review of related research is conducted to identify factors influencing the use of truck rest areas. Define the study area, and questionnaires are prepared to gather data from the population and sample groups. Data collection follows, leading to data analysis. A model is then developed to estimate the required truck parking spaces. The model's accuracy is validated using field data, and the methodology is concluded.

3.1. Study Area

The study area focuses on a segment of Highway Route No.2 from Km.486+306 to Km. 509+113 in Nong Khai Province adjacent to border checkpoint area. This area is a key freight route to Laos via the First Thai-Lao Friendship Bridge. The journey for trucks from Bangkok or Laem Chabang Port, a major logistics hub, takes over four hours. Additionally, the area has few intersections, making it easier to control truck access.

3.2. Sample Population

To obtain an appropriate sample size for the study and representativeness that can provide reliable population information, the sample size will be determined using the formula by Yamane (Yamane, 1973). In this study, a confidence level of 95% will be set for the sample group, and a margin of error of 5% will be accepted for the sampling variability (Equation 2).

$$n = \frac{N}{1+Ne^2} \tag{1}$$

where n represents the sample size.
N represents the number of trucks on the highway segment considered.
e represents the margin of error.

To determine the sample population, we referenced the truck traffic volume data from the 1/2023 Traffic Information Management System (TIMS) of the Department of Highways, which reported a daily traffic volume of 34,815 vehicles, with trucks accounting for 33.95%. By setting a confidence level of 95% and an acceptable sampling error of 5%, the calculated sample population size is 387 samples.

3.3. Field Data Collection

The field data collection will be divided into two parts. The first part involves gathering information to understand driver behavior, and the second part involves counting the number of trucks to determine the actual demand in the field.

- ***Truck Driver Behavior***

To understand the behavior of truck drivers in choosing truck stops services, amenities, and travel information, surveyors will distribute questionnaires to collect data from a sample population on the highways segment within the study area. The data collected from the questionnaire will be input into the Truck Parking Demand Model to estimate truck parking spaces needed. This data will then be compared to the actual demand for truck parking in the field for subsequent analysis.

- ***Truck Parking Demand from Field Surveys***

The purpose of the truck parking field survey was to record trucks parked during the peak hour in public rest areas, private truck stops, pull- out areas, interchange ramps, mainline and highway shoulders, fueling stations, etc. Surveyors consisting of drivers and field recorders will count parked trucks every 3 hours starting at 12:00 AM to 21:00 PM to find the highest demand for truck parking.

3.4. Truck Parking Demand Model

The first step in the parking demand estimation is to calculate the seasonal peak daily truck volume, V_t is expressed in trucks per day (Equation 2).

$$V_t = AADT \ X \ P_t \ X \ FS \tag{2}$$

where $AADT$ = annual average daily traffic (vehicles/day)
P_t = percent of total traffic that is trucks
FS = 1.15, seasonal peaking factor

Next, using the length of the analysis segment and the speed limit, the average truck travel time, TT, for the segment is calculated in hours per truck (Equation 3).

$$TT = \frac{L}{S} \tag{3}$$

Where L = analysis segment length (km)

S = speed limit or average truck speed (kph)

Then, using V_t, TT, and the proportion of trucks that are short-haul and long-haul, the total daily truck-hours of travel, THT, for short-haul (Equation 4) and long-haul (Equation 5).

$$THT_{SH} = P_{SH}\ x\ V_t\ x\ TT \tag{4}$$

$$THT_{LH} = P_{LH}\ x\ V_t\ x\ TT \tag{5}$$

where P_{SH} = proportion of total trucks that are short-haul

P_{LH} = proportion of total trucks that are long-haul

After THT have been computed the daily short-haul truck -hours of parking demand, THP_{SH}, can be estimated based on the time parking per time driving (Equation 6).

$$THP_{SH} = \frac{D_{ST} x\ THT_{SH}}{60} = \frac{5xTHT_{SH}}{60} = \frac{THT_{SH}}{12} \tag{6}$$

Where D_{ST} = duration of short-term stops per hour traveled (5min/hour)

For long-haul drivers, the weekly parking time can be calculated by taking the total hours in a week and subtracting average number of hours spent driving, the average number of hours spent at home, the average number of hours spent loading/unloading, and the average number of hours spent parked while resting at shippers/receivers. The THT_{LH} in Equation 5, can then be used to estimate the daily long-haul truck-hours of parking demand, denoted as THP_{LH}, on the segment (Equation 7).

$$THP_{LH} = \frac{Parking\ Time/Week}{Driving\ Time/Week}\ x\ THT_{LH}\ x\ \frac{D_{ST}xTHT_{LH}}{60} \tag{7}$$

Now that the daily truck-hours parking demand for the segment has been estimated, the number of trucks demanding a parking space in the peak hour needs to be determined. This conversion can be made by considering the proportion of the daily truck-hours of parking demand that occurs during the peak hour can be made with a peak-hour parking factor (PPF). the peak-hour short-haul and long-haul parking demand, PHP_{SH} and PHP_{LH}, respectively, can be calculated (Equation 8, 9).

$$PHP_{SH} = PPF_{SH}\ x\ THP_{SH} \tag{8}$$

$$PHP_{LH} = PPF_{LH}\ x\ THP_{LH} \tag{9}$$

where PPF_{SH} = peak-parking factor for short-haul trucks

PPF_{LH} = peak-parking factor for long-haul trucks

The total peak-hour parking space demand is distributed between public rest areas (RA) and private truck stops (TS) using responses from driver survey (Equation 10 to 13).

$$PHP_{SH,RA} = P_{RA} \ x \ PHP_{SH} \tag{10}$$
$$PHP_{SH,TS} = P_{TS} \ x \ PHP_{LH} \tag{11}$$
$$PHP_{SH,RA} = P_{RA} \ x \ PHP_{SH} \tag{12}$$
$$PHP_{SH,TS} = P_{TS} \ x \ PHP_{LH} \tag{13}$$

Where P_{RA} = proportion of demand for rest area spaces
P_{TS} = proportion of demand for private truck stops spaces

3.5. Model Reliability Verification

The reliability of the model will then be assessed based on the inspection criteria of the Department for Transport UK Highways Agency's Design Manual for Roads & Bridges (DMRB) of England using the GEH in Equation 14. If the GEH value is ≤ 5.0, it indicates that the model's results are in good agreement with the field survey. If 5 < GEH ≤ 10, the results are consistent, but the model's demand estimates should be re-evaluated. If GEH > 10, the model's results do not align with the actual field survey findings.

$$GEH = \sqrt{\frac{2(M-C)^2}{M+C}} \tag{14}$$

Where M = represents the truck parking demand obtained from the model.
C = represents the actual truck parking demand observed in the field survey.

4. RESULTS

Results of this study can be divided into 3 parts as follows.

4.1. Truck Driver Behavior

Equation 1 will be used to calculate the appropriate number of samples. which equals 387 samples. But to get more accurate information. This study therefore used a total of 532 questionnaires. The results from the questionnaires were summarized as follows.

- ***Working days***

Data obtained from questionnaires found that the average number of working days was 5.312 days per week. Most work 6 days, minimum 2 days, and maximum 7 days per week. As shown in Figure 1, the average driving time per day is 12.216 hours per day, resulting in an average driving time of 64.89 hours per week. which exceeds the legal limit

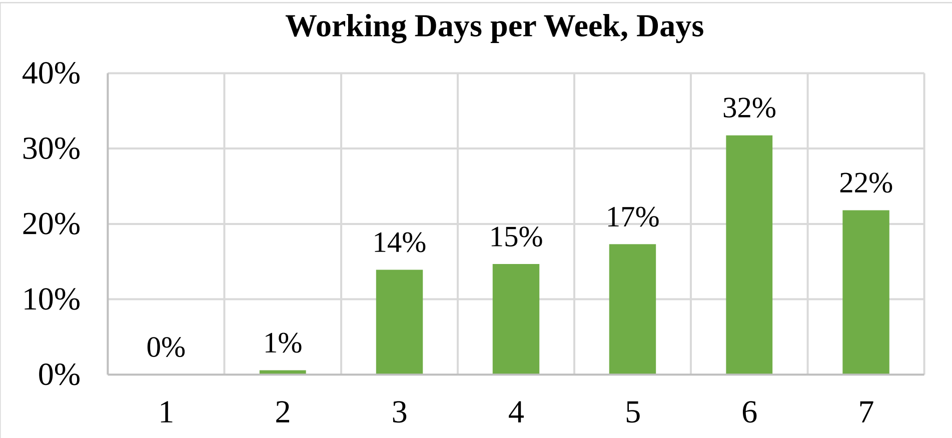

Figure 1 Driving time per week

- ***Short-Haul to Long-Haul Ratio***

There were 61 samples of respondents who were short-haul drivers with a travel radius of no more than 400 kilometers, which is the distance that can be traveled round trip in one day, and 471 samples were long-haul drivers, representing a ratio of 0.1147/0.8853 as shown in Figure 2.

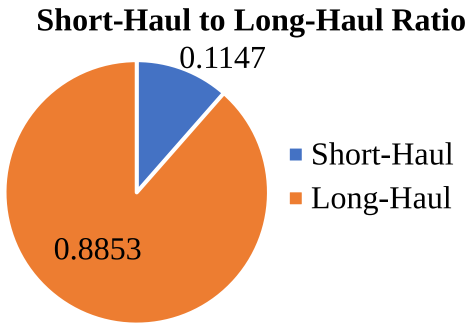

Figure 2 Short-Haul to Long-Haul Ratio

- ***Average Parking Time***

When drivers were asked to answer questions about the average parking time for each activity, it was found that the activity that keeps drivers parked the longest during driving is Extended rest. Calculated as an average of 16.46 hours per week. This is followed by the Load/Unload and Shipper/Receiver which takes 12.30 and 9.56 hours per week. Next is Eating, Restroom, and Quick nap, accounting for 5.00, 3.23, and 0.92 parking hours per week, respectively, as shown in Figure 3.

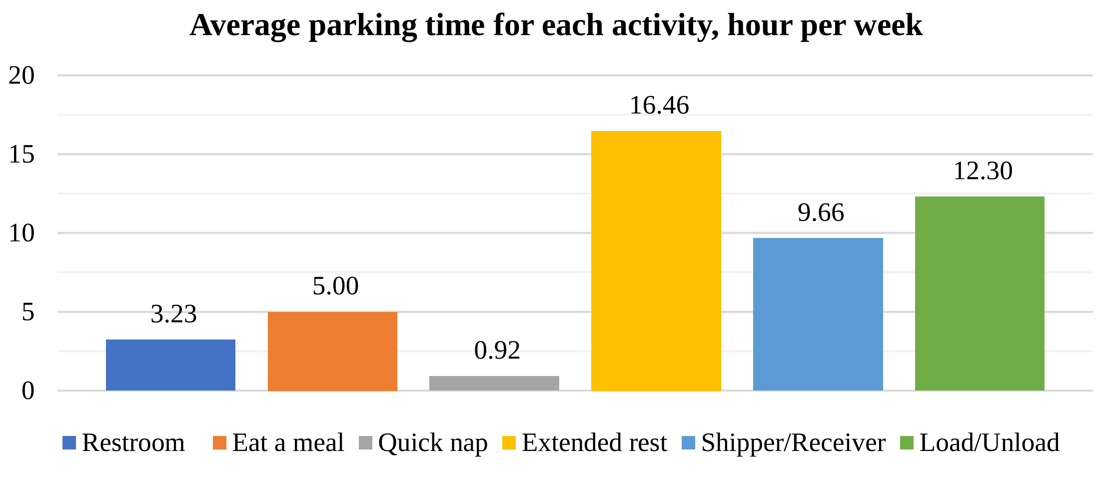

Figure 3 Average parking time for each activity

- ***Parking Location Preference***

When drivers were asked where they preference to park for each activity, they were asked to choose between Rest areas, no preference or private truck stops. Most drivers answered that they chose convenience rather than a specific type of rest areas, except for Extended rest, Shipper/Receiver or Quick a nap where most drivers choose to stop at the rest areas, which is a government rest stop. Because there is a large area Convenient entry and exit and not being chased out If you must park for a long time. Preferences for where drivers like to park for each activity Shown as shown in Figure 4.

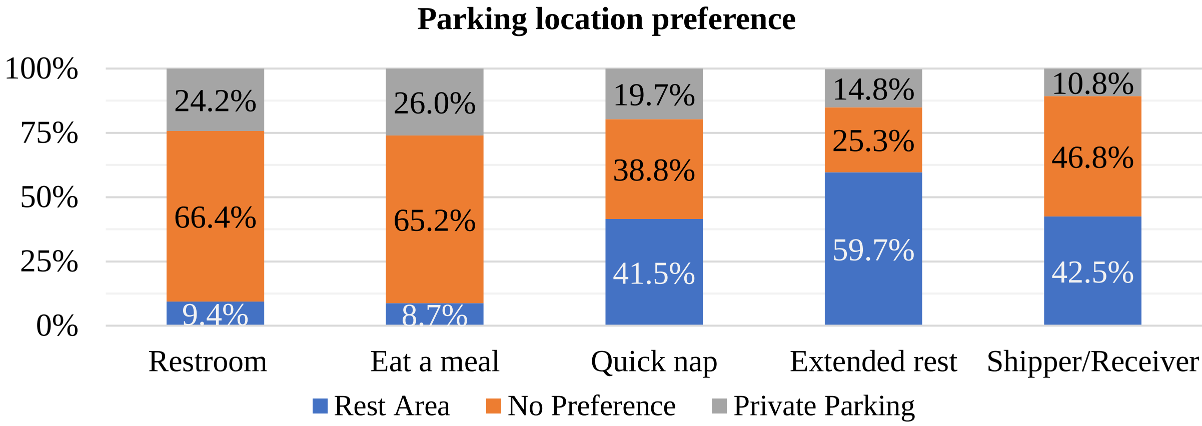

Figure 4 Parking location preference

▪ ***Importance of Features When Parking***

Truck drivers rated the amenities they need when parking their vehicles on a scale from 1 to 5, where 1 indicates not important and 5 indicates very important. The top four amenities that truck drivers prioritize are Restroom (5.0), Bathroom (4.8), Well-lighted (4.5), and Facilities maintenance (4.4). The ranks with the lowest average scores were Power plug, Wi-Fi internet, and Fuel, with scores of 2.99, 2.48, and 2.23, respectively, which did not differ between short-haul and long-haul drivers. As shown in Figure 5.

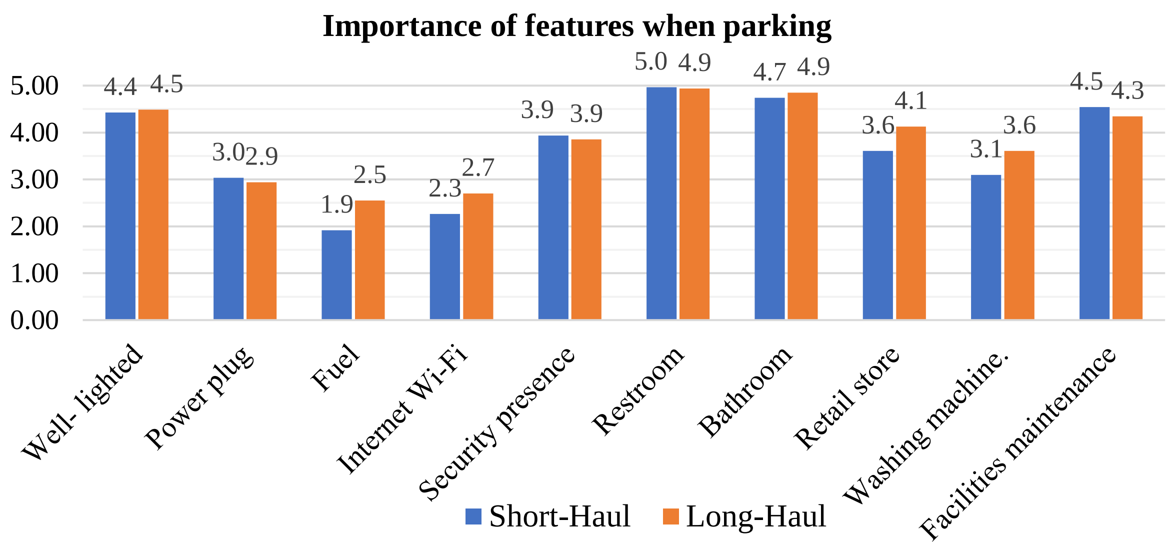

Figure 5 Importance of features when parking (as rated by drivers)

▪ ***Proportion of Parking Demand for Rest Area and Private Truck Stop Spaces***

Based on responses when asked what types of rest area drivers prefer to park in for various activities, Table 3 presents the data obtained from the field survey. It is obtained by multiplying the number of people who choose to park in each type of rest area by the average parking time for each activity. will be the number of truck-hours according to the parking needs of each type of rest area. Requirements listed as No Preference will be divided equally among Rest area and Private truck stops. Then add all truck hours together and find the proportion between rest areas and private rest stops. As a result, the proportion of parking demand for rest areas and private rest stops is 62.9 percent and 37.1 percent, respectively.

Table 3 Proportion of parking demand for rest areas and Private truck stops by drivers

Facility	Demand (truck-hours)	Proportion of Total Demand
Rest area	11,080.02	62.9%
Private truck stops	6,542.25	37.1%
Total	17,622.28	100.00%

- ***Parameter Values Obtained from The Questionnaire.***

The Peak-parking factor, PPF can be obtained from a questionnaire by finding the proportion by type of drivers (short-haul or long-haul) who park during peak parking demand periods more than 4 hours, in the highway segment considered divided by the total type of drivers, divided by 7 days, and divided by 2 periods (peak hours and non-peak hours).

Peak-parking factor for short-haul trucks PPF_{SH} can be found from the total number of respondents There are 61 sets of short-haul drivers, including short-haul drivers who need to stop during rush hour 29.5 times per week. Therefore, PPF_{SH} is equal:

$$PPF_{SH}=\frac{29.5}{61x7}\ x\ 100\% = 6.91\%$$

And peak-parking factor for long-haul trucks PPF_{LH} can be found from the total number of respondents There are 471 sets of long-haul drivers, including long-haul drivers who need to stop during rush hour 314 times per week. Therefore, PPF_{LH} is equal:

$$PPF_{LH}=\frac{314}{471x7}\ x\ 100\% = 9.52\%$$

From field survey data using questionnaires. The values obtained from the survey were used to determine the following parameters are the average hours spent loading/unloading, spent at home, spent parking for rest at Shipper/Receiver per week and the proportion of demand for rest between rest areas and private truck parking areas as per Table 4.

Table 4 Demand model parameters.

Model Variable	Description	Default Value	Source
FS	Seasonal peaking factor	1.15	Professional
D_{ST}	Short-term parking duration per hour traveled (min/hour)	5	Professional
$T_{DRIVING}$	Average hours driven per week	64.89	questionnaire
$T_{LOAD/UNLOAD}$	Average hours spent Load/Unload per week	12.30	questionnaire
T_{HOME}	Average hours spent at home per week	40.51	questionnaire
$T_{SHIPPER/RECEIVER}$	Average hours spent parking for rest at Shipper/Receiver per week	9.66	questionnaire
P_{RA}	Proportion of demand for rest area spaces	62.90%	questionnaire
P_{TS}	Proportion of demand for truck stops spaces	37.10%	questionnaire
P_{SH}	Proportion of total trucks that are short-haul	11.47%	questionnaire
P_{LH}	Proportion of total trucks that are long-haul	88.53%	questionnaire
PPF_{SH}	Peak-parking factor for short-haul trucks	6.91%	questionnaire
PPF_{LH}	Peak-parking factor for long-haul trucks	9.52%	questionnaire

4.2. Truck Parking Demand from Field Surveys

From counting trucks parked in the study area, including rest areas, private rest stops, road shoulders, and intersections from 00:00. until 21:00., it was found that the time of peak demand for parking is in the morning, around 9:00. And trucks started accumulating on Sunday evening. and there is the least number of trucks during 3:00 As shown in Figure 6.

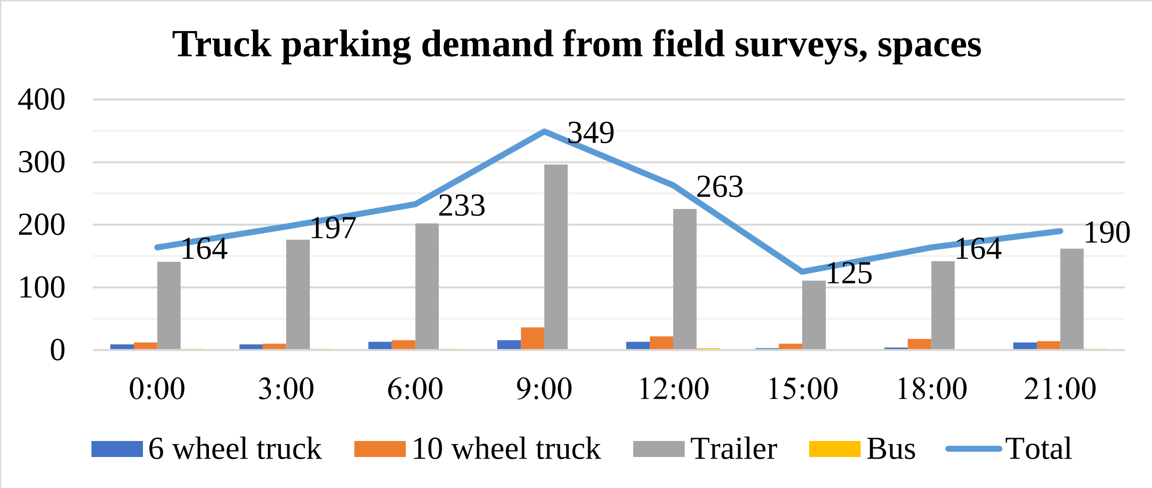

Figure 6 Truck parking demand from field surveys

4.3. Truck Parking Demand from TPD

The highway segment under consideration has a speed limit of 60 km/h, a length of 22.807 km, an AADT (Average Annual Daily Traffic) of 34,815 vehicles per day, and a truck ratio of 33.95%. Average truck travel time, TT, can be calculated from equation 4, which is equal to 0.38 hours. When combined with the data in Table 2, the THT_{SH} value can be found from Equation 4, which is equal to 592 truck-hours per day , and the THT_{LH} value according to Equation 5, which is equal to 4,574 truck-hours per day on the segment.

The next step is to determine the daily short-haul truck-hours of parking demand, THP_{SH}, can be estimate by equation 6 and the daily long-haul truck-hours of parking demand, THP_{LH}, can be estimate by equation 7, which are equal to 49 and 3,246 truck-hours per day respectively. Then multiply with PPF in Table 2 according to Equations 8 and 9 to get PHP_{SH} and PHP_{LH} values equal to 3 spaces and 309 spaces, respectively.

Now that the peak-hour short-haul and long-haul parking demand for the segment has been calculated, resulting in a total demand of 312 parking spaces (3+309) Finally, the total peak-hour parking demand will be distributed between public rest areas (RA) and private truck stops (TS) using the settings determined from driver survey responses and Equations 10 to 13. which has the following values:

Proportion of Short-Haul Truck-Hours Parking in Public Spaces, $PHP_{SH,RA}$ =1 spaces
Proportion of Short-Haul Truck-Hours Parking in Private Spaces, $PHP_{SH,TS}$ = 2 spaces
Proportion of Long-Haul Truck-Hours Parking in Public Spaces, $PHP_{LH,RA}$ = 194 spaces
Proportion of Long-Haul Truck-Hours Parking in Private Spaces, $PHP_{LH,TS}$ =115 spaces

Once the demand for truck parking has been obtained from both TPD and the number of trucks parked in the field. The next step is to validate the model.

4.4. Model Reliability Verification

When comparing the parking demand estimated TPD, which is M = 312 spaces, with the actual number of parked trucks in the field, C = 349 spaces, this resulted in a Goodness of Fit (GEH) can be calculate by equation 14

$$GEH = \sqrt{\frac{2(M-C)^2}{M+C}} = \sqrt{\frac{2(312-349)^2}{312+349}} = 2.03$$

The GEH value was found to be 2.03 which has a value less than 5. It indicates that the model's results are in good agreement with the field survey.

5. CONCLUSIONS

A study truck driver behavior to estimate appropriate parking spaces the objective is to study the behavior of truck drivers. and create a model to estimate the number of truck parking spaces at present and in the future using the Truck Parking Demand Model method, TPD which was studied on Highway 2, km. 486+306 to km. 509+113 next to the Thai-Lao border checkpoint area, Using a questionnaire that collected personal preferences in choosing rest areas. Parking time for each activity Including the amenities that drivers want to have in rest areas. To find the facilities that drivers need and the appropriate number of truck parking slots The results of the study can be summarized as follows. From the study it was found that Activities that cause drivers to park for a long time in truck rest area, if not including extended rest. It will be parking to wait for Shipper/Receiver or Load/Unload not driven by the needs of truck drivers. And an equation can be created to estimate the number of parking spaces appropriate for rest areas or private truck stops according to Equation 15 and Equation 16.

$$PHP_{RA} = 0.01446 \text{ x } AADT \text{ x } Pt \text{ x } FS \quad (15)$$

$$PHP_{TS} = 0.00853 \text{ x } AADT \text{ x } Pt \text{ x } FS \quad (16)$$

Where PHP_{RA} = demand for Rest area spaces
PHP_{TS} = demand for Private truck stops spaces

Because it may not make sense to specify that short-haul drivers require parking based on minutes, because some short-haul drivers need to park for long time during rush hour on the highway segment that is a border checkpoint area. If this equation is to be applied to other border economic zones, the distribution of cities must be considered, which will affect the proportion of short-haul and long-haul trucks. Trucks using rest areas for long-term parking should be considered. Because this group of drivers was not surveyed using a questionnaire. This may be the reason that the demand from the model is lower than the reality.

6. ACKNOWLEDGMENTS

I would like to thank Associate Professor Supornchai Utainarumol for providing valuable guidance in planning and providing a holistic research perspective. Thank you to the team that helped collect the questionnaire until it was successful And thank you to all respondents who participated in answering the questionnaire and contributing information.

7. REFERENCES

Office of Strategic Development for Logistics Systems, Office of the National Economic and Social Development Council. (2023). Thailand's Logistics Report 2022 (p. 5). https://www.nesdc.go.th/download/logistics/report/LogisticsReportTH.pdf

Land Transport Safety Bureau. (2023). Truck accident situation analysis report. Department of Land Transport.

Office of Transport and Traffic Policy and Planning. (2014). Study project on the development of truck rest areas along the country's main freight routes. https://www.otp.go.th/uploads/tiny_uploads/ProjectOTP/2557/Project07/01_Final_Report_PDF.pdf

Pécheux, K. K., Chen, K. J., Farbry, J. Jr., & Fleger, S. A. (2002). Model development for national assessment of commercial vehicle parking (Final report). Federal Highway Administration, March 2002.

Chen, K. J., Pécheux, K. K., Farbry, J. Jr., & Fleger, S. A. (2002). Commercial Vehicle Driver Survey: Assessment of Parking Needs and Preferences (Final Report). Federal Highway Administration, March 2002.

Kelley, K., Pécheux, K. J., Chen, J., Farbry, J., & Fleger, S. A. (2002). Model development for national assessment of commercial vehicle parking. Federal Highway Administration.

Wanichsirikul, A., & Utainarumol, S. (2015). Factor influencing the demand of service area in motorway (Master's thesis). King Mongkut's University of Technology North Bangkok.

Mahannopnatee, C., & Pongprasert, P. (2020). A feasibility study of expressway service area development (Master's thesis). Thammasat University.

The Role of Knowledge and Awareness in Road Safety: An Evaluation of Road Traffic Accidents in Indonesia

Firza Aulia Syafina[1,*], Ni Kadek Dinda Paramitha[2] and Hadi Mizan Nur Arifin[3]

[1] Bangka Belitung National Road Implementation Center, Ministry of Public Works and Housing, Pangkalpinang, Indonesia, firzasyafina@pu.go.id
[2] East Java-Bali National Road Implementation Center, Ministry of Public Works and Housing, Denpasar, Indonesia, nkdindaparamitha@pu.go.id
[3] Southeast Sulawesi National Road Implementation Center, Ministry of Public Works and Housing, Kendari, Indonesia, hadimizan@pu.go.id

ABSTRACT

This paper examines the role of road safety knowledge and its awareness in Indonesia, one of the developing countries in Southeast Asia, as a factor in establishing a safer road. Currently, high road traffic injury remains the leading cause of death of young people and is one or more leading causes of death when all ages are considered. The highest number of fatalities occur in the Southeast Asia Region, especially for those living in low and middle-income countries. Incorporating evidence from previous data, personal correspondence, and statistical analysis, this study evaluates that road safety knowledge was an important element in building a safer road rather than the quality of the road itself. It argues that the results are different for some age groups. A comparison between a city with a high number of accidents rate and a city with less is made therefore the discrepancy can be seen.

Keywords: road safety, safety awareness, traffic accidents, developing country

1. INTRODUCTION

Traffic accidents have become one of the factors that contribute most to the death rate in several countries, especially developing countries and countries with low or middle income as nine in 10 deaths occur in low- and middle-income countries. Furthermore, they also continue to face the highest risk of death per population. This is something that is worrying, especially considering that most victims are in productive age, where if this continues to happen it will have an impact on decreasing the productive population in the country, thus reducing the country's productivity in order to become a more developed country in the future.

Losses resulting from traffic accidents are not only felt by the victims or their families. If the victim is the backbone of a family's livelihood, the social impact will be greater. Remarkably, until 2023, there are only 25 countries that mandate provision of psychological assistance to road traffic crash victims and their families (WHO, 2023). Not to mention, if it causes damage to facilities and hampers the activities of a production or logistics cycle, it will certainly cause economic losses in a wider scope, even to the state. Based on data portal of Ministry of Transportation, the total loss due to traffic accidents in 2022 is around 280 billion rupiah.

These road accidents occur in all regions, even though these locations have different traffic quantities and road quality. Therefore, it is necessary to evaluate the conditions of road accidents, especially in the author's country, Indonesia which is places in Southeast Asian. Death tolls there is mostly higher than Covid-19 fatalities, makes Southeast Asian Road accidents are some of the most dangerous in the world (Hutt, 2022).

Many factors affect road traffic accidents, one of which, and perhaps the most influence is the knowledge and awareness of the road users. Before traveling from some place to another or deciding to behave in some situation on the road, road users will consider their preferences based on their understanding. Consequently, the knowledge and awareness of road users can be the basis in strengthening the safety of the road itself while ignorance of people must have a significant part in taking traffic accidents place.

This evaluation will focus on assessing the level of knowledge and awareness of road users and their relationship to road accidents considering other factors such as traffic quantity, road quality and the age of the road users themselves. Traffic quantity can be assumed as environmental condition or society of the road and road quality is an infrastructure that facilitates road user to mobilize. In addition, age is one requirement of Indonesian driving license, a legal document issued by the Indonesia National Police (POLRI) for a person to be allowed to drive a motor vehicle in Indonesia.

This study will begin with an introduction that explains the background, purpose, and objectives from authors then followed by some theoretical review based on existing literature. After that, focusing on how the research conducted and how the analysis results are. At the end, conclusions and recommendations will be created to show the findings and give some advice for further research.

2. LITERATURE REVIEW

2.1 Road traffic accidents

Accidents are an unwanted or unintended sudden event or a specific chain of such events which has harmful consequences. Road Traffic Accident is any accident involving at least one road vehicle in motion on a public road or private road resulting in at least one or killed person. Accidents that occur on the road are caused by several factors while many factors underpin the speedy enhancement of incidence rate, which has become a major social problem. For example, in capital city such as Jakarta, Indonesia, traffic jam happens almost all the time, and causes drivers easily lose focus on driving. On the other hand, in a small village that is not very developed, there are still many roads of inadequate quality that can endanger road users. It may be expected to increase the occurrence of road traffic accidents due to many vehicles on the road, they may also decrease due to a reduction in speed. This suggests that accidents may be caused by the number of cars on the road as it affects the result of speeds itself. This study will classify those factors into three simplified types: human factors, traffic factors, infrastructure factors. Two of these factors have their respective responsibilities in the government, such as the Ministry of Public Works and Public Housing is responsible for infrastructure, the Ministry of Transportation and the police are responsible for traffic. While the human factor is the responsibility of all entities, including road users themselves. Therefore, studying these factors will be useful in evaluating accidents that occur.

Human factors

Many studies have shown that human behavioral factors correctively represent the main causes of road traffic crashes, and their good understanding about these matters can go a long way to help prevent road traffic injuries. Numerous studies have demonstrated that human behavior accounts for more than 85% of road traffic accidents. The World Health Organization report attributes 71% of road traffic accidents to human factors (Lakhan, 2020). A reckless driver who usually lacks adequate training and education impairs their judgment and concentration then makes them more vulnerable to fatal accidents.

Infrastructure factors

The fact is we mobilize from one place to another by passing through road infrastructure, except for air and water travel. Furthermore, the infrastructure is one of the essential factors that either will save us from crashes or push us to a fatal injury. With that in mind, one element of the infrastructure is the quality of it that in this case the road quality.

Traffic factors

Numerous studies have been conducted in recent years to investigate the frequency and severity of accidents in different parts of the rural and urban area. Some of them concluded that the high volume of traffic plays a significant role in accidents. Its report contradictory results. One finds that higher exposure to traffic is associated with increased crash risk. On the other hand, some others believe that the low traffic makes people speed moreover which can be dangerous for the road users.

2.2 Road safety

In the simplest terms, safety can be defined as the absence of risk or danger. Focusing this term to address transportation, road safety can be characterized by the ability of person to travel freely without injury or death. (Carter, 2013) Road safety professionals typically measure safety by the number and rate of crashes and by the severity of those crashes. Crashes frequency or accidents frequency which is the number of crashes occurring per year or any other unit of time is another commonly used metric. Crash rates are numbers of accidents normalized by a particular population or metric of exposure.

Criteria for The Road Saftey includes three aspects: Forgiving Road, Self-explaining road, and Self-regulation road (Mulyono, 2021). Forgiving road is the road must be able to anticipate accidents by adding safety features to reduce the fatality rate of accidents, Self-explaining road means that the road must be able to communicate its conditions to the drivers by being equipped with signs (warnings, prohibitions, commands, and instructions), and Self-regulation road means that the road must comply with road planning regulations and standard.

2.3 Road quality

There are many aspects in determining the road's quality. For example, road lighting enhances visual comfort and alertness of the road users; skid resistance, a relationship between the vertical force and the horizontal force developed as a tire slides along the pavement surface (Ibrahim M.Asi, 2007); and pavement roughness which will detailed.

Pavement roughness is generally defined as an expression of irregularities in the pavement surface that adversely affect the ride quality of a vehicle and thus the user. The World Bank found road roughness to be a primary factor in the analyses and tradeoffs involving road quality. Roughness is also referred to as smoothness although both terms refer to the same pavement qualities.

Today, roughness is typically quantified using some form of either present serviceability rating (PSR), international roughness index (IRI), and others. As index with IRI being most prevalent and becoming the standard used in Ministry of Public Works and Housing Indonesia, in this research road quality will be referred to IRI value. IRI was developed by the World Bank in the 1980s and is used to define a characteristic of the longitudinal profile of a traveled wheel track and constitutes a standardized roughness measurement.

2.4 Traffic volume

Traffic volume is the number of vehicles passing a cross section during a certain period of time. Average annual daily traffic (AADT) is the number of vehicles passing a road in a year, divided by 365. (Hesjevoll, 2016) Traffic volume estimates can be based either on continuous counting known as traffic sensor, or short-term data collection adjusted for relevant variations such as seasonal, weekday, and hourly variations.

2.5 Knowledge and awareness of road safety

Knowledge on road safety refers to the knowledge of the regulations, do and do not, and the importance of making the whole system of the road become safer for the users. Road safety awareness refers to having recognition, knowledge, and understanding of road safety. Awareness is divided into seven levels, that are: 1. animal – fight or flight, 2. mass – follow the masses, 3. aspiration – desire for something greater, 4. individual – express your individual powers, 5. discipline – the ability to give yourself a command and stick to it, 6. experience – action and results, 7. mastery – respond, think, and plan.

2.6 Maturity Based on Brain Development

The prefrontal cortex is defined as the part of cerebral cortex that receives projections from the mediodorsal nucleus of the thalamus. The prefrontal cortex undergoes one of the longest periods of development of any brain region, taking over two decades (until near the age of 25 years) to reach full maturity in humans (Kostovic et al., 1988; Sowell et al., 1999a).

This brain region is known to be the higher-order association center of the brain as it is responsible for decision making, reasoning, personality expression, maintaining social appropriateness, and other complex cognitive behaviors.

3. SAMPLES AND METHODS

3.1 SAMPLES

The sample selected for this study was specifically citizens representing two age group (based their maturity) from two characters of domicile (high road accident rate and the less one). A Google Form utilized questionnaire was conducted to collect and assess the knowledge and awareness of road users. The constructs in the questionnaire were adapted from published literature, tailored to information needs, scoring yes/no/not sure questions, and open opinion to gain insight. The survey instrument was first developed in Indonesian language and afterwards independently translated into English by research member.

The secondary data was collected from official institution who has responsibility in those sectors, that are POLRI for accidents data, Central Agency of Statistics (BPS) for population and vehicle volume, and Ministry of Public Works and Housing for road quality data. Road quality is using IRI as the measure of the good road profile, and it is covered in several standards from American Society for Testing and Materials (ASTM) International.

3.2 METHODS

Coefficient correlation (R) was the method applied to the research model for data analysis. This technique is known for being used when we want to quantify the linear relationship between two variables and neither of the variables represents a response or outcome variable. In this case calculation will be examined by Pearson correlation coefficient. Microsoft Excel was the software used to evaluate both the measurement and analysis.

4. RESULTS

4.1 Number of road accidents

Table 1 shows the number of road accidents rate in provinces with the highest rate (North Kalimantan, Bangka Belitung Islands, and Yogyakarta) and provinces with lowest rate (East Java, West Java, and Central Java) in 2022.

Table 1 Road traffic accidents rate.

Province	Accidents (times)	Population (1000 s)	Accident Rate
North Kalimantan	8583	727,8	11,79
Bangka Belitung Islands	11389	1494,6	7,62
DI Yogyakarta	13041	3761,9	3,47
Central Java	9881	37032,4	0,27
East Java	5073	41150	0,12
West Java	1409	49405,8	0,03

(POLRI & BPS, 2022)

Based on Table 1, North Kalimantan, Bangka Belitung Islands, and DI Yogyakarta are provinces with the highest accident rate in 2022. The number of their rates are above 3,4, moreover in North Kalimantan, accidents occur 11,79 times per population. In contrast, Central Java, East Java, and West Java have a fewer number of accidents even though the populations are much higher (more than 10 times higher) than the three provinces before, however their accident rates are below 0,3 which West Java has the lowest rate totaled only 0,03 times per population.

4.2 The causes of road accidents

The causes of road traffic accidents according to the in-depth interview with the road users who represent each age group and from each type of accident rate area (high and low) as informants, here are the results with the respondent about road traffic accidents:

- "The driver plays the most important role when an accident occurs, I think around 50% is due to the driver. While the quality of the road affects around 30% and the mechanical condition of the vehicle around 20%." (Informant 1, 2024)
- "Accidents occur due to negligence of people, speeding on narrow roads because the traffic is low, even markings are connected but drivers still overtake other vehicle, varying tonnage of heavy vehicles, road conditions that lanes are not wide enough, minimal lighting so that at night accidents often occur, lack of public awareness, they don't wear a helmet and feel uncomfortable if wear a safety belt" (Informant 2, 2024)
- "First, it is because people violate traffic laws and signs. Second, the vehicle speed is too high, yet they tend to brake suddenly. Third, road conditions factor such as dirt on the road due to sand or the condition of the asphalt with holes." (Informant 3, 2024)

From the interview it is known that the causes of road traffic accidents are classified as 3 big factors, they are: traffic factors, infrastructure factors, human factors.

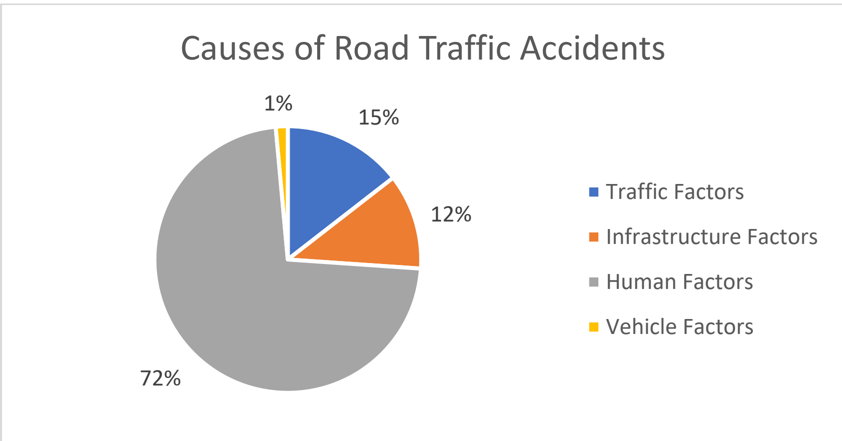

Figure 1 Causes of Road Accidents
(Syafina, et. al, 2024)

For traffic factor, it is said that the low traffic volume makes the driver tend to over speeding. On the other hand, from Table 1 it is illustrated that a city with high population density apparently doesn't mean there are more accidents, so it is necessary to analyze whether the traffic volume has the characteristics or not. For infrastructure factor, there are many elements that have been mentioned like the quality of the pavement, the street lighting facilities, and the clarity of traffic signs. Because this is a very broad factor, the analysis will only concentrate on the quality of the road. For human factors, the main cause is due to negligence of the regulation by the road users. When there is a prohibition sign such as not allowed to overtake, speed limit, do not enter road, they still do the opposite. There is a regulation to use helmet while driving motorbike, however people don't always wear it as same as using safety belt in the car. This factor will be analyzed in level of awareness and will be focused on how people's general point of view regarding safe roads and road traffic accidents.

4.3 Qualities of the roads

Road condition survey is conducted every semester to determine the road quality rating. One data point used in determining road quality is the International Roughness Index (IRI) value. The IRI values are divided into four conditions: values 1-4 indicate good condition, 4-8 indicate Fair condition, 8-12 indicate Lightly Damaged condition, and values above 12 indicate Severely Damaged condition. Good and Fair conditions are categorized as Good Quality, while Lightly Damaged and Severely Damaged conditions are categorized as Poor Quality. The Comparison of the length of the roads in good quality condition with the total length of the roads which is used as a Road Quality Rating Condition.

The road qualities are divided into National Road Qualities, Province Road Qualities, and District Road Qualities because the authority for its road preservation is carried out by different agencies. The data is presented in Table 2.

Table 2 Road qualities.

Province	National Road Quality	Province Road Quality	District Road Quality
North Kalimantan	91,23	14,97	37,66
Bangka Belitung Islands	99,85	94,64	78,42
DI Yogyakarta	97,97	70,52	75,54
Central Java	93,74	90,86	81,69
East Java	97,36	97,56	80,96
West Java	97,48	88,77	79,67

(Ministry of Public Works and Housing, 2022)

Based on Table 2, National Road is inclined to have good quality rather than Province Road and District Road. Province Road has its lameness variation from 14,97 (very poor quality) until 97,56 (very good quality), while District Road variation tends to be more consistent to have 37,66 as the lowest quality and 81,69 as the peak.

4.4 Traffic volume

The Average Traffic Data, estimated by dividing total traffic volume during a given observation period ranging from 2 to 364 consecutive days with number of days in that period, expressed in vehicles per day (VPD) in each province is given in Table 3.

Table 3 Traffic volume.

Province	Average Traffic Data
North Kalimantan	189.091
Bangka Belitung Islands	1.160.091
DI Yogyakarta	3.112.170
Central Java	19.534.880
East Java	23.605.425
West Java	97,48

(Ministry of Public Works and Housing, 2022)

This average traffic data appears highly positive correlated with the population data shown in Table 1 as it will be illustrated in Figure 2 which means the more population in one province, the more traffic volume there.

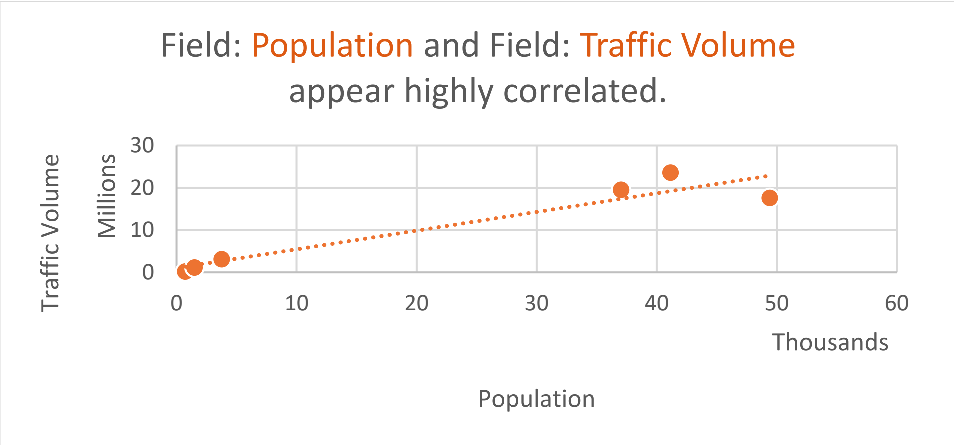

Figure 2 Correlation between population and traffic volume
(Syafina, et. al, 2024)

4.5 Level of awareness

Level of awareness was examined by scoring from yes/no/not sure questions in each level. Each level has two questions and will be counted 0 if the answer is yes, 1 if the answer is no, and 0.5 if the answer is not sure. If the accumulation of the score from the lowest level until the higher reach 2 points, it shows where the level of the respondent is.

The assessment's data, consisting of 14 main questions, was analyzed for validity to determine each question's feasibility. A total of 68 respondents filled out this survey, so a reference correlational value (r Table) was taken with a significance level of 5% at 0.235. As a result, it was found that each main question in this survey scored higher than the r Table and can be considered valid, as shown in the following table.

Table 4 Validity test result.

	p1	p2	p3	p4	p5	p6	p7	p8	p9	p10	p11	p12	p13	p14
r	0,354	0,412	0,486	0,535	0,486	0,500	0,281	0,370	0,368	0,563	0,532	0,586	0,651	0,682
r Table	0,235	0,235	0,235	0,235	0,235	0,235	0,235	0,235	0,235	0,235	0,235	0,235	0,235	0,235
Result	Valid	Valid	Valid	Valid	Valid	Valid	Valid	Valid	Valid	Valid	Valid	Valid	Valid	Valid

(Syafina, et. al, 2024)

The Cronbach's Alpha value obtained for this data is 0.707, which indicates that the data is reliable based on the minimum Cronbach's Alpha value for reliability tests, according to Eisingerich and Rubera (2010), which is 0.7.

Table 5 Reliability test result.

N	Cronchbach's Alpha Value	Reliability level
68	**0,707**	**Reliable**

(Syafina, et. al, 2024)

Based on the assessment and scoring the form, the result is illustrated in Figure 3 which the age group described in Table 6.

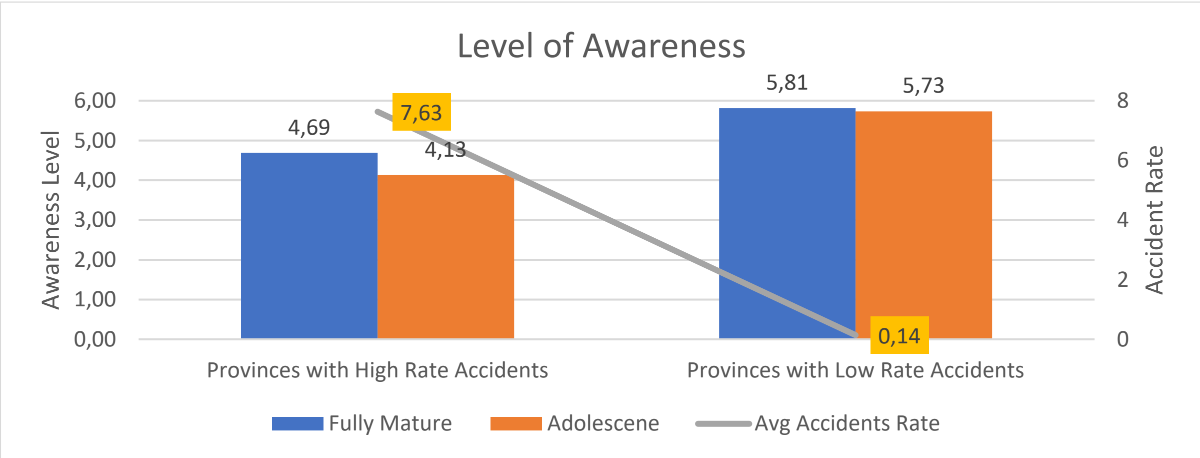

Figure 3 Level of awareness in each group
(Syafina, et. al, 2024)

Table 6 Maturity by brain development.

Brain Development	Age
Fully Mature	>= 25
Adolescence	< 25

(Sowell et al., 1999a)

From Figure 3 it can be known that for provinces that have the highest and lowest average accident rates, the Adolescence people have lower level of awareness regarding road safety rather than Fully Mature people. Moreover, the average awareness level in provinces that have a high accident rate is about 4,69 for the Fully Mature and 4,13 for the Adolescence, which is lower than provinces that have a low accident rate with the average awareness level about 5,81 for Fully Mature and 5,73 for Adolescence. From these data, the level of awareness influences the accident rate that occurs. The lower level of awareness increases the risk of accident.

4.6 Outcomes

The results of calculating the correlation of each factor with accidents using the Pearson formula and the Microsoft Excel application are described in Table 7.

Table 7 Coefficient Correlative.

	Accidents	Population	Accident Rate
Accidents	1,00		
Population	-0,79	1,00	
Accident Rate	0,43	-0,85	1,00
Traffic Volume	-0,64	0,95	-0,87
National Road Quality	0,03	0,05	-0,35
Province Road Quality	-0,18	0,56	-0,78
District Road Quality	-0,11	0,55	-0,83
Average Awareness	-0,60	0,83	-0,89

(Syafina, et. al, 2024)

Based on Table 7, the factors that have a large correlation with the number accidents or the accidents rates are factors that have a coefficient correlative value higher than 0.6 or less than -0.6 (the font-colored red). Where a negative value means that it is inversely correlated, and a positive value indicates that the two factors are correlated in line, with the following outcomes:

- More accidents occur in areas that have less population and traffic volume. This is indicated by the results of interviews which stated that in areas with small populations, they tend to have positive traffic volumes, drivers tend to speed.
- More accidents occur when road conditions are worse, this applies to provincial and district roads. whereas on national roads there is no significant relationship seen from the cc value of -0.35. This is because national roads in Indonesia tend to have IRI values which tend to be very good.
- In addition, the outcome based on Figure 3 is explained as more accidents occur in areas with a low level of awareness where the correlation of it (-0,89) is very relevant to accident rate compared to other factors such as quality (-0,35 until -0,83) and traffic volume (-0,87).

4.7 Implications

As far as the outcome is determined, one of the things that needs attention is the condition of district roads. This is because the negative correlation value is the largest, therefore it can be concluded that more and more accidents occur on district roads because the quality of the roads there is the worst. Also, the low level of awareness in The Adolescence age group needs to be considered because it contributed to accidents. Where if an area has poor road quality and least awareness that accidents often occur, this means that the road is unsafe for the users.

4.8 Limitations

This study can provide an overview of the relevance between the high occurrence of accidents and road safety knowledge in several cities in Indonesia. However, there are several limitations in this research process.

Firstly, the data used did not consider factors related to vehicle suitability and the environment (such as weather, etc.). Secondly, the data assessment was collected through questionnaires distributed to individuals categorized by age and city. Despite being randomly sampled, time constraints in conducting the research resulted in a limited number of samples taken, thus this data does not fully represent these categories. Besides that, interviewees were not differentiated by educational background and were not differentiated by gender.

5. CONCLUSIONS

Based on the analysis, this study proposes an insight into evaluation of road traffic accidents and the relationship between its factors. The findings confirm that; besides the condition of the road and traffic, road user's awareness also works as a relevant factor that needed to be considered. Among the results it is known that the higher awareness of the people the lower rate of accident in the road occurs.

An effective raising knowledge on road safety and its awareness campaign and action is needed to reduce the burden of road traffic accidents and establish a safe road for everyone. It will be great if there is further research from this one that considers the detailed elements such as gender, the occupation of the road users, or any background necessary. The more provinces that would be analyzed also will gain evaluation and insight of this theme.

6. ACKNOWLEDGMENTS

The unwavering support from peers and collages have been a constant source of motivation, providing crucial encouragement, and pursuing innovative ideas. Their expertise and constructive feedback played a significant role in refining the overall research. Authors also indebted to World Health Organization, Ministry of Public Works and Housing, POLRI, and BPS for serving as a source of information and inspiration for the framework of this study.

7. REFERENCES

Blackburn, Alexander et. al., (2019). Road Transport. Glossary for Transport Statistics 5th Edition, 31-56. doi:10.2785/53349

Carter, Daniel et. al., (2013). Road Safety Fundamentals: Concepts, Strategies, and Practices that Reduce Fatalities and Injuries on the Road. US Department of Transportation. Report no. FHWA-SA-18-003.

Central Agency of Statistics. (2022). Jumlah kendaraan bermotor menurut provinsi dan jenis kendaraan (unit), 2022 [Motor vehicle statistics by province and vehicle type (units), 2022]. Retrieved June 15, 2024, from https://www.bps.go.id/id/statistics-table

Eisingerich, A. B., & Rubera, G. (2010). Drivers of brand commitment: A cross-national investigation. Journal of International Marketing, 18(2), 64-79.

El-Baba RM, Schury MP. Neuroanatomy, Frontal Cortex. 2023 May 29. In: StatPearls [Internet]. Treasure Island (FL): StatPearls Publishing; 2024 Jan–. PMID: 32119370.

Hesjevoll, I. S., & Elvik, R. (2016). Effect of traffic volume on road safety. European Road Safety Decision Support System. Retrieved from http://www.roadsafety-dss.eu

Hutt, David. (2022, January 26). Southeast Asia's roads more dangerous than Covid With death tolls higher than Covid-19 fatalities, Southeast Asian roads are some of the most dangerous in the world. *Asia Times*. https://asiatimes.com/2022.

Ibrahim M. Asi, (2007). Evaluating skid resistance of different asphalt concrete mixes. Building and Environment Volume 42 Issue 1, Pages 325-329, ISSN 0360-1323. doi.org/10.1016/j.buildenv.2005.08.020.

Indonesian National Police. (2023). Annual crime report (Report No. 123). Indonesian National Police. https://www.polri.go.id/annual-crime-report-2023

Kostovic, I., Slavic J., & Strinovic D. (1988). Acetylcholinestetase in the human frontal associative cortex during the period of cognitive developement: early laminar shifts and late innervation of pyramidial neurons. *Neuroscine Letters,* 90, 107-112

Lakhan, Ram et. al., (2020). Important Aspects of Human Behavior in Road Traffic Accidents. Neurotrauma Society of India, page 2-4. doi.org/10.1055/s-0040-1713079

Md. Shamsul Hoque et al., (2006). Involvement of vehicle factors in road accidents. Department of Civil Engineering, Bangladesh University of Engineering and Technology. Retrieved August 5, 2024, from http://mail.jce-ieb.org/doc_file/3402008.pdf

Ministry of Public Works and Housing. (2022). Konektivitas. Retrieved June 15, 2024, from https://data.pu.go.id/search/field_topic/konektivitas-1

Ministry of Transportation. (2022). Dataset: 10029. Retrieved June 15, 2024, from https://portaldata.kemenhub.go.id/content/dataset/10029

Mulyono, Agus Taufik. (2021). Uji Laik Fungsi Jalan Berkeselamatan Dan Berkepastian Hukum. Yogyakarta : UGM Press

Sowell, E.R., Thompson, P.M., Holmes, C.J., Jerningan, T.L., & Toga, A.W. (1999a). Localizing age-related changes in brain structure between childhood and adolesence using statistical parametric mapping. *NeuorImage, 9, 587-597*

World Health Organization. (2023). Global status report on road safety 2023. Geneva. Retrieved from https://www.who.int/publications/i/item/

Enhanced YOLOv8-Based Object Detection of Road Assets Utilizing Generalized Focal Loss: A Case Study on Thai Highway Imagery

Natthasiri Rattanachona[1], Pawarisorn Thungthin[1], Nattapat Subsompon[1], Sittinun Thongbai[2], Weerachai Wongweeranimit[2], Ruttanawadee Phukham[3], and Teerapong Panboonyuen[4,5]*

[1] InfraPlus Co., Ltd., Bangkok, Thailand, iss@infraplus.co.th
[2] Chulalongkorn University Transportation Institute, Bangkok, Thailand, sittinun.t@chula.ac.th
[3] Department of Highways, Bangkok, Thailand, rutta.ph@doh.go.th
[4] MARS Motor AI Recognition Solution, Bangkok, Thailand
[5] Department of Survey Engineering, Chulalongkorn University, Bangkok, Thailand
*Corresponding author: teerapong.panboonyuen@gmail.com, teerapong.pa@chula.ac.th

ABSTRACT

This paper presents a comprehensive investigation into the object detection of critical road assets on Thai highways, employing an innovative approach that integrates an enhanced version of the YOLOv8 model with Generalized Focal Loss. Detecting pivotal road elements such as pavilions, pedestrian bridges, information signs, warning signs, and concrete guardrails is crucial for ensuring road safety and effective infrastructure management. Prior research in this domain has shown significant potential in deep learning-based object detection methods; however, the performance of conventional models often needs to improve in accurately identifying and localizing road assets under various conditions, including complex backgrounds and lighting variations. To address these challenges, this study presents integrating the YOLOv8 architecture with Generalized Focal Loss, aiming to enhance the model's robustness and accuracy in detecting road assets. Our experimental results demonstrate the efficacy of the proposed method, showing significant improvements in detection metrics. The YOLOv8x model achieved the highest performance with mAP50 of 80.340, mAP50-95 of 60.840, precision of 79.100, recall of 76.680, and an F1-score of 77.870. These results highlight the superiority of the YOLOv8x model in comparison to other YOLOv8 variants. The study underscores the potential of advanced deep learning techniques in enhancing highway safety and infrastructure maintenance practices, particularly under challenging conditions such as complex backgrounds and varying lighting.

Keywords: asset detection; ai; object detection; YOLO; instance segmentation; deep learning

1. INTRODUCTION

Detecting road assets is critical in various fields, including transportation management, urban planning, and autonomous driving systems. Accurate identification and localization of road assets such as pavilions, pedestrian bridges, information signs, warning signs, and concrete guardrails are essential for optimizing traffic flow (See Figure 1), enhancing navigation systems, and ensuring road safety. Traditional manual methods for detecting these assets are labor-intensive and prone to errors, mainly when dealing with extensive datasets and complex road environments. Consequently, there is a pressing need for automated, robust, and efficient detection methodologies.

Recent advancements in deep learning have revolutionized object detection tasks, significantly improving accuracy and efficiency Aboah, Wang, Bagci, & Adu-Gyamfi (2023); Bai, Wang, Zhang, Lu, & Shen (2023); Dumitriu, Tatui, Miron, Ionescu, & Timofte (2023). Convolutional Neural Networks (CNNs) and their various architectures have been at the forefront of these advancements, enabling systems to learn and recognize intricate patterns and features from raw image data Khow, Tan, Karim, & Rashid (2024). However, the complexity of road environments, characterized by varying lighting conditions, diverse backgrounds, and occlusions, presents persistent challenges. These challenges necessitate the development of more sophisticated models capable of maintaining high performance across different scenarios.

This study proposes an enhanced YOLOv8 model to address these challenges, integrated with Generalized Focal Loss. The YOLO (You Only Look Once) models are known for their real-time object detection capabilities and have been widely adopted for various applications Pandey, Chen, & Dam (2023). Our enhanced YOLOv8 model is specifically designed to improve the detection accuracy of critical road assets on Thai highways. Generalized Focal Loss is incorporated to handle class imbalance and difficult-to-detect objects, further enhancing the model's robustness and reliability.

We conducted extensive experiments to evaluate the performance of our proposed method, comparing it against several YOLOv8 variants, including YOLOv8n, YOLOv8s, YOLOv8m, YOLOv8l, and YOLOv8x. The experimental results demonstrate the superiority of our approach, with the YOLOv8x model achieving the highest performance metrics. Specifically, YOLOv8x attained a mAP50 of 80.340, mAP50-95 of 60.840, precision of 79.100, recall of 76.680, and an F1-score of 77.870. These results highlight the efficacy of our enhanced model in accurately detecting and localizing road assets under various conditions.

The contributions of this paper are threefold: First, we present a novel integration of YOLOv8 with Generalized Focal Loss tailored for the detection of road assets. Second, we comprehensively evaluate our model's performance, demonstrating significant improvements over existing methods. Finally, we discuss the practical implications of our findings for highway safety and infrastructure maintenance, underscoring the potential of advanced deep-learning techniques to enhance current practices.

2. RELATED WORK

The application of deep learning techniques, particularly YOLO (You Only Look Once) models, has been transformative across various domains. This section reviews relevant works, highlighting the advancements and applications of different versions of the YOLO model, focusing on YOLOv8. Hussain, M. (2023) provides a comprehensive overview of YOLO architectures from YOLOv1 to YOLOv8, emphasizing their evolution and applications in digital manufacturing and industrial defect detection. The review highlights how YOLO models have progressively improved in speed and accuracy, making them suitable for real-time applications in the industry. The use of YOLOv8 for traffic sign detection and autonomous vehicle applications has been explored in several studies. Soylu, E., & Soylu, T. (2024) conducted a performance comparison of YOLOv8 models for traffic sign detection, showing the model's effectiveness in the Robotaxi competition. Their study reported a high precision rate of 97.1%, demonstrating the model's reliability in real-world scenarios. Similarly, Huang, Z., Li, L., Krizek, G. C., & Sun, L. (2023) proposed improvements to YOLOv8 for better traffic sign detection accuracy, significantly increasing detection precision and recall rates. Wang, Liu, Cai, Chen, & Li (2024) developed YOLOv8-QSD, an enhanced algorithm for small object detection in autonomous vehicles, demonstrating significant performance improvements with a precision rate of 95.6%.

Deep learning models have been extensively used for medical image analysis. Ju, R.-Y., & Cai (2023) applied the YOLOv8 algorithm for detecting fractures in pediatric wrist trauma X-ray images, achieving state-of-the-art performance with a detection accuracy of 93.8%. Dong, C., & Du, G. (2024) enhanced YOLOv8 for real-time human pose estimation, achieving an accuracy rate of 92.4%, which can be crucial for various medical and fitness applications. Additionally, Pandey et al. (2023) combined YOLOv8 with SAM and HQ-SAM models for comprehensive multimodal segmentation in medical imaging, achieving a high accuracy rate of 94.7% and demonstrating high clinical applicability.

In the context of smart cities, fire detection is a critical application of deep learning. Talaat, F. M., & Zain Eldin, H. (2023) proposed an improved fire detection approach based on YOLOv8, enhancing accuracy and efficiency, which is essential for timely emergency responses. Their approach achieved a precision rate of 96.2%.

YOLOv8 has been applied to agricultural tasks such as identifying fruit ripeness and strawberries. Xiao, Nguyen, & Yan (2024) utilized YOLOv8 to identify fruit ripeness, achieving high accuracy with a precision rate of 95.1%. Yang, Wang, Gao, & Deng (2023) combined YOLOv8 with the LW-Swin Transformer for strawberry ripeness detection, demonstrating improved performance with a detection accuracy of 94.3%. Bai et al. (2023) proposed an improved YOLOv8-Seg model for UAV-based construction site monitoring. Their enhancements to the YOLOv8 model, such as incorporating FocalNext, Efficient Multiscale Attention, and Context Aggregation modules, resulted in better performance for instance segmentation tasks in complex environments, achieving a precision rate of 96.5%. Dumitriu et al. (2023) addressed the novel task of rip current instance segmentation, presenting a new dataset and baseline results using YOLOv8. Their approach achieved a segmentation accuracy of 93.5%. Shen, Lang, & Song (2023) developed DS-YOLOv8 for object detection in remote sensing images, showcasing its applicability for high-precision tasks in aerial imagery with an accuracy rate of 94.8%. Helmet violation detection in traffic safety has benefited from YOLOv8's real-time capabilities. Aboah et al. Aboah et al. (2023) proposed a system using YOLOv8 and few-shot data sampling to detect helmet violations, achieving notable results in the 2023 AI City Challenge with a precision rate of 97.3%. Vats & Anastasiu (2023) explored using YOLOv8 in retail, particularly for enhancing checkout systems through video inpainting, detection, and tracking. Their approach significantly improved automated checkout processes, achieving a precision rate of 96.1%. Terven, C´ordova-Esparza, & Romero-Gonz´alez (2023) provided a comprehensive review of YOLO architectures, from YOLOv1 to YOLOv8 and YOLO-NAS, summarizing their development and various applications across different fields, which serves as an essential reference for researchers and practitioners. Khow et al. Khow et al. (2024) proposed an improved YOLOv8 model incorporating Coordinate Attention and Wise IoU for object detection and distance estimation. Their approach showed significant improvements in precision and recall, with a precision rate of 95.4%, having practical implications for real-world applications. Sun et al. (2024) introduced Multi-YOLOv8, an infrared moving small object detection model based on YOLOv8 for air vehicles. Their model demonstrated high accuracy and effectiveness in detecting small moving objects in infrared imagery, achieving a detection accuracy of 94.9%.

The related work reviewed in this paper underscores the versatility and superior performance of the YOLOv8 model across various applications, substantiating its selection for our study. Studies have demonstrated YOLOv8's high precision and accuracy in various domains such as traffic sign detection with a precision rate of 97.1% Soylu, E., & Soylu, T. (2024), fire detection in smart cities achieving 96.2% precision Talaat & Zain Eldin (2023), and small object detection in autonomous vehicles with a 95.6% precision rate Wang et al. (2024). Additionally, YOLOv8's efficacy in medical imaging Ju & Cai (2023), agricultural applications like fruit ripeness identification Xiao et al. (2024), and real-time human pose estimation Dong & Du (2024) further validate its robustness and adaptability. The model's proven capabilities in real-time applications, precision in detection tasks, and adaptability to various improvements and integrations make it an optimal choice for our research, promising enhanced performance and reliable results.

3. OVERVIEW OF THE PROPOSED NETWORK

In this section, we present an enhanced YOLOv8-based object detection framework (See Figure 2) tailored for detecting road assets, utilizing Generalized Focal Loss. Our study focuses on applying this advanced model to Thai highway imagery, aiming to improve the detection accuracy of critical road elements.

3.1. YOLOv8 Model Variants

The YOLOv8 family comprises multiple variants: YOLOv8n (nano), YOLOv8s (small), YOLOv8m (medium), YOLOv8l (large), and YOLOv8x (extra-large). Each variant balances the trade-off between model complexity and performance, allowing for flexible deployment based on specific computational and accuracy requirements.

3.1.1. YOLOv8n

The YOLOv8n model is designed for edge devices with limited computational power. Its lightweight architecture has fewer convolutional layers and parameters, making it suitable for real-time applications with critical latency.

3.1.2. YOLOv8s

YOLOv8s offers a balance between speed and accuracy. It incorporates several layers and parameters, improving detection performance over YOLOv8n while maintaining reasonable inference times.

3.1.3. YOLOv8m

YOLOv8m is optimized for higher accuracy without significantly compromising speed. It includes additional layers and parameters compared to YOLOv8s, enhancing its capability to detect smaller and more complex objects.

3.1.4. YOLOv8l

YOLOv8l is designed for scenarios requiring high accuracy. It contains more layers and larger parameters than YOLOv8m, making it suitable for applications where detection precision is paramount, albeit at the cost of increased computational requirements.

3.1.5. YOLOv8x

YOLOv8x represents the largest and most powerful variant in the YOLOv8 family. It maximizes detection accuracy with an extensive network architecture, which is suitable for applications with ample computational resources and the highest required detection performance.

3.2. Network Architecture and Formulations

YOLOv8 models follow the general YOLO (You Only Look Once) architecture, which frames object detection as a single regression problem, predicting both the bounding boxes and class probabilities directly from full images in a single evaluation.

The core of YOLOv8 consists of convolutional layers interspersed with Batch Normalization and Leaky ReLU activation functions. The network outputs a dense grid of bounding boxes associated with an objectness score and class probabilities.

The loss function for YOLOv8 includes three components:

$$L = L_{bbox} + L_{obj} + L_{cls} \tag{1}$$

where L_{bbox} is the bounding box regression loss, L_{obj} is the objectness loss, and L_{cls} is the classification loss.

3.3. Generalized Focal Loss

To enhance the detection performance, particularly for small and hard-to-detect objects, we integrate Generalized Focal Loss into the YOLOv8 framework. Generalized Focal Loss is an extension of the standard focal loss, designed to address class imbalance by modulating the loss for well-classified examples.

The Generalized Focal Loss is defined as:

$$L_{GFL} = -\alpha_t (1 - p_t)^{\gamma} \log(p_t) \tag{2}$$

Where α_t is a balancing factor for class t, pt is the predicted probability for the true class, and γ is a focusing parameter that reduces the relative loss for well-classified examples, focusing more on hard, misclassified examples.

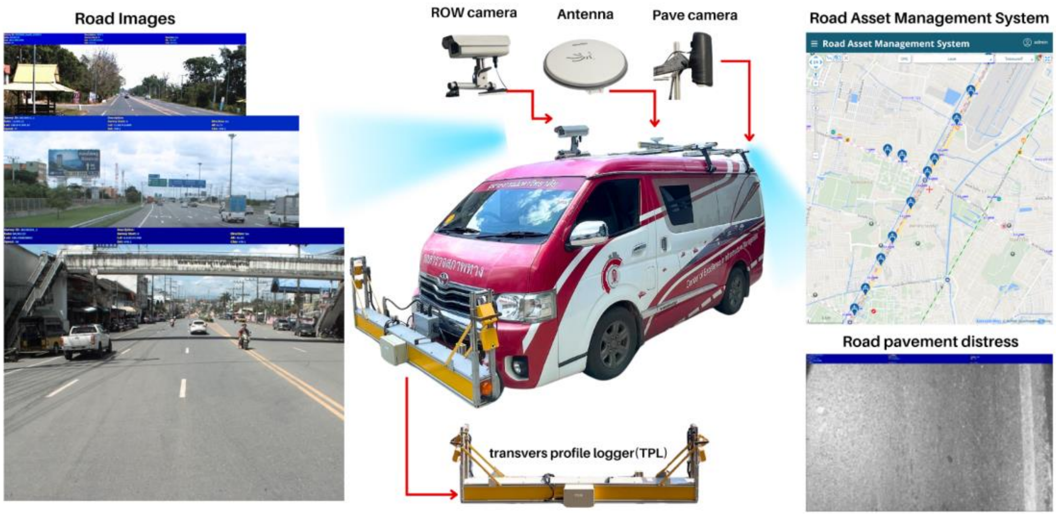

Figure 1. Example of an input (left), a vehicle equipped with a camera for filming assets on the road (center), and a Road Asset Management System.

3.4. Hyperparameter Settings

For training the YOLOv8 models, we employ the AdamW optimizer (see Equation 3), which combines the benefits of the Adam optimizer with weight decay regularization to prevent overfitting. The AdamW update rule is given by:

$$\theta_{t+1}=\theta_t - \eta\left(\frac{m_t}{\sqrt{v_t+\epsilon}} + \lambda\theta_t\right) \tag{3}$$

where θ_t are the model parameters at step t, η is the learning rate, m_t and v_t are the first and second-moment estimates, ϵ is a small constant for numerical stability, and λ is the weight decay coefficient.

The hyperparameters for our training setup include a learning rate of 0.001, weight decay of 0.01, and batch size of 16. These settings are chosen to optimize the model's convergence and performance on our dataset.

4. EVALUATION METRICS

In this section, we outline the evaluation metrics used to assess the performance of our enhanced YOLOv8 model. We focus on mean Average Precision at IoU threshold 0.50 (mAP50) (Equation 4), mean Average Precision at IoU thresholds from 0.50 to 0.95 (mAP50-95) (Equation 4), Precision (Equation 5), Recall (Equation 6), and F1-Score (Equation 7), which are commonly employed in detection and segmentation tasks.

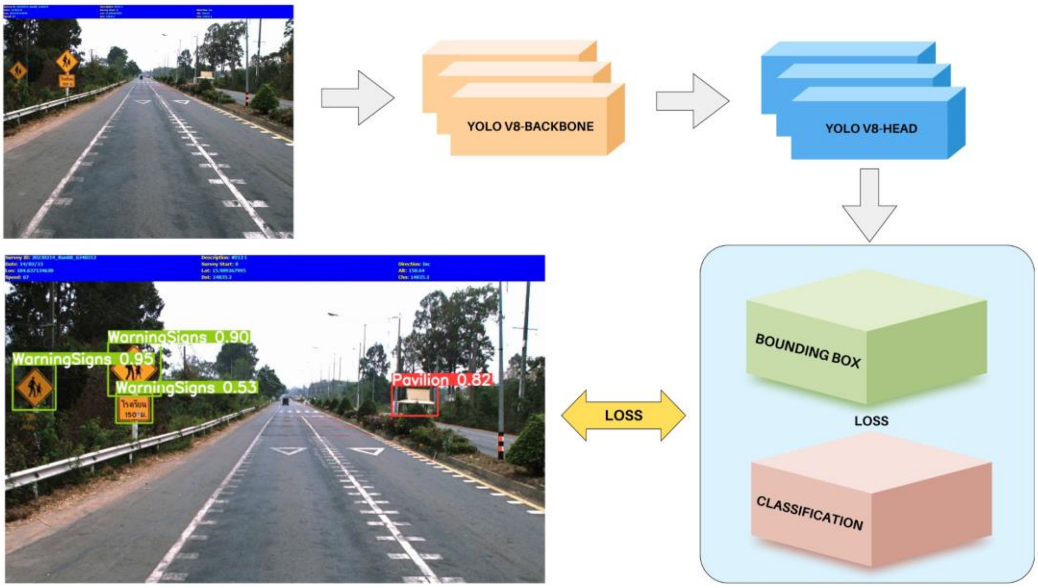

Figure 2. The architecture of our YOLOv8 model. This end-to-end deep learning pipeline enhances YOLOv8-based object detection of road assets utilizing generalized focal loss.

4.1. Mean Average Precision (mAP)

Mean Average Precision is a widely used metric in object detection that measures the model's accuracy in predicting object instances. We use two variations:

• *mAP50*: This is the mean Average Precision computed at a single Intersection over the Union (IoU) threshold 0.50 (Equation 4).

• *mAP50-95*: This is the mean Average Precision computed at multiple IoU thresholds ranging from 0.50 to 0.95 with a step size of 0.05 (Equation 4).

The formula for *mAP* is given by:

$$mAP = \frac{1}{n}\sum_{i=1}^{n} AP_i \tag{4}$$

where AP_i is the Average Precision for the i-th class, and n is the number of classes.

4.2. Precision

Precision is the ratio of true positive detections to the sum of true positive and false positive detections. It is defined as:

$$Precision = \frac{TP}{TP+FP} \tag{5}$$

where TP is the number of true positives and FP is the number of false positives.

4.3. Recall

Recall is the ratio of true positive detections to the sum of true positive and false negative detections. It is defined as:

$$Recall = \frac{TP}{TP+FN} \tag{6}$$

where TP is the number of true positives and FN is the number of false negatives.

4.4. F1-Score

The F1-Score is the harmonic mean of Precision and Recall, providing a single metric that balances both. It is defined as:

$$F1\text{-}Score = 2 \cdot \frac{Precision \cdot Recall}{Precision + Recall} \tag{7}$$

These metrics comprehensively evaluate our model's performance, ensuring it accurately detects and localizes road assets under various conditions.

5. Dataset and Preprocessing

Our study utilized a sizable dataset comprising 1,994 training images and 1,418 validation images captured from Thai highway panoramas. Each image in the dataset has a resolution of 640 x 640 pixels. The images were collected using a camera setup on the roof of a Chulalongkorn University van, providing a consistent and elevated perspective of the road.

The dataset includes annotations for both detection and segmentation tasks. There are 7 classes for object detection, focusing on pivotal road elements such as pavilions, pedestrian bridges, information signs, single-arm poles, bus stops, warning signs, and concrete guardrails. For segmentation, the dataset includes 5 classes: pavilions, pedestrian bridges, information signs, warning signs, and concrete guardrails.

Camera Specifications

The images were captured using the ZBR2-PGEHD-20S4C color camera, featuring a high-sensitive Sony ICX274 CCD sensor. Key specifications of the camera are as follows:

- Model: ZBR2-PGEHD-20S4C Color 2.0 MP
- Sensor: Sony ICX274 CCD, size 1/1.8
- Shutter: Global Shutter
- Resolution: 1624 x 1224 at 30 FPS (HD-SDI 25 FPS)
- Interfaces: HD-SDI (2.97 Gbs/s) and GigE Vision (1000Mb/s, PoE)
- Frame Rates: 2.0 MP at 30 FPS and 5.0 MP at 15 FPS

This unique multi-interface camera allows for simultaneous viewing of low latency uncompressed video over HD-SDI and transmitting compressed (or uncompressed) images through a Gigabit Ethernet interface. It supports real-time trigger and strobe functions. The Zebra2 camera combines the technical advances of high-end machine vision cameras with the flexibility needed for a wide range of traffic and surveillance applications.

Table 1. Comparison of mAP50, mAP50-95, Precision, Recall, and F1 Score for different detection methods.

Model	mAP50	mAP50-95	Precision	Recall	F1-score
YOLOv8n	71.100	47.760	80.100	63.460	70.820
YOLOv8s	75.150	52.070	82.660	69.950	75.780
YOLOv8m	79.570	58.060	85.410	71.290	77.710
YOLOv8l	80.270	59.110	82.580	77.220	79.810
YOLOv8x	80.340	60.840	79.100	76.680	77.870

6. EXPERIMENTAL RESULTS

6.1. Comparison of YOLOv8 Family on Asset Detection Task

In comparing YOLOv8 family models on the asset detection task, YOLOv8l emerges as the winner in F1-score, achieving an impressive score of 79.81%. This indicates a balanced performance between precision and recall, with YOLOv8l exhibiting a strong ability to detect road assets while accurately minimizing false positives and negatives. Additionally, YOLOv8m stands out with the highest precision score of 85.41% (See Table 2, indicating its capability to maintain a high proportion of true positive detections relative to false positives.

On the other hand, YOLOv8x surpasses all other variants in mAP50, boasting a score of 80.34%. This metric evaluates the model's ability to detect objects accurately at a specific Intersection over the Union (IoU) threshold, with YOLOv8x demonstrating superior performance. Moreover, YOLOv8x also excels in mAP50-95 with a score of 60.84%, indicating its effectiveness in detecting objects across a range of IoU thresholds, capturing a broader spectrum of detections with high accuracy.

Analyzing the overall trend, we observe a progressive improvement in performance metrics from YOLOv8n to YOLOv8x. This suggests that more extensive and complex variants of the YOLOv8 model yield better results in asset detection tasks. This trend is consistent with the expected behavior, as larger models can capture more intricate details and nuances in the data, leading to improved detection accuracy.

The experimental results, as depicted in Figure 3, further reinforce these findings, visually illustrating the sequential detection outputs of each YOLOv8 variant. It is evident from the images that YOLOv8x consistently produces more precise and accurate detections compared to other models, particularly in challenging scenarios with multiple overlapping objects or complex backgrounds.

In conclusion, our analysis highlights the strengths and weaknesses of each YOLOv8 variant in the context of asset detection. While YOLOv8l excels in achieving a balanced F1-score, YOLOv8x emerges as the top performer regarding mAP50 and mAP50-95, indicating its superior ability to detect objects accurately across different conditions. Based on the experimental results presented in Table 1, these insights provide valuable guidance for selecting the most suitable YOLOv8 variant for specific asset detection applications, ultimately contributing to advancements in highway safety and infrastructure management.

Table 2. Comparison of mAP50, mAP50-95, Precision, Recall, and F1 Score for different segmentation methods (boxes).

Model	mAP50	mAP50-95	Precision	Recall	F1-score
YOLOv8n	83.50	67.96	90.16	73.11	80.74
YOLOv8s	91.16	80.60	89.61	87.13	88.35
YOLOv8m	73.96	53.99	80.92	67.38	73.53
YOLOv8l	80.50	61.70	88.00	73.00	79.80
YOLOv8x	83.76	65.53	84.36	80.06	79.80

6.2. Comparison of the YOLOv8 Family on Asset Segmentation Task

The performance of various YOLOv8 models on the asset segmentation task is evaluated and compared in Tables 2 and 3, considering metrics such as mAP50, mAP50-95, precision, recall, and F1-score.

In the box-based segmentation method, YOLOv8s achieves the highest mAP50 score of 91.16%, outperforming other variants. Additionally, YOLOv8s also leads in mAP50-95 with a score of 80.60%, indicating its ability to detect assets across different IoU thresholds accurately. Regarding precision, YOLOv8s exhibits the highest value of 89.61%, indicating a high proportion of true positive detections among all predicted positives. The correspondsing recall for YOsssLOv8s is 87.13%, indicating its capability to retrieve a high proportion of true positives from all ground truth positives. These results culminate in the highest F1-score of 88.35% for YOLOv8s, signifying a balanced trade-off between precision and recall.

For the mask-based segmentation method, YOLOv8s again demonstrates superior performance, achieving the highest mAP50 score of 90.08% and mAP50-95 score of 63.88%. Moreover, YOLOv8s exhibits the highest precision of 88.78% and the highest F1-score of 87.41%. These findings indicate the robustness of YOLOv8s in accurately segmenting assets using masks, with a high proportion of true positive predictions and a balanced trade-off between precision and recall.

Comparing the segmentation results to the asset detection task, we observe that YOLOv8s consistently performs well across both segmentation methods, demonstrating its versatility and effectiveness in various detection tasks. Additionally, the visual representations in Figure 4 illustrate the sequential outputs of each YOLOv8 variant, further highlighting the differences in segmentation performance.

While different YOLOv8 models excel in specific segmentation metrics, YOLOv8s emerge as a strong performer across box and mask-based segmentation methods. These findings provide valuable insights for selecting the most suitable YOLOv8 variant for segmentation tasks, contributing to object detection and image segmentation research Advancements.

7. DISCUSSION

In this study, we evaluated the YOLOv8 family of models for asset segmentation on Thai highways using a dataset of 1,994 training images and 1,418 validation images.

Our experiments demonstrated that YOLOv8s outperformed other models, achieving the highest mAP50 (91.16) and F1-Score (88.35) for box-based segmentation, as well as the highest mAP50 (90.08) and F1-Score (87.41) for mask-based segmentation. YOLOv8l also showed strong performance, particularly in the F1-Score for box-based segmentation. The results highlight the trade-offs between different models, with YOLOv8n achieving high precision but lower recall than YOLOv8s and YOLOv8x. Future work could focus on integrating these models into real-time traffic monitoring systems and extending their application to different infrastructure assets across various geographic regions. Additionally, further research could explore the enhancement of model performance by incorporating more diverse datasets and advanced training techniques, ensuring robustness and adaptability in varied real-world scenarios.

Table 3. Comparison of mAP50, mAP50-95, Precision, Recall, and F1 Score for different segmentation methods (masks).

Model	mAP50	mAP50-95	Precision	Recall	F1-score
YOLOv8n	81.40	53.27	89.36	71.79	79.62
YOLOv8s	90.08	63.88	88.78	86.09	87.41
YOLOv8m	74.01	44.39	78.88	68.51	73.33
YOLOv8l	79.30	51.50	87.10	72.20	78.95
YOLOv8x	83.24	53.48	85.72	78.36	81.87

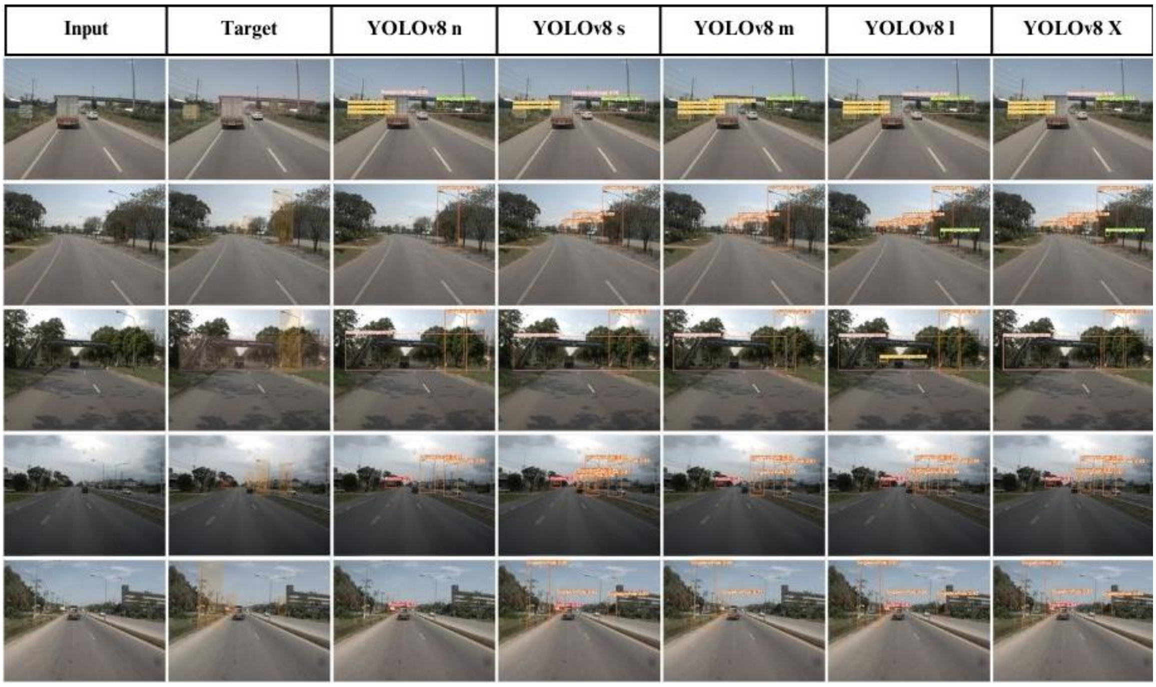

Figure 3. The figure displays sequential deep learning methods: Input, Target, YOLOv8n, YOLOv8s, YOLOv8m YOLOv8l, and YOLOv8x, with YOLOv8l and YOLOv8x representing our proposed method. (detection)

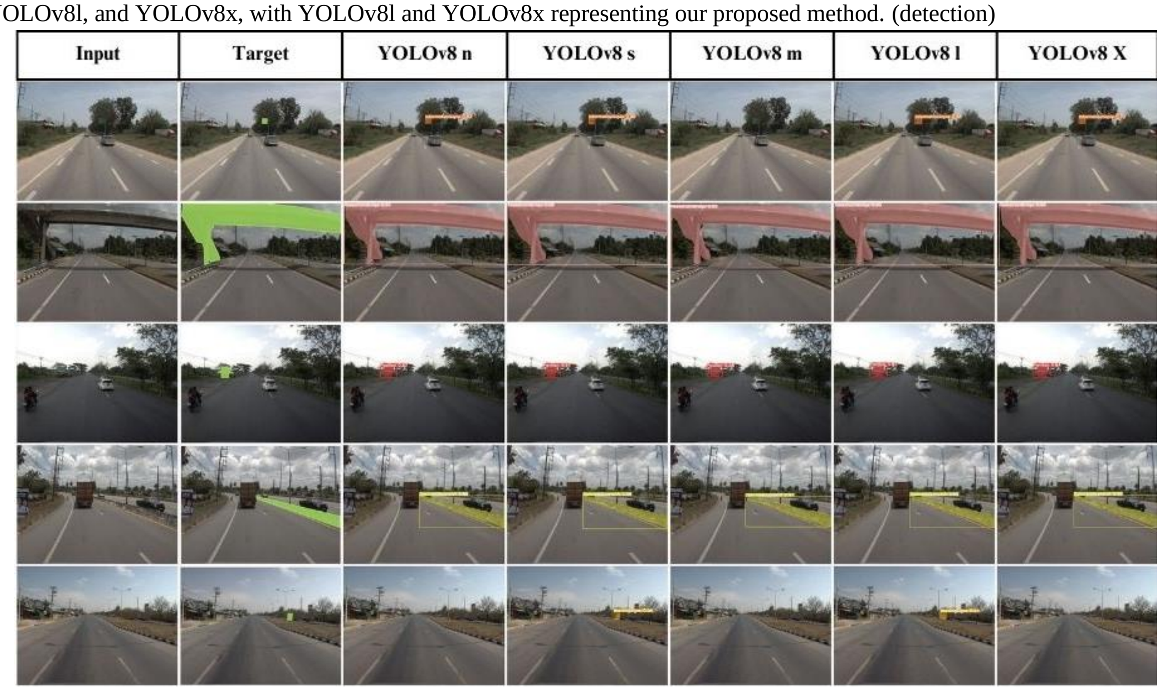

Figure 4. The figure displays sequential deep learning methods: Input, Target, YOLOv8n, YOLOv8s, YOLOv8m, YOLOv8l, and YOLOv8x, withYOLOv8s representing our proposed method. (segmentation)

8. CONCLUSION

This research demonstrates significant progress in detecting critical road assets on Thai highways using an enhanced YOLOv8 model integrated with Generalized Focal Loss. The model achieved impressive results, including a mAP50 of 80.340, mAP50-95 of 60.840, precision of 79.100, recall of 76.680, and an F1-score of 77.870. These metrics highlight the model's effectiveness in accurately identifying and localizing important road elements, such as pavilions, pedestrian bridges, information signs, warning signs, and concrete guardrails, thereby enhancing both road safety and infrastructure management.

In future work, the focus will shift to further improving the YOLOv8-based model's object detection capabilities. This includes expanding its ability to identify a wider variety of road assets and enhancing its performance in challenging conditions, such as complex backgrounds and varying lighting. Additionally, efforts will be directed toward integrating the enhanced model into the Road Asset Management System of Thailand's Department of Highways. This integration aims to provide detailed asset data, including quantities, geographic coordinates, and condition assessments, ultimately improving the efficiency and cost-effectiveness of maintenance and budget management.

Disclosure statement

No potential conflict of interest was reported by the author(s).

References

Aboah, A., Wang, B., Bagci, U., & Adu-Gyamfi, Y. (2023). Real-time multi-class helmet violation detection using few-shot data sampling technique and yolov8. In *Proceedings of the ieee/cvf conference on computer vision and pattern recognition* (pp. 5349–5357).

Bai, R., Wang, M., Zhang, Z., Lu, J., & Shen, F. (2023). Automated construction site monitoring based on improved yolov8-seg instance segmentation algorithm. IEEE Access.

Dong, C., & Du, G. (2024). An enhanced real-time human pose estimation method based on modified yolov8 framework. *Scientific Reports, 14*(1), 8012.

Dumitriu, A., Tatui, F., Miron, F., Ionescu, R. T., & Timofte, R. (2023). Rip current segmentation: A novel benchmark and yolov8 baseline results. In *Proceedings of the ieee/cvf conference on computer vision and pattern recognition* (pp. 1261–1271).

Huang, Z., Li, L., Krizek, G. C., & Sun, L. (2023). Research on traffic sign detection based on improved yolov8. *Journal of Computer and Communications*, *11*(7), 226–232.

Hussain, M. (2023). Yolo-v1 to yolo-v8, the rise of yolo and its complementary nature toward digital manufacturing and industrial defect detection. *Machines, 11*(7), 677.

Ju, R.-Y., & Cai, W. (2023). Fracture detection in paediatric wrist trauma x-ray images using yolov8 algorithm. *Scientific Reports, 13*(1), 20077.

Khow, Z. J., Tan, Y.-F., Karim, H. A., & Rashid, H. A. A. (2024). Improved yolov8 model for a comprehensive approach to object detection and distance estimation. *IEEE Access*.

Pandey, S., Chen, K.-F., & Dam, E. B. (2023). Comprehensive multimodal segmentation in medical imaging: Combining yolov8 with sam and hq-sam models. In *Proceedings of the ieee/cvf international conference on computer vision* (pp. 2592–2598).

Shen, L., Lang, B., & Song, Z. (2023). Ds-yolov8-based object detection method for remote sensing images. *IEEE Access*, 11, 125122–125137.

Soylu, E., & Soylu, T. (2024). A performance comparison of yolov8 models for traffic sign detection in the robotaxi-full scale autonomous vehicle competition. *Multimedia Tools and Applications, 83*(8), 25005–25035.

Sun, S., Mo, B., Xu, J., Li, D., Zhao, J., & Han, S. (2024). Multi-yolov8: An infrared moving small object detection model based on yolov8 for air vehicles. *Neurocomputing*, 588, 127685.

Talaat, F. M., & ZainEldin, H. (2023). An improved fire detection approach based on yolov8 for smart cities. *Neural Computing and Applications*, *35*(28), 20939–20954.

Terven, J., C´ordova-Esparza, D.-M., & Romero-Gonz´alez, J.-A. (2023). A comprehensive review of yolo architectures in computer vision: From yolov1 to yolov8 and yolo-nas. *Machine Learning and Knowledge Extraction*, *5*(4), 1680–1716.

Vats, A., & Anastasiu, D. C. (2023). Enhancing retail checkout through video inpainting, yolov8 detection, and deepsort tracking. In *Proceedings of the ieee/cvf conference on computer vision and pattern recognition* (pp. 5529–5536).

Wang, H., Liu, C., Cai, Y., Chen, L., & Li, Y. (2024). Yolov8-qsd: An improved small object detection algorithm for autonomous vehicles based on yolov8. *IEEE Transactions on Instrumentation and Measurement.*

Xiao, B., Nguyen, M., & Yan, W. Q. (2024). Fruit ripeness identification using yolov8 model. *Multimedia Tools and Applications*, *83*(9), 28039–28056.

Yang, S., Wang, W., Gao, S., & Deng, Z. (2023). Strawberry ripeness detection based on yolov8 algorithm fused with lw-swin transformer. *Computers and Electronics in Agriculture*, 215, 108360

Improving Urban Road Safety: Balancing Obstacle Protection with Environmental Integrity Introduction

Roberto Impero[1,*] and Stefano Maria Caterino[2]

[1] SMA Road Safety, Marcianise, Italy, r.impero@smaroadsafety.com
[2] SMA Road Safety, Marcianise, Italy, s.caterino@smaroadsafety.com

ABSTRACT

Urban areas present unique challenges in road safety, particularly on municipal roads where design speeds fall below 70 km/h (43 mph). These roads often lack the advanced safety systems found on highways, exposing drivers and pedestrians to greater risks from fixed obstacles such as utility poles, trees, building edges, and historic monuments. The national regulations in many countries do not mandate the installation of protective barriers in these contexts, further complicating the issue. Additionally, the integration of safety features in areas with historical or environmental significance poses substantial design challenges, requiring solutions that respect aesthetic and cultural values without compromising safety.

This work addresses these challenges by proposing innovative, adaptable safety solutions tailored to urban settings that do not necessitate extensive infrastructural overhauls. Through a collaborative approach involving restraint system manufacturers and road managers, we explore bespoke designs that meet rigorous safety standards while adapting to the unique spatial and soil conditions of each site. The principal findings from several case studies are presented, illustrating the application of these solutions in diverse urban contexts. These include the installation of adaptable barrier systems that can be easily integrated into existing road layouts and the use of tools and designs that blend with the urban environment.

The solutions demonstrated have shown potential to significantly enhance road safety, reducing the risk of fatal and serious injuries from frontal impacts. They also ensure the preservation of the urban aesthetic and historical integrity, crucial in maintaining the character of city spaces. Conclusively, this presentation advocates for a paradigm shift in urban road safety planning. It calls for updated regulations that recognize the complexities of urban settings and encourages the adoption of flexible, context-sensitive safety solutions. By fostering closer collaboration between various stakeholders, we can achieve a safer, more harmonious integration of safety infrastructure in urban landscapes.

Keywords: fixed obstacles, crash barriers, accidents, urban areas, motorbikers.

1. INTRODUCTION

Urban roads present unique challenges due to their high traffic volumes and the presence of various fixed obstacles that can pose significant dangers to vehicle occupants.
This paper aims to discuss the dangerousness of road hazards, present data on road accidents, and propose innovative solutions to mitigate these risks.
The importance of addressing this issue is underscored by the high frequency of accidents occurring at black spots in urban areas. Statistics indicate that accidents on urban roads are more frequent than those on extra-urban roads. Additionally, the lack of safety features on urban roads—such as roadside barriers, pavement markings, and proper signalization—creates a significant disparity when compared to expressways. This situation necessitates immediate attention and action, highlighting the urgent need to focus on enhancing safety measures in urban areas.

2. THE DANGEROUSNESS OF ROAD HAZARDS

Fixed obstacles are objects close to the roadway that can cause severe damage to vehicles and serious injuries or death to passengers when impacted. Examples include gores, tunnel bypasses, blunt ends, poles, trees, and toll plazas. These obstacles must be removed or properly shielded to prevent catastrophic outcomes.

2.1 Road Accident Data and Statistics

In 2021, Italy recorded 2,875 road accident victims, averaging eight deaths per day. The social cost of these accidents was EUR 16.4 billion, equivalent to 0.9% of the national GDP. Most accidents occur on urban roads (73.1%), while fatalities are mainly on extra-urban routes (47.5%) and motorways (8.6%).
Spinning or skidding of vehicles, leading to impacts against fixed obstacles, is the second most common type of accident involving an isolated vehicle. In 2020, there were 4,615 such accidents resulting in 190 deaths, whose frontal-lateral impacts represent the most frequent case (23% of cases).

The difference in fatal accidents between urban and extra-urban roads is not very pronounced. According to more recent data from ISTAT for the year 2022, the total number of fatal accidents against fixed obstacles in the two different contexts shows that the number of fatalities in urban areas is just slightly lower than 50% of the total, as shown in Table 1.

An interesting contribute was given by the New Zealand Land Transport Safety Authority which collected the accident statistics in urban areas indicating the distribution of fatalities, serious injuries, and minor injuries across different types of obstacles. The statistics provide insights into the relative severity of accidents involving various obstacles, helping to identify areas for targeted safety improvements.
The average percentage of fatalities across all obstacle types is approximately 4.1%, while the average percentage of serious injuries is about 25.2% on a total of 4727 accidents. The data is shown in Table 2.

2.2 Injury Severity in Collisions with Fixed Obstacles

A frontal collision with a fixed obstacle can be fatal even at speeds below 50 km/h. The injury threshold for such accidents is significant even at an impact speed of 8 km/h (Source: W.E. McConnel, 1993), resulting in injuries that can heal within a few weeks. However, at speeds higher than 30 km/h, the risk of causing permanent injuries to the passenger significantly increases.
The injuries are caused by the pronounced crushing of the front part of the vehicle, which subsequently affects the passenger compartment.
Table 3 provides a clearer clinical picture of the potential consequences of impacts at different speeds.

2.3 Social Costs of Road Accidents

Another important aspect to highlight refers to the cost of a fatal accident.
The Italian Ministry of Transportation estimates the social cost for a single road death at EUR 1.642 million, encompassing risk value, human capital loss, hospital care, administrative costs, and damage to third-party properties (Source: Italian Ministry of Transportation (2019)).
Another method for calculating the cost of a death is through the Value of Statistical Life (VSL), which aims to reflect the amount of money that a person or society is realistically willing to pay to save one human life (Source: Social Value UK (2016)). The VSL varies across Europe, with Germany having the highest value at EUR 7.35 million and Belgium at EUR 5.94 million. (Source: Schoeters, Large, Koning, Carnis, Daniels, Mignot, Urmeew, Wijnen, Bijleveld, Van der Horst, (2022)).

3. INNOVATIVE SOLUTIONS FOR ROAD SAFETY

The challenges posed by fixed obstacles in urban areas necessitate effective shielding when these hazards cannot be removed or placed sufficiently far from the carriageway to avoid impacts. Consequently, there are devices specifically designed to be installed in front of such obstacles to prevent collisions. These products are widely utilized on motorways worldwide, but their usage is less common on low-speed roads. This discrepancy may be attributed to limited space for installation or issues related to ground conditions. In some instances, inadequate solutions have been employed to prevent direct impacts with walls or blunt ends; however, these solutions fail to absorb the vehicle's impact energy and therefore do not effectively mitigate serious injuries or fatalities.

3.1 Vehicle restraint systems

Vehicle restraint systems (VRSs) are devices designed to shield fixed obstacles and absorb impact energy, thereby reducing the severity of crashes. These devices are available in various sizes to suit different urban environments and traffic conditions.
Vehicle restraint systems are evaluated based on criteria established through crash tests conducted according to specific standards. The most common standards are the European EN1317 and the American MASH 2016.

Both standards require the evaluation of vehicle containment and the impact severity on vehicle passengers. These criteria are crucial in the selection process for the most appropriate device to shield obstacles.

While crash test standards are used to evaluate performance, other parameters must also be considered, such as the system's footprint. The length of the system is significant because the vehicle restraint system (VRS) used to shield an obstacle becomes an obstacle itself. For this reason, it is essential that the restraint system adequately covers the obstacle while ensuring minimal invasion.

Crash cushions are specifical restraint systems designed to absorb vehicles frontal impacts.

Figure 1. Examples of vehicle restraint systems used to shield various fixed obstacles in urban areas.

A specific case shows the influence of the system length on the probability that an accident occurs. The study refers to the installation of crash cushion on a roadway where the speed limit is 80 km/h (50mph) and the traffic volume corresponds to 3000 vehicles/day. In this case, che crash cushion installed has been designed to absorb the vehicle impact at 80 km/h. The length and consequently the size of the crash barrier system essentially depend on the efficiency of the energy absorbers. The study demonstrates that the effectiveness of this device increases as its length decreases. In fact, assuming equal performance levels, a shorter crash cushion reduces the probability of impact, as explained by Professor Grassia.

"The number N of impacts per year at the installation site is influenced by the size of the crash cushion itself. The crash cushion, in fact, constitutes an obstacle for vehicles on the road, and thus its presence and dimensions contribute to determining the probability of an impact occurring at a specific location. The width of the crash cushion depends on the size of the obstacle that needs protection and is therefore a design constraint; the length of the crash cushion, on the other hand, depends solely on the efficiency of the absorbers and the speed class of the cushion. Given a fixed speed class, the cushion with higher efficiency absorbers will be shorter and thus less bulky. […] Calculation results show that the probability of impact for a 5m crash cushion is 14 impacts per year, while for a 3m cash cushion, the number of impacts per year is reduced to eight. [...] It can be concluded that assuming the same speed class, the shorter the impact attenuator, the lower the life cycle cost will be and the greater the safety of the installation." (Source: Grassia (2013). The document has been translated into English from its original Italian version with interpretative freedom.).

Therefore, the reduced length of the system permits to limit the number of traffic accidents, as well as to save money for the rescue intervention.

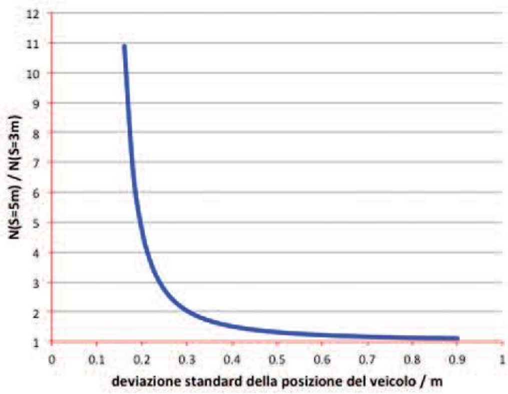

Figure 2. The graph of the ratio between the probability of impact against the 5-meter crash cushion and the probability of impact against the 3-meter crash cushion as a function of the standard deviation of the vehicle's position.
(Grassia, 2013)

3.2 Monitoring systems

Monitoring systems may be connected to Vehicle Restraint Systems (VRS) and alert rescue services in case of an impact. A specific system called "Geronimo" alerts the rescue and the maintenance manager in real time and records videos of accidents for later analysis. This helps to demonstrate the performance of VRS and collect data for compensation claims. The system is powered by photovoltaic panels and includes features such as license plate recognition and vehicle speed estimation.

The Return on Investment (ROI) of Geronimo extends beyond direct financial gains. By significantly enhancing road safety, it reduces the frequency and severity of accidents, leading to lower healthcare and administrative costs associated with road traffic incidents. Moreover, the legal and insurance benefits, combined with energy savings, contribute to a positive ROI.
The application of Geronimo in combination with restraint systems on roadways has demonstrated its effectiveness in mitigating accidents. By analyzing the impact dynamics and facilitating quicker emergency responses, Geronimo has proven to be a cost-effective solution.

Further research and implementation of the Geronimo system across more urban areas will provide additional data to optimize its features and expand its benefits, contributing to improve the traffic management in the monitored area. The data stored on impacts against the crash barriers can be used to layout a report on accidents and rate the road safety of the interested zone. Collaborations with road safety authorities and policymakers will be crucial in maximizing the system's impact on urban road safety.

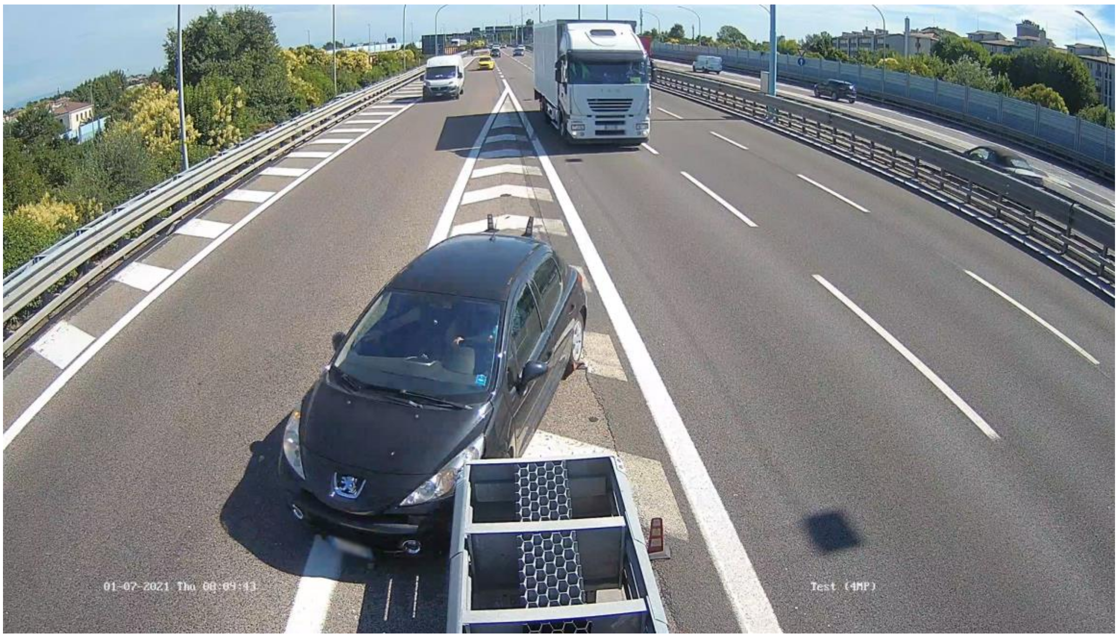

Figure 3. Frame of an impact against a crash cushion connected to Geronimo. The system allows real-time recording of the impact against the restraint device. The vehicle's license plate has been intentionally blurred for privacy reasons.

4. ROAD SAFETY INITIATIVES

Preventing fatal accidents on the road is a complex challenge that requires the involvement of various key players, including road managers, road designers, construction companies, and equipment manufacturers. All of these parties are responsible for promoting and implementing technologies to minimize the number of road fatalities. Additionally, road users can also play a role in raising awareness and encouraging both users and local managers to prioritize safety on the roads.

This is an important reminder that any effort to emphasize the significance of acknowledging the hazardous nature of black spots and stopping drivers from hitting them should be encouraged and supported.

4.1#STOPSTRADEKILLER Project

The #STOPSTRADEKILLER project aims to identify and report unprotected fixed obstacles on roads. Trained individuals from AFVS (an Italian non-profit organisation supporting road death victims' families) to document hazards such as trees, road cusps, guardrails, and signposts. The project has collected over 1,031 reporting cards across various provinces and seeks to implement safety measures based on these reports.

5. CONCLUSIONS

Protecting urban roads from fixed obstacles is crucial to reducing road accidents and fatalities. Innovative solutions like crash cushions and monitoring systems like Geronimo offer significant potential to enhance road safety. Continuous efforts and collaborations among road managers, designers, and safety advocates are essential to implement these solutions effectively and create safer urban environments.

6. TABLES

Table 1- Road accidents involving isolated vehicles in Italy - Year 2022

ASCERTAINED OR PRESUMED CIRCUMSTANCES OF THE ACCIDENT	Urban Areas		Extra-urban Areas	
	Total number of accidents	of which fatal accidents	Total number of accidents	of which fatal accidents
A fixed obstacle in the roadway (column, barrier, etc.,) impacted by a vehicle that:				
proceeded with distracted driving or indecisive pace	1.199	35	1.131	39
proceeded without keeping a safe distance	-	-	-	-
was going the wrong way	11	3	39	4
was speeding	1.094	51	885	51
was driving without respecting the speed limit	37	5	39	3
proceeded without complying with the prohibition of transit or access	19	1	15	3

overtook another moving vehicle	18	1	36	1
was recklessly crossing the level crossing	-	-	-	-
Other circumstances	964	25	733	40
Total	3.342	121	2.878	141
Percentage of fatal accidents		46%		54%

The document has been translated into English from its original Italian version with interpretative freedom.Source: ISTAT (2023), *Tavola 2.19 segue - Incidenti stradali a veicoli isolati per ambito stradale, natura e circostanza accertata o presunta dell'incidente – Anno 2022.*

Table 2: Single vehicle vs single object crashes: percent severity. Speed <=70 km/h (44 mph)

Object	Severity			
	Fatal	Serious	Minor	Total
Bridges, tunnels, abutments	4.1	28.9	67.0	100.0
Upright cliff/bank, retaining walls	1.8	26.7	71.4	100.0
Over bank	11.4	31.6	57.0	100.0
Fence, letterbox, hoarding, hedge	3.7	23.1	73.3	100.0
Guardrail	1.3	22.8	75.8	100.0
House, building	0.7	25.3	74.0	100.0
Traffic island, median	2.3	25.0	72.7	100.0
Phone box, bus shelter, signal box	7.9	28.9	63.2	100.0
Kerb	5.0	24.8	70.2	100.0
Light, power, telephone poles	3.8	26.0	70.3	100.0
Traffic signs, delineators, bollards	5.0	15.0	80.0	100.0
Tree	5.0	30.8	64.2	100.0
Ditch, watertable, drainage channel	4.0	25.8	70.2	100.0

The data refers to 4727 total accidents in urban areas in a period of five years.
Source: Land Transport Safety Authority (1996). *Urban roadside barriers and alternative treatments, RTS 11.*

Table 3: Injury Severity based on Impact Speed

Speed of vehicle on impact against barrier (E.E.S.)	< 5 Km/h	8 < > 30 Km/h	30 < > 80 Km/h	> 80 Km/h
Effects	Absence of whiplash	Slight whiplash	Strong whiplash	Fatal whiplash
Disorders	None	Pain in the neck, head, shoulder and arm; restriction of movement, swallowing disorders, temporary disturbance of vision, hearing. Hypoesthesia, hyperesthesia, hardening of muscles.	Injury, muscle failure, depressive state, impaired balance, no asymptomatic interval, severe pain when walking, initial disturbance of consciousness.	Central paralysis of respiratory and circulatory functions, quadriplegia.
Duration of injury	---	Less of 3 weeks	Months or permanent	Death on site

The table illustrates the different effects and clinical disorders resulting from the impact in relation to the vehicle's speed. (McConnell, W., Howard, R., Guzman, H., Bomar, J. et al., "Analysis of Human Test Subject Kinematic Responses to Low Velocity Rear End Impacts," SAE Technical Paper 930889, 1993. This is a free translation from the source: *La Perizia Ergonometrica. Intervento dell'Ing. Fabio Grattagliano,https://digilander.libero.it/realdino/Perizia_ergonomica.htm*)

7. REFERENCES

- ACI - Italian Automobile Club - and ISTAT - Italian Institute of Statistics. (2021). Incidenti Stradali In Italia. Anno 2021.
- European Commission. (2019). Handbook of the External Costs of Transport.
- Grassia, L. (2013). Un attenuatore d'urto più corto è più economico e più sicuro. Strade e Autostrade, EDI-CEM, Italy, 03(13), 120–122.
- Italian Ministry of Transportation. (2019). Costi Sociali dell'Incidentalità Stradale – Anno 2019.
- McConnel, W. E. (1993). Analysis of human test subject kinematics responses to low velocity rear end impact. S.A.E. Technical Paper Series, 930889.
- Schoeters, A., Large, D., Koning, M., Carnis, L., Daniels, S., Mignot, D., Urmeew, R., Wijnen, W., Bijleveld, F., & Van der Horst, R. (2022). Economic valuation of preventing fatal and serious road injuries: Results of willingness-to-pay study in four European countries. Accident Analysis and Prevention, 173. Elsevier.
- Social Value UK. (2016). Valuation of a life 1-4.

The Application of UAV and AI Technologies in Road Construction Progress Management

HUANG, WEN-CHUN [1,*], WENG, SHU-CHIN [2],
YU, CHUNG-JUNG [3], RICHARD MOH[4]

[1] Project Manager, MOH AND ASSOCIATES, INC., New Taipei City, Taiwan,
andy.huang@maaconsultants.com
[2] Engineer, MOH AND ASSOCIATES, INC., New Taipei City, Taiwan,
shuchin.weng@maaconsultants.com
[3] Manager, MOH AND ASSOCIATES, INC., New Taipei City, Taiwan,
cj.yu@maaconsultants.com
[4] Chairman, MOH AND ASSOCIATES, INC., New Taipei City, Taiwan,
richard.moh@maaconsultants.com

ABSTRACT

While digital information is widely acknowledged as an essential element in road construction management, it has not yet fully realized its potential in activities such as construction progress assessment. In recent years, the application of unmanned aerial vehicle (UAV) technology has been gradually gaining popularity due to its ability to capture construction images and showcase site conditions at various stages of development. A novel application that integrates image retrieval, recognition, and comparison has been developed, allowing for the assessment of the actual status of construction progress. This application provides six major functions: (1) detection of land cover change, (2) detection and alert for elevation differences, (3) assessment of pipeline construction progress, (4) assessment of roadside ditch construction progress, (5) assessment of areas covered by dust netting, and (6) assessment of asphalt paving progress. A web-based computer platform was developed to integrate AI-recognized digital data with various types of geographical information. This platform is utilized for automated construction progress tracking, providing baselines for decision-making and prioritizing control over construction progress management, which is expected to enhance the quality of road construction.

Keywords: UAV, AI, Road construction progress management, GIS

1. INTRODUCTION

This application primarily focuses on the automated tracking and evaluation of specific tasks and objectives to enhance the quality of task execution. The main structure of this paper firstly introduces the development site, the standardization work flow of producing ortho-rectified images, AI applications on road construction progress management. Finally it summarizes the AI analysis and comparison functions and the outcomes to an integrated web-GIS platform for digital archive and query for the engineers.

2. Project Overview

To enhance the efficiency of traditional road and land development construction progress management, MAA has developed UAV and AI technology for automated progress comparison in related projects. The Taoyuan City Zhongli Sports Park section expropriation project serves as the development site for this initiative. The project site is located in Zhongli District, Taoyuan City, covering a total area of approximately 72.97 hectares. The plan aims to stimulate the revitalization and transformation of surrounding industries through regional development. It envisions creating a green living zone that fosters a symbiotic relationship between water and forest, combining green and blue belts to establish a forest-like sports park. The concept of the planned development is illustrated in Figure 1.

Figure 1 Project development concept.

3. Development Process and UAV Image Standardization Operations

3.1 Overall Workflow

The overall technical development process begins with the collection of aerial image data. After collecting the images, the data is integrated and processed. The images are then imported into the developed AI comparison system for analysis and comparison. Finally, the compared data is imported into the platform for data querying and storage purposes. The complete automated progress comparison and analysis workflow is illustrated in Figure 2.

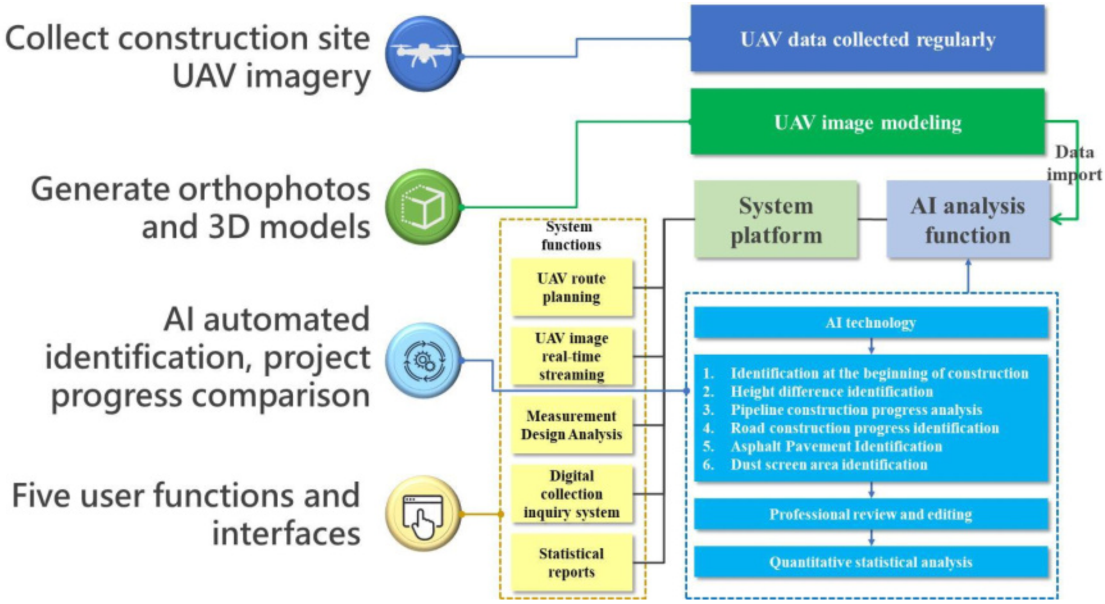

Figure 2 Development workflow.

3.2 Overall Workflow

For regular photography of the construction site to accurately record the progress changes, this project uses a self-assembled UAV system. The UAV has a maximum flight altitude of 1000 meters, a maximum flight time of 45 minutes, and a real-time image transmission system with a maximum transmission distance of 10 kilometers, enabling real-time monitoring of the shooting conditions during flight.

This project uses standardized UAV flight route planning based on open-source software architecture to develop a route planning system that meets the needs of different construction sites. Additionally, a standardized image production process has been established (as shown in Figure 3) to obtain uniformly ortho-rectified images. The flight altitude for this project is 120 meters, with an average ground resolution of 3.70 cm for the captured images.

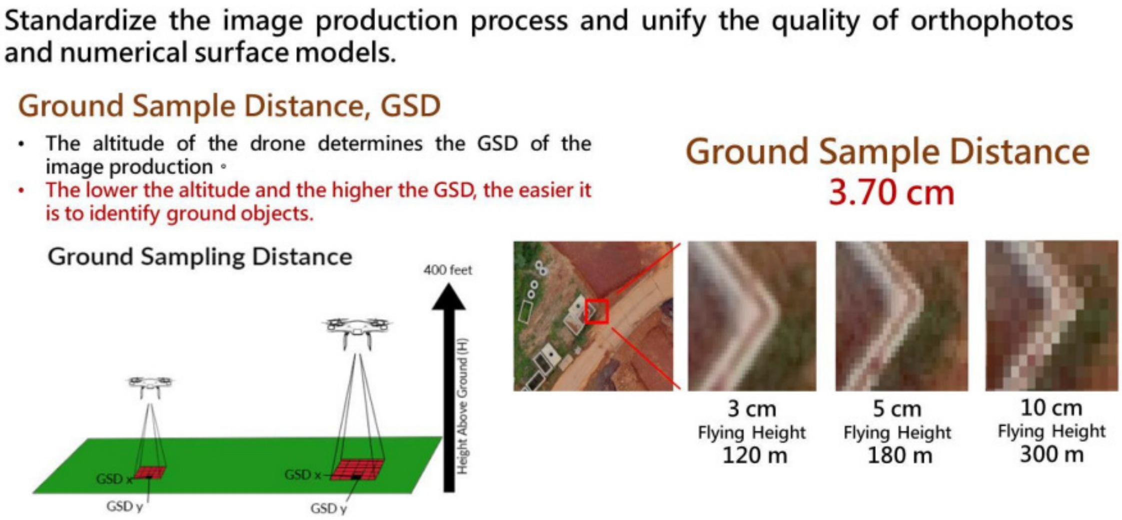

Figure 3 Standardization of ortho-rectified images and digital surface models.

4. RESULTS

4.1 Development of AI Engineering Analysis Techniques

The project uses AI comparison development through a convolutional neural network system, employing SVM image classification for deep learning and recognition of images. A total of more than 20 image data sets which were took from 2021/05 to 2023/03 were captured, serving as the foundation for AI recognition training.

Currently, this project has developed six major AI analysis techniques (as shown in Figure 4), including: (1) Detection of land cover change , (2) Detection and alert of elevation differences, (3) Assessment of pipeline construction progress, (4) Assessment of roadside ditch construction progress, (5) Assessment of areas covered by dust net, and (6)Assessment of asphalt paving progress. These functions assist in various construction management applications.

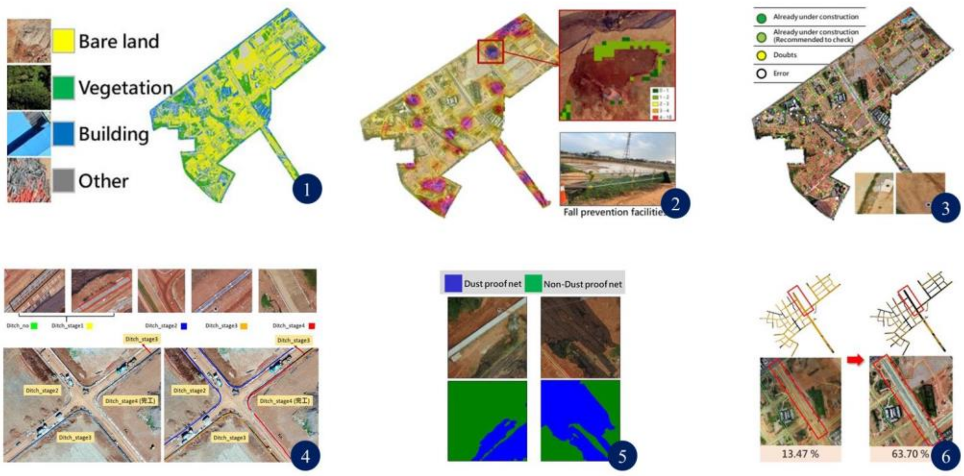

Figure 4 Six major AI analysis functions.

- Detection of land cover change

Land cover is categorized into four major types, including bare land, vegetation, buildings, and others (as shown in Figure 5). Through the analysis of images from different time periods, changes in land cover within the development area can be understood, allowing for the monitoring of construction progress at the site.

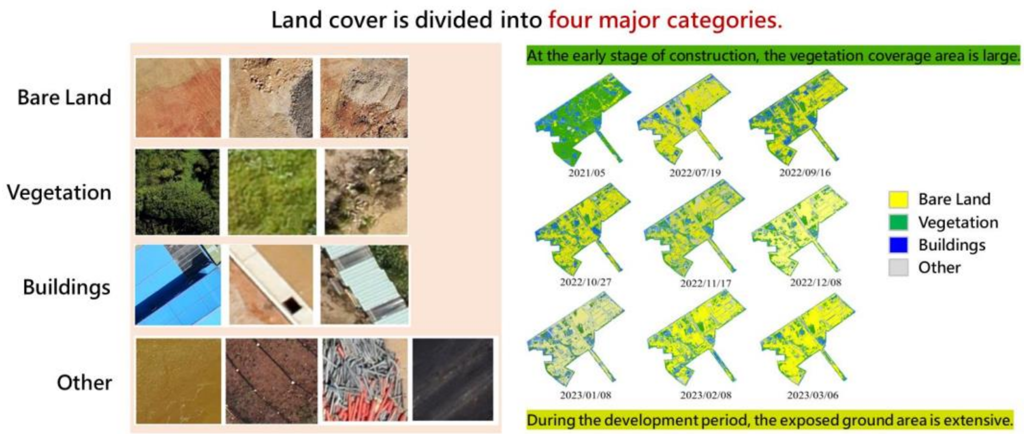

Figure 5 Land cover change detection.

- Detection and alert of elevation differences

By quantifying the standard deviation of the ground elevation, the degree of elevation change in the terrain can be measured. Smart analysis is then applied to identify areas with significant elevation differences, allowing for the implementation of relevant safety measures in those areas (as shown in Figure 6).

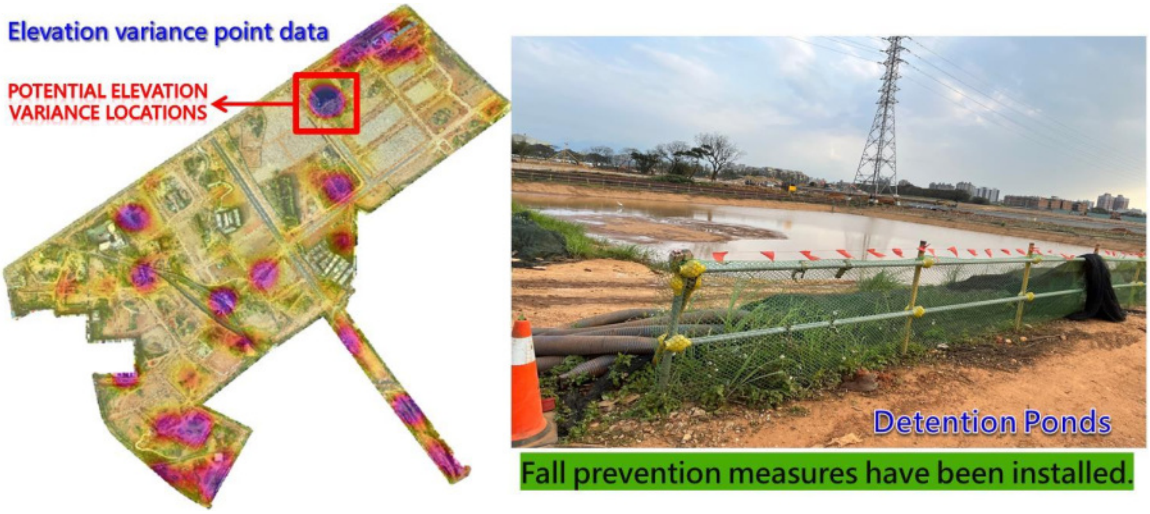

Figure 6 Interpretation and alert analysis of elevation differences.

- Assessment of pipeline construction progress

By analyzing images, we can interpret the existing sewage and manholes on the surface, overlay them with manhole layout plans, and conduct analysis of the differences in construction locations. This allows for the verification of areas where the actual construction location differs significantly from the plan (as shown in Figure 7), effectively monitoring construction conditions and progress.

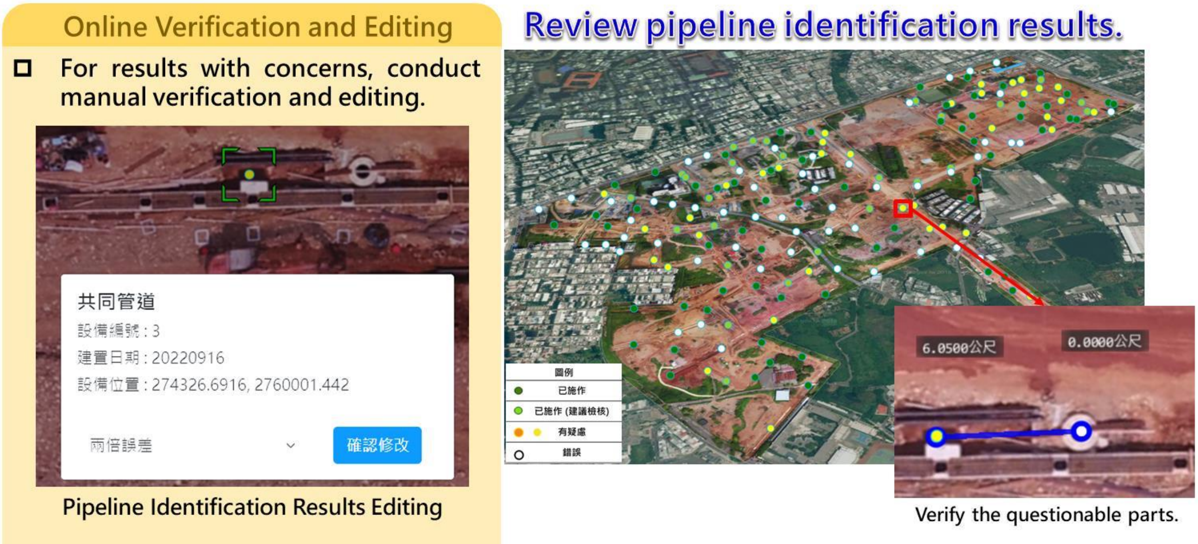

Figure 7 Automated assessment of pipeline construction progress.

- Assessment of roadside ditch construction progress

The road construction progress images are categorized into four construction stages: 1. Side wall bottom plate formwork assembly and concrete pouring, 2. Formwork removal, 3. Reinforcement assembly of trench cover plate, and 4. Pouring concrete for trench cover plate. This includes the state of the trench not yet constructed, totaling four types of construction stage categories (as shown in Figure 8). This allows for the rapid calculation of the progress of each roadside ditch construction stage, with an identification and analysis accuracy reaching 98%.

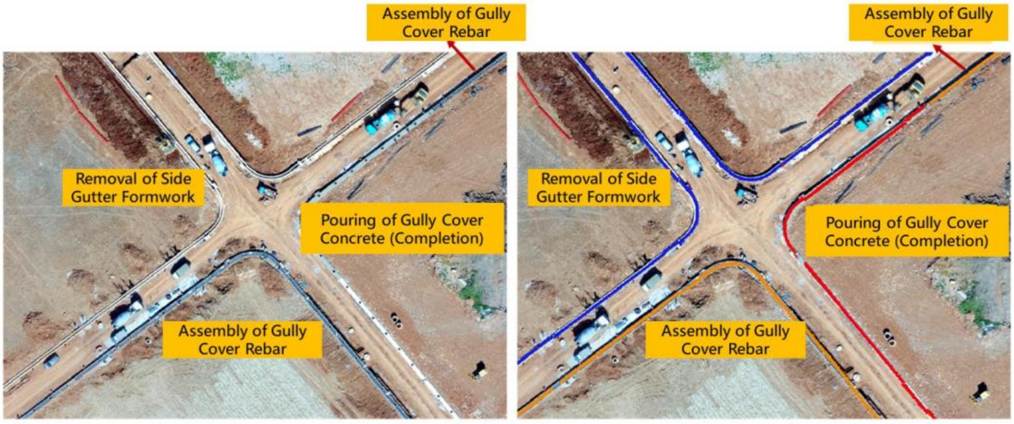

Figure 8 Evaluation of roadside ditch construction progress.

- Assessment of areas covered by dust net

Through AI image training and recognition, the deployment area of dust netting is analyzed (as shown in Figure 9), effectively monitoring the status of dust netting deployment in the construction area. The identification and analysis accuracy reaches 94%.

Using AI image training and recognition, we analyze the deployment area of dust nets (as shown in Figure 9). The ortho-rectified images data is segmented into smaller image blocks for analysis and recognition. The entire construction area is divided into a total of 402 blocks, which are split into training, validation, and test data in a 7:2:1 ratio for deep model training. After validation, the recognition analysis accuracy reaches 94%, effectively monitoring the deployment status of dust nets in the construction area.

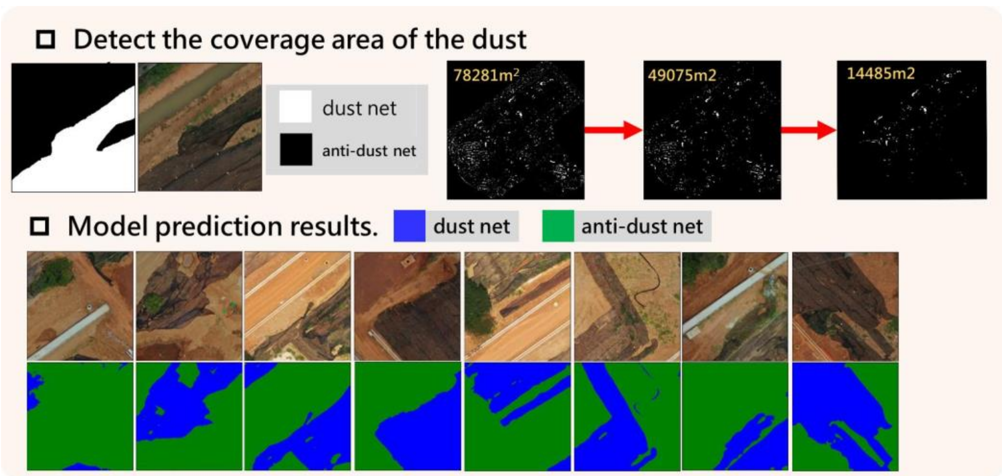

Figure 9 Recognition of dust net coverage areas.

- Assessment of asphalt paving progress

Combining images from each phase with the designed road map data, road images are segmented and combined with the map data. Through AI analysis and recognition, the road paving progress is calculated, allowing for an accurate understanding of the actual road paving status on-site (as shown in Figure 10).

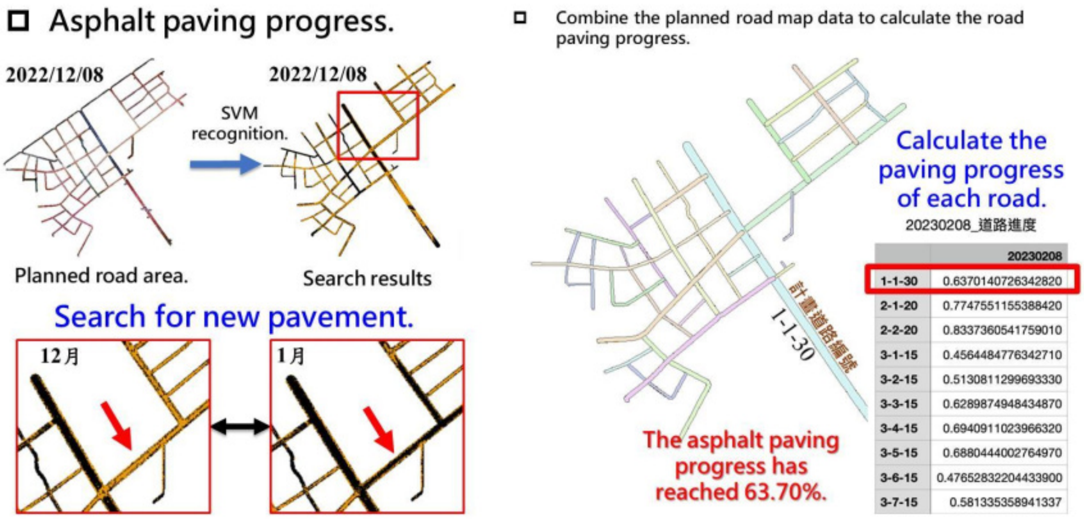

Figure 10 Identification of asphalt paving progress.

4.2 System Platform Establishment

To integrate relevant data and provide rapid display and query applications for land development construction progress management, MAA has also developed a 3D GIS system platform. This platform integrates 3D GIS and BIM data, providing the necessary map data integration, measurement, statistical analysis reports, and management functions for road and land development construction progress management applications (as shown in Figure 11).

Figure 11 System Platform Establishment.

5. CONCLUSIONS

To provide intelligent control of road development progress, MAA systematically collects construction site images, incorporating images from different periods into an AI model training database to enhance analysis accuracy. Leveraging feedback from supervisory construction management experiences, the AI analysis modules are continually optimized for precision, thereby rapidly assisting on-site construction management. Additionally, UAV aerial operations and AI analysis comparison tasks are completed within one to two days, allowing for the swift compilation of progress in various specialized construction areas. This significantly reduces the manpower required for on-site supervision of construction progress and enables the pre-emptive prevention of potential fall hazards, thereby enhancing safety standards.

Moreover, the established map data platform can incorporate construction process images and analysis for comprehensive documentation of the construction progress. Through this innovative application of technology, MAA aims to achieve intelligent construction management that ensures quality, adherence to schedules, budget compliance, environmental sustainability, and safety.

In UAV shooting operations, in addition to standardizing the complete workflow to ensure consistent ortho-rectified images quality, it is necessary to consider the constraints of weather conditions on site. Furthermore, the UAV must be operated by personnel with professional flight licenses to ensure flight safety. For the continued development of UAV combined with AI comparison technology, it is hoped that its application can be extended beyond road engineering to include such as land development, building, bridge and any other construction projects for AI automatic progress comparison. This can reduce labor costs and, through the digital archiving of data, enhance the overall engineering environment and quality, thereby creating sustainable engineering value.

6. ACKNOWLEDGMENTS

The information presented in this paper is provided by MAA. I would like to express my gratitude to the colleagues at MAA for their valuable data, models, and integration of relevant work experience. Additionally, I would like to thank Professor Han Jen-Yu and his team from the Department of Civil Engineering at National Taiwan University for their invaluable technical contributions. Special thanks also go to the New Construction Engineering Department of the Taoyuan City Government for providing the construction site, which enabled the completion of this innovative technological application.

Traffic Operational Performance for A Corridor Analysis: A Case Study of Main Road Link Type 1 and 2 of Department of Highway

Ladda Tanwanichkul[1], Pattharin Sarutipand[2], Wuttikrai Chaipanha[3] and Jumrus Pitaksringkarn[4]

[1*]Department of Civil Engineering, Engineering Faculty
Khon Kaen University, ladpit@kku.ac.th
[2] Bureau of Planning, Department of Highways,
psarutipand@gmail.com
[3]Department of Civil Engineering, Engineering Faculty,
Rajamangala University of Technology Isan Khonkaen Campus,
wuttikrai.ca@rmuti.ac.th
[4] Department of Civil Engineering, Engineering Faculty
King Mongkut's Institute of Technology Ladkrabang,
jumrus@gmail.com

ABSTRACT

Roadway Corridor Improvements are one of the key improvements of road network, mainly aiming to solve problems in term of mobility and accessibility of the Highways in Thailand. Mid-block, Intersection, and Median Opening are the three main bottlenecks of traffic congestion on road corridor related to its corridor operation. Thus a project under a supervision of Thailand Department of Highways—Planning Division named "A Strategic Planning Study of Major Roadway Corridor Improvements focusing on its Mobility and Safety" have been undertaken to explore traffic operational performance of the 15 selected corridors covering all four regions in Thailand representative as Road Link Type one and two as main road links of country road network. In order to assess a traffic operational performance, various traffic surveys and the traffic demand forecast with its traffic simulation have been developed for these individual 15 selected corridors. Traffic parameters and operational performance of each corridor have been examined. Consequently, this case study aims to examine and develop relationship between traffic parameters such as number of lane, traffic volume and level of service. It is found that the trends of this relationship can be classified regarding to the Level of Service and the related traffic parameters on both Mid-blocks and Intersections as mentioned previously. In addition, the traffic operational performance of Median Open has been examined using a typical section varying main road and U-turn traffic volume. Two categories of the median opening have been considered i.e. at grade median opening (Inner-to-Outer and Inner-to-Inner U-turn types) and grade-separation median opening

(Short-span bridge and Elevated U-turn). It is also found that at a similar condition of traffic volume for the Inner-to-Inner at grade U-turn type is better than Inner-to-Outer because of less conflict points and higher speed on the U-turn maneuver whereas a grade-separation median opening outperforms ones as at-grade types in term of average delay from micro simulation model. Therefore, the study results depict that the potential trends have been developed from those relationships being used as the primarily decision-making tool for a planning-level stage of the traffic operational improvements on a major roadway corridor.

Keywords: Road Corridor Improvement, Traffic Operational Performance Analysis, Traffic Simulation, and Traffic Parameter

1. INTRODUCTION

The major highways system remains the backbone of the transportation system, as it is heavily traveled, provides the most important link in the nation's supply chain, and serves as the primary connection both between and within urban communities. Highway corridors play a vital role as to facilitate economic development by connecting economic entities and activities both within and between regions (Vyas et al., 2018).

The goal of the road corridor improvement is to develop recommendations to enhance safety and mobility in order to design a roadway (City of Austin, 2023). A planning in corridor improvement are preliminary engineering documents that provide a roadmap for further analysis and development of potential projects. Kotkar & Bhorkar (2023) review of improvements for road corridors has explained some suitable suggestions, such as road widening, including appropriate road furniture, and incorporating a diversion island for left-turn traffic separation. Additionally, improving junctions helps in reducing pollution. Vehicles making U-turns at median openings with wide medians (median nose width of 6.4m) have a larger capacity than those making U-turns at median openings with narrow medians (median nose width of less than 6.4m) (Liu et al., 2008). Traffic lights in corridors at the arterial level produced higher total emissions (over 6%), while stop-controlled intersections produced lower emissions (12%) compared to roundabouts. (Fernandes et al., 2015). Moreover, Romadhona et al., (2019) suggested that U-turn location with bad performance should be omitted and also reducing the number of U-turn locations will improve more than 50% of the traffic performance in the urban street. In fact, there are still many projects and studies being conducted to improve road networks in order to make them more efficient for traffic and safer for driving (Nicoli et al., 2015; Gichaga, 2017; Kebe, 2023; Sandeep, 2023).

The works of this paper have been originated, created and developed from study results of "Study of Strategic Planning for Main Road Corridor Improvement of Road Mobility and Safety" Project under Bureau of Planning, Department of Highway, Ministry of Transport Thailand (DOH, 2024).

DOH (2020) classified the national highways into 6 types based on Link Role Connectivity, Context, and Function of each road: (1) Motorway: Highways designed for fast and uninterrupted traffic flow, especially linking Bangkok with various regions of the country and neighboring countries. (2) Link 1 - National Highway and AH Highway: Primary network linking between regions. (3) Link 2 – Regional Highway: Main routes within regional highway networks. (4) Link 3 – Provincial Highway: Main provincial highway network linking travel between districts within provinces or connecting to Link 2. (5) Link 4 – District Highway: Highway network at the district level linking travel between sub-districts within districts or extending from Link 3 and, (6) C-Link – Connecting Link: Other types of highways or roads not managed by government sector that connect to the highways.

The project focused on Road Link Type 1 and 2 categorized in Road Hierarchy System as main road in Thailand Road Network. study objective focuses on road corridor improvement in term of mobility and safety. Measurement on traffic operational performance were often used to examine road components along a road corridor. In the project, 15 corridors were then selected as study area for the project in order to working on traffic studies in order to do corridor analysis improvement. In travel demand model, forecast traffic volume in 5 committed years would be determined and then traffic simulation model would be employed to evaluate traffic operational performance along corridors for without- and with- project conditions. Acharya & Marsani (2019) building a mathematical model based on the prevailing unauthorized pedestrian crossings observed in mid-block road sections of Kathmandu city shows that traffic speed is a significant factor for illegal mid-block pedestrian crossings. Othayotha & Rao (2020) investigate the relationship between the level of service and the v/c ratio at signalized intersections under heterogeneous traffic conditions. The results show that the delay distributions under different degrees of saturation are overlapping, making it difficult to establish v/c thresholds for each LOS category.

Therefore, study of relationships between traffic parameters and traffic operational performance were then commenced to see the trends of those results from corridor analysis from the aforementioned project. Trends from this relationship could then be used as a preliminary threshold to cut of improvement traffic efficiency of components in any corridors especially at planning level.

2. STUDY METHODOLOGY

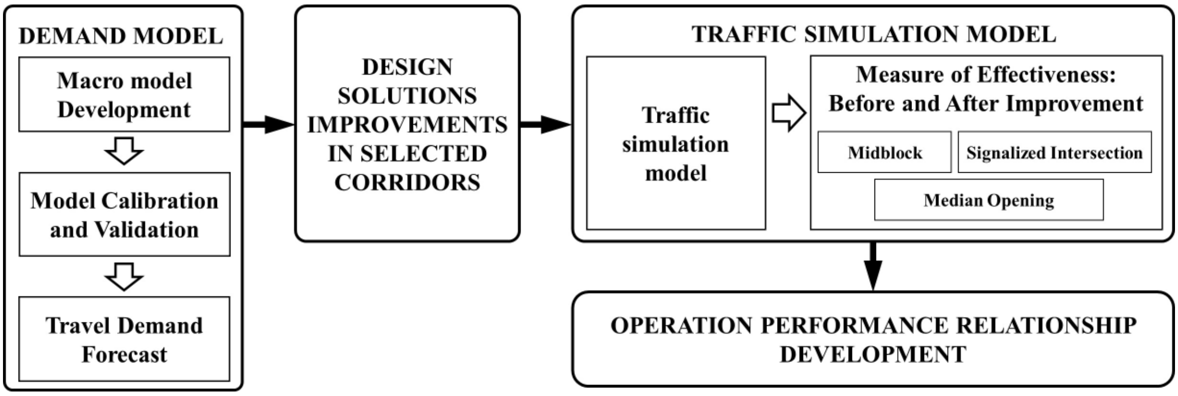

Figure 1 Study Framework

The initial phase of the study involves defining the study area, which comprises 15 main corridors with traffic issues. Traffic data was collected to develop a macroscopic model for forecasting future traffic volumes in order to serve as input for developing a traffic simulation model to evaluate proposed roadway design improvements. The simulation compares Measure of Effectiveness (MOEs) before and after improvements, based on traffic volume forecasts. Afterward, an analysis of the relationship between traffic data and road physical characteristics was conducted. A summary of the study procedure is shown in **Figure 1**. Traffic data collections for the 15 selected corridors covering 4 regions in Thailand with 433.484 kilometers (as illustrated in **Figure 2**) were conducted for one weekday and one weekend. The data collections included total of 106 Mid-Block Classified Counts (MB), 86 Turning Movement Counts (TMC), 48 Origin-Destination Survey (OD), and Travel Time Survey along corridors.

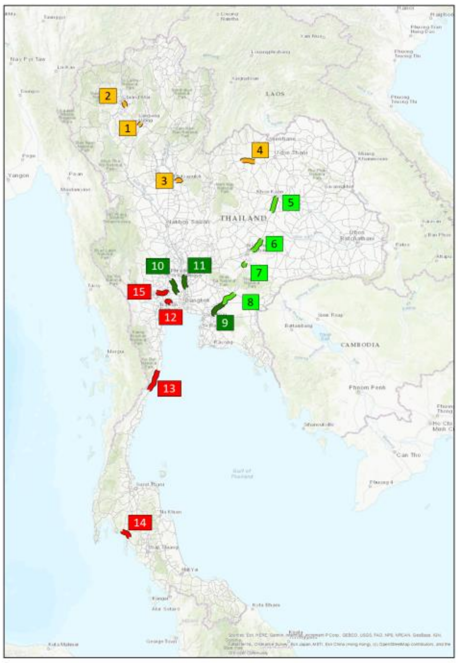

No.	Regions	Corridors
1	North	Highway no.1 (Lampang)
2		Highway no.11 (Chiang Mai)
3		Highway no.12 (Phitsanulok)
4		Highway no.210 (Nongbualamphu)
5	North East	Highway no.2 (Khon Kaen)
6		Highway no.2 (Nakhon Ratchasima)
7		Highway no.304 (Nakhon Ratchasima)
8		Highway no.304 (Prachinburi)
9	Central	Highway no.331 (Chachoengsao)
10		Highway no.340 (Pathum Thani)
11		Highway no.347 (Pathum Thani)
12	South	Highway no.4 (Nakhon Pathom)
13		Highway no.4 (Prachuap Khiri Khan)
14		Highway no.4 (Krabi)
15		Highway no.346 (Nakhon Pathom)

Figure 2 The selected network consisting of 15 corridors (DOH, 2024)

2.1 Macro Traffic Model

The analysis of traffic conditions in various forecast years has been applied using data from the National Model (NAM) and then the development into a Study Area Model (SAM) for use in predicting future traffic volumes. This involves analyzing current and future traffic conditions on the network, considering changes in travel demand and infrastructure plans/projects for road network improvement. The model developed will be constructed from traffic data, highway network data, travel data, and socio-economic data of travelers obtained from surveys conducted within the study area. Predictions are made for forecast years of the 5th, 10th, and 20th years of service from 2028 as opening year. The development approach of the traffic and transportation model of the project will involve calibration before the application of the developed model. Calibration ensures the accuracy and reliability of the model. The accuracy of the model will be validated by comparing predicted traffic volumes on the road network for the current year with actual traffic volumes obtained from project traffic data surveys. The travel demand forecasted for the future years.

2.2 Traffic Simulation Model

Traffic Simulation Model has been developed for analyzing Level of Service (LOS) which is an integral part of the effectiveness evaluation process (Measure of Effectiveness, MOEs) for various traffic measures on roadways. PTV VISSIM and VISTRO software (shown in **Figure 3**) were used to develop traffic simulation model with forecasted traffic volumes from the Macro Model and is used to analyze and evaluate traffic conditions following physical and management improvements such as mid-block widening, traffic signal intersection improvements as grade-separation improvements.

In this study, model calibration involved adjusting certain parameters to verify that the results closely match real-world conditions and also are at acceptable criteria and threshold. Traffic volume and travel speed were used as Measure of Effectiveness (MOEs) for calibrating the model. The travel speeds in each direction were examined to meet the calibration criteria recommended by the Design Manual for Roads and Bridges (DMRB) (WisDOT, 2002). Comprehensive comparison with the GEH statistic between the traffic model and observed hourly volumes indicated that a GEH value of less than 5.0 is considered satisfactory.

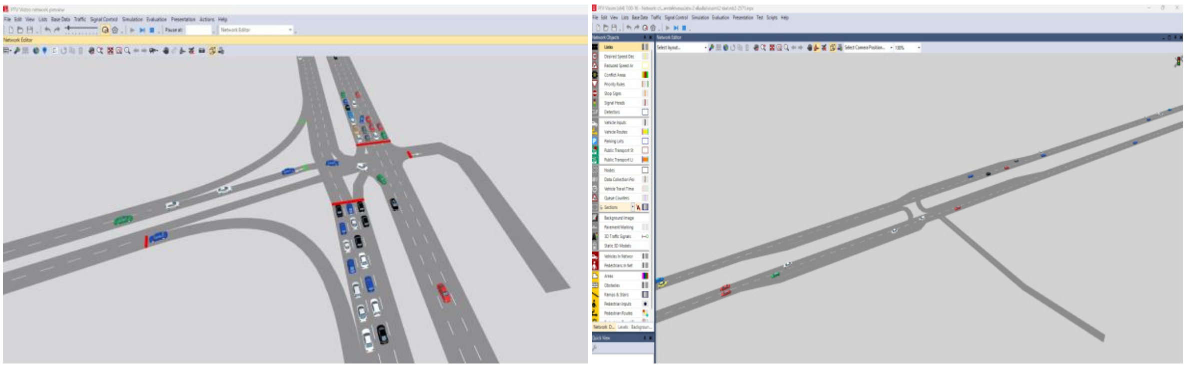

Figure 3 Examples of analysis results using the PTV VISTRO and VISSIM simulation models

The calibrated model will be applied to analyze improvements for mid-block sections and intersections. Level of Service (LOS) is used as an indicator of mid-block sections and intersections to compare traffic operational performance of two main scenarios: The Existing Scenario and the Proposed Scenario. Traffic Simulation Model was used to evaluate performance before and after the improvement of corridors. As referencing to the criteria of North Carolina Department of Transportation (2014), at planning level, LOS D serves as an indicator of deficiencies in the performance of road segments and suggests improvement measures to enhance their efficiency of Mid-block. Moreover, this study adapted and proposed to use LOS E for evaluating deficiencies of intersection performance. The example of Highway 12 (Phitsanulok Province) shown in **Figure 6** The Existing Scenario and the Proposed Scenario representing Level of Service of before and after the improvement both Mid-blocks and Intersection along the corridor.

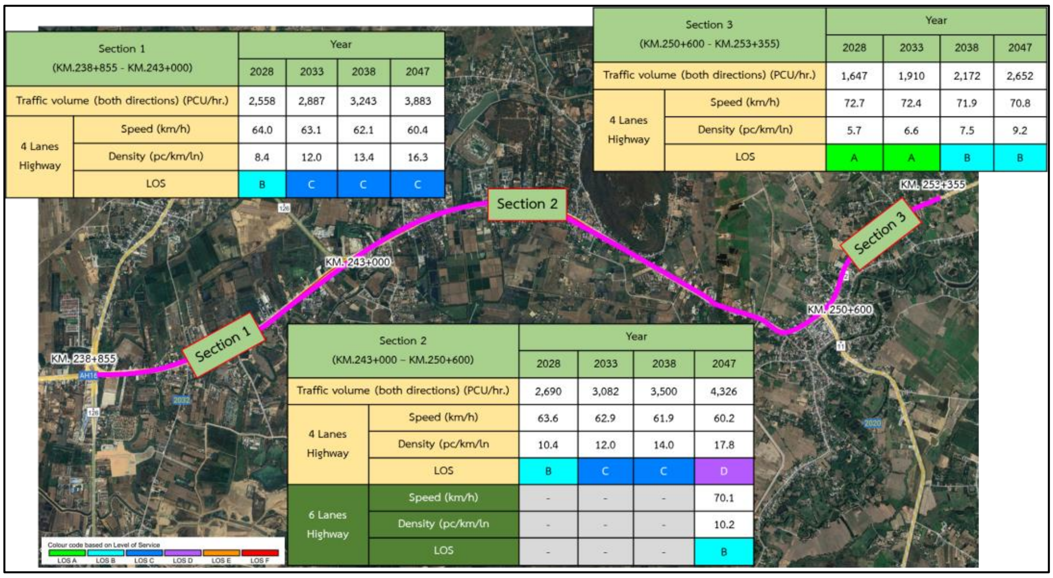

(a) Mid-block sections

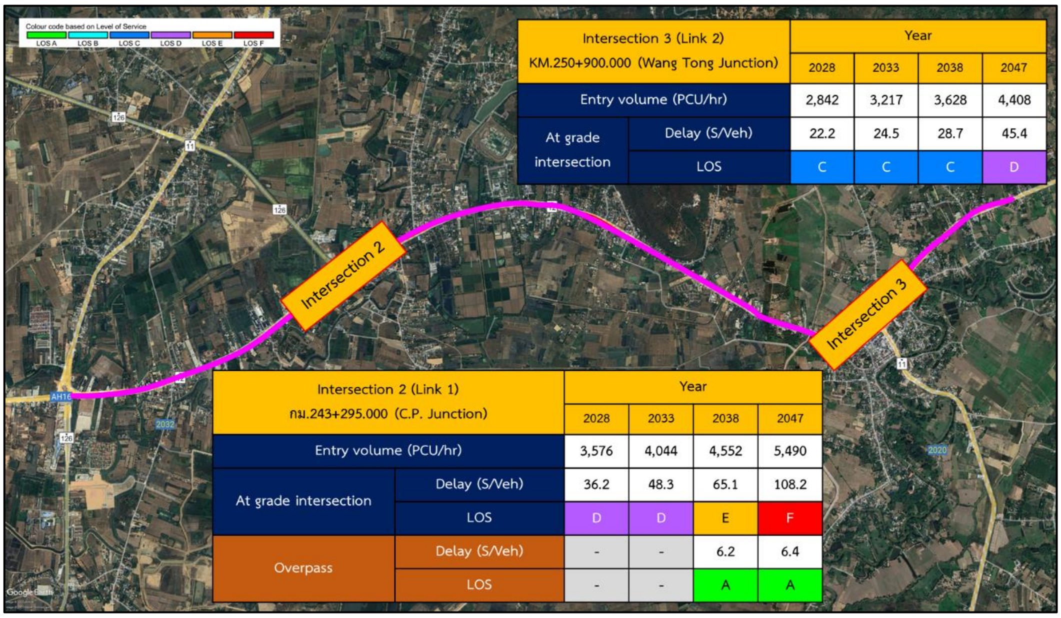

(b) Intersections

Figure 6 Analysis of Service Levels along Mid-block sections and Intersections of Highway 12 in Phitsanulok Province

3. RESULTS

In corridor analysis, road element efficiency along corridor is to be examined in term of traffic operational performances including both mid-block sections and intersections along 15 corridors in study area. Results of traffic operational performances are generally represented in term of Level of Service (LOS) following to Highway Capacity Manual guideline. As traffic operational performance, LOS of elements (both mid-blocks and intersections) along 15 corridors in the study area were determined. Then, relationships between traffic operational performance data and road geometry characteristics were examined from those results. Moreover, traffic simulation models were also used to develop typical models for Median Opening in both at grade and separate grade types by increasing different traffic volumes of main roads and U-turn. Three road geometry characteristics to represent relationships were categorized details shown in **Table 1**.

Table 1 Traffic Data and Road Geometry Characteristics

Road Geometry Characteristics	Traffic Data
1. Mid-block: 4 and 6 lanes per two directions	- Number of lanes - Level of service, LOS - Traffic Volume and Condition Speed
2. Intersection: 3 and 4 legs of signalized intersections	- Number of Lane on Main and Minor Road - Level of service, LOS - Traffic Volume on Main and Minor Road
3. Median Opening: at grade and separate grade	
3.1 At grade: Inner-to-Outer and Inner-to-Inner 3.2 Separate grade: Short Flyover and Elevated U turn	- Delay - Main road traffic volume - U-turn traffic volume

3.1 Mid-blocks Analysis

There was an analysis of relationships between traffic volume (two directions), condition speed, and level of service (LOS) concerning with land use characteristics (suburban and rural) for 4- and 6- lane mid-block segments along 15 corridors. It was found LOS for suburban highways tends to have lower condition speeds than rural highways at the same level of service (LOS). The lower condition speeds on suburban highways are attributed to higher roadside friction during traveling along a highway corridor compared to rural highway ones. Generally, roadside friction during traveling may comprise various activities on the roadway, such as different travel modes, vehicle types, and travel purposes, resulting in varying frictional effects on travel speeds through areas with different surrounding land use characteristics. Trends in the relationship between traffic volume and LOS of roadway segments with 4 and 6 lanes were then grouped and compared. It was found that the trends in the aforementioned relationship for both suburban and rural areas are consistent across all two category road types in term of suburban and rural highway were harmonized as illustrated in **Figure 7**.

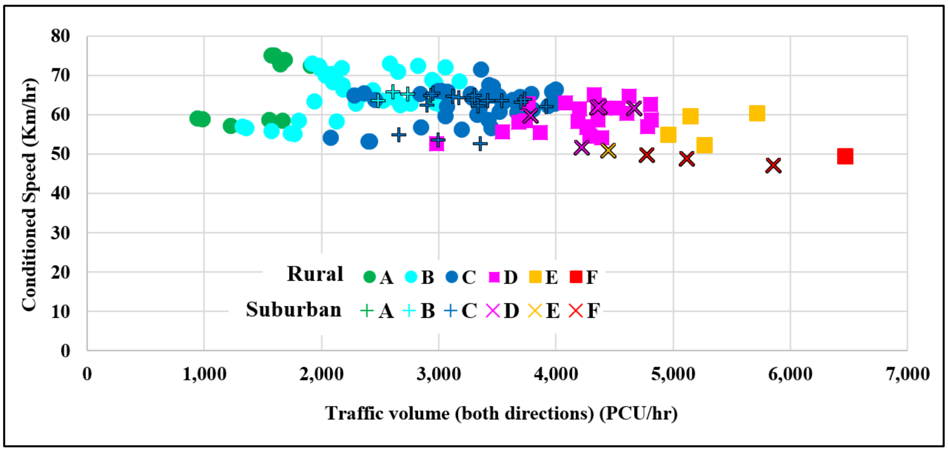

(a) 4-Lane Highways

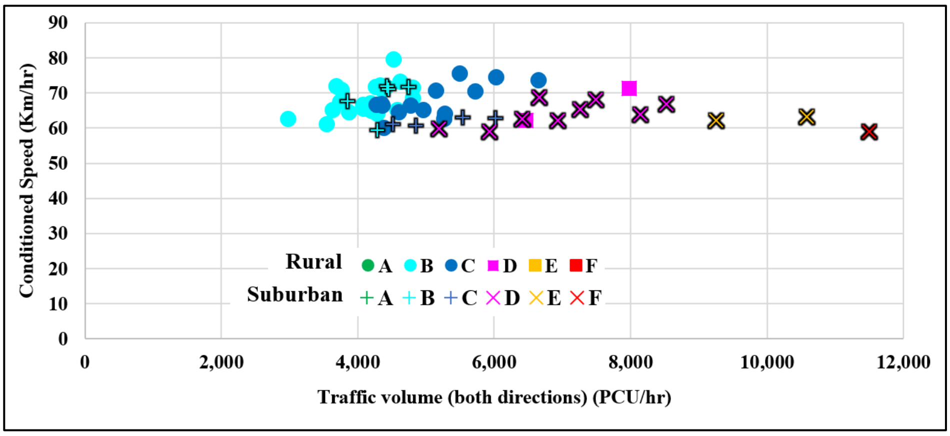

(b) 6-Lane Highways

Figure 7 The Relationship between Traffic Volume and Level of Service on Highway Segments in Suburban and Rural Areas for 4- and 6- Lane Highways

3.2 Intersection Analysis

Concurrently, analysis of relationship between traffic volume of main and minor road associated with LOS of intersections along 15 corridors were also developed. The analysis results were grouped according to three- and four-leg intersections. The total number of intersections evaluated included 16 three-leg intersections and 24 four-leg intersections by varying to main road of 4 lanes and minor road of 4 and 2 lanes. It was found that results from four-leg intersection (main road 4 lanes - minor road 4 lanes) and three-leg intersection (main road 4 lanes - minor road 2 lanes) are not adequately explained the trends. However, there are two category of analysis trends could be described as following:

- **Four-leg intersection (main road 4 lanes - minor road 2 lanes):** the relationship shows that increasing traffic volume on both the main and minor roads affects congestion and also the trend suggests that intersection efficiency needs improvement when traffic volume more than 2,500 and 500 pcu/hr (both directions) for main road and minor road respectively.

- **Three-leg intersection (main road 4 lanes - minor road 4 lanes):** from the graph, the relationship was depicted that increasing traffic volume on both main and minor roads affects congestion and it was suggested that intersection capacity could be improved when the traffic volume (per two directions) entering the intersection on the main road exceeds 4,000 pcu/hr.

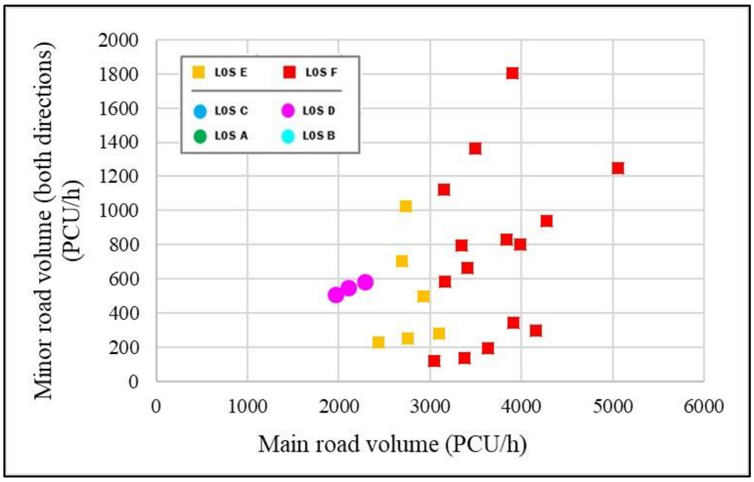

(a) Four-leg intersection (main- minor road 4-2 lanes)

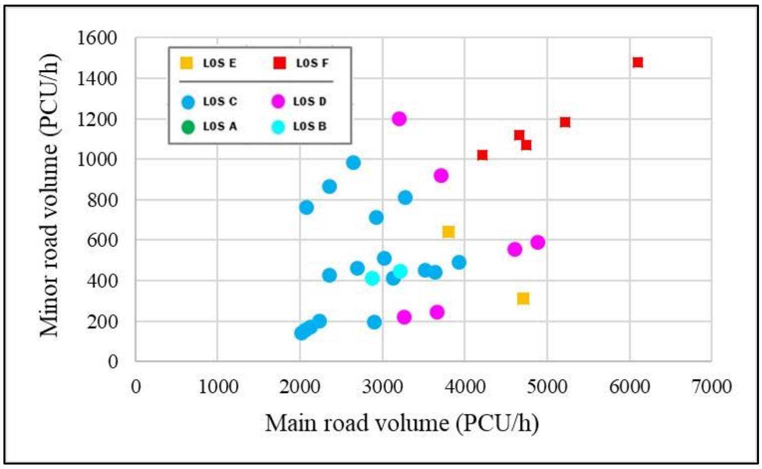

(b) Three-leg intersection (main-minor road 4-4 lanes)

Figure 8 Relationship between main road and minor road traffic volume and intersection level of service: Four-leg and three-leg intersection

3.3 Median Opening Analysis

Traffic operational analysis for median opening is adopted from unsignalized intersection behavior by using a traffic simulation model to analysis to assess the efficiency by increasing traffic volume in main road and u-turn direction. Traffic evaluation efficiency (Level of service, LOS) will be referenced from the Highway Capacity Manual (2016) (TRB, 2016) for unsignalized intersections. This is because median openings have a service pattern similar to unsignalized intersections in controlling vehicle reversals. This will be used as a guideline for evaluating the efficiency of median openings in each configuration. The researchers have proposed the service levels that should be enhanced, which is LOS E with an average delay exceeding 35 seconds per vehicle. The analysis results of Median Opening have been divided into two groups as following:

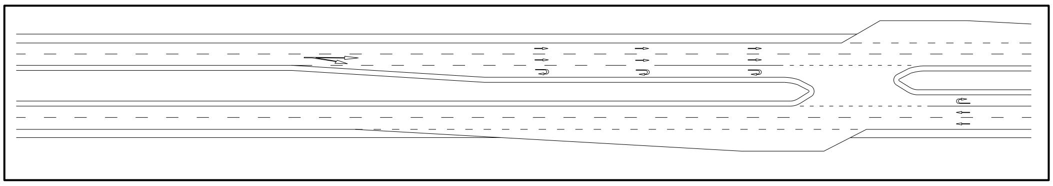

(a) Inner-to-Outer Median Opening

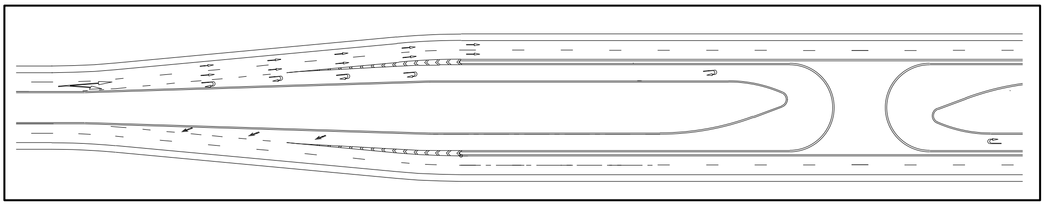

(b) Inner-to-Inner Median Opening

Figure 9 At Grade Median Opening: (a) Inner-to-Outer (b) Inner-to-Inner

1) **At Grade Median Opening:** There are two different types of at grade median opening in this study to be analyzed i.e. Inner-to-Outer and Inner-to-Inner types. They are different in radius of turning at median opening. For Inner-to-Outer type, a vehicle would be able to make a turn from the most inner-lane into the most outer-lane whereas inner-to-inner type is from the most inner-lane into the most inner-lane in opposite direction as shown detail in **Figure 9**. Generally, inner-to-inner type would have a wider radius curve of median which could facilitate a vehicle to be more continuous traffic flow comparing with ones on inner-to-outer type. By using LOS E as threshold value (total average delay of 35 seconds per pcu), it was found that the Inner-to-Outer type represents higher average delay per pcu comparing with the Inner-to-Inner type at the same ratio of main and u-turn traffic volume as shown in **Table 4.** Moreover, by overlaying the analysis data, as shown in **Table 5**, it is found that in cases where the traffic volume on the main road is equal, the Inner-to-Inner type can accommodate a higher volume of reversing traffic than the Inner-to-Outer reversing point. This is because vehicles could do more continuous movement (less conflict points and higher speed) at the Inner-to-Inner type comparing to ones at the Inner-to-Outer type. However, the trend indicates that the efficiency of the Inner-to-Inner type can be at a certain level and if it exceeds this trend, it is suggested to manage the median opening to be improved into Grad-Separation Median Opening.

Table 4 The relationship between the traffic volume on the main road, the percentage of traffic volume reversing, and the average delay at ground-level median openings (DOH, 2015)

Inner-to-Outer U-turn									
Average delay (Sec./PCU)		**The percentage of U-turn traffic volume reversing on the main road (%)**							
		1%	**3%**	**5%**	**7%**	**10%**	**15%**	**20%**	**25%**
Traffic volume per direction (PCU/hr)	1,000	0.89	0.95	1.03	1.12	1.28	1.49	1.80	2.13
	1,500	1.66	1.73	1.86	2.04	2.28	3.24	4.83	11.87
	2,000	2.69	2.85	3.09	3.53	4.59	31.53	124.74	337.89
	2,500	3.82	4.15	6.87	51.41	161.39	390.35	543.60	678.37
	3,000	5.27	7.35	172.61	329.65	448.92	646.11	693.43	843.04
	3,500	7.90	234.82	437.35	518.53	597.82	791.74	833.34	969.44
	4,000	263.37	534.15	639.67	687.02	786.50	945.60	967.84	1044.11
Inner-to-Inner U-turn									
Average delay (Sec./PCU)		**The percentage of U-turn traffic volume reversing on the main road (%)**							
		1%	3%	5%	7%	10%	15%	20%	25%
Traffic volume per direction (PCU/hr)	1,000	0.89	0.92	0.96	0.99	1.10	1.25	1.45	1.72
	1,500	1.65	1.69	1.75	1.82	1.96	2.22	2.57	3.08
	2,000	2.64	2.70	2.83	2.92	3.22	3.84	4.54	6.47
	2,500	3.67	3.81	4.03	4.29	4.97	8.07	28.30	178.01
	3,000	4.87	5.13	5.69	6.85	14.98	184.81	355.77	521.82
	3,500	6.95	7.64	17.82	145.16	329.73	539.16	661.32	765.25
	4,000	24.68	117.73	331.97	450.22	598.28	726.51	836.58	919.25

Note: - Average delay refers to the combined delay of both mainline traffic and turning traffic for the 4-lane main road.

Table 5 Comparison of Traffic Capacity for U-turns between Inner-to-Outer and Inner-to-Inner Median Openings

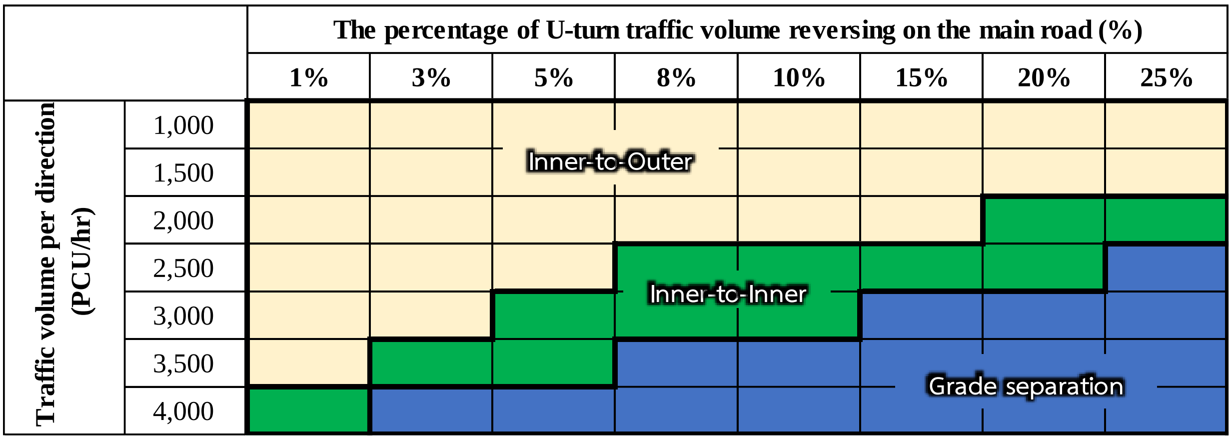

2) **Grade-Separated Median Openings**: The analysis of grade-separated median openings, using an initial threshold of 35 seconds as the average delay. It was found that Elevated U-turn offer slightly better delay performance Short-Span Overpass as demonstrated in **Table 6**. Nonetheless, grade-separated median openings can handle higher U-turn traffic volumes compared to at-grade median openings. This is because grade-separated median openings segregate the mainline traffic and U-turn traffic,

providing a higher level of safety for U-turn maneuvers compared to at-grade median openings. However, the necessity of constructing grade-separated median openings should consider the cost-effectiveness and anticipated traffic volume.

Table 6 The relationship between the traffic volume on the main road, the percentage of U-Turn traffic volume on the main road, and the average delay of short-span bridge and elevated U-Turn

Short-span bridge U-Turn									
Average delay		**The percentage of U-turn traffic volume reversing on the main road (%)**							
(Sec./PCU)		1%	3%	5%	7%	10%	15%	20%	25%
Traffic volume per direction (PCU/hr)	1,000	0.87	0.89	0.90	0.91	1.08	1.20	1.41	1.68
	1,500	1.62	1.64	1.75	1.79	2.01	2.19	2.52	2.99
	2,000	2.61	2.65	2.75	2.88	3.24	3.88	4.60	5.36
	2,500	3.64	3.73	3.83	4.21	5.09	7.62	10.74	20.10
	3,000	4.74	4.95	5.32	5.81	10.49	33.62	78.49	253.75
	3,500	6.36	7.31	10.69	44.01	126.12	260.42	428.49	550.15
	4,000	14.90	30.23	141.34	238.17	306.37	484.36	630.09	789.19
Elevated U-Turn									
Average delay		**The percentage of U-turn traffic volume reversing on the main road (%)**							
(Sec./PCU)		1%	3%	5%	7%	10%	15%	20%	25%
Traffic volume per direction (PCU/hr)	1,000	0.86	0.87	0.88	0.90	1.03	1.15	1.24	1.31
	1,500	1.61	1.62	1.66	1.72	2.00	2.16	2.44	2.65
	2,000	2.60	2.64	2.67	2.69	3.22	3.79	4.17	5.08
	2,500	3.61	3.64	3.73	3.88	5.05	6.60	10.02	17.86
	3,000	4.63	4.90	5.16	5.64	10.38	30.23	76.11	239.95
	3,500	6.32	7.17	9.16	16.65	112.81	193.11	360.63	520.61
	4,000	14.29	27.00	114.74	226.48	299.48	462.76	613.32	747.64

Note: - Average delay refers to the combined delay of both mainline traffic and turning traffic for the 4-lane main road.

4. CONCLUSIONS

This study has examined traffic operational performance of three road key bottle necks by using corridor analysis of 15 selected corridor representative of Road Link Type 1 and 2. Three key road components generally causing bottleneck along a road corridor including Mid-blocks, Intersections and Median Openings. For Mid-blocks, relationship between traffic volume and condition speed resulting were illustrated in different LOS for 4 and 6 lane road. Moreover, it was also found that LOS for suburban highways tends to have lower condition speeds than rural highways at the same level of service (LOS). Whereas for four-leg (main/minor as 4 and 2 lanes) intersections and three-leg (4-lane main/4-lane minor) intersections, relationship between main and minor roads could be identified in certain number of traffic volume in either main or minor roads as a guideline for intersection improvement. Therefore, it recommended that four-leg intersections (main road 4 lanes - minor road 2 lanes) with traffic volume exceed 2500 and 500 pcu/hr respectively and when traffic volume on main road more than 4,000 pcu/hr for three-leg intersections (main road 4 lanes –

minor road 4 lanes) it is recommended to intersection improvement should be considered. Two groups of Median Opening i.e. At-Grade and Separate Grade types have been explored. It was found that Inner-to-Inner type is outperform to Inner-to-Outer type because of less conflicts between main road and U-turn traffic. However, once traffic volume of main road and U-turn exceed some point, grade separation either types of Median Opening is required to improve traffic operational performance.

Relationships of traffic operational performances and other traffic parameters of three key components in corridor analysis were developed. From this, trends and relationships could then be used as preliminary guidance for road designers and road planners for making decisions in key components along a corridor at planning level.

5. REFERENCES

Acharya, S., & Marsani, A. (2019). Modelling the Relationship between Pedestrian Illegal Mid-Block Crossings with Traffic and Geometric Parameters. International Journal of Advanced Engineering and Management, 4(1).

City of Austin (2023). Corridor Improvement Programs, Retrieved July 2, 2024, retived from https://www.austintexas.gov/department/corridor-improvement-programs

Department of Highways (2015).Standard drawing for highway design and construction (revision 2015). Department of highway, Ministry of transportation.

Department of Highways (DOH) (2024). Study of Strategic Planning for Main Road Corridor Improvement of Road Mobility and Safety Project. Bureau of Planning, Department of highway, Ministry of transportation.

Department of Highways. (2020). Study project and data compilation for categorizing the classification levels of the national highway network nationwide to enhance efficiency in development planning and management of highways. Bureau of Planning, Department of highway, Ministry of transportation.

Fernandes, P., Fontes, T., Neves, M., Pereira, S. R., Bandeira, J. M., Rouphail, N. M., & Coelho, M. C. (2015). Assessment of corridors with different types of intersections: Environmental and traffic performance analysis. Transportation Research Record, 2503(1), 39-50.

Gichaga, F. J. (2017). The impact of road improvements on road safety and related characteristics. IATSS research, 40(2), 72-75.

Kebe , E. hadj A. K., Gomis , J. S., Dangoura , M., & Cisse, I. . (2023). Diagnostic, entraves et importance des corridors de transport routier dans le processus d'intégration régionale en Afrique de l'Ouest : le cas du Sénégal et ses pays voisins. Revue Internationale De

La Recherche Scientifique (Revue-IRS), 1(2), 181–189. https://doi.org/10.5281/zenodo.7851118

Kotkar, S. & Bhorkar, M. (2023). Junction improvement on urban corridor using traffic simulation model – A review. *AIP Conf. Proc.* 12 May 2023; 2747 (1): 040003. https://doi.org/10.1063/5.0133847

Liu, P., Lu, J. J., Hu, F., & Sokolow, G. (2008). Capacity of U-turn movement at median openings on multilane highways. Journal of Transportation Engineering, 134(4), 147-154.

Nicoli, F., Pratelli, A., & Akçelik, R. (2015). Improvement of the west road corridor for accessing the new hospital of Lucca (Italy). Urban Transport XXI, WIT Transactions on the Built Environment, 146, 449-460.

Othayoth, D., & Rao, K. K. (2020). Investigating the relation between level of service and volume-to-capacity ratio at signalized intersections under heterogeneous traffic condition. Transportation Research Procedia, 48, 2929-2944.

Romadhona, P. J., & Nurkumala, L. (2019). Traffic Performance of U-Turn Effects at Median Opening on Four-Lane Divided of Urban Street (Study Case: Yogyakarta, Indonesia). In MATEC Web of Conferences (Vol. 280, p. 02002). EDP Sciences.

Sandeep R G, Yateen Lokesh, Nikhil T R, "Improvements to Road Geometrics of Aluva to Kothamangalam Section of State Highway 16 in the State of Kerala," SSRG International Journal of Civil Engineering, vol. 10, no. 4, pp. 8-12, 2023. Crossref, https://doi.org/10.14445/23488352/IJCE-V10I4P102

Transport Research Board (TRB) (2016). Highway Capacity Manual, Sixth Edition: A Guide for Multimodal Mobility Analysis.

Vyas, M., Harris, J., Knowlton, T., LaBonty, G. J., Milam, R. T., Seager, S., ... & Zundel, L. (2018). Applying innovative performance metrics for corridor evaluation. Transportation Research Record, 2672(44), 93-102.

Wisconsin DOT (WisDOT). (2002). Paramics Calibration and Validation Guideline, Freewey System Operational Assessment, Technical Report I-33, District 2, Milwaukee, WI. June 2002.

Innovation of Bridge Slab Maintenance Development of Specialized Waterproofing Materials for Manual Pavement Work

Gaku Suzuki & Yuki Hiramatsu

Kuwana Office, Central Nippon Highway Maintenance Nagoya Company Limited
g.suzuki@c-nexco-hmn.jp   y.hiramatsu@c-nexco-hmn.jp

ABSTRACT

As the existing Japanese expressway network ages, the amount of repair work increases dramatically. Especially, many of the bridges facing severe deteriorations of concrete slab produce numerous numbers of potholes on the pavement surfaces. Although a lot of effort has been made every day, it is impossible to complete all the necessary repair work immediately within very limited allowable hours at midnight lane closure. To deal with this difficulty, we have developed a new bridge waterproofing material, especially for the extremely small area of repair by manual paving works. This product enabled us to do high quality, easy and safe work within a short period of time, compared with conventionally used methods. The construction process of the developed waterproofing material takes only 10 minutes, by avoiding heating operation on site and skipping need for curing time. We have confirmed its efficiency and durability on concrete bridge slabs for repair. We confirmed performance for concrete bridge slabs, the next goal is to expand its application to steel bridge slabs. This paper introduces the development of the new method for targeting concrete bridge slabs and presents test results for steel bridge slabs.

Keywords: waterproof, bridge slab, pothole, manual paving work, expressway

1. Overview

Many of the minor pavement repairs are needed due to concrete slab deterioration of the bridge decks. When repairing the slabs, vulnerable portions of deteriorated concrete have to be removed, new concrete for the repair to be placed, and then waterproofing is applied on the slabs. However, waterproofing for such small repair areas in manual pavement work has posed difficulties in terms of quality, work efficiency, and work safety. To solve such concerns, we interviewed with many people including paving industries, manufacturers of bridge slab waterproofing materials but could not find optimal materials. Therefore, we decided to develop a new waterproofing material, specialized for small-scale manual pavement work, in collaboration with a resin manufacturer.
In the course of development, we referred to the epoxy-based resin used to bond the deck plate and asphalt on steel bridges in China. The development of this product was aimed at ensuring high quality and safe construction in a brief time using simple equipment, while

assuring its applicability to both concrete and steel slabs.

The product developed has solved the concerns of quality, work efficiency, and safety. It has finally passed a strict waterproofing standard prescribed by Nippon Expressway Company Limited (hereafter referred to as "NEXCO).

Following that, we are using this product (Figure 1 and 2) on the Japanese Expressway. Additionally, there had been demand for using this material for steel bridge slabs. Consequently, we confirmed its performance for steel bridge slabs. This paper outlines the development efforts undertaken thus far.

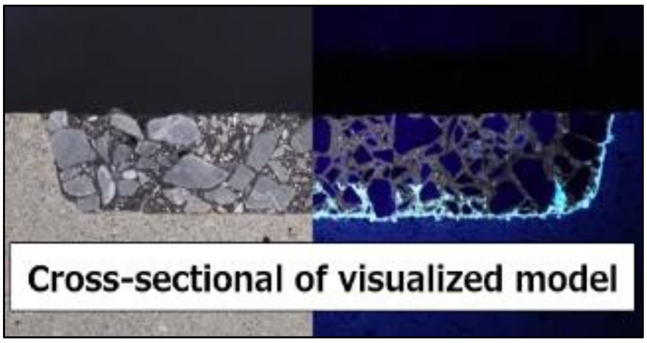

Figure 1. Blue paint part is new material

Figure 2. Packing component

2. The state of problems

The total length of Japan's expressways has reached over 9,000 km since the first route opened to traffic in 1963. About 40% (about 3,700 km) of those bridge sections have been in service for more than 30 years. Meanwhile, bridges constructed before 2002 were not waterproofed. Even if waterproofing was implemented, many bridges must have been damaged and are no longer functional. Rainwater and anti-icing agents spread on the roadway penetrate through cracks into the deck slabs, causing corrosion of the steel bars inside, and resulting in deterioration of the slabs and occurrence of potholes. (Figures 3 and 4)

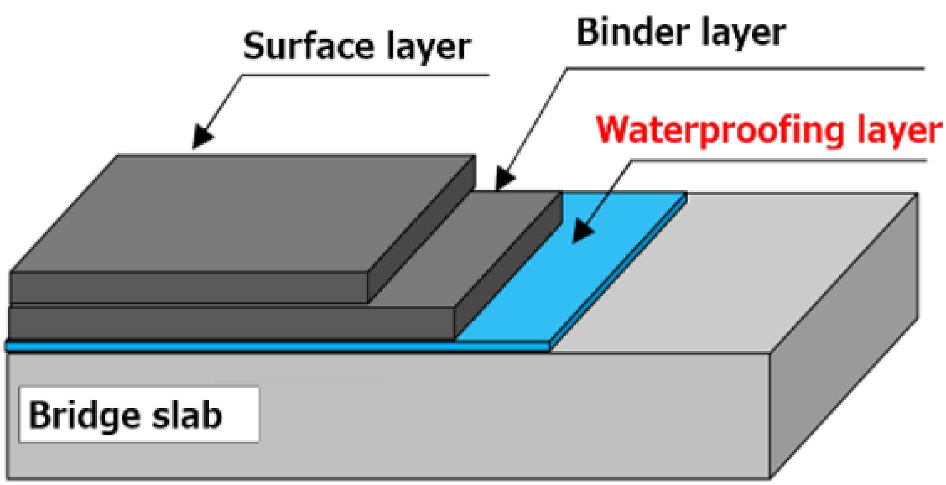

Figure 3. Pavement structure on the bridge

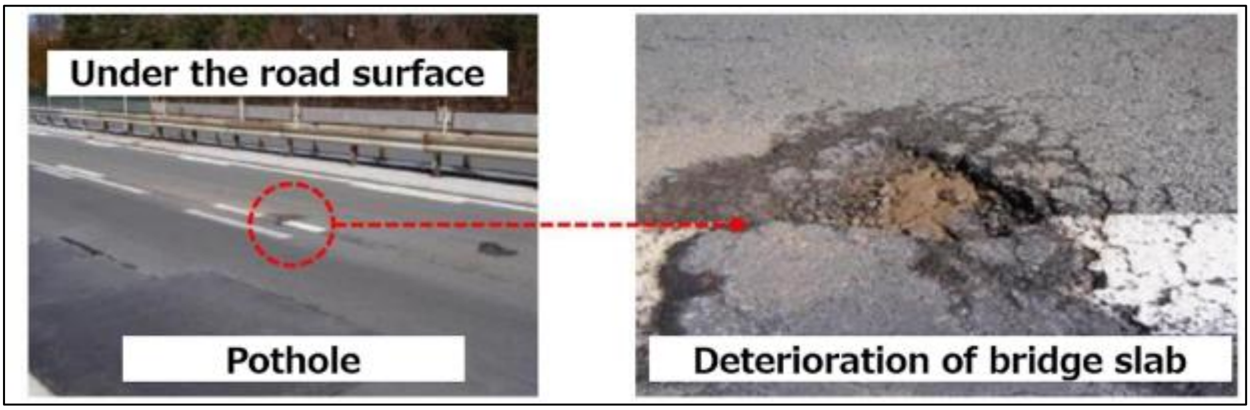

Figure 4. Example of pavement damages caused by concrete slab deterioration.

3. Issues of waterproofing

The currently used waterproofing sheet method in our maintenance job sites is classified as the "asphalt heating type of waterproof layer," which faces the three focus points below.

(1) Quality
Due to the lack of electric pots for small-scale manual pavement work, gas burners are used to melt materials (Figure 5). As a result, proper temperature control is difficult.

(2) Work efficiency
When working at low temperatures in winter, it takes longer time to dry and cure the organic solvent in the primer.

(3) Work safety
There is a risk of fire when transporting heated materials and accidents may happen during loading or unloading heavy materials.

Figure 5. Melted waterproofing material by gas burner.

4. Overseas survey

To solve the above-mentioned work difficulties, we consulted with some major Japanese manufacturers of waterproofing materials but found no existing materials best suited for extremely small-scale, manual pavement work. We thus investigated slab waterproofing on overseas expressways and found that epoxy resin was employed to waterproof steel deck and to prevent anti-rutting in heavy traffic sections in China. The epoxy resin eliminates the use of fire to heat and melt materials. In addition, it is possible to control curing time by designing the resin composition. We started development with a resin manufacturer based on the condition that a waterproofing material best suited for manual pavement work can be composed using simple equipment and without special techniques or hazardous work (Figure 6).

Figure 6. Steel bridge slab adhesive using epoxy-based material in China

5. Development goals

Since the waterproofing material for manual pavement work is to be used at expressway maintenance sites, the material would have to pass the tests of six items as per the Required Performance Grade I for Waterproof Layers for Slabs specified in the Japan Society of Civil Engineer's Guidelines for Pavement Construction Management. Development goals were set to solve four challenges facing job sites as shown in Table 1.

Table 1. Development goals

Premise: Passing the tests of six items as per the Required Performance Grade I※
1. Reduce of work time for waterproof Layers
2. Simplification of tools used
3. Improved construction safety
4. Capability to re-bond damaged waterproof sheets

※Performance Grade I is a standard for bridge waterproofing material for highway repair as determined by NEXCO.

The development was carried out by enhancing the adhesive, which was used on steel deck in China with additional waterproofing and flexibility agents. We tried laboratory tests on multiple prototypes, with a chemical composition that would significantly change the characteristics of the existing product.

6. Verification and field evaluation

Since the results of laboratory tests satisfied the criteria of the six items in accordance with the Required Performance Grade I for Waterproof Layers for Slabs, we asked a third-party for verification. The new materials were officially confirmed to pass the criteria, as specified in Table 2.

Table 2. Results of third-party testing

Test item	Pavement laying load	Pass/fail guideline	Test result	Pass/fail
Waterproofness test Ⅱ	Ⅰ	No leaks	None	Pass
	Ⅱ		None	Pass
Crack follow-up performance test Ⅱ	None	0.3mm or more	4.1mm	Pass
Tensile bond strength test	Ⅱ	0.6N/mm² or more	1.7N/mm²	Pass
	Ⅲ	0.6N/mm² or more	1.7N/mm²	Pass
Shear test	Ⅱ	0.15N/mm² or more	0.87N/mm²	Pass
	Ⅲ	0.15N/mm² or more	0.58N/mm²	Pass
Water immersion tensile bond strength test	Ⅱ	50% or higher tensil bond strength compared to before water immersion	1.0N/mm² 59%	Pass
Chemical resistance test	None	No abnormalites	No abnormalites	Pass

(1) Reduction of work time

The conventional method, as shown in Figure 7, requires a total of about 3 hours for the application work and primer-drying under low temperatures in winter. Drying by a heater is attempted to shorten the curing time, but this approach is problematic because the primer can be ignited, and the surface of the repair mortar will be cracked due to rapid drying. On the other hand, the new method does not need a curing time. Because the heat from the asphalt mixture after application accelerates curing of the epoxy, and the time required for waterproofing work is only 10 minutes.

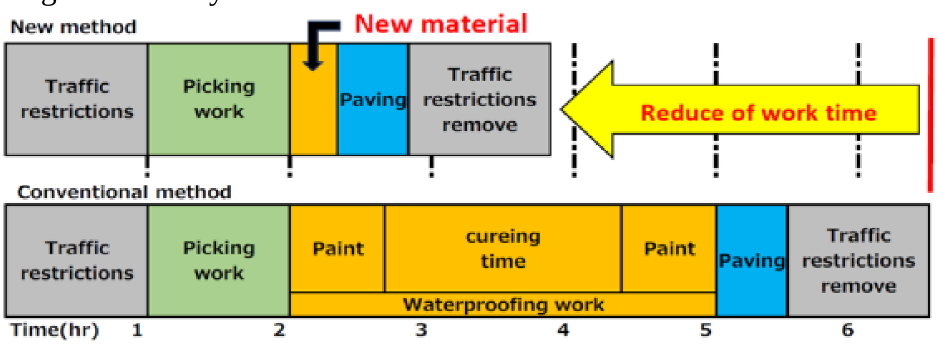

Figure 7. Comparison of work time between the new and conventional methods.

(2) Simplification and Safety

The conventional method requires waterproofing materials to be melted on site, where time and labour is limited for transporting many tools such as melting pots and gas burners and for unloading them. However, with the introduction of new method, waterproofing work can now be performed using only rechargeable agitators and brushes. The weight of the tools has been reduced by 95%, and the labour involved in preparation greatly reduced, too. The paving workers also commended that the field work became much safer with no risk of heavy lifting, fire, or accidents (Figure 8).

Figure 8. Comparison of tools

(3) Capability of re-bonding

We conducted a bond verification test to re-bond peeled waterproof sheets using the new method. As a result, the bond strength between the waterproof sheet and concrete was 1.20 N/mm2 or higher, the specimen fracture surface was remained on the sheet interface, and the bond strength exceeded the sheet strength. This confirms that the new method can be substantially used as an adhesive to bond existing damaged deck slabs (Figure 9).

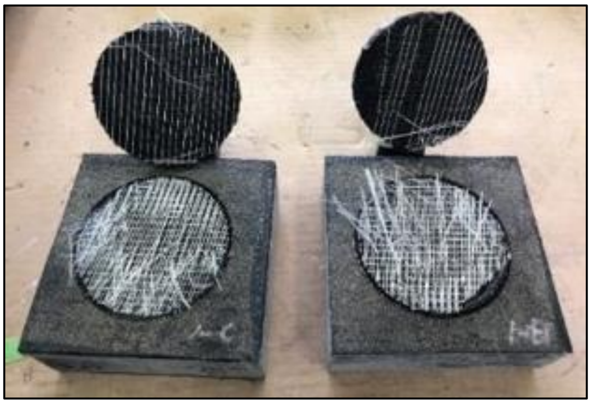
Figure 9. Bond verification test of waterproof sheets and deck slabs

We tried an initial test construction on April 4, 2022. Although the construction was done at a low temperature of 10°C for both the outside air and concrete slabs, we were able to verify that all the problems that the conventional method had faced have been solved sufficiently (Figure 10). At NEXCO, we have done approximately 400 or more repairs using this material, but there have been no damages caused by the waterproofing material (Figure 11). Typically, epoxy-based waterproof materials ensure durability for about 10 years. Since this product is also epoxy-based, it is expected to have similar durability. However, the areas where it has been applied since April 2022 will be regularly monitored to verify its durability.

Measure

Mixing

Painting

Waterproofing just finished

Manual paving

Figure 10. Construction procedures

Figure 11. Appearance 60 days after repair work

7. Field evaluation for steel bridge slabs

This product is primarily composed of epoxy resin that has good compatibility with iron and provides strong adhesive strength, making it suitable for use in concrete bridge slabs as well as for steel bridge slabs.
If the steel slab is rusted, it is necessary to polish the surface before application.
Polishing the slab removes rust and dust from the surface, ensuring strong adhesive strength. Typically, shot blasting is used for removing rust and dust steel slabs. However, for small-scale repair work like this, manual polishing, as shown in Photo 10, can be done cost-effectively. By performing waterproofing, a strong adhesive waterproof layer is formed between the steel slab and the pavement, enhancing the durability of the repair (Figure 12). Furthermore, steel slabs have bolts and rivets at the joints due to their structural design. Conventional asphalt sheet waterproof materials cannot be used where bolts and rivets are present. However, since this product is a liquid type, it can be applied even with bolts or rivets in place, providing a significant advantage (Figure 13). Additionally, steel slabs tend to become extremely hot in the summer, making them prone to flow rutting. However, this product uses epoxy resin with a softening point of 130°C, which is higher than that of asphalt bitumen, allowing it to be used without any issues.

Figure 12. Polishing work to remove rust and dust.

Figure 13. Repair work for steel bridge slab using new material.

The test results for the steel bridge slab also meet the standard values, and the results are shown in Table 3.

Table 3. Results of Third-Party Testing for Steel Slab Bridge

Test item	Test Temperature	Pass/fail guideline	Test result	Pass/fail
Tensile bond strength test	23℃	0.6N/㎟ or more	1.6N/㎟	Pass
	−10℃	0.6N/㎟ or more	2.8N/㎟	Pass
Shear test	23℃	0.15N/㎟ or more	0.4N/㎟	Pass
	−10℃	0.15N/㎟ or more	0.9N/㎟	Pass
Water immersion tensile bond strength test	23℃	50% or higher tensile bond strength compared to before water immersion	1.9N/㎟ 118%	Pass

8. Acknowledgement

For over 20 years, I have been engaged in small pavement repairs and long wanted to make a waterproofing layer safe, easy-handling, and durable during limited manual pavement work. I am proud of the fact that the newly developed material has passed the strict NEXCO standard and achieved substantial results in the actual field. This method will surely lead to the realization of an extended pavement and bridge lifespan. I hope that this paper serves as a reference, and I express my great wish that this new remedy will be utilized worldwide.

9.References

Gaku Suzuki (2023). Reformation of Bridge Slab Maintenance
Development of Specialized Waterproofing Materials for Manual Pavement Work.

Utilizing 3D Point Cloud Data for Effective Road Maintenance Work in Thailand

Kimura Shun[1,*], Mashiko Naoto[2], Witchukreangkrai Eakarat[3] and Chullabodhi Pongsakorn[4]

[1]Engineering Consultants Department, Metropolitan Expressway Co., Ltd., Japan,
s.kimura3424@shutoko.jp
[2]Engineering Consultants Department, Metropolitan Expressway Co., Ltd., Japan,
n.mashiko1013@shutoko.jp
[3]Engineering Consultants Department, Metropolitan Expressway Co., Ltd., Japan,
w.eakarat164@shutoko.jp
[4]Bureau of Highways Maintenance Management, Department of Highways, Thailand,
tuetee2000@hotmail.com

ABSTRACT

This paper presents the results of pilot project partially granted by JICA to contribute to the sustainable development in Thailand by utilizing innovative technology such as 3D point cloud data. Through the project, it has been confirmed the lead-time required in various work processes and the overall time for traffic restriction has been reduced, hence enhancing the effectiveness and efficiency of road maintenance work in Thailand.

Keywords: 3D point cloud data, InfraDoctor, effective road maintenance, preventive maintenance, sustainable development

1. INTRODUCTION

In Thailand, there has been significant dynamism in infrastructure development since the 1980s. Decades of road construction have resulted in a substantial aging infrastructure, necessitating extensive maintenance and repair over the next 10 to 20 years. Consequently, there is an urgent need to transition from conventional corrective maintenance to establishing a preventive maintenance system.

Moreover, Thailand faces relatively rapid demographic changes, characterized by a low birthrate and aging population compared to other ASEAN countries. These demographic trends raise concerns about potential future economic contraction and declining labor force. Hence, enhancing efficiency in maintenance work of road infrastructure becomes one of imperative issues.

According to this background, this project aims to contribute to the sustainable development and to promote innovation in road maintenance work in Thailand. A pilot project was carried out by a joint venture of 6 Japanese companies led by Metropolitan Expressway Co., Ltd. (MEX) with a partial financial support from Japan International Cooperation Agency (JICA) together with the technical cooperation from the counterpart organization, Department of Highways (DOH), Thailand. This project is implemented for contributing enhancement of optimizing maintenance costs through preventive measures, extending the lifespan of structures, and enhancing awareness of maintenance practices through shifting utilization of innovative digital technology such as 3D point cloud data of this project from conventional corrective maintenance of current maintenance system.

2. DIGITAL TECHNOLOGY IN ROAD MAINTENANCE IN JAPAN

In Japan, aging infrastructure that was developed during the high economic growth period has progressively deteriorated. This causes a dramatic increase in the numbers of structural damages detected from the routine and periodic inspection work. However, there is a shortage of inspection and maintenance engineers due to a reduction of working-age population, which causes one of major social issues.

Concerning the above-mentioned issues, MEX, which is the operator of urban expressway network in Tokyo Metropolitan Area, has developed an innovative maintenance and management system (i-DREAMs: intelligence-Dynamic Revolution for Asset Management system) in order to enhance effectiveness and efficiency in maintenance and management work for achieving the sustainable expressway network (Dobashi, 2018). This system has been developed by adopting various digital technologies that have made remarkable progress in recent years, such as ICT (Information and Communication Technology), AI (Artificial Intelligence), IoT (Internet of Things) and RT (Robotic Technology).

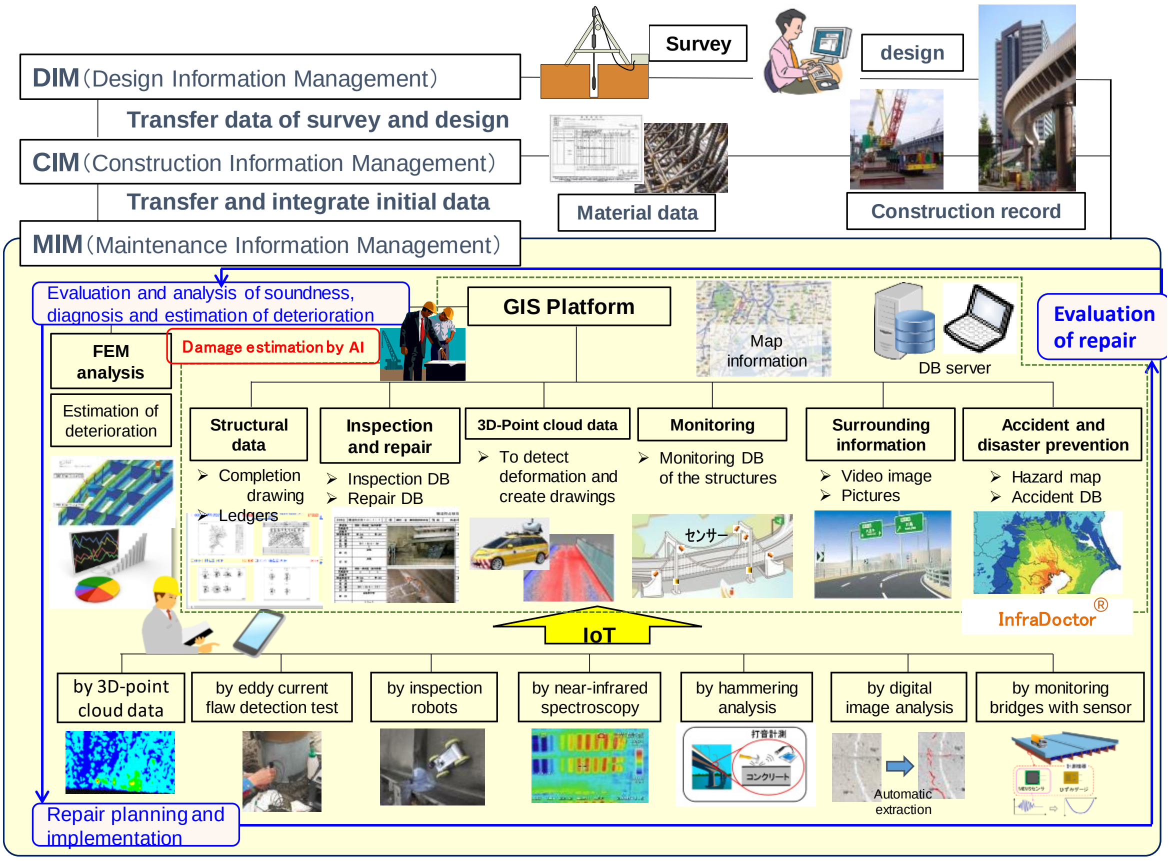

Figure 1 Overall concept of smart infrastructure management system (i-DREAMs).

2.1 Integrated Asset Management System (i-DREAMs, InfraDoctor)

As shown in Figure 1, i-DREAMs is an integrated system that can help implement an efficient maintenance and management work by linking and integrating all relevant data and information obtained during the work processes of survey and design (DIM: Design-Information-Management), construction (CIM: Construction-Information-Management) and maintenance (MIM: Maintenance-Information-Management).

The core technology of i-DREAMs is InfraDoctor, which is a cutting-edge system for supporting infrastructure maintenance utilizing GIS and 3D point cloud data by integrating various data obtained from each work process for various stages of maintenance work on cloud server, as indicated inside of the dashed line box in Figure 1. This system can help support an efficient maintenance and management work of expressway network in MEX.

2.2 Practical Application of 3D Point Cloud Data and Digital Technology

The 3D point cloud data of 320-km urban expressway network in MEX has been obtained and put into practical operation since 2017. Various application currently adopted in the system has been implemented by utilizing the basic and advanced functions of InfraDoctor system as shown in Figures 2 and 3. In addition, by utilizing digital technologies such as image processing analysis and AI, a comprehensive evaluation and assessment of structural

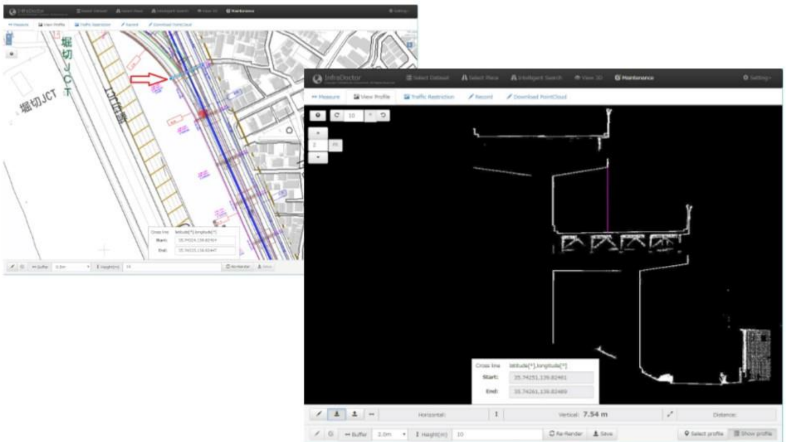

Figure 2 Basic function of InfraDoctor (cross-sectional viewing).

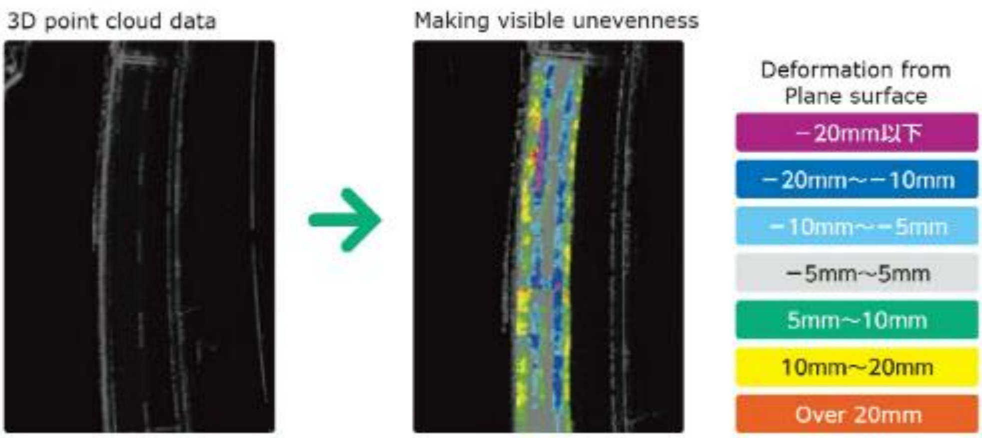

Figure 3 Advanced function of InfraDoctor (damage detection).

deterioration and damage can be achieved, thus allowing the condition of expressway network to be visibly checked. By repeating and conducting the required processes in a maintenance cycle, an advanced and innovative maintenance and management can be implemented in MEX.

3. IMPLEMENTATION OF PILOT PROJECT IN THAILAND

A pilot project was conducted to evaluate the effectiveness and efficiency of utilizing 3D point cloud data in road maintenance work in Thailand. The implementation organization of the pilot project is illustrated in Figure 4. The pilot site under a jurisdiction of DOH was selected by considering the site condition of elevated highway in urban area with at-grade road beneath the elevated sections for ease in the measurement work of 3D point cloud data.

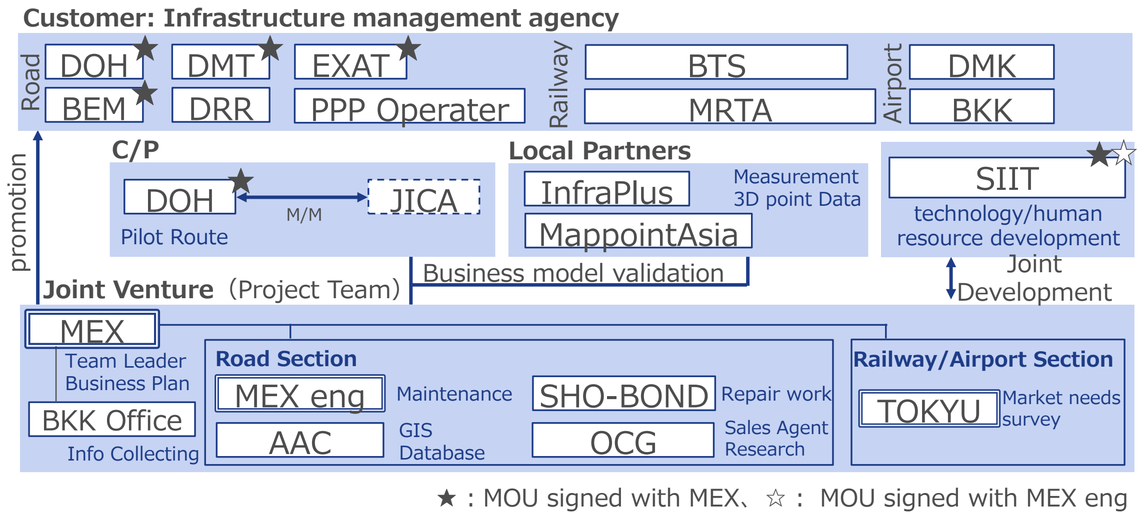

Figure 4 Implementation organization of the pilot project.

3.1 Measurement and Processing of 3D Point Cloud Data

The 3D point cloud data and omnidirectional video of the pilot site were obtained using Mobile Mapping System (MMS) technology by 2 local survey companies. The elevated sections were measured by MappointAsia (MPA), while the frontage road and at-grade road beneath the elevated sections were measured by InfraPlus (IFP), as shown in Figure 5. Since a relative high density of point cloud data is necessary to meet the requirement of practical application of advanced function in InfraDoctor system, the Trimble MX9 as shown in Figure 6 was adopted with the specification as specified in Table 1.

Since the MMS vehicle could run at the regulated speed according to the Thai law, there was no necessity for any road closure during the measurement work, which can help reduce any risk of accident that may occur during the survey work. Moreover, to ensure safety of the surveyors, a warning vehicle provided by DOH followed the MMS vehicle throughout the measurement work (Figure 7).

Basically, MMS is measurable for multiple-lane by once travelling. However, traffic flow had been constantly congested especially in frontage road, hence measurement works were implemented on each lane for obtaining high precision data.

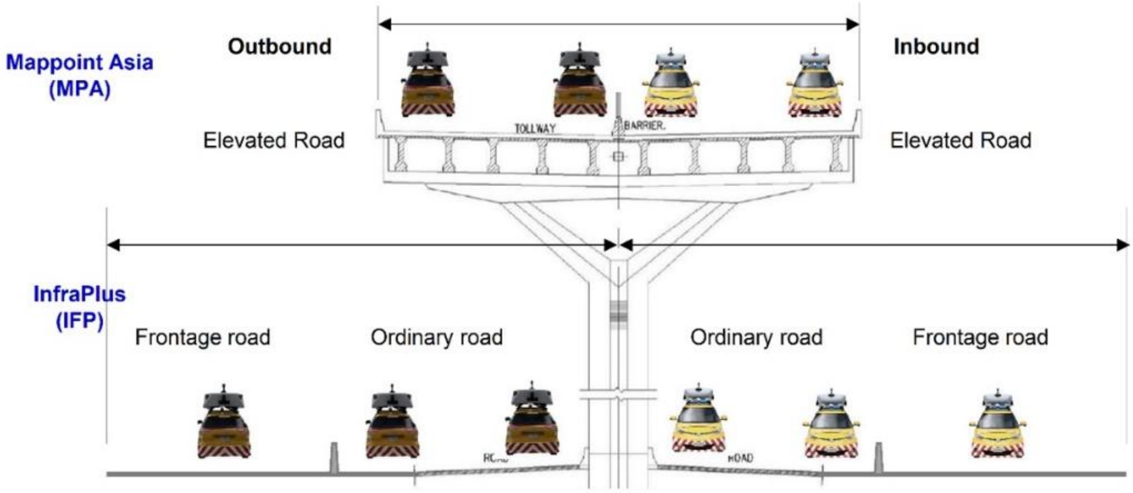

Figure 5 On-site measurement work by MMS.

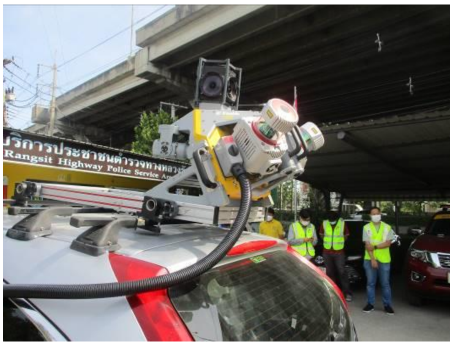

Figure 6 MMS Trimble MX9.

Figure 7 Warning vehicle by DOH.

Table 1 Specifications of Trimble MX9.

MX9 SYSTEM						
Scan speed	500 scans/sec					
Number of laser scanners	2					
Laser positions	Adjustable in 3 horizontal and 3 vertical positions					
MX9 LASER SCANNER						
Laser class	1, eye-safe					
EFFECTIVE MEASUREMENT RATE[1]	300 kHz	500 kHz	1000 kHz	1250 kHz	1500 kHz	1800 kHz
Maximum range target reflectivity > 80%[2]	475 m	370 m	235 m			
Maximum range target reflectivity > 10%[2]	170 m	130 m	85 m			
Maximum number of targets per pulse	up to 15	up to 15	up to 9	up to 7	up to 5	up to 4
Minimum range	1 m @ PRR ≥ 1 MHz, 1.2 m @ PRR < 1 MHz					
Accuracy[3]/precision[4]	5 mm/3 mm					
Field of view	360° "full circle"					

The 3D point cloud data were generated from the collected raw data and were colorized using images captured simultaneously during the survey process, while any irrelevant points on the road surface, e.g., noise data from moving vehicles, were manually removed. Examples of the processed 3D point cloud data are shown in Figure 8. As shown in

Table 2, it is confirmed that the average densities of measured point cloud data exceed the minimum requirement of 400 points/m^2 for this pilot project.

Figure 8 Examples of 3D point cloud data (Left: MPA, Right: IFP).

Table 2 Density of measured point cloud data (road surface, point/m^2).

Elevated sections (MPA)	At-grade sections (IFP)
5,359 points	8,251 points

The coordinates of 3D point cloud data were established based on UTM zone 47N/WGS84 coordinate system, along with the altitude information based on TGM2017. In addition, the absolute accuracy of horizontal and vertical coordinates of processed 3D point cloud data was verified to be within the required tolerance (equivalent to map scale of 1:500) by using Ground Control Points (GCP) as shown in Table 3.

Table 3 Absolute accuracy of coordinates of measured point cloud data.

Direction	Elevated sections (MPA)	At-grade sections (IFP)
Horizontal	6.3 cm	4.8 cm
Vertical	6.3 cm	13.9 cm

3.2 Structural Database Establishment

Related document provided by DOH, including the hard copy of plan-view drawings, completed construction drawings, design documents, specifications and basic ledgers were organized and integrated into the InfraDoctor system, so that they can be easily retrieved from

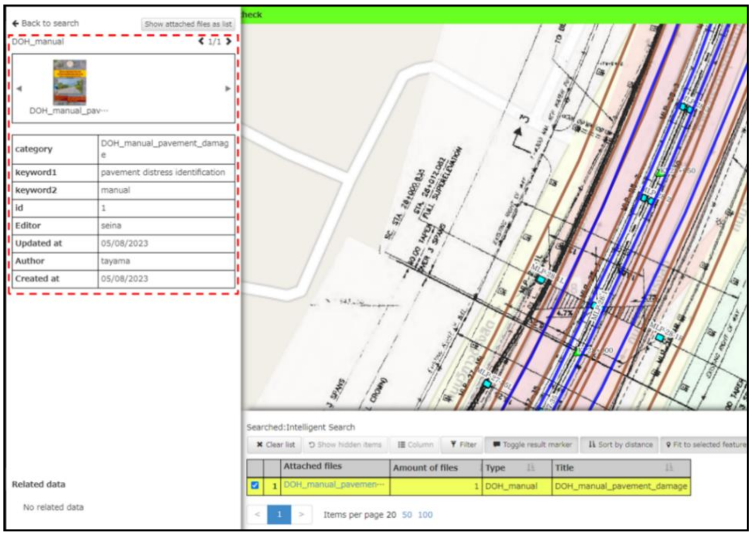

Figure 9 Structural database system (DOH manual).

the cloud platform. The pavement related manual of DOH (Pavement Distress Identification Manual) was also loaded into the system as illustrated in Figure 9.

3.3 Pavement Inspection Database Establishment

In this pilot project, the pavement damage results, such as International Roughness Index (IRI) and rutting, for each evaluation section were computed from 3D point cloud data by utilizing the analysis program jointly developed by the University of Tokyo, Shutoko Engineering Co., Ltd. and Aero Asahi Corporation (Hirano et al., 2018). The computed results were then uploaded into the pavement inspection database system, so that the following functions can be practically utilized, including (1) visualization of pavement damage results on GIS map, (2) aggregation of results based on specified criteria and (3) display of information for each evaluation section, as shown in Figure 10.

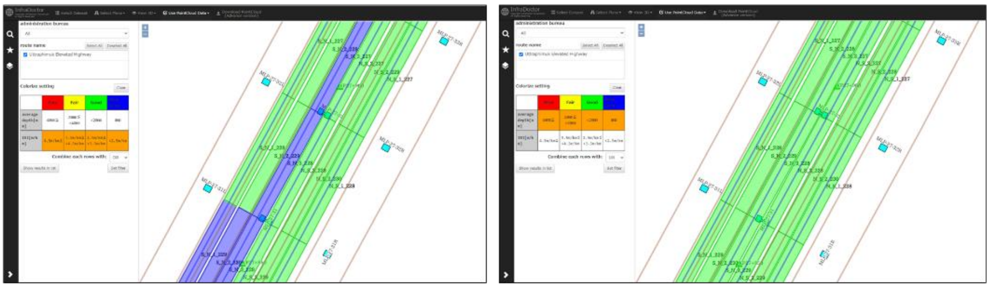

Figure 10 Pavement inspection database system (Left: IRI, Right: Rutting).

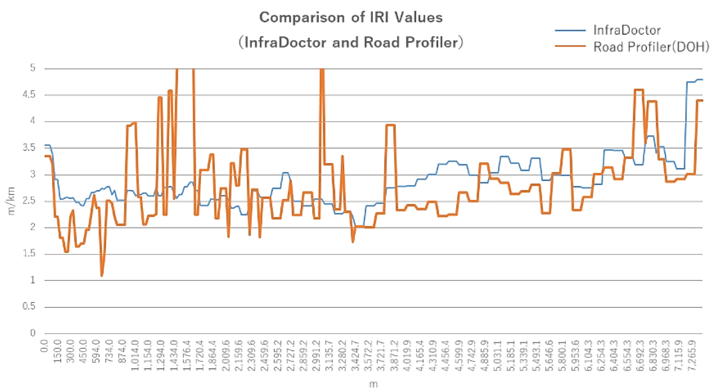

Figure 11 Comparison of IRI values (InfraDoctor and Road Profiler).

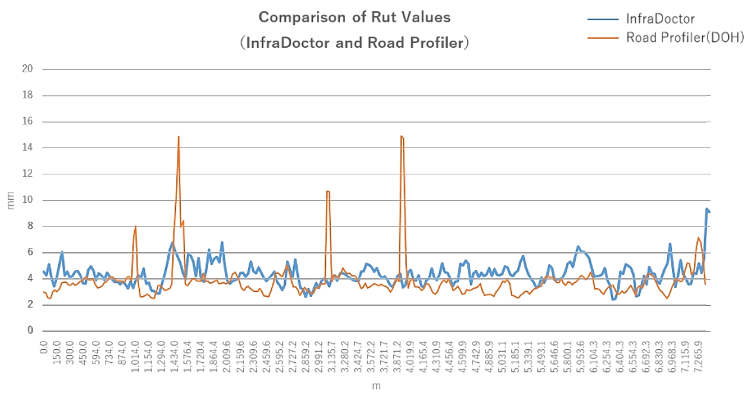

Figure 12 Comparison of rutting values (InfraDoctor and Road Profiler).

The accuracy of calculated IRI and rutting was verified by comparing with the results from the conventional method (road profiler) in DOH as shown in Figures 11 and 12. It can be seen that although there are some discrepancies in some locations, both results are in generally consistent to each other. These discrepancies are assumed to include change of pavement status by difference of measurement period between each measurement method and data-noise from level difference near expansion joints in road profiler. Further study with different parameters such as road surface condition, traffic volume, etc. shall be implemented to improve the accuracy of the pavement damage results calculated by this method.

4. TRIAL OPERATION OF 3D POINT CLOUD DATA IN DOH

The measured 3D point cloud data and related information such as as-built drawings, design manual, pavement damage results, etc., were formulated and loaded into GIS database in the cloud server. The trial operation of such data through the basic and advanced functions of InfraDoctor were carried out by the counterparts in DOH. The followings are examples of such practical application of 3D point cloud data in DOH.

4.1 Dimension Measurement (Site Condition Survey)

Since the coordinates of each point cloud have an equivalent accuracy with that obtained from a conventional on-site surveying, it is possible to accurately measure the dimension of an arbitrary designated part such as road width as shown in Figure 13. Moreover, the clearance limit of road structure can be also verified directly from the system. This implies that the check of site condition can be easily and completely carried out from the GIS system without necessity of work zone traffic control for road closure as required in the conventional method.

Figure 13 Dimension measurement (Left: web-based version, Right: advanced version).

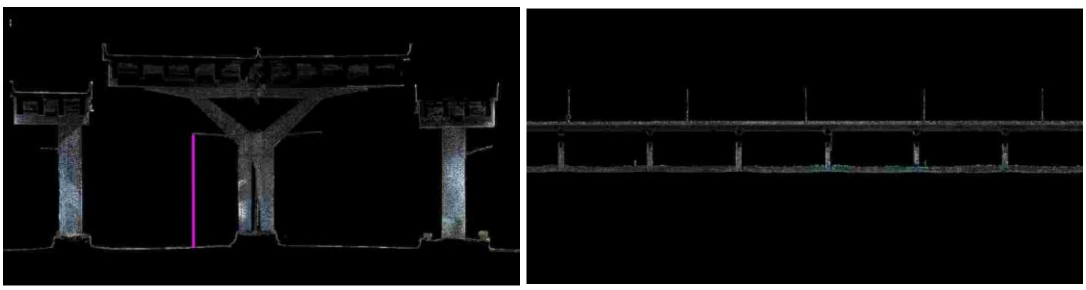

Figure 14 Cross-sectional view of the pilot site (Left: vertical, Right: longitudinal).

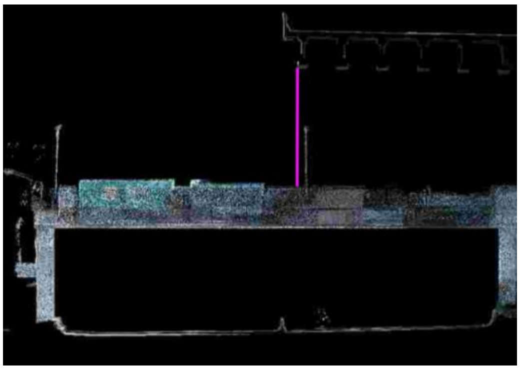

Figure 15 Check of vertical clearance with elevated pedestrian bridge.

4.2 Cross-Sectional View Creation

As shown in Figure 14, any cross-sectional views (vertical and longitudinal section) can be promptly created from the basic function of InfraDoctor. This means that the current site condition (i.e., vertical and horizontal clearance) of structures under a jurisdiction of various organizations can be easily grasped and checked even without any as-built drawings of such structures. Figure 15 shows an example of the measurement of vertical clearance between the elevated highway of DOH and the pedestrian bridge. Moreover, these cross-sectional views can be also exported to various types of drawing file.

4.3 3D Simulation of Bridge Inspection Vehicle

As shown in Figure 16, one of the advanced functions enables a dynamic simulation of any construction machine such as bridge inspection vehicle in the work space of 3D point cloud data. As a result, it is possible to confirm in advance the selection of heavy construction or inspection vehicle that is suitable for the actual site condition, arrangement position, and interference with surrounding structures. Hence, it is possible to provide work safety and to minimize any rework in the actual field.

4.4 3D Simulation of Work Zone Traffic Control

By semi-automatically arranging the traffic control equipment such as safety cones based on stipulated rules on 3D point cloud data, a simulation of work zone traffic control can be easily conducted as illustrated in Figure 17. Therefore, it is possible to confirm in advance whether the work zone traffic control plan is appropriate or not from the driver's point of view.

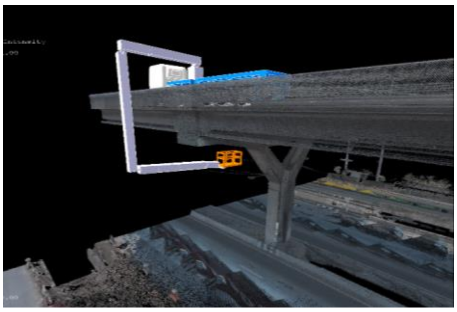

Figure 16 Simulation of bridge inspection vehicle.

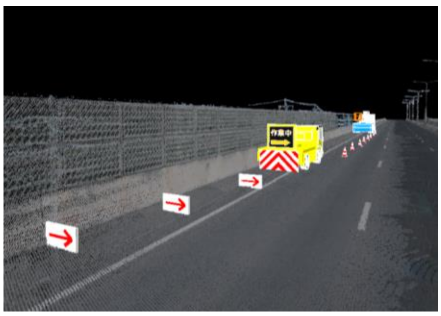

Figure 17 Simulation of work zone traffic control.

4.5 Check of Pavement Damage Results (IRI, Rutting)

The pavement damage results (IRI and rutting) can be displayed and checked on the GIS map by showing different colors according to the damage level. This function can be useful for considering pavement repairment area and pavement repairment prioritization. Thus, this can help reduce the lead-time required for implementation of pavement maintenance work in DOH.

5. CONTRIBUTION TO ROAD MAINTENANCE WORK IN THAILAND

Beneficial impact and contribution of the utilized technology (3D point cloud data, ICT, etc.) adopted in this pilot project on road maintenance work in Thailand were evaluated and summarized in the viewpoints of Sustainable Development Goals (SDGs) adopted by the United Nations as follows.

5.1 Goal 9.b: Technology Development and Innovation

The pilot project has yielded a promising result, as evidenced by the average satisfaction level of more than 80% from the DOH counterparts. This indicated an augmented interest in ICT technology and increased proficiency in utilizing 3D point cloud data for practical applications in road maintenance work. The technology transfer regarding the utilization of 3D point cloud data can create value addition for road maintenance work in Thailand, thereby contributing to Goal 9.b, which emphasizes the support for technology development and innovation.

5.2 Goal 11.3: Capacity for Sustainable Human Settlement Planning and Management

Through the interviews conducted with DOH, it was confirmed that a significant reduction in lead-time, ranging from approximately 50% to 80%, can be achieved by utilizing

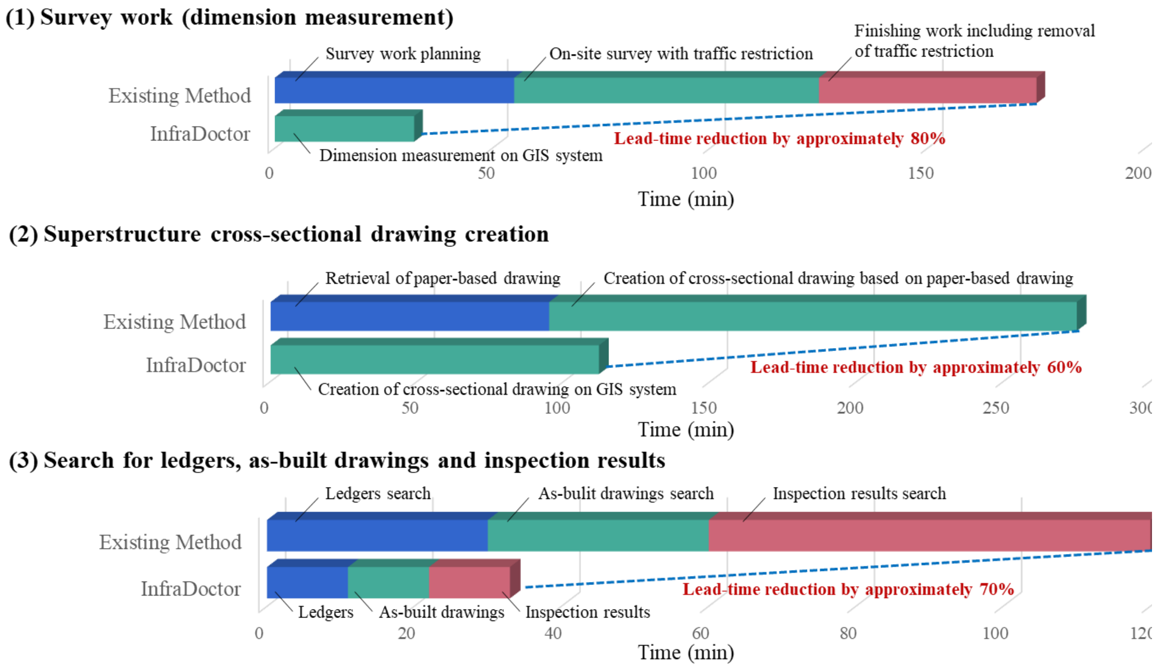

Figure 18 Reduction in lead-time by utilizing 3D point cloud data in DOH.

3D point cloud data, particularly in the following work fields: 1) survey work (dimension measurement), 2) creation of superstructure cross-sectional drawings, and 3) retrieval of ledgers, as-built drawings and inspection results, as shown in Figure 18. This implies that an increased efficiency and optimization of road maintenance operations can be achieved, hence it can contribute to Goal 11.3, which aims to strengthen the capacity for sustainable human settlement planning and management.

5.3 Goal 11.a: Support Positive Social and Environmental Links Between Cities

Figure 19 shows the details of actual time required for traffic restriction in the pilot section of DOH. By utilizing 3D point cloud data, the traffic restriction works for on-site measurement are not required, which can reduce the overall time for traffic restriction by approximately 10%. This implies that the traffic safety in road network could be improved, thus creating an environment where road users can access safe and secure road infrastructure services. This can contribute to Goal 11.a, which focuses on "Strengthening development planning and fostering good connections between cities."

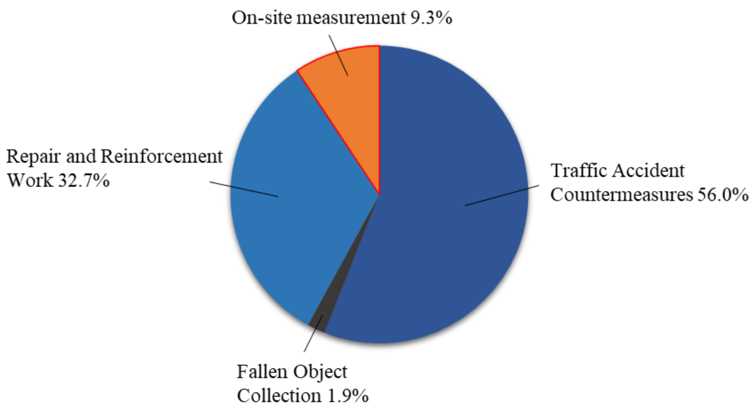

Figure 19 Actual traffic restriction time in DOH (pilot section).

6. TECHNICAL SEMINAR

A technical seminar was conducted for infrastructure management organizations with the objective of enhancing their comprehension of maintenance work through the technical presentations and opinion exchange among the participants (Figure 20). During the discussions in the seminar, it became evident that the adoption of new technology such as 3D point cloud data into a series of maintenance cycles through GIS database system, received positive feedback from the participants since it can enhance the effectiveness and efficiency in maintenance works. Moreover, some comments from the participants suggested that it would be better if the system can seamlessly execute a series of maintenance works ranging from the arrangement and ranking of inspection results to the prioritization and budget allocation for road maintenance work, which can alleviate the required lead-time for each work process.

7. RECOMMENDATIONS AND CONCLUSIONS

7.1 Recommendations

To enhance the accuracy of coordinate information of the measured 3D point cloud data, the sufficient number of GPS-based Control Station should be provided. Moreover, it was observed from the pilot project that there is a room to improve the technical skills of Thai local engineers regarding the data processing and registration of 3D point cloud data, especially the misalignment of different measured point cloud data. For enhancing the technical skills of Thai local engineers, training by dispatched Japanese expert engineers and the creation of manuals formalizing their know-how are effective methods. Additionally, there is a crucial need for flexibility in system modification or customization to ensure adaptable and detailed responses to the requirements of road authorities in Thailand.

7.2 Conclusions

The pilot project on the utilization of new technology such as 3D point cloud data in InfraDoctor system was implemented to evaluate the effectiveness and efficiency in road maintenance work in DOH, Thailand. It was confirmed that a significant reduction in lead-time, ranging from approximately 50% to 80%, could be achieved by utilizing 3D point cloud data. Moreover, the time required for traffic restrictions could be reduced by approximately 10%. These results imply an increase in productivity and efficiency in road maintenance work, while an increase in road safety could be achieved by a reduction in traffic restriction time. However, further studies such as introducing this system on a trial basis to Thai other road organizations and verifying the changing of cost-benefit effect with time shall be carried out to accurately evaluate the detailed cost-benefit effect of utilizing 3D point cloud data in DOH and other road agencies in Thailand.

8. ACKNOWLEDGEMENTS

This project was implemented with a partial financial support from Japan International Cooperation Agency (JICA), Japan, together with the technical cooperation from Department of Highways (DOH), Thailand, through the Minutes of Meetings among JICA, DOH and Metropolitan Expressway Co., Ltd. (MEX) who is the leader firm of the joint venture team of 6 Japanese companies (MEX, Shutoko Engineering Co., Ltd., Aero Asahi Corporation, SHO-BOND corporation, TOKYU Corporation, Oriental Consultants Global Co., Ltd.). The survey works of 3D point cloud data were conducted by 2 local companies (InfraPlus, MappointAsia). The authors would like to express their sincere appreciation for the tremendous supports and cooperation from the above-mentioned organizations throughout the project period.

9. REFERENCES

Dobashi, H. (2018). Innovative management system for infrastructure by utilization of 3D point cloud data based on GIS platform. International Press-in Association News Letter (Special Contribution), 3(2), 3–9.

Hirano, H., et al. (2018). Evaluation of local deterioration of pavement surface by spatial frequency analysis based on short-time fourier transform. Journal of Japan Society of Civil Engineers, 77, I_121–I_129.

PathWatcher: AI-Enabled Automated Footpath Inspection System

Benjamin W.L. Aw[1], Andy S.C. Low[1], Desmond A.B. Lim[1], Cadmon Kwan[1], Dean D.Y. Su[1], Daniel W.T. Cheng[1], Evan R.C. Sim[1], P.B. Phua[1]

Colin Khor[2], Z.Q. Lim[2], S.Y. Foo[2]

[1] LightHaus Photonics, Singapore, ppohboon@lighthaus.com.sg
[2] Land Transport Authority, Singapore

ABSTRACT

Global land transport sector is being transformed by AI, automation, mobile connectivity, and big data, creating opportunities for improvement and job creation. In Singapore, land transport sector's footprint occupies 12% of the land, with extensive roads, footpaths, rail, and cycling paths. Regular and efficient maintenance is essential to enhance usability and safety, but current manual inspection methods are inefficient. Inspectors walking the pavements often miss defects due to human error and physical limits. Communication issues further waste time and resources in fixing problems.

LightHaus Photonics and Land Transport Authority (LTA) of Singapore have collaborated to reduce manual inspection inefficiencies with PathWatcher, an AI-enabled device that captures pavement defects. Compact and lightweight, PathWatcher is bicycle-mounted and compliant with Singapore's Active Mobility Act. Its modular design also allows for man-pack configurations for less accessible pavements.

PathWatcher is equipped with pavement-facing high-resolution camera that can resolve defects of <1mm, four high-resolution panoramic cameras to create an equirectangular panorama projection for panoramic scene. Precise geo-localization of defects is achieved with multiband GNSS receiver equipped with Real Time Kinematics (RTK) capabilities.

The AI model is trained on CNN-based algorithms that can run real-time inferences of footpath defects. The model can detect concrete cracks, tactile tile cracks, grating cover defects, tiles cracks, etc. with overall detection probabilities of >80%. Well-calibrated pavement-facing camera imaging parameters also allows for assessment of defect severity.

Data is pushed to and managed in the cloud where it serves as a central hub for information visualization through a web application. Semi-autonomous generation of defect reports and push notifications facilitates maintenance contractors for quick turnaround of repairs.

PathWatcher increases efficiency, enabling staff to cover more ground and reducing reliance on manual inspections, also aiding in structural inspections of linkways and bus stops.

Keywords: pavement defect inspection, machine learning, computer vision, artificial intelligence

1. INTRODUCTION

In Singapore, the total inventory of pavements/cycling paths is close to 5,500 km and over five thousand of commuter facilities including the bus shelters. There are also around 228 km of covered linkways on some of the pavements. It is essential for these commuter and road-related facilities to be inspected regularly to ensure their safety and functionality to serve the public.

LTA has in place a routine inspection regime to inspect and monitor the condition of the commuter and road-related facilities such as pavements, cycling paths, railings and traffic signs, etc. The regime includes capturing of potential safety concerns and defects (i.e., cracked pavement, dislodged tiles, illegal advertisements, overgrown foliage, etc.) conducted by inspectors on foot. Upon the identification and tabulation of defects in manual reports, the necessary rectification work will then be carried out by the maintenance contractor.

This routine inspection is a visual inspection that is carried out by qualified inspectors with relevant civil engineering background and road pavement knowledge. Close to 40 walking inspectors are deployed daily to inspect the pavements, commuters and road related facilities and it takes a 3-month cycle to complete a round of the inventory pavements. The process is tedious and laborious. Great effort is also needed to tabulate the defects sheet through excel to incorporate description of defects, location as well as severity of defect.

Figure 1 Conventional visual inspection of pavement defects carried out by inspectors on foot, spotted defects are manually captured with a handheld camera.

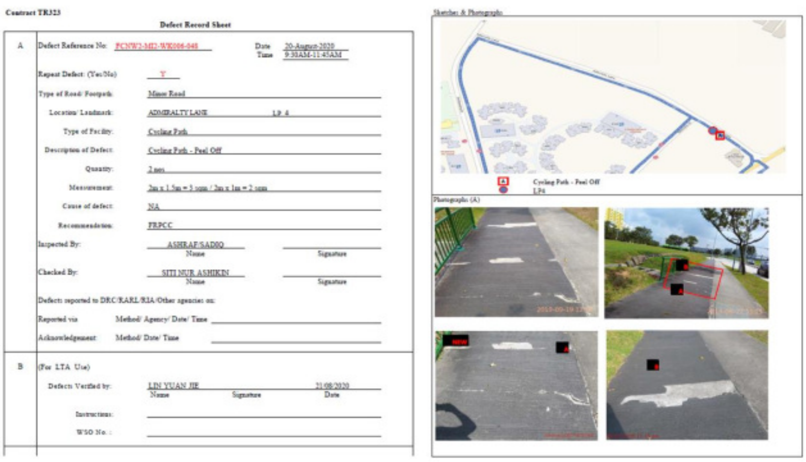
Contract TR323

Defect Record Sheet

A
Defect Reference No: PCNW2-MI2-WK006-048 Date 20-August-2020 Time 9:30AM-11:45AM
Repeat Defect: (Yes/No) Y
Type of Road/ Footpath: Minor Road
Location/ Landmark: ADMIRALTY LANE LP 4
Type of Facility: Cycling Path
Description of Defect: Cycling Path - Peel Off
Quantity: 2 nos
Measurement: 2m x 1.5m = 3 sqm / 2m x 1m = 2 sqm
Cause of defect: NA
Recommendation: FRPCC
Inspected By: ASHRAF/SADIQ (Name) (Signature)
Checked By: SITI NUR ASHIKIN (Name) (Signature)
Defects reported to DRC/RARL/RIA/Other agencies on:
Reported via Method/ Agency/ Date/ Time
Acknowledgement Method/ Date/ Time

B
(For LTA Use)
Defects Verified by: LIN YUAN JIE (Name) (Signature) 21/08/2020 (Date)
Instructions:
WSO No.:

Sketches & Photographs
Cycling Path - Peel Off
LP4
Photographs (A)

Figure 2 Typical Defect record sheet manually prepared after walking inspections.

2. PATHWATCHER SYSTEM

To improve the efficiency and effectiveness of our footpath inspection work, we have conceptualized and developed PathWatcher – an integrated system specialized for footpath inspection. Pavement defects are automatically detected using artificial intelligence (AI) which is trained to pick out a wide variety of defect types.

The PathWatcher integrated system comprises of its Front-end Unit, Data Processing Software and Cloud-hosted Web App. Each of these shall be presented in further detail in the following sections.

PathWatcher is designed to be operated by using the Front-end Unit as the surveying instrument during inspection runs, collected data are post-processed by the Data Processing Software, finally all processed data outputs are uploaded to the cloud through the Cloud-hosted Web App. Defect reports are automatically generated through the Cloud-hosted Web App for maintenance personnel to carry out repair works on the ground.

In its bike-mounted configuration, the hardware platform measures 1.66m long, 0.61m wide, 1.43m tall with an unladen weight of 19.3kg including bicycle. The compact and lightweight mechanical design of PathWatcher enhances safety and handling during operation on public roads, abiding to Singapore's Active Mobility Act which is a set of rules and code of conduct to foster safer sharing of public paths among various users. A manpack configuration is being developed to allow PathWatcher to be used in less-accessible pavements.

Figure 3 PathWatcher Front-end Unit performing pavement inspection.

2.1 Front-end Unit

The Front-end Unit is a custom hardware platform fitted with a multitude of sensors. The embedded system features a downward pointing high resolution camera with diffraction limited optical lens system, a 360° panoramic camera, a high precision Global Navigation Satellite Systems (GNSS) receiver capable of real time kinematic (RTK) positioning, and related interfacing electronics which allows for real-time recording of high-resolution images which can be geolocated down to centimeter-level accuracy.

The Front-end Unit contains a power-efficient single board computer serving as the data recorder. The single board computer can be equipped with up to 8TB solid state memory allowing for data storage of up to an equivalent of >500km of surveyed footpath. A 20Ah Lithium-Iron-Phosphate (LiFePO4) battery provides the electrical power required to sustain continuous image streams for up to 5 hours of operation time. It is integrated with an internal battery management system which protects again fault conditions such as over-charging and over-discharging.

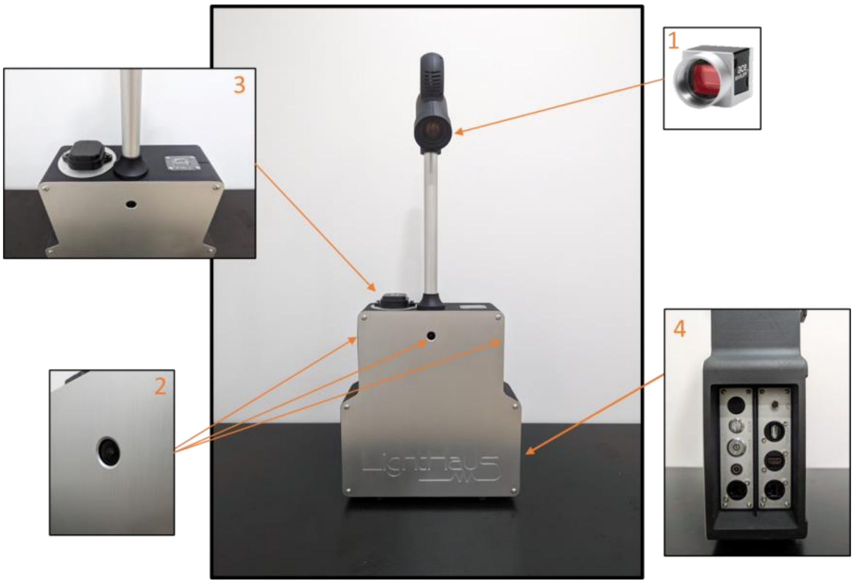

Figure 4 PathWatcher Front-end Unit in standalone configuration, equipped with (1) high resolution pavement camera, (2) embedded panoramic cameras, (3) GNSS active antenna and lux sensor, (4) operator access panel.

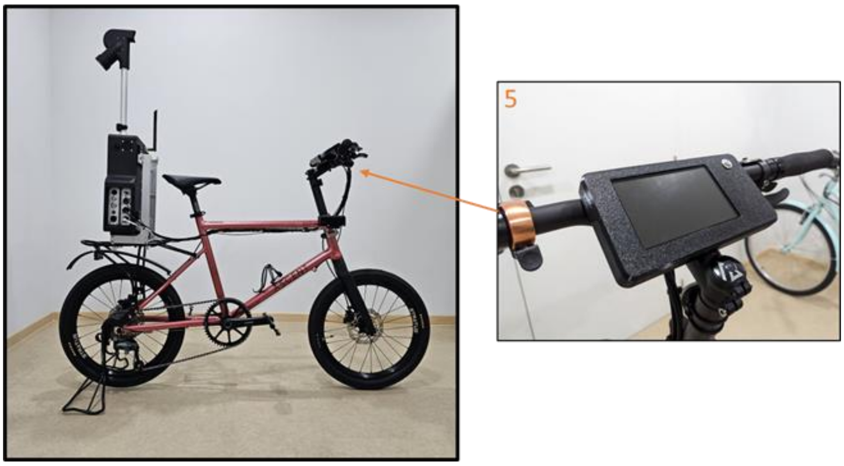

Figure 5 PathWatcher Front-end Unit in bike-mounted configuration, securely mounted onto a lightweight bicycle with custom designed mountings, equipped with (5) touchscreen panel.

Imaging Sensors

The pavement-facing camera is an industrial-grade detector using the Sony IMX183 image sensor with 20 megapixels, running at a maximum of 17 frames per second via high data throughput USB3.0 interface with rates of up to 350MB/s. Coupled with a 6mm F/1.8 diffraction-limited optical lens, the pavement-facing camera has an instantaneous field-of-view (FOV) of 400µrad, providing a center ground sampling distance of 0.7mm at the designed mounting configuration of the camera in the PathWatcher system. This optical setup allows the monitoring of a pavement 3.5m wide while capturing defect details of below 1mm in dimensions. The raw image is distortion-corrected to remove lens distortion artifacts, flat-field corrected to ensure uniformity, and finally color-balanced for accurate color reproduction.

All-round panoramic images are captured using an array of four identical industrial-grade detectors running the OnSemi MT9J003 10MP sensors. The camera arrays are Gigabit-ethernet enabled, interfaced and controlled via a 4-port switch, and are embedded in the Front-end Unit, pointing forwards, backwards, to the left and to the right of the operator. Each detector is coupled to a 3.12mm F/1.8 lens, providing a 150 degrees horizontal FOV per camera, with a 60 degrees overlapping FOV for image stitching. The instantaneous FOV of the panoramic image is 535µrad, providing good spatial resolution of the vicinity around the PathWatcher system.

Processing of the all-round panoramic images is performed as follows: each individual image was first distortion-corrected, flat-field corrected and color-balanced. The corrected image is then projected to a cylindrical plane to map a 2D "flat" image to a 3D-like surface. Finally, each adjacent image is aligned and stitched together using feature detection and matching.

Figure 6 Image of pavement containing crack defects with estimation of the crack length.

Real-time Kinematic (RTK) Positioning

With RTK positioning, the geocoordinates measured by the embedded GNSS receiver reach centimeter-level precision when operating in RTK-mode. High precision positioning is highly favored in surveying applications with its obvious advantages. Without RTK, the traditional positioning accuracy is around 5 meters and is susceptible to measurement errors such as clock errors, orbit errors, satellite biases, atmospheric errors and multipath errors. RTK positioning addresses these shortcomings using a fixed base station to deliver correction data called RTCM (Radio Technical Commission for Maritime) corrections. RTCM corrections are interpreted by the embedded GNSS receiver in real-time in conjunction with satellite navigation signals to filter out the measurement errors, ultimately unlocking centimeter-level positioning accuracy for PathWatcher.

PathWatcher subscribes to the Singapore Satellite Positioning Reference Network (SiReNT) service initiated by the Singapore Land Authority (SLA), which provides real-time RTCM correction data over-the-air through a protocol known as Network Transport of RTCM with Internet Protocol (NTRIP). By tapping on the SiReNT service and its infrastructure, users need not set up their own fixed RTK base stations.

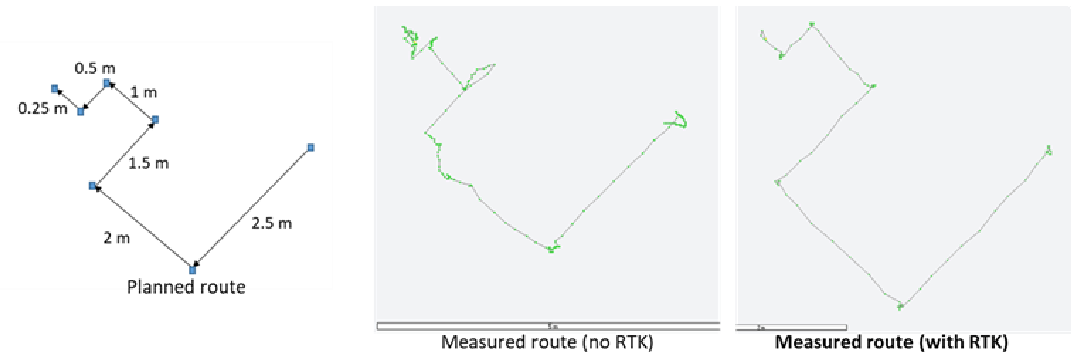

Figure 7 Measured travelled routes without RTK positioning (middle) and with RTK positioning (right). Without RTK positioning, the recorded positions are prone to errors and drifts.

2.2 Data Processing Software

While the Front-end Unit is being operated on ground during an inspection run, it continuously captures and stores data into its internal onboard memory. The stored data is then transferred out of the onboard memory into a separate desktop personal computer (PC) at the end of every inspection run over a Secure File Transfer Protocol (SFTP) link. The PC is housed indoors and is equipped with the necessary hardware (i.e. GPU, RAM) and software packages to automatically perform data pre-processing and pavement defect detection. The processed data is then uploaded to the Cloud-hosted Web App for archival and coordination of repair works.

Data Pre-processing

In the initial stage of data pre-processing, the captured images undergo a series of image processing techniques such as distortion correction, image stitching and equirectangular projection. This will ensure that any imaged objects or targets maintain their true shape and dimensions for the later stages of data processing. An interactive all-round panoramic scene, similar to Google Street View, is also created in this stage to enhance spatial awareness and accurate pinpointing of locations.

Data pre-processing is executed on the PC in batches, each containing large numbers of images split across multiple CPU threads in parallel. At the end of this stage, the distortion-free and rectified images are then added into the AI pipeline for inferencing.

Figure 8 Flattened stitched image of a sample panoramic scene.

Machine Learning

The AI-enabled PathWatcher employs machine learning (ML) technology at its core, unlocking the ability to process enormous volumes of data efficiently, enabling the automatic detection of defective pavements by performing inferences at real-time speeds, potentially discovering new insights and trends that may not be noticeable through existing methods.

Traditionally, footpath inspection is predominantly conducted through manual inspection which are labor-intensive and prone to inconsistencies introduced by human factors. To address these challenges, various traditional frameworks have been developed to automate crack detection using Gabor filter (Zou et al., 2012) and minimum spanning tree construction (Salman et al., 2013). However, these frameworks suffer in real-world situations due to the variations in lighting conditions and variety of pavement texture. Currently, there is an increasing focus on the application of deep learning-based methodology to automate pavement defect detection. The advancements of deep learning have introduced object detection and segmentation models that can effectively localize and classify pavement defects present within images.

In (Zhang et al., 2016), Zhang et al. proposed training a convolutional neural network (CNN) to classify image patches as either crack or non-crack. Gou et al. (Gou et al., 2019) proposed an improved Faster R-CNN (Ren et al., 2017) model for pavement crack detection and localization. Gou et al. noted that traditional crack detection methods suffer in performance when the images are of low quality. The improved Faster R-CNN model incorporated ResNet101 (He et al., 2016) for feature extraction and a modified region proposal network. Their research findings yield improvements in results even when dealing with images affected by noise and illumination. However, despite having better detection accuracy, their improved model pales in inference speed when compared to single-stage detectors such as YOLOv3 (Redmon & Farhadi, 2018) which can perform object detection in real-time.

Nie and Wang (Nie & Wang, 2019) discusses particularly the comparison between YOLOv3, RetinaNet (Lin et al., 2017) and Faster R-CNN on the detection of pavement cracks. The results demonstrated that while YOLOv3's accuracy was slightly lower than Faster R-CNN, its detection speed was markedly superior. In (Mandal et al., 2020), Mandal et al. compares the difference between popular single-stage object detection models, YOLOv4 (Bochkovskiy et al., 2020), CenterNet (Zhou et al., 2019) and EfficientDet (Tan et al., 2019) in detecting various classes of pavement cracks. Their results showed that the YOLO-based model achieved the best performing results amongst the detectors. Qiu and Lau (Qiu & Lau, 2023) also explored various YOLO models integrated with UAV technology to provide real-time detection of cracks on tiled sidewalks. The YOLO models showed a robust adaptability to a range of environmental conditions. In segmentation tasks, Sarmiento (Sarmiento, 2021) uses DeepLabv3 (Chen et al., 2017) for the segmentation of road defects in the Philippines. Sarmiento observed that DeepLabv3 effectively detected and segmented complex defects.

Previous studies have compared and found that R-CNN detectors, which follows a two-stage process, is usually capable of higher accuracy and precision against real-time single-stage detectors like YOLO, the additional computational steps inherently slow down the detection pipeline at inference time. In our scenario where the slower inference times of R-CNN detectors can be a significant drawback, it is imperative that the collected images are processed and delivered swiftly to the maintenance personnel. This rapid turnaround ensures that any critical defects and safety concerns are promptly addressed, allowing for immediate repairs and minimized downtime.

While these studies have made significant strides in pavement defect detection using deep learning methodologies, it is important to note that many of the image datasets were taken with smartphones mounted on mobile platforms. This may lead to inconsistencies within the collected datasets like varying perspectives and image quality which may impact the detection models' performance. Comparatively, the images captured by the Front-end Unit are likely to be more consistent throughout inspection runs due to its rigidly mounted optical setup and thus removes some layer of complexity towards building a balanced training dataset.

The AI model was constructed with an ensemble of YOLO-based single-stage detectors for when inference speed is critical, and R-CNN-based two-stage detectors for when accuracy is vital. A set of training data consisting of about 3350 labelled images, created from a combination of historical images containing defects stored by LTA and images captured by the Front-end Unit, was used to train the detectors. The resultant AI model can detect concrete cracks, tactile tile cracks, missing tactile tiles, cracks and large gaps on tiled footpaths, grating cover defects, and uneven footpaths with overall recall rate probabilities of >80%. Both training and inference are executed on the PC, accelerated with the help of an equipped Nvidia RTX3090 GPU. When defects are detected within the images, the defective areas are highlighted by drawing bounding boxes around it with each bounding box tagged with the predicted defect type. These bounding box outputs from AI model alongside the remaining captured data are then uploaded into the cloud.

It is observed that environmental effects such as brightness of the scene, presence of fallen leaves and twigs can negatively impact predictions by a reduction in confidence score and/or inducing an increase in false positive predictions. This shall be studied and addressed in future development of the system.

At present, the focus is placed on pavement defects where the probability of needing repair works is higher and occurrence of pedestrian safety concerns is also higher. Hence, only the pavement images are used as inputs to the automated defect detection process in the current development. The list of defect types detectable is expected to grow as more data is captured and fed into the machine learning iterative training process.

The AI model is also planned to be scaled up to include detection of defects on other forms of infrastructure above ground (e.g., bus stop infrastructures) by including panoramic images for ML training and inference.

Figure 9 List of defect types currently detectable by the AI model and planned defect types in active development (top), images of pavement defects detected by AI model (bottom).

Cloud-hosted Web App

A web application was developed on the Amazon Web Services (AWS) framework as a centralized hub for users of the PathWatcher system to interact with the fully processed data in the cloud archive storage.

The Web App allows users to input parameters (e.g. date, time, defect type, location) for a filtered search and calls up a list of datasets from the storage database which matches the parameters. The locations of these datasets are also plotted on a map view window for geospatial visualization. The geolocations of the datasets are plotted in grouped clusters to prevent cluttering on the map view window, which automatically re-clusters itself depending on the map zoom levels. The user can select a dataset for detailed viewing of its captured pavement and panoramic images, with bounding box overlays if any defects are predicted by the AI model. If the pavement defect detected by the PathWatcher system is deemed necessary for repair, a standardized report containing relevant information (i.e. images, location, defect types, etc.) can be easily generated to facilitate the maintenance team for repair works on the ground.

The Web App also features a length estimation tool (Figure 6) to indirectly measure the size of the defect on the pavement for assessment of defect severity. Through this feature, the user avoids the need to physically measure the dimensions of the defects onsite, instead can simply obtain the dimensions through software conveniently. This is possible due to the well-calibrated and well-characterized optical properties of the pavement-facing camera. Telegram Instant Messaging service is also integrated into the Web App, which allows for customizable notifications to be pushed automatically to Telegram users during defined events (e.g., critical defects found requiring urgent repair).

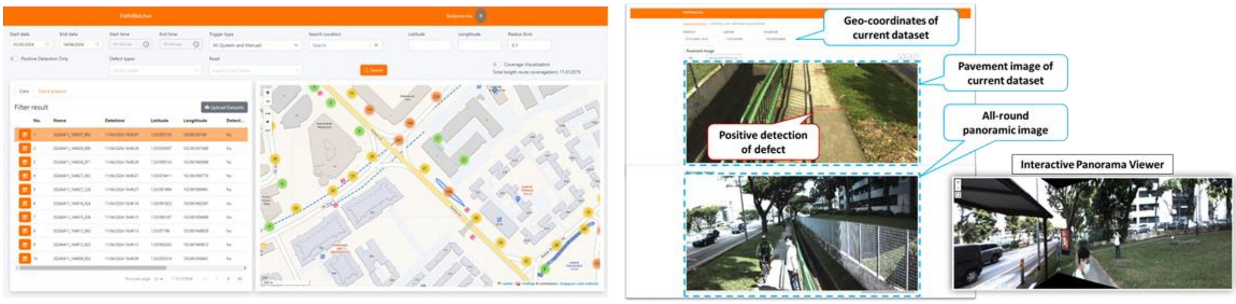

Figure 10 Cloud-hosted Web Application – dataset selection with map view (left), detailed view (right).

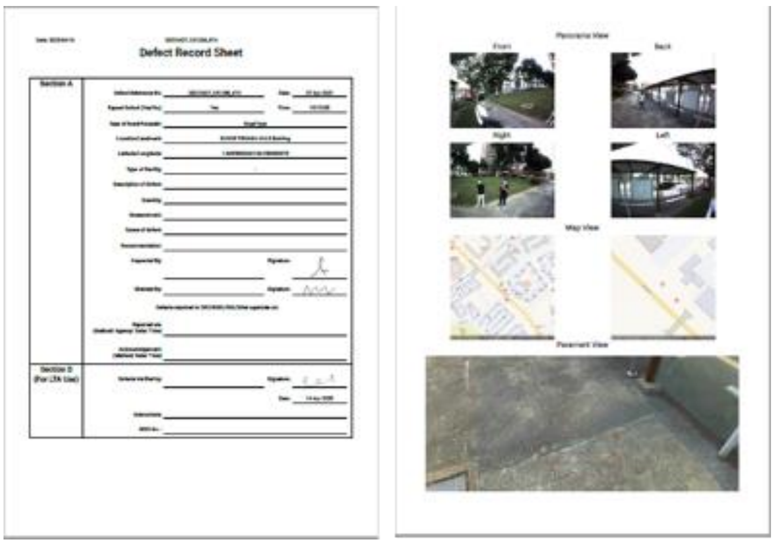

Figure 11 Standardized report automatically generated by the Web App.

3. RESULTS

An outdoor trial was conducted as a measure of performance of the PathWatcher system. The objective of the trial was to subject the bike-mounted instrument to real-world pavement conditions while testing its effectiveness at detecting defects along travelled pavements. A 1.5 km stretch of defect-ridden pavement was identified as the user acceptance testing (UAT) environment for the outdoor trial.

The Front-end Unit in its bike-mounted configuration was found to be simple to handle and rides comfortably along the identified pavement in which cracked surfaces, slopes and uneven surfaces were encountered. All electrical connectors and mechanical fixtures were inspected post-trial to be intact with all screws holding their torque.

A total of 916 datasets, each containing one pavement image, four all-round images for panoramic stitching, a set of logged measured sensor values made up of GNSS geocoordinates, location uncertainty, ground speed, acceleration in XYZ axis, platform orientation in XYZ axis, ambient light measurement values and power measurements, were continuously acquired and stored by the Front-end Unit during the conduct of the trial. Out of the 916 pavement images, 481 contained pavement defects regardless of size or severity.

Upon processing the captured data through the Data Processing Software, the AI model reports a defect detection overall recall rate of 93.3% and an overall precision rate of 71.3%, despite the low amount of training data used to train the AI model. While the high recall rate suggests that the PathWatcher AI model is highly performant, it should be taken into account that the AI model was trained on images that are local to part of Singapore island and may not generalize itself to other types of pavements globally at this stage.

The positive results demonstrates that the PathWatcher system can reliably produce quality data while operating under real-world conditions, allowing the AI model to maximize its probability of achieving its objective – autonomous detection of pavement defects along our footpaths.

With the successful development of the PathWatcher, the manual regime of walking inspection would be further enhanced with efficiency and productivity. The manpower reduction upon adopting PathWatcher reduced significantly to more than 50% from original. AI detection of defects on pavement from video captured and with autogenerated defects' report as well as the various functions within the Web App, it provides a streamline and improved processes in LTA's inspection and maintenance operation.

Table 1 ML training data size, recall rate, precision rate breakdown across defect types.

Defect Type	Training Data Size	Recall Rate (%)	Precision Rate (%)
Footpath Cracks	1169	89.2	95.2
Grating Cover Defects	589	97.9	92.3
Tactile Tile Defects	556	93.3	95.4
Tile Defects	552	74.4	97
Uneven Footpath	304	86.9	76.9
Uneven Grating Cover		53.8	63.6

4. CONCLUSIONS

LightHaus Photonics and Land Transport Authority of Singapore has jointly designed and developed the PathWatcher, an automated footpath inspection system fully integrated with customized hardware and software.

The front-end hardware is engineered for outdoor conditions and designed with ease-of-use in mind. The back-end software works well with the front-end hardware and presents the captured data to the user in an intuitive manner through the Web Application. The AI model was constructed with a suite of single-stage detectors and two-stage detectors, each uniquely trained to detect a specialized defect type. Together, the PathWatcher system achieved a remarkable defect detection rate and with its automated report generation feature, shall increase efficiency and supplement our current efforts in keeping our footpath infrastructure safe for all pedestrians and footpath users.

As PathWatcher is progressively operated throughout Singapore's footpath network, it is expected that the system will be exposed to more types and variants of pavement defects as well as a buildup in volume of training data. Being the key enabler of PathWatcher, its AI capabilities are expected to expand beyond its current and bring about significant benefits to all in the industry.

5. ACKNOWLEDGMENTS

The authors wish to express their gratitude to fellow colleagues and organizations in the success of development and deployment of the PathWatcher.

We wish to thank Enterprise Singapore (ESG) Mr. Nicholas Tey, LTA Technology & Industry Development (TID) Mr. Mark Tan, Ms. Caroline Tan and Mr. Irving Toh for their efforts and initiatives in open innovation and industry collaboration through the "Accelerating Co-Innovation for Transformation & Export (Xcite)" program and co-funding this project through two important phases of development.

We also wish to thank our colleagues from LTA Traffic and Road Operations (TRO) / Commuter Facilities Management (CFM) and Active Mobility Acts (AMA) for conceiving the project's problem statement, making the project possible, and guiding the technical team with their valuable insights and expertise on footpath infrastructure.

6. REFERENCES

Bochkovskiy, A., Wang, C.-Y., & Liao, H.-Y. M. (2020). YOLOv4: Optimal Speed and Accuracy of Object Detection. arXiv.Org. https://arxiv.org/abs/2004.10934

Chen, L.-C., Papandreou, G., Schroff, F., & Adam, H. (2017). Rethinking Atrous Convolution for Semantic Image Segmentation. arXiv.Org. https://arxiv.org/abs/1706.05587

Gou, C., Peng, B., Li, T., & Gao, Z. (2019). Pavement Crack Detection Based on the Improved Faster-RCNN. 2019 IEEE 14th International Conference on Intelligent Systems and Knowledge Engineering (ISKE), 962-967. https://doi.org/10.1109/iske47853.2019.9170456

He, K., Zhang, X., Ren, S., & Sun, J. (2016). Deep Residual Learning for Image Recognition.

2016 IEEE Conference on Computer Vision and Pattern Recognition (CVPR), 770-778. https://doi.org/10.1109/cvpr.2016.90

Lin, T.-Y., Goyal, P., Girshick, R., He, K., & Dollár, P. (2017). Focal Loss for Dense Object Detection. arXiv.Org. https://arxiv.org/abs/1708.02002

Mandal, V., Abdul Rashid Mussah, & Yaw Adu-Gyamfi. (2020). Deep Learning Frameworks for Pavement Distress Classification: A Comparative Analysis2020 IEEE International Conference on Big Data (Big Data), 5577-5583. https://doi.org/10.1109/bigdata50022.2020.9378047

Nie, M., & Wang, C. (2019). Pavement Crack Detection based on yolo v3. 2019 2nd International Conference on Safety Produce Informatization (IICSPI), 327-330. https://doi.org/10.1109/iicspi48186.2019.9095956

Qiu, Q., & Lau, D. (2023). Real-time detection of cracks in tiled sidewalks using YOLO-based method applied to unmanned aerial vehicle (UAV) images. Automation in Construction, 147, 104745–104745. https://doi.org/10.1016/j.autcon.2023.104745

Redmon, J., & Farhadi, A. (2018). YOLOv3: An Incremental Improvement. arXiv.Org. https://arxiv.org/abs/1804.02767

Ren, S., He, K., Girshick, R., & Sun, J. (2017). Faster R-CNN: Towards Real-Time Object Detection with Region Proposal Networks. IEEE Transactions on Pattern Analysis and Machine Intelligence, 39(6), 1137–1149. https://doi.org/10.1109/tpami.2016.2577031

Salman, M., S. Mathavan, Kamal, K., & Rahman, M. (2013). Pavement crack detection using the Gabor filter. 16th International IEEE Conference on Intelligent Transportation Systems (ITSC 2013), 2039-2044. https://doi.org/10.1109/itsc.2013.6728529

Sarmiento, J.-A. (2021). Pavement Distress Detection and Segmentation using YOLOv4 and DeepLabv3 on Pavements in the Philippines. arXiv.Org. https://arxiv.org/abs/2103.06467

Tan, M., Pang, R., & Le, Q. V. (2019). EfficientDet: Scalable and Efficient Object Detection. arXiv.Org. https://arxiv.org/abs/1911.09070

Zhang, L., Yang, F., Yimin Daniel Zhang, & Ying Julie Zhu. (2016). Road crack detection using deep convolutional neural network. 2016 IEEE International Conference on Image Processing (ICIP), 3708-3712. https://doi.org/10.1109/icip.2016.7533052

Zhou, X., Wang, D., & Krähenbühl, P. (2019). Objects as Points. arXiv.Org. https://arxiv.org/abs/1904.07850

Zou, Q., Cao, Y., Li, Q., Mao, Q., & Wang, S. (2012). CrackTree: Automatic crack detection from pavement images. Pattern Recognition Letters, 33(3), 227–238. https://doi.org/10.1016/j.patrec.2011.11.004

Introducing Big Data Analysis in the Cause of Traffic Congestion and the Improvement Strategies of National Freeway Widening Project

Shing-hau Jaw[1], Sheng-fa Lin[2], Ge-ping Pan[3], Yi-Hsien Chen[4]

1. Director General of Freeway Bureau, MOTC, Taipei, Taiwan, jaw666@freeway.gov.tw
2. Deputy Chief Engineer of Freeway Bureau, MOTC, Taipei, Taiwan, senfa@freeway.gov.tw
3. Vice President of T.Y. Lin Taiwan, Taipei, Taiwan, gppan@tylin.com.tw
4. Managing Director of Integrated Engineering Evaluations, Corp., Taipei, Taiwan, yihsienchen@pavement.com.tw

ABSTRACT

The section of National Freeway No.1 from Yangmei(YM) to Toufen(TF) is approximately 40 kilometers long and is a major congestion point in the northern part of Taiwan. This project has been undergoing preliminary evaluation since 2017, and the design work is currently underway.

Freeway Bureau works with T.Y. Lin Taiwan, introducing big data analysis of national freeways into the operation process. Using ETC (Electronic Toll Collection), and VD (Vehicle Detector)data, we conducted spacetime diagram, confirming traffic bottlenecks kilometer by kilometer, lane by lane, minute by minute, and proposing improvement strategies. This study showed that the traffic congestion in each section does not happen at the same time, they are not related to each other. The cause of traffic congestion in each section are different. To effectively improve the level of service, freeway widening along the entire mainline is necessary.

This widening project passes through 10 urban planning divisions. Improvement strategies were proposed for each section based on the engineering environment. The starting and ending sections of Yangmei(YM) and Toufen(TF) have a simple environment along the freeway mainline, and the embankment is simply widened to reduce the cost; the alignment of freeway mainline in Hukou(HK) section is curved and sloped and close to industrial zone, so a detoured tunnel used to pass through a military base to avoid recurring congestion; the Hsinchu(HS) section has no widening space, and an Accelerated Bridge Construction strategy is planned in the limited area, taking into account construction safety and traffic maintenance requirements.

Key words: big data, recurring congestion, space-time heat map

1. INTRODUCTION

National Freeway No. 1 is the most important traffic artery in western Taiwan. Since its full opening in 1978, traffic volume has been increasing day by day. The entire mainline nowadays is at least a six-lane dual carriageway. The Xizhi to Wugu section and the Wugu to Yangmei section have been widened by elevated viaducts due to insufficient clear distance, and the improvement effect is great. The Hsinchu(HS) area is currently the most serious recurring congestion section, with many short and medium-term traffic, which cannot be relieved in a short time. Therefore, the widening project of National Freeway No. 1 from Yangmei(YM) to Toufen(TF) is promoted to solve traffic problems effectively.

The evaluation stage of this project is to understand the time and characteristics of freeway congestion, so it uses traffic big data for segmented analysis by time and lane, to judge whether the congestion of each section is related to each other. This article explains the process and results of how the big data analysis is used.

The scope of this project starts from the end of the Wugu-Yangmei widening project (Yangmei End) and extends south to the Toufen(TF) interchange, with a total length about 39-kilometer, passing through 4 interchanges connecting local roads(Hukou(HK), Zhubei(ZB), Hsinchu(HC), Toufen(TF)), 1 system interchange connecting different freeways(Hsinchu System IC(HC Sys IC)), and a service area (Hukou Service Area).

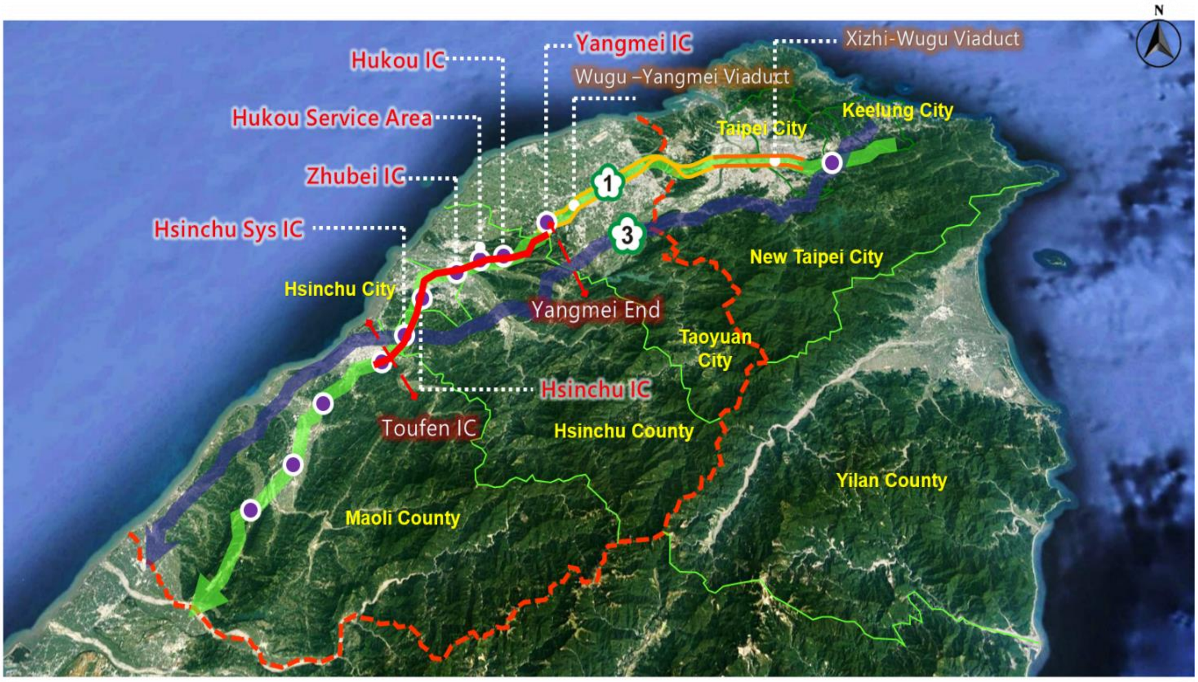

Figure 1 Scope of the Project

2. Use of Big Data to Analyze Freeway Traffic Characteristics

The freeway has implemented distance-based electronic toll collection (ETC) since December 30th, 2012. Every 5 minutes, it counts the traffic volume, travel time, and average speed of each section by vehicle type. More than 20 billion data have been accumulated so far. This project cites relevant statistical data, combined with SQL database system, and related big data analysis software such as Tableau, to count the probability of congestion occurring in each section and each time-period, to show the changes of speed in time-space diagram. The research divides the analysis objects into three time periods: weekdays, weekends, and long holidays.

2.1 Data Collection

In Taiwan, mainline ETC gantries (Figure 2) are constructed between freeway interchanges (IC). There are 14 ETC gantries between Yangmei and Toufen. At each ETC gantry, LPR (license plate recognition) camera, RFID readers, and LiDAR (light detection and ranging) vehicle detectors are installed and used to detect vehicles' travelling speed, travelling time. Trip Details (the origination and destination of each vehicle) are also processed by ETC system for data analysis.

Source: Google Map

Figure 2 ETC Gantry

2.2 Congestion Probability

The concept of "congestion probability" is used in some research [Ossenbruggen et al. (2012)] for a better understanding of roadway performance. And the same concept is also used in this research as an indicator to our freeway performance. It is general accepted in Taiwan that when travelling speed less than 40 kph is a congested situation in our freeway. So, in the paper that the definition of congestion probability is that referring to a specific time and section, the number of days when the average speed is less than 40 kph accounts for the ratio of all days. The drawing is shown in Figure 3. It is clear in the drawing that during the morning and evening peak hours, some freeway sections have a probability exceeds 30% for the average speed less than 40 kph. It is a recurring congestion section.

The traffic data of the whole length between Yangmei(YM) and Toufen(TF) is analyzed.

From Figure 3, the congested sections on weekdays are southbound Yangmei(YM) in the morning and the northbound Hsinchu(HC) to Zhubei(ZB) section in the evening. The probability of southbound congestion in the morning has a gradual improvement trend. However, the probability of northbound congestion increases year by year, and the congestion probability of the Hsinchu(HC) section is the highest, presumably due to the increase in work trips after getting off work.

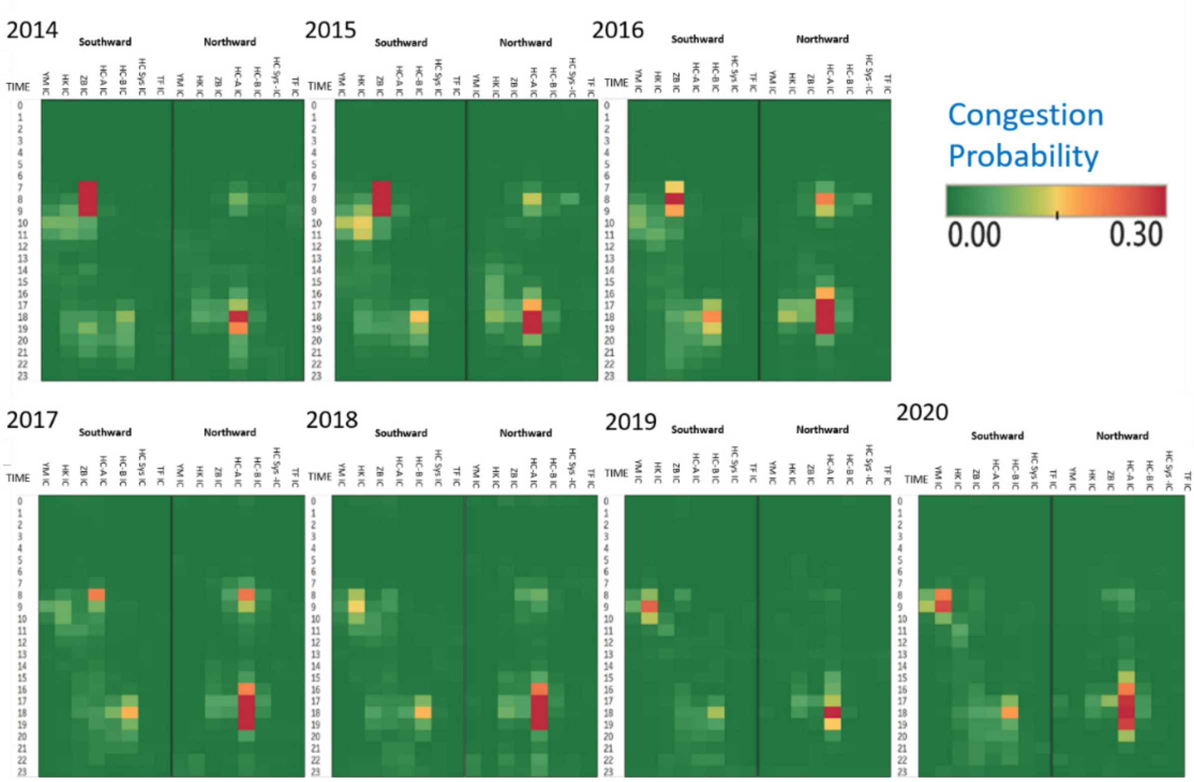

Figure 3 Congestion probability of National Freeway No. 1 from Yangmei to Toufen from 2014 to 2020 (weekdays)

3. Analysis of Trip Characteristics

The following analyzes the data of some certain weekday (May 29th, 2018) to find out the all-day vehicle speed changes in space-time heat map, traffic composition, and congestion characteristics.

3.1 Vehicle speed changes in space-time heat map

Vehicle detectors (VD) is a inductive loop installed at freeway pavement to detector passing vehicles. Using VD data, draw the vehicle speed in space-time heat map to find out the congestion bottleneck section and congestion time characteristics between Yangmei (YM) and Toufen (TF).

3.1.1 Southbound

As can be seen from Figure 4, the congestion is quite serious on this day. The serious congestion happened from Hukou IC (HK IC) to Hsinchu IC (HS IC)from 6 am to 12 pm, and another obvious congestion occurred from Hukou IC(HK IC) to Hukou Service Area(HK Ser. Area) from 3 pm to 7 pm.

3.1.2 Northbound

As can be seen from Figure 5, in addition to the occurrence of congestion in the afternoon, there is also serious congestion from Hsinchu IC (HS IC) to Hukou IC (HK IC) from about 8 am to 12 pm in the morning.

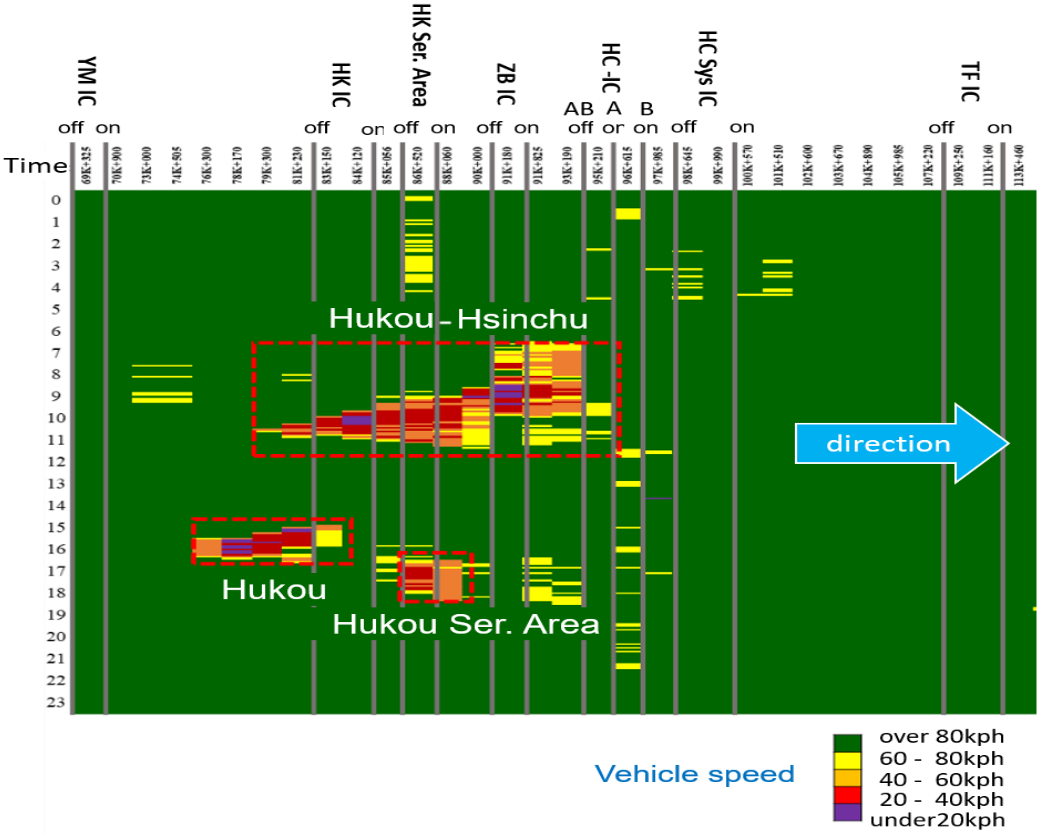

Figure 4 Yangmei IC to Toufen IC Southbound Speed Heat Map

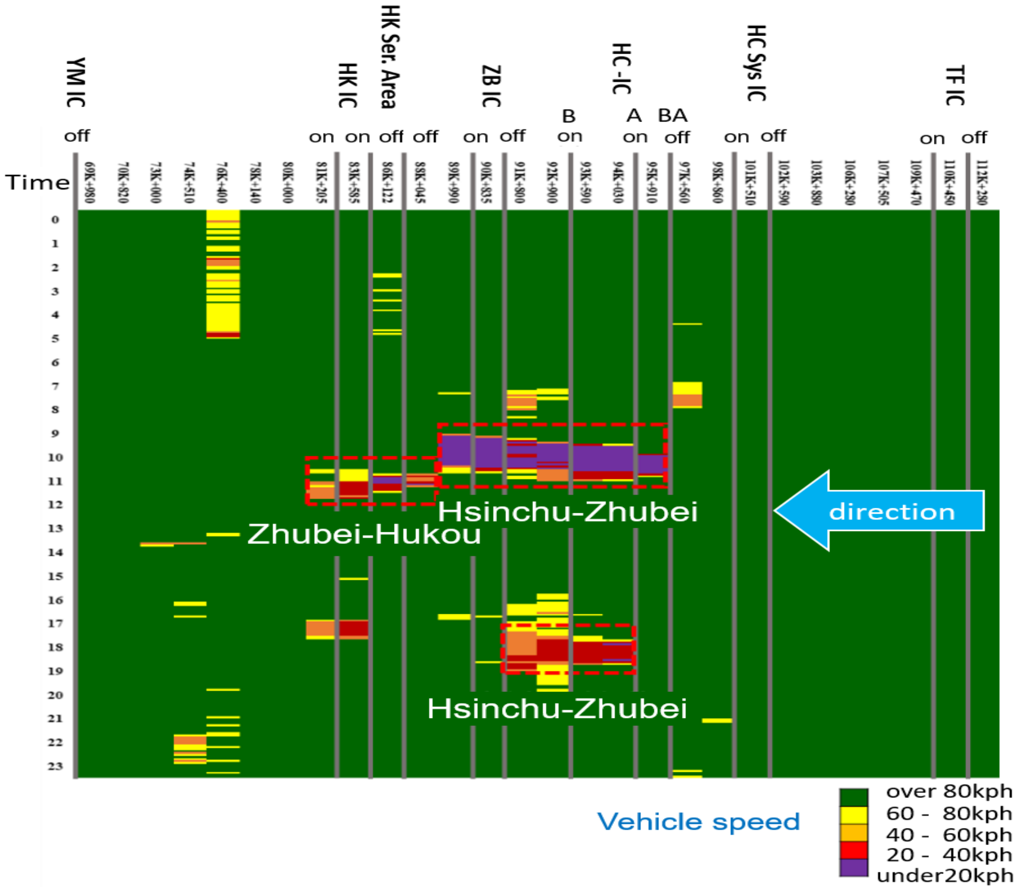

Figure 5 Toufen IC to Yangmei IC Northbound Speed Heat Map

3.2 Traffic Composition Analysis

To understand the traffic composition characteristics of the main congestion sections, this project divides the traffic into three types: external traffic, interzonal traffic, and intrazonal traffic. The definitions are as follows:

- External Traffic: trips whose two O/D points are both outside the scope of the project.
- Interzonal Traffic: trips with one O/D point in the scope of the project.
- Intrazonal Traffic: trips whose two O/D points are both within the scope of the project.

3.2.1 Southbound

As can be seen from Figure 6, the total number of trips from Yangmei End (YM End)to the Hsinchu System IC (HC Sys IC)is about 82,000 trips, of which the proportion of external traffic is about 34%; interzonal traffic is about 36%; intrazonal traffic is about 30%. In addition, the intrazonal traffic is highest in the Zhubei IC(ZB IC) to Hsinchu IC(HC IC) section. And it is also the section with highest congestion probability in Figure 3. So, it is believed that a high intrazonal traffic is the cause of congestion.

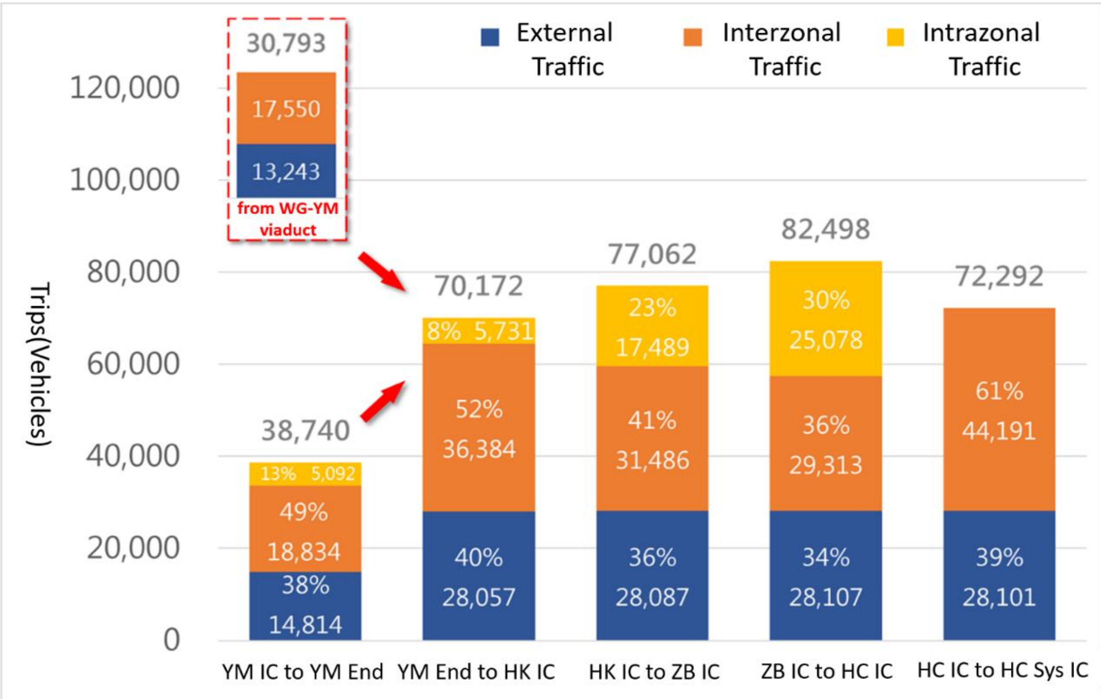

Figure 6 Yangmei IC to Hsinchu Sys IC Southbound Traffic Composition

3.2.2 Northbound

From Figure 7, the composition of northbound traffic is like that of southbound.

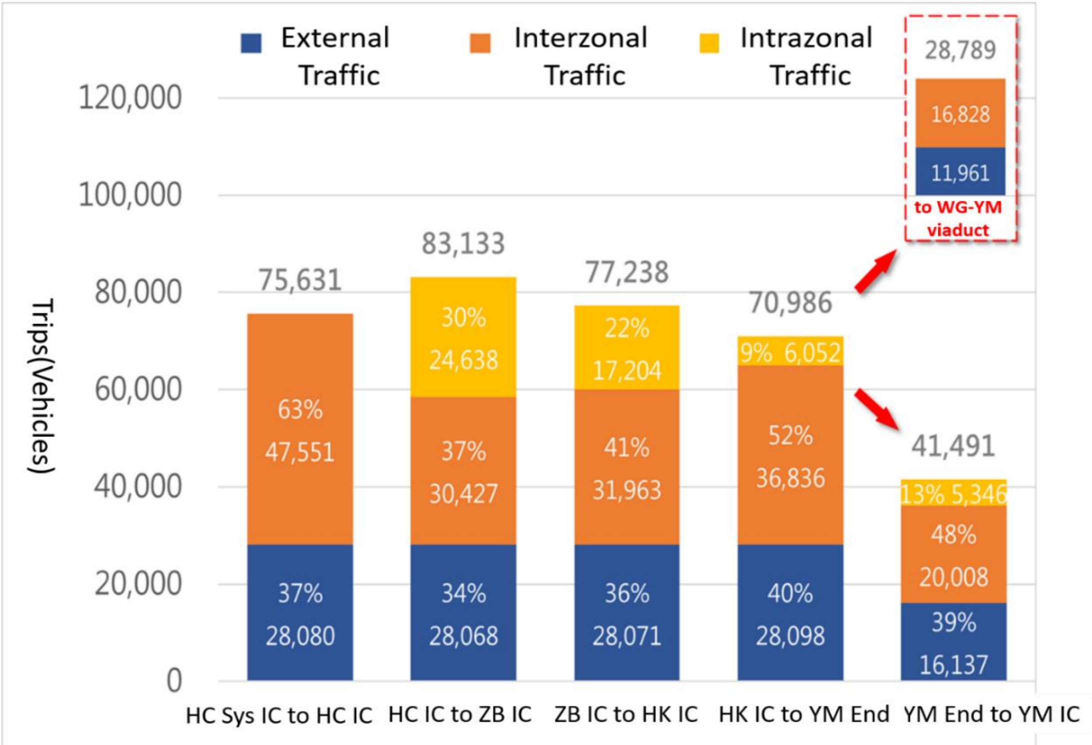

Figure 7 Hsinchu Sys IC to Yangmei IC Northbound Traffic Composition

4 Analysis of Congestion Characteristics and Causes

For the main congestion time-period in Figure 4, we enlarge and view the speed heat map of this section, mark the relative positions of on-ramps and off-ramps of each interchange, to find out the node causing congestion. We also combine the traffic composition of the section, the average speed of the section, and the traffic volume from on-ramps and off-ramps of each interchange to understand the congestion characteristics of the section.

4.1 Congestion Time Period Traffic Composition

Figure 8 is the vehicle speed space-time heat map from 6 am to 12 pm and from 3 pm to 7 pm on a randomly selected ordinary weekday (May 29th, 2018). The main congestion period is from 7:30 am to 11:50 am from Hukou to Hsinchu, and the upstream speed of the on-ramp of Hukou IC (HK IC) and Zhubei IC (ZB IC)is less than 20 kph. In the afternoon, it is from 3:20 pm to 6:50 pm at the upstream of the off-ramp of Hukou IC(HK IC), and its average speed is also less than 20 kph.

Figures 9 and 10 are respectively the traffic composition of that day. During the congestion period, the proportion of intrazonal trips in the Hukou to Zhubei (HK to ZB)section and the Zhubei to Hsinchu(ZB to HC)section is 24%~35%, which is higher than the proportion in Figure 6. In Figure 9 shows that the core of the congestion problem should be that there is a high proportion of short distance intrazonal trips during the congestion period. Such short-distance intrazonal trips cause traffic weaving, the mainline traffic being disturbed and leads to serious congestion.

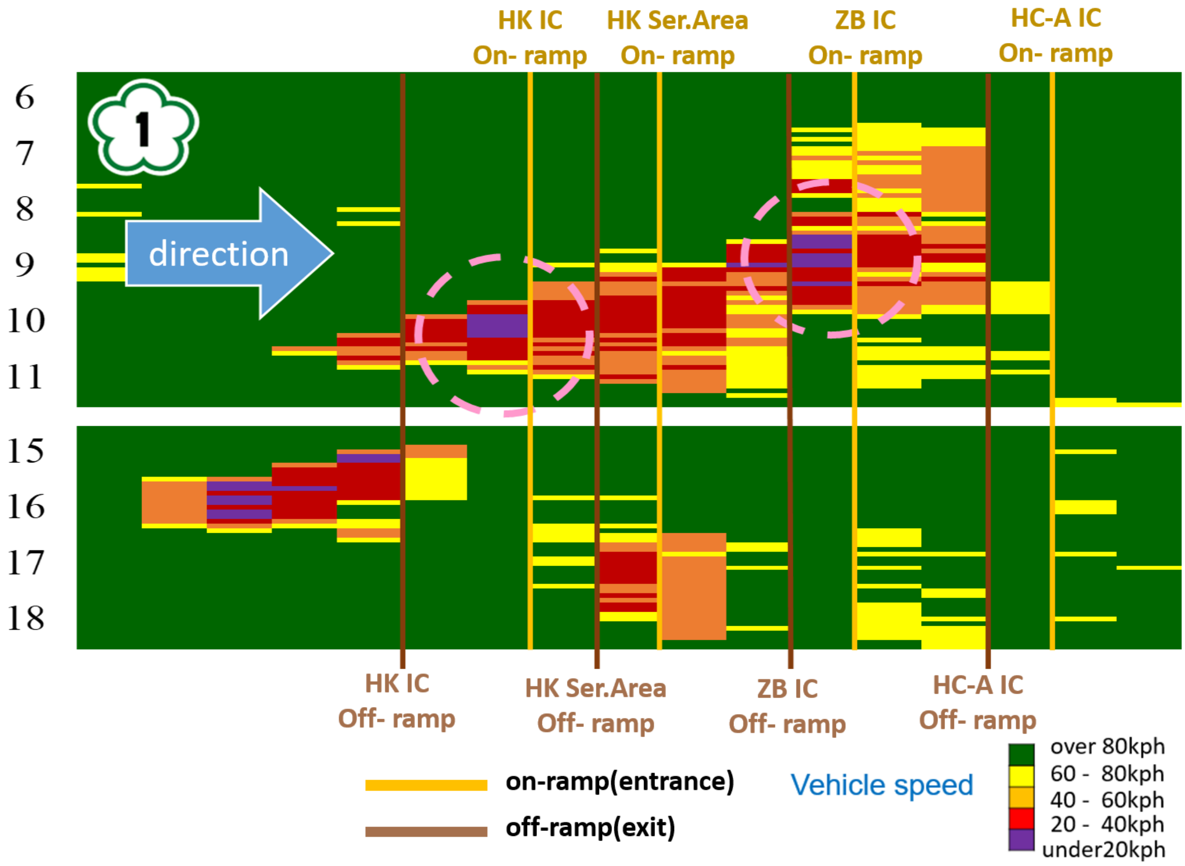

Figure 8 Yangmei IC to Hsinchu System IC Southbound Speed Space-Time Heat Map

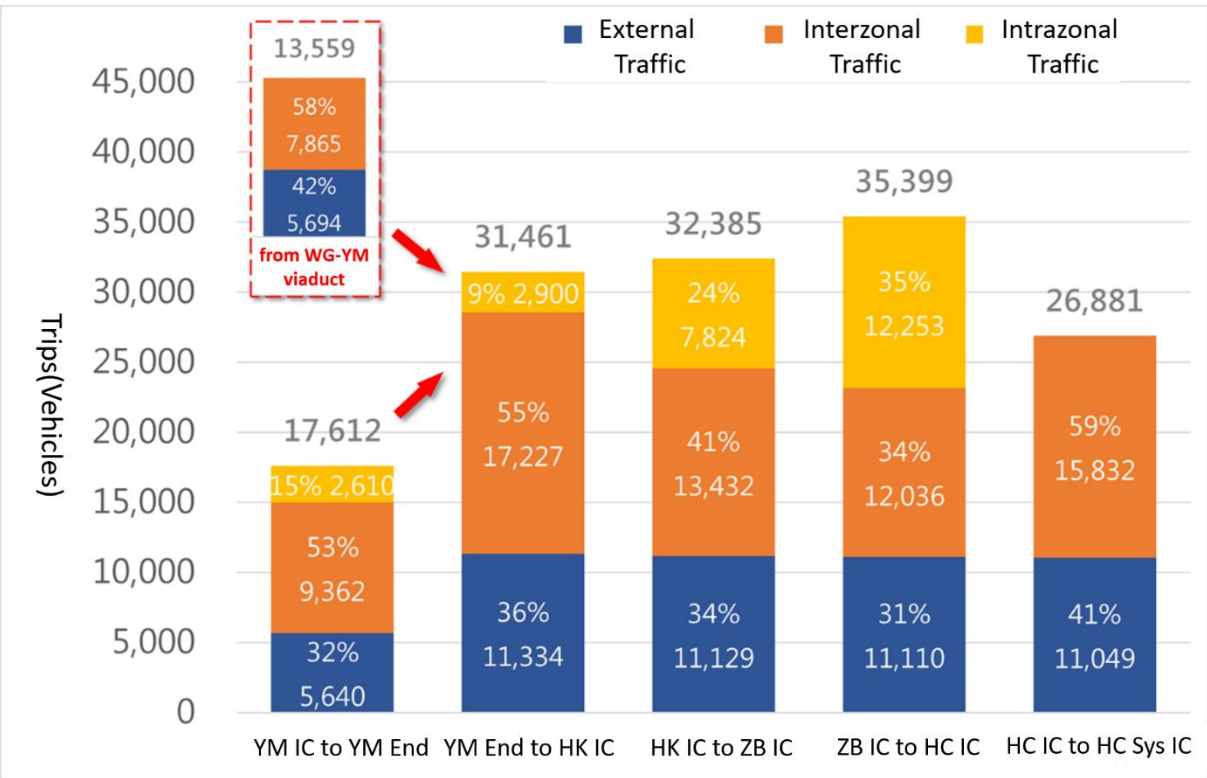

Figure 9 Yangmei IC to Hsinchu Sys IC Southbound Traffic Composition (06:00 am~ 1:00 pm)

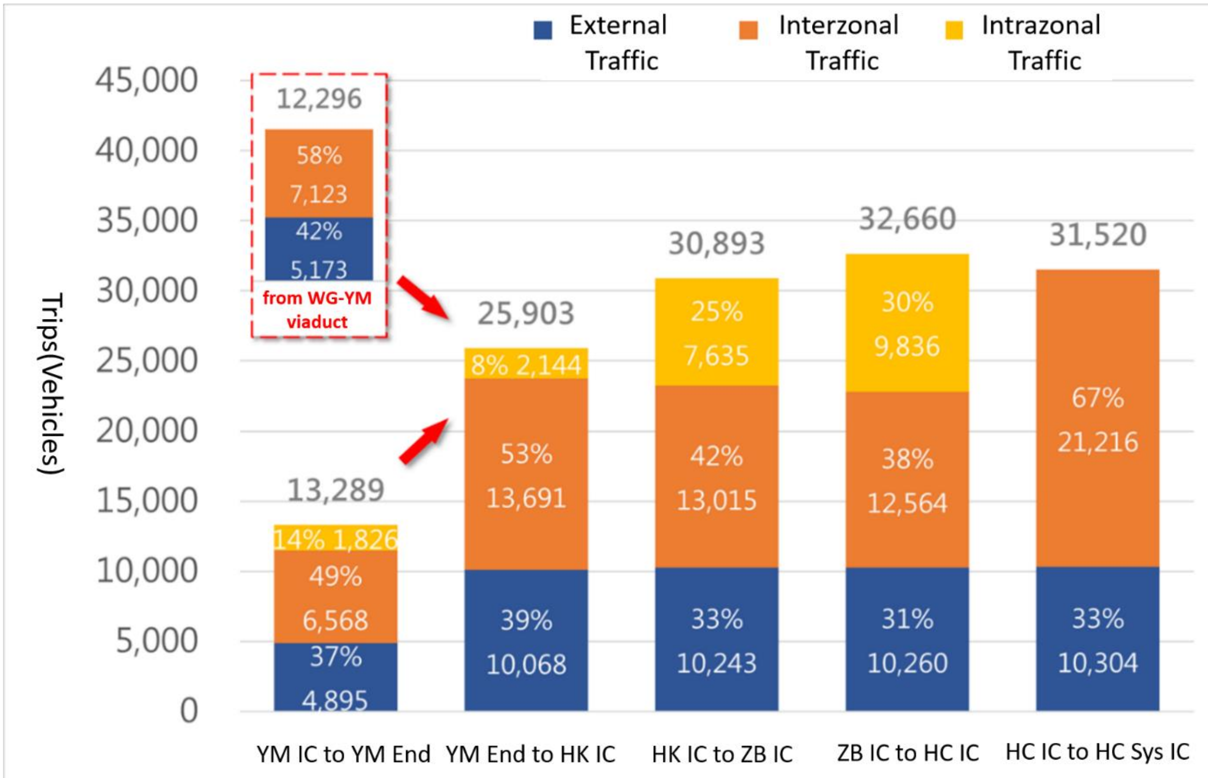

Figure 10 Yangmei IC to Hsinchu Sys IC Southbound Traffic Composition (1:00 pm ~ 8:00 pm)

4.2 Time Flow Speed Analysis

The traffic composition and speed distribution are shown in Figures 11 and 12. The traffic volume of the Hukou IC to Zhubei IC section starts to grow rapidly from about 6 am, mostly interzonal traffic and interzonal traffic, and the traffic volume reaches the peak at about 7 am. Both the flow and average speed from 8 am to 11 am both began to decline, and the speed dropped to the lowest at 10:30 am, about 40 kph. The average speed of the Zhubei IC to Hsinchu IC section dropped to the lowest 20 kph at 9:30 am, and the congestion began to ease from 11 am to 12 pm, and the speed and flow gradually increased. In the afternoon, Hukou IC to Zhubei IC section has about 500 vehicles passing every five minutes. Due to the open of the shoulder, the Zhubei IC to Hsinchu IC section has a traffic volume of about 500 to 600 vehicles every five minutes, that is, about 6,000 vehicles per hour, which has reached the saturation flow of this section. The average speed of the two sections is reduced to the lowest 40 kph, and the congestion begins to ease until 7 pm.

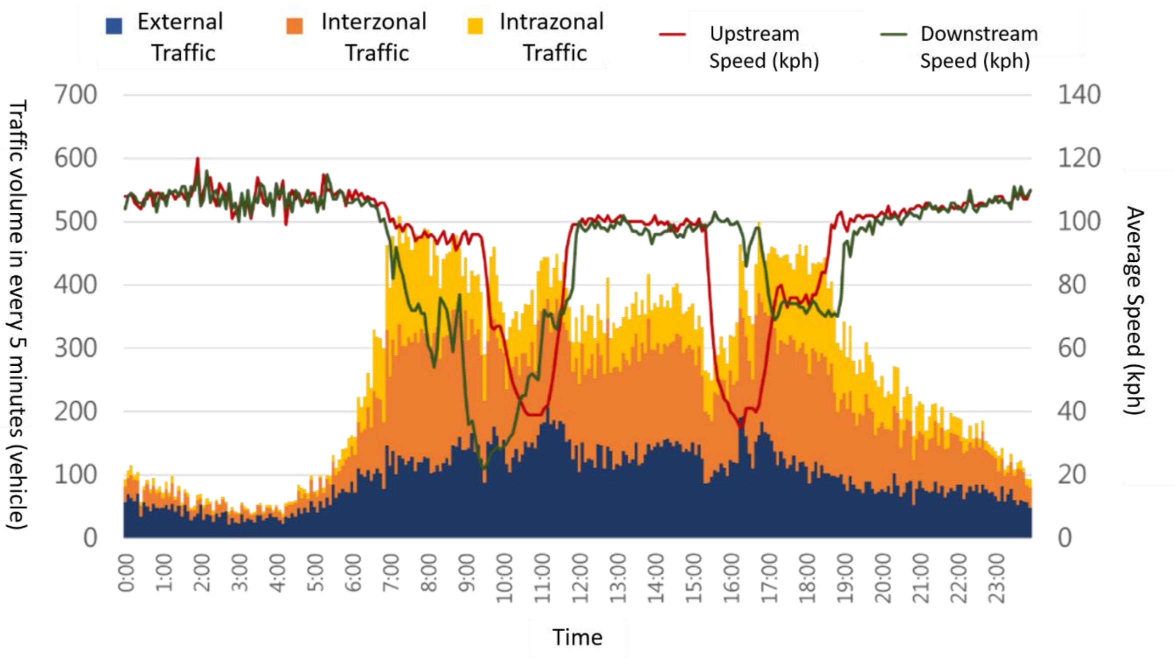

Figure 11 Hukou IC to Zhubei IC Southbound Volume and Speed Distribution Chart

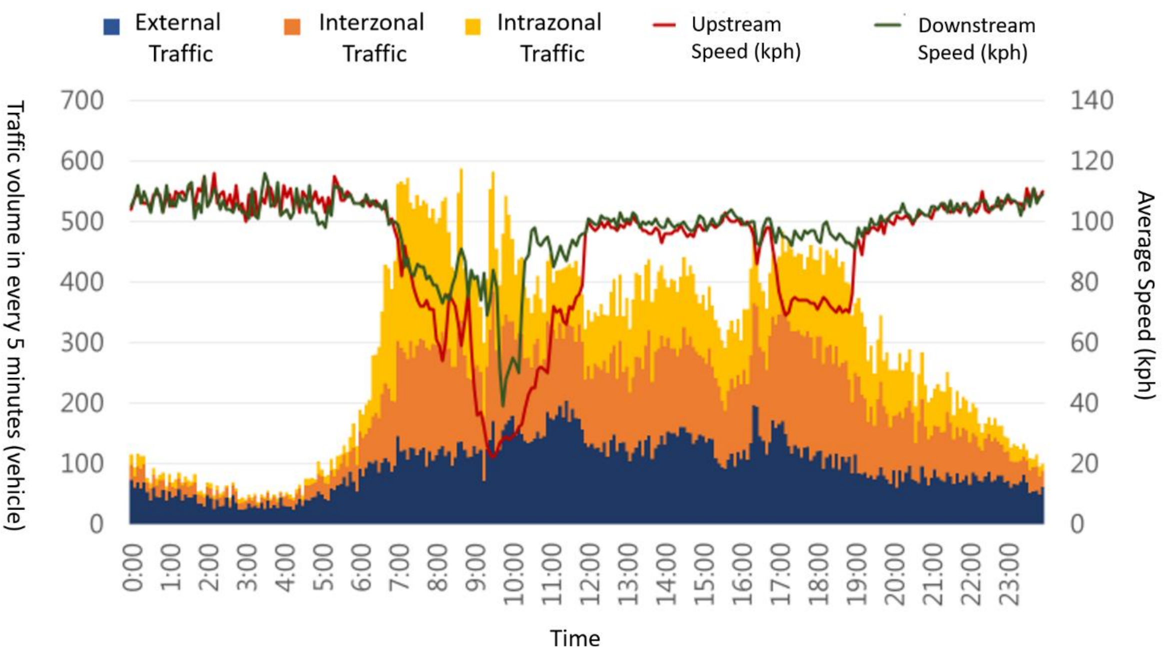

Figure 12 Zhubei IC to Hsinchu IC Southbound Volume and Speed Distribution Chart

4.3 Speed by Lane

This section tries to find out the speed rate changes of each section lane by lane by using vehicle detector (VD) data.

4.3.1 Hukou to Zhubei section

As can be seen from Figure 13, the VD at 83K+150 is located upstream of the off-ramp of Hukou IC, and the average speed of the outside lane is lower than the inner lane during the morning period. The average speed of the three main lanes at 84K+120 is less than 20 kph because it is located on the mainline upstream of the on-ramp of Hukou IC, it is supposed that a large amount of traffic flow into the Hukou on-ramp causes congestion.

The downstream 88K of Hukou Service Area is a downslope section with a smaller curvature radius, and the drivers face the east. It may be due to the direct sunlight in the morning affecting driver's sight, which decreases the road capacity. Therefore, as the Hukou IC on-ramp continues to import a large amount of traffic, the downstream 88K+060 reaches the saturated flow, and it starts to congest and queue to the upstream, and the VD speed at the further downstream 90K+000 is higher than 88K+060, showing that the alignment and sight problem at 88K should be the reason for the slower speed of this section.

However, there are congestion queues at the upstream of 81K+230K and 86K+560 in the afternoon. It is speculated that both places are downslope sections with a smaller curvature radius, which decreases the road capacity, and the mainline traffic flow has been saturated from 3 pm to 7 pm, causing congestion.

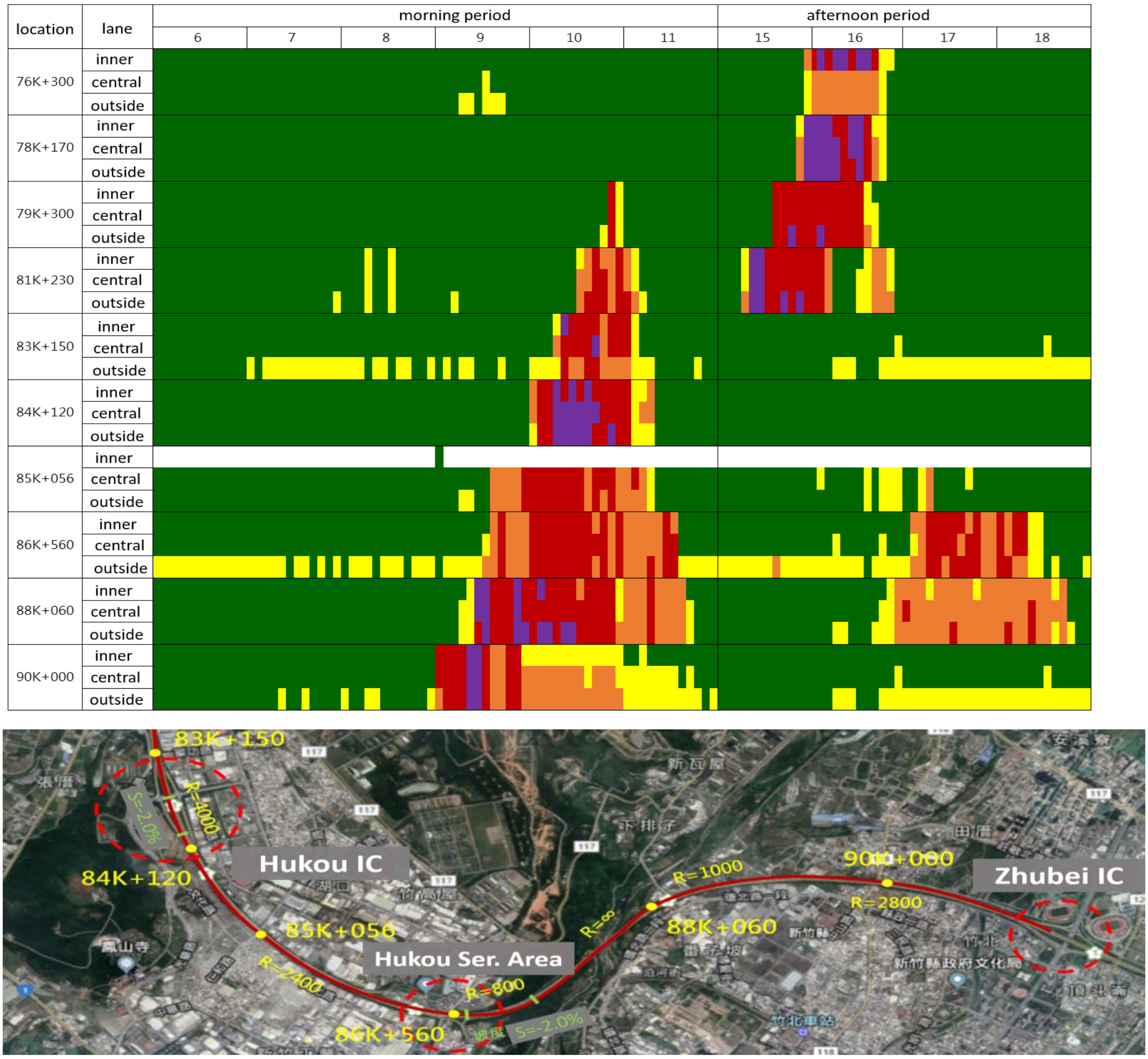

Figure 13 Hukou IC Nearby Mainline Southbound VD Data Analysis Schematic Diagram

Also, from Figure 14 and Figure 15, in the congestion period, the Hukou IC on and off ramp does not have obvious congestion, but the Hukou IC on-ramp maximum traffic flow can also reach 175 vehicles every five minutes, nearly 2,000 vehicles per hour. Therefore, a large amount of inflow traffic, alignment, and driver's sight problems are speculated to be the main reason of serious congestion in the downstream section of Hukou IC.

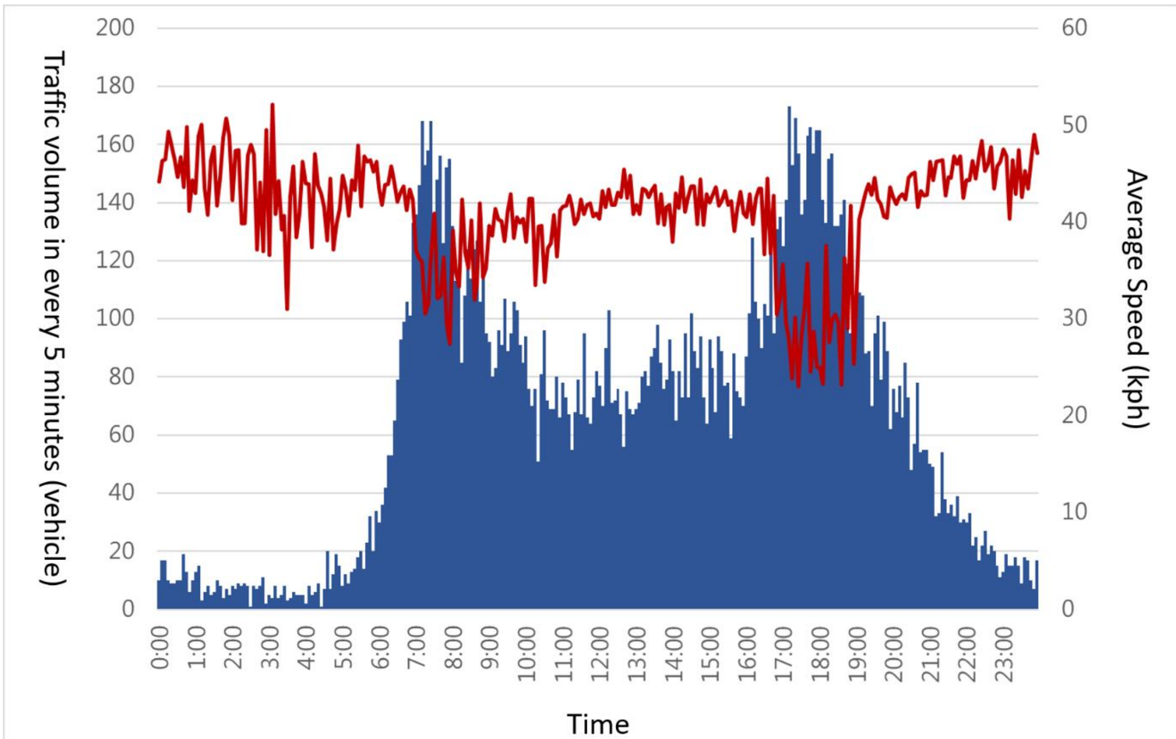

Figure 14 Hukou IC On-Ramp Flow Speed Chart

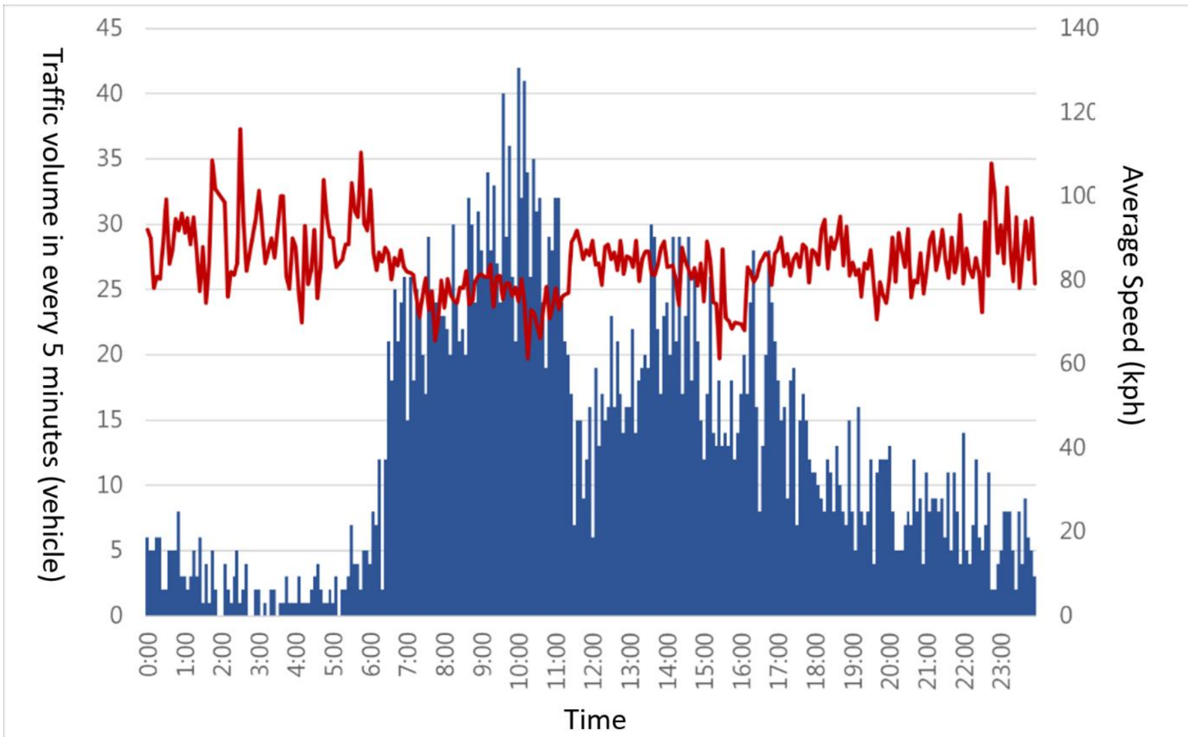

Figure 15 Hukou IC Off-Ramp Flow Speed Chart

4.3.2 Zhubei to Hsinchu Section

From Figure 16, the speed of the outer lane of the mainline section near the ramp starts to drop first, and then the speed of the inner and central lanes start to drop. 93K+190 is the downstream section of Zhubei IC in-ramp and upstream of Hsinchu IC off-ramp, and the severe situation of its outer lane is much more severe than the inner lane. It is speculated that the in-ramp of Zhubei IC is too close to the off-ramp of Hsinchu IC, only 1.7 kilometers, which causes serious congestion of the outer lane due to traffic weaving.

Again, from Figure 17 and Figure 18, in the congestion period, the traffic flow of Zhubei in-ramp also has congestion, and the maximum traffic flow can reach 200 vehicles every five minutes, that is 2,400 vehicles per hour. Its speed is less than 20 kph, and finally severe congestion every five minutes traffic flow is only 50 vehicles, that is 600 vehicles per hour. The speed of the off-ramp during the congestion period is also affected, but the traffic flow can mostly maintain between 40 kph and 80 kph, so there should be no congestion caused by exit queues. The cause of congestion in the Zhubei section should be the traffic flow from the in-ramp of Zhubei IC into the mainline.

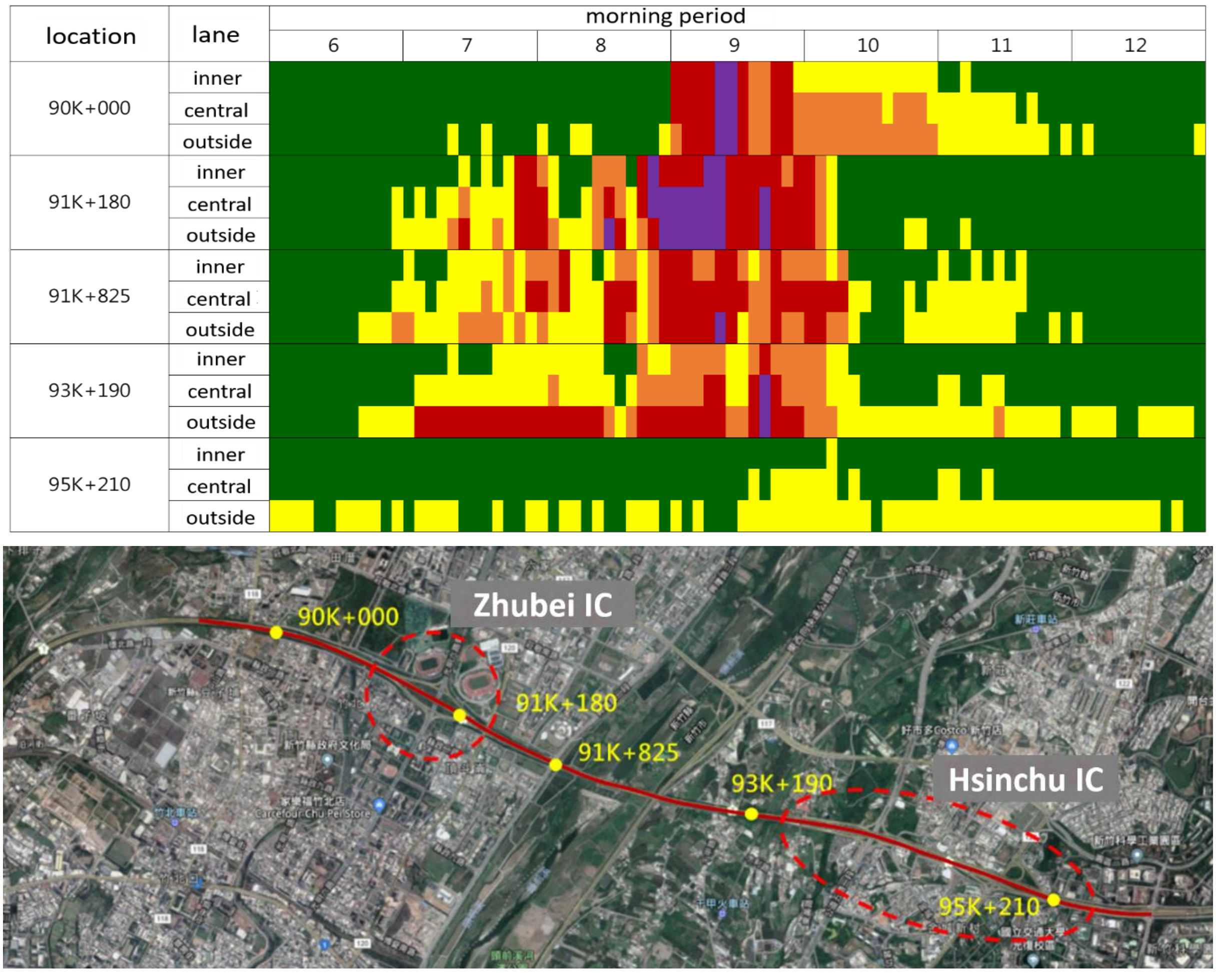

Figure 16 Zhubei IC Nearby Mainline Southbound VD Data Analysis Schematic Diagram

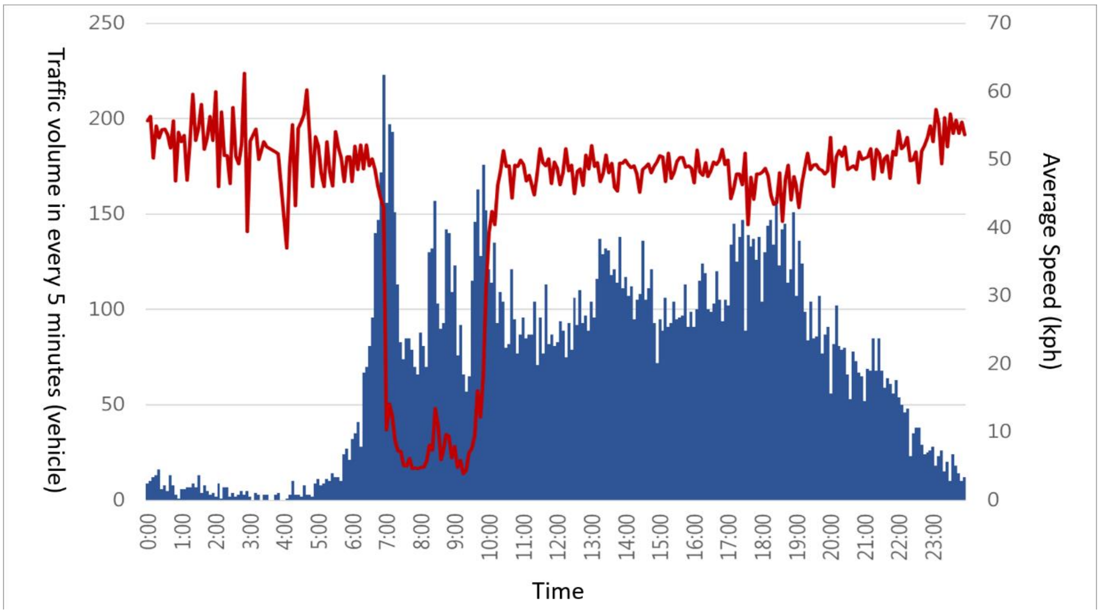

Figure 17 Zhubei IC On-Ramp Flow Speed Chart

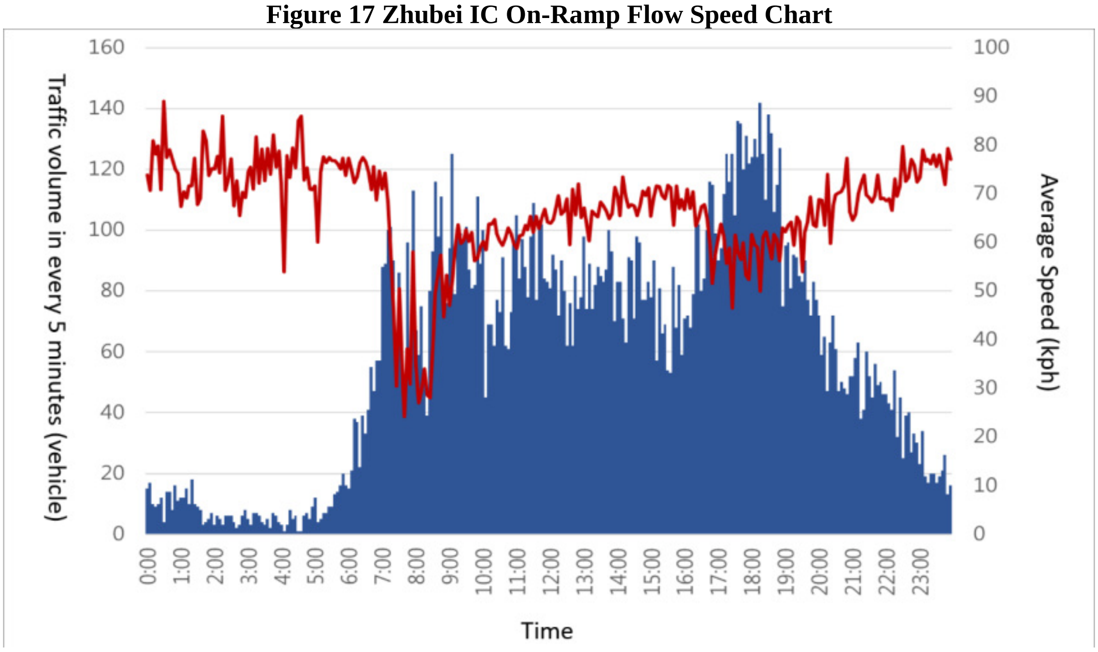

Figure 18 Zhubei IC Off-Ramp Flow Speed Chart

4.4 Explanation of Congestion Causes and Improvement Strategies

The analysis results of the previous section show that the main cause of congestion on weekdays differs from each other. From Hukuo to Zhubei, the mainline is a downslope alignment with a smaller curvature radius, which decreases the road capacity. Also the drivers face the east, the direct sunlight in the morning affecting driver's sight, which also decreases the capacity. From Zhubei to Hsinchu, due to the increase in intrazonal and interzonal traffic, the interchange continuously has a large amount of outflow and inflow traffic, and the mainline vehicles weaves, causing the freeway mainline to reach a saturated state, and queueing to the upstream section. The cause of congestion on weekends and long holidays is mainly affected by the increase in external traffic, causing the mainline to reach the saturated flow.

It shows that the causes of congestion are not simply due to insufficient capacity in certain sections leading to traffic queues. To effectively improve the level of service, freeway widening is necessary. The traffic congestion in the starting and ending sections of Yangmei and Toufen are not so serious, but taking "lane balancing" into account, the freeway widening area is along the entire mainline.

5. Widening Project

This widening project passes through 10 urban divisions. There are several engineering constrains along the divisions. Strategies were proposed for each section based on the engineering constrains. The starting and ending sections of Yangmei and Toufen have a simple environment along the mainline, so the embankment is simply widened to reduce the cost. The alignment of the mainline in Hukou section is curved and sloped and close to industrial zone, so a detoured tunnel used to pass through a military base to avoid recurring congestion. the Hsinchu section has no widening space, and an Accelerated Bridge Construction strategy is adopted in the limited area, taking construction safety and traffic maintenance into account.

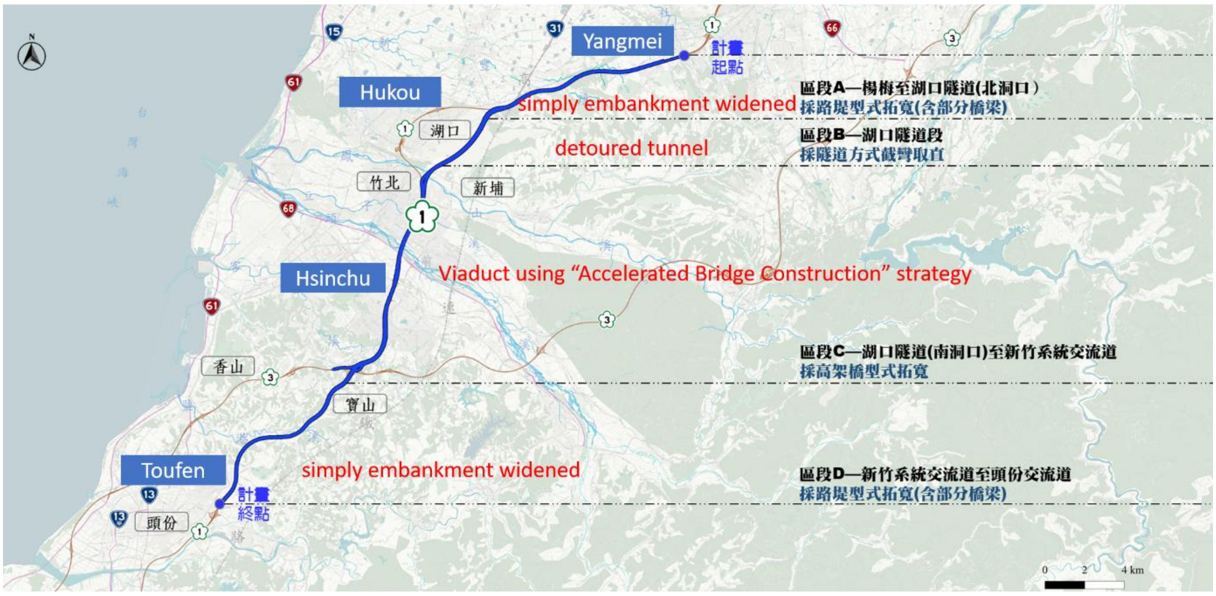

Figure 19 Freeway No1 Widening Project

In addition to widening the mainline from Yangmei to Toufen, it also aims to improve the bottleneck points where the traffic weaving distance is not enough, or the capacity of the entrance and exit ramp is insufficient. The improvement strategies are explained as follows:

- Zhubei IC to Hsinchu IC: Add one lane in both directions (the 4th lane, auxiliary lane) and maintain the standard 3m shoulder.
- Southbound and northbound Hsinchu-B IC off-ramp improvement; extend the exit lane length
- Hukou Service Area to Hukou Interchange (northbound): Use the marking method to adjust the original 3+1 lane configuration to 2 (mainline lane) +2 (exit lane).

6. Conclusions and Recommendation

6.1 Conclusions

This project cites relevant statistical data, combined with SQL database system, and related big data analysis software such as Tableau, to count the probability of congestion occurring in each section and each time-period, and the changes of speed in time-space diagram. The research process divides the analysis objects into three time periods: weekdays, weekends, and long holidays., to investigate the causes of congestion in each section and lane step by step. It is found that the periods of congestion and their causes are not the same across different sections. The causes of congestion are not simply due to insufficient capacity in individual sections leading to traffic queues. To effectively improve the level of service, freeway widening along the entire mainline is necessary.

6.2 Recommendation and Limitation

Freeway Bureau has fully established a traffic management system for Taiwan's freeway and expressway networks by setting up automatic traffic monitoring and control systems as well as information display equipment. This aims to enhance the speed of incident detection and handling, to improve driving safety, and increase overall traffic management efficiency by integrating advanced technology and traffic management strategies. Using big data can also upgrade freeway traffic management efficiency and alleviate traffic congestion. This study utilizes national freeway big data, with a rigorous and detailed analysis process that has been highly recognized by various experts. We would like to take this opportunity to share the research process, hoping that all our honored experts will provide valuable opinions.

This research is the first one using ETC and VD data to evaluate the freeway performance in Taiwan. Due to the time constrains, only some factors are used in this research. There are still more factors, such as truck proportions, safety statistics and so on can be considered in the future. And it is also a great idea to explore alternative strategies other than widening to make the whole research more comprehensive.

7. References

Ossenbruggen, P. J., Laflamme, E. M., & Linder, E. (2012). Congestion probability and traffic volatility. Transportation research record, 2315 , 54–65.

Detecting Lateral Offset Distance on Rural Road in Thailand by Using Point Cloud Data : A Case Study

Nutvara Jantarathaneewat[1], Chenxi Liu[2], Shucheng Zhang[3], and Yinhai Wang[4,*]

[1] Department of Civil and Environmental Engineering, University of Washington, Seattle, USA, nutvaraj@uw.edu
[2] Department of Civil and Environmental Engineering, University of Utah, Utah, USA, chenxi.liu@utah.edu
[3] Department of Civil and Environmental Engineering, University of Washington, Seattle, USA, sz224@uw.edu
[4] Department of Civil and Environmental Engineering, University of Washington, Seattle, USA, yinhai@uw.edu

ABSTRACT

The lateral offset distance refers to the horizontal clearance that serves as an essential buffer for vehicle operation. Illegal permanent and temporary obstacles along roadsides, such as privately owned signs or building expansions, can obstruct visibility and increase the risk of collisions. Traditionally, road agencies have relied on manual inspections to estimate these distances, a process that is both time-consuming and often inaccurate. To overcome these challenges, this study introduces an automatic process for determining lateral offset distance using point cloud data. Approximately 10 kilometers of point cloud data were collected from rural roadways in Thailand using a Mobile Laser Scanning system. Clustering algorithms, specifically RANSAC and DBSCAN, were employed to identify road lines and walls within the point cloud data and calculate the lateral offset distance. The dataset encompasses a variety of road characteristics, including residential areas, high-traffic volume roads, and roads along rivers. Mean Absolute Error (MAE) was used to measure the accuracy of this algorithm by comparing the automated results to manual detection. The algorithm demonstrated the highest accuracy for high-traffic volume roads, achieving an MAE of 0.343 meters per kilometer. The study also reported average lateral offset distances across the different road classes, with roads along the river having the widest average lateral distance at 10.787 meters, and residential roads having the shortest average lateral distance at 4.911 meters. Suggestions for further improvements to the algorithm were also provided based on these findings.

Keywords: Point Cloud Data, LiDAR, Rural Roads

1. INTRODUCTION

Roadside features have significant impacts on transportation safety. In 2022, approximately 20% of motor vehicle crash fatalities occurred when vehicles left the roadway and collided with fixed objects on the roadside, such as trees, utility poles, and traffic barriers (Insurance Institute for Highway Safety, 2022). A research (Lee and Mannering, 2022) reveals that the severity of these accidents is impacted by the lateral offset distance (e.g., road shoulder width) significantly. The lateral offset distance refers to the horizontal clearance that provides a buffer for vehicle operation. According to the AASHTO Green Book (AASHTO, 2018), a minimum horizontal clearance of 18 inches to objects behind curbs is the standard offset that allows for normal traffic operations. However, it is acknowledged that providing such a clearance may not always be feasible in low-speed curbed areas due to right-of-way constraints and other practical limitations of the built environment (FHWA, 2023).

Many countries and regions like Thailand, particularly in rural areas, often suffer from limited horizontal clearance due to illegal permanent and temporary obstacles along roadsides, such as privately owned signs or building expansions (as shown in Figure 1). Based on the latest five-year accident records (2019-2023) reported in Accident Report Management System (ARMS) from the Department of Rural Roads of Thailand, run-off-road (ROR) crashes were the leading type of accident and resulted in the highest number of fatalities (DRR, 2024). This type of crash accounted for 37% of the total collisions (2,291 cases) and caused 632 deaths over the five-year period. Fixed roadside objects such as trees, electrical poles, and kilometer posts were identified as significant roadside hazards in Thailand (Se, 2020; Somchainuck et al., 2013).

Figure 1 Illegal permanent and temporary obstacles along the roadside.
(Google Street View, 2024)

Therefore, the concept of a 'Forgiving Roadside' was introduced over a decade to emphasize the importance of designing safer roadsides that allow vehicles to safely traverse a verge with gentle gradients and that are free of hazardous ground profiles and objects (iRAP, 2024). To mitigate the severity of ROR accidents, Highway setback guidelines set up the minimum lateral clearance distance to provide clear zones free of obstructions and dangerous roadside conditions (Lorenz, 2024). The recent research (Road Safety Thailand Road Safety Policy Foundation, 2024) highlighted the performance of the policy to remove or relocating roadside fixed objects to safer road. However, road agencies still relied on physical inspections to manually estimate this distance, often using public light poles as reference points. This kind of manual measurement is time-consuming with low accuracy, which highlights the demand for technologies for a more efficient, accurate, and economic measurement.

Therefore, since 2014, the Department of Rural Roads (DRR) has developed the Rural Road Network Management (RM) System. The RM system employs Mobile Mapping System (MMS) technology for image processing, capturing detailed images of road assets and locations. The MMS system is equipped with various sensors, including dual antenna GNSS for precise heading determination and wide-angle cameras, aiming to reduce the need for onsite surveying by staff and replace it with high-quality data (Bamrungwong et al., 2017). In 2019, DRR enhanced the RM system by incorporating laser scanning technology to generate 3D point cloud data for high-accuracy object detection. Many studies (Zhong et al., 2019; Hou et al, 2020; González-Gómez et al. 2014) have proven the performance of LiDAR in distance measurement and 3D scene reconstruction, however, most of them are applied for vertical clearance measurement (Gargoum, 2018). Therefore, this research aims to take advantage of the 3D point cloud data collected in the program and develop an innovative automated processing system for horizontal clearance distance measurement for transportation safety enhancement

The proposed system is structured into six main steps. Firstly, the point cloud data is preprocessed to remove noise, which enhances the efficiency and accuracy of subsequent processes. Next, the point cloud is separated into ground and non-ground points to improve the effectiveness of object detection tasks. Following this, edge line detection and wall detection are performed separately, with both processes capable of running in parallel. For these tasks, the study employs clustering algorithms to fit the point cloud data to lines for edge detection and to planes for identifying wall configurations. Once these objects are detected, the system calculates the distance between them. To validate the results, manual measurements are taken using point cloud processing software, and the Mean Absolute Error (MAE) is used as the metric for accuracy assessment. Approximately 10 kilometers of point cloud data were collected from rural roadways in Thailand and used as a dataset for developing and testing the detection algorithm. This study's contributions are:

- **Automated Calculation of Lateral Offset Distance**: The research introduces an innovative for lateral offset distance measurement through 3D point cloud data, eliminating the needs for manual physical inspections. The proposed system provides a more accurate and efficient method for estimating lateral offset distances compared to traditional manual methods.
- **Comprehensive Dataset**: Approximately 10 kilometers of point cloud data were collected from rural roadways in Thailand, covering residential areas, high-traffic volume roads, and roads along the river.
- **Support for Right-of-Way Inspections**: Offers valuable data for right-of-way inspections and supplementary roadside improvements, helping to address issues with visibility and collision risks due to illegal obstacles along roadsides.

2. LITERATURE REVIEW

Object detection using point cloud data has been extensively utilized in various industries, most notably in autonomous vehicles. Meanwhile, it also approaches for creating asset inventory. For instance, point cloud data has been primarily employed for automatic traffic sign detection by analyzing parameters such as retro-intensity, elevation, and hit count (Ai, 2012). Ai's study concluded that certain constraints, including retroreflectivity and the height of objects, need to be adjusted to eliminate false negative detections. Clustering techniques such as RANSAC (Random Sample Consensus) and DBSCAN (Density-Based Spatial Clustering of Applications with Noise) have been successfully applied to extract road boundaries and pole-like objects from point cloud data (Yin and Zhu, 2022; Gouda et al., 2022). These methods are particularly effective in dealing with noisy data and identifying distinct geometric structures within point clouds.

Point clouds collected from Mobile Laser Scanning (MLS) have demonstrated their utility in detecting both on-road and off-road objects. On-road objects include road surfaces, road markings, driving lines, and road cracks, while off-road objects encompass pole-like structures such as traffic signs, light poles, trees, and power lines (Ma et al., 2018). Learning-based point cloud processing algorithms, particularly those employing machine learning techniques, have become prevalent in existing studies. For instance, random forests have been utilized for urban road environment classification, demonstrating the capability to extract a variety of objects beyond traditional road assets, including buildings, trash cans, and vegetation (Mohamed et al., 2022). Despite their effectiveness, there is a need for larger-scale studies to thoroughly evaluate the efficiency and scalability of these methods. In addition, these methods often rely on the prior knowledge of human operators, which poses significant challenges, especially in complex urban environments.

In addition to clustering and machine learning techniques, neural networks have also been extensively utilized for point cloud object detection. One notable neural network architecture is PointNet, which is a unified framework designed for a range of applications, including object classification, part segmentation, and scene semantic parsing (Qi et al., 2016). While PointNet introduced significant advancements in processing point cloud data, it faced limitations in capturing local structures induced by the metric. To address this, PointNet++ was developed, enhancing PointNet by incorporating hierarchical feature learning, which allows it to recognize fine-grained details and local patterns more effectively (Qi et al., 2017). Numerous studies have applied PointNet and PointNet++ for object detection in the transportation domain. These techniques have proven effective in detecting various roadside infrastructures such as poles, traffic signs, light poles, trees, and power lines. For instance, Balado et al. (2019) and Wang et al. (2019) demonstrated the successful application of PointNet++ in identifying and classifying roadside objects, thereby contributing to the development of detailed and accurate infrastructure inventories.

Furthermore, PointNet++ has been effectively used for creating sidewalk inventories. Hou et al. (2020) utilized a deep neural network based on PointNet++ for the segmentation of sidewalks, showcasing its capability to segment and classify urban features accurately. This application is particularly valuable for urban planning and maintenance, providing detailed information about pedestrian pathways and related infrastructure. However, despite the significant advancements offered by PointNet and PointNet++, these approaches come with certain limitations. One major challenge is the requirement for extensive annotations to train the neural networks effectively. Annotating large datasets is labor-intensive and time-consuming, posing a bottleneck for widespread implementation. Additionally, the high computational resources needed for training and deploying these deep neural networks can be prohibitive, especially for large-scale deployments.

A concept of lateral distance calculation was presented in a study on point cloud classification for detecting roadside safety attributes and distances (Zhong et al., 2019). This study utilized a comprehensive approach where roadside objects were first detected and labeled by leveraging both point-wise and grid-wise features. The identified objects were then used to calculate the distance to the attribute center, providing precise measurements for roadside safety analysis. In our study, we aim to simplify this method by selecting clustering methods as the main approach for object detection. By employing clustering methods, we ensure that the object detection process is not only efficient but also scalable. This approach allows us to handle large datasets with minimal computational resources, making it feasible for large-scale deployments. The clustering approach is practical for our objectives, as it reduces the reliance on extensive annotations and high computational power, which are significant constraints in many existing methodologies.

3. METHODS

The workflow for the system, as shown in Figure 2, begins with a preprocessing step focused on noise removal from raw point cloud data. Following this, the data undergoes segmentation to distinguish between ground and non-ground points. For the ground points, line detection is performed to identify the border lines of pathways or roads. Concurrently, non-ground points are processed for wall detection to identify vertical structures and obstacles. After the initial detection, the results are validated by checking with panoramic images manually. This validation step ensures accuracy and allows for adjustments to the detection algorithm if necessary. Finally, the system calculates the lateral distance between the detected lines and walls, providing essential spatial measurements.

The algorithm was implemented using two different libraries on separate workstations. The environment for working with Point Cloud Library (PCL) (Rusu et al., 2011) was set up on a system equipped with an AMD Ryzen 9 5900HX CPU, running on WSL2. The environment for working with python-pcl (Sirokujira, 2018) was set up on a system equipped with an Intel Core i9-7900X CPU running Ubuntu 18.04.

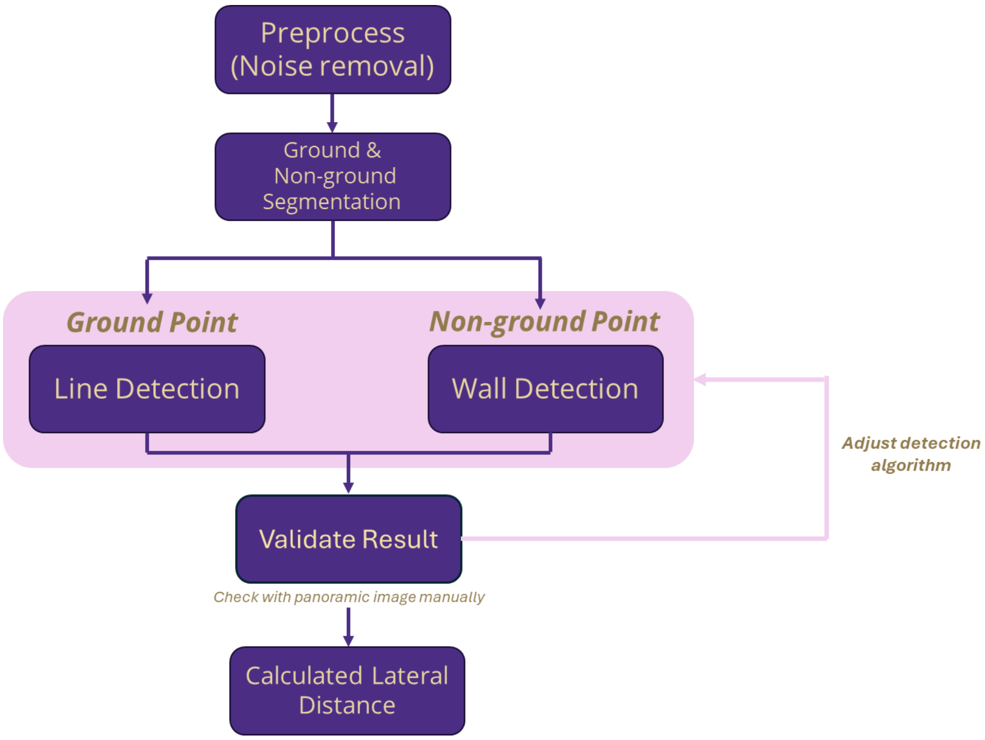

Figure *2* Workflow for a system

3.1 Preprocessing

Point clouds are considered large datasets that provide accurate and robust information but may contain high-density noise and scattered distributions due to being acquired by scanning equipment. Noise can arise from measurement errors, sensors, and environmental factors. Preprocessing processes can address these issues by reducing noise and the amount of data to process. Techniques for preprocessing point cloud data include point filtering, removing outliers, and holding out some data to decrease the size of raw data (Kharroubi, 2023).

Noise removal refers to the process of eliminating unwanted or spurious points from a point cloud dataset. Manual cleaning can remove noise data, but this method is inefficient as it is time-consuming. Double scanning can also help but is costly. Some mathematical techniques for noise removal include applying mean, median, or Gaussian filtering. These methods help ensure that the dataset is cleaner and more suitable for further processing and analysis. Downsampling is another technique used to reduce noise, but it requires careful parameter setting, as overly aggressive downsampling can eliminate important features, leading to inaccurate detection.

This study employed a downsampling technique to remove noise during the preprocessing step (Point Cloud Library, 2020). This method not only cleans the data but also reduces the size of the point cloud, resulting in more efficient analysis. Specifically, the VoxelGrid class in Point Cloud Library was used to create a 3D voxel grid over the input point cloud data. In each voxels, represents of the 3D cube with a fixed size, all points are reduces (i.e., downsampled) by their centroid. For this study, a voxel grid leaf size of 1 cm was set, which successfully reduced the point cloud size by 50% while retaining the original shape, as shown in Figure 3. This efficient reduction in data size without significant loss of detail is crucial for further processing and analysis.

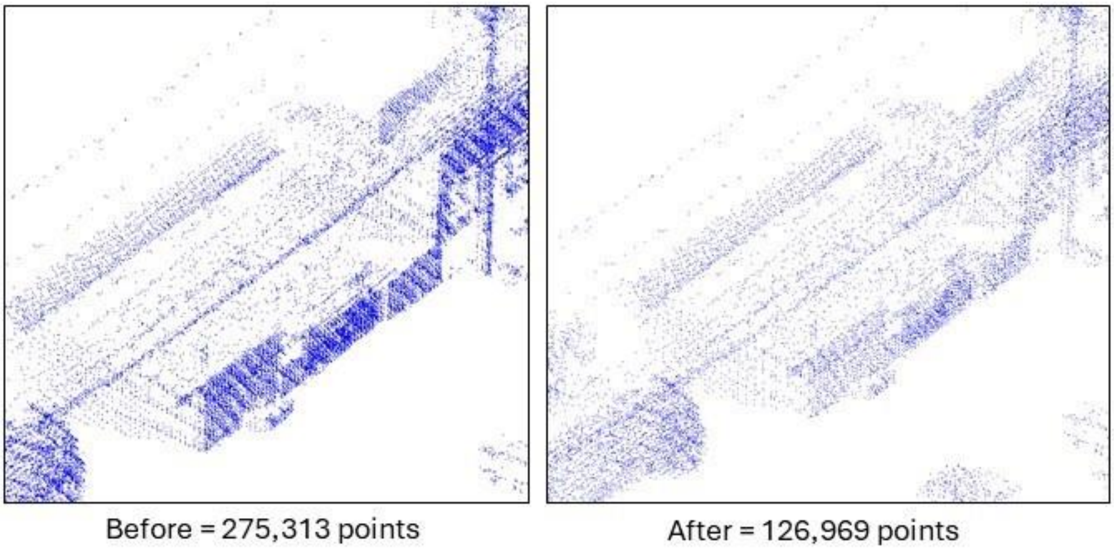

Figure 3 Applying Downsampling Method for Preprocessing (Leaf Size = 1 cm)

3.2 Ground Separation

To reduce computation time and increase the accuracy of object detection, it is essential to separate ground and non-ground objects (Figure 4). This study employed a filtering method known as the Cloth Simulation Filter (CSF) for this purpose (Zhang W, 2016). The CSF method simulates cloth using 3D computer graphics algorithms to cover an inverted LiDAR point cloud. The upside-down LiDAR terrain is assumed to be rigid, and the shape of the cloth, which drops due to gravity, forms the digital terrain model (DTM). The ground surface is determined from the interaction between the cloth and the corresponding LiDAR points.

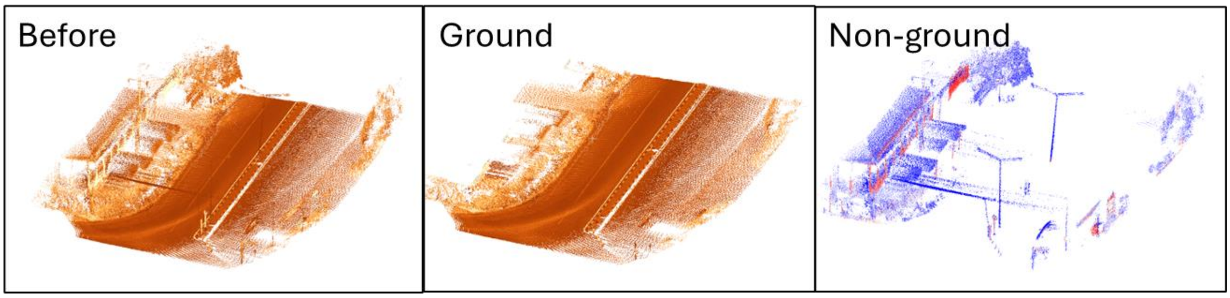

Figure 4 Applying Cloth Simulation Filtering (CSF) for ground and non-ground segmentation

In order to customize this method to the particular data we are working with, the Cloth Simulation Filter (CSF) enables users to adjust parameters based on their own needs. The first parameter is **cloth resolution**, which determines the grid size of the cloth used to cover the terrain; a larger cloth resolution results in a coarser Digital Terrain Model (DTM). The second parameter is **max iteration**, which specifies the maximum number of iterations for the terrain simulation. Lastly, the **classification threshold** defines the threshold for classifying the original point cloud into ground and non-ground parts based on the distances between the original point cloud and the simulated terrain. In this study, we used the default values for all parameters: 0.5 for cloth resolution, 500 for max iteration, and 0.5 for the classification threshold. These settings were chosen to balance accuracy and efficiency in the ground Separation process.

3.3 Line Detection

The road pavement marking contains an outstanding intensity value, therefore, we will utilize it. To prepare the data for the clustering algorithm, the separated ground point cloud is filtered based on intensity values before proceeding to the next step. In this study, an intensity range of 40 to 999 was set to ensure that the retained point cloud does not include pavement, which make up the majority of data in the ground point cloud. After the filtering process, the size of the point cloud is reduced, which enhances both the accuracy and efficiency of the subsequent processing steps.

Afterward, this study employed the Density-Based Spatial Clustering of Applications with Noise (DBSCAN) method, which is well-known for its ability to detect clusters of various shapes and sizes, making it suitable for identifying road alignments. Previous studies have utilized DBSCAN to process point cloud data for clustering tasks (Wang, W. and Wang, F., 2018; PointCloud Slam Image Web3, 2024; Peng et al., 2020). Generally, DBSCAN requires two parameters:

- **eps**: This is the maximum distance between two points for them to be considered part of the same neighborhood. In this study, the default value of 0.5 was used.
- **min_points**: This is the minimum number of points required to form a dense region, also known as the minimum cluster size. The default value of 5 was used in this study.

This section utilizing *python-pcl* library for process the point cloud data , and use *sklearn* library, which is machine learning library , for applying DBSCAN clustering. Each road segmented will be fitted to a line using polynomial regression, chosen for its capacity to handle nonlinear relationships. Different degrees of polynomials were examined to determine the best match. The equation is illustrated in the following form:

$$y = \beta_0 + \beta_1 x + \beta_2 x^2 + \cdots + \beta_n x^n \quad (1)$$

Where y = Dependent variable
x = Independent variables
n = Degree of a polynomial
β = Coefficient

In this study, a second-degree polynomial was chosen as it provided the best fit. To enhance the accuracy of data fitting, the point cloud data were divided into multiple segments, resulting in smaller straight lines (Figure 5).

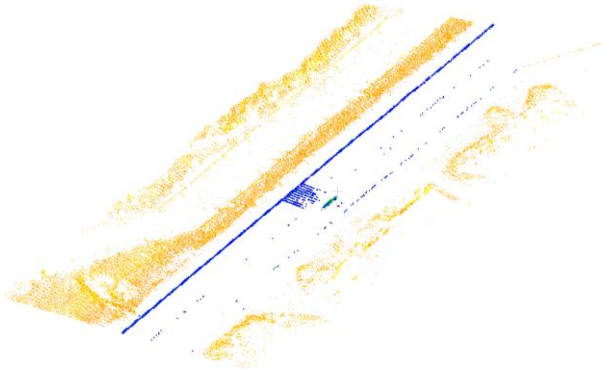

Figure 5 Segmented line detection from point cloud on the ground

3.4 Wall Detection

Plane segmentation of a set of points is used for wall detection. Plana surface is estimated by using RANdom Sample Consensus (RANSAC) algorithm to fit the point clouds in the plane model as the following equation:

$$ax + by + cz + d = 0 \quad (2)$$

Where x, y, z = Point cloud coordination
a, b, c = The x, y, z coordinate of the plane's normal (normalized)
d = The fourth Hessian component of the plane's equation

The RANdom Sample Consensus (RANSAC) technique was initially employed to identify the most significant plane, which corresponds to wall object. RANSAC (Random Sample Consensus) is an iterative method used to estimate a model from data that includes outliers (Fischler and Bolles, 1981). It works by repeatedly selecting random subsets of data, fitting linear models to these subsets, and identifying the model that best fits the inliers, thereby excluding outliers. The model with the best fit, based on the inliers, is chosen as the final result.

For RANSAC to function effectively, a distance threshold must be set to determine the maximum allowable distance from the model to a potential inlier point. Table 1 presents the various thresholds tested on a point cloud of approximately 120,000 points. We found that a threshold of 0.250 meters is the most suitable for our data, as it yields a reasonable number of clusters that represent planes in the point cloud. The maximum number of iterations was set to 1,000 by default.

After obtaining the plane from the RANSAC algorithm, the next step is to determine if the plane represents a wall. A plane that represents a wall should be perpendicular to the x-y plane or parallel with the z-plane. To determine the plane's configuration, surface normals are used. Surface normals are vectors that are perpendicular to a surface at a given point and are essential properties of a geometric surface.

Tabel 1 Distance Threshold for RANSAC Algorithm tested on 120k Point Cloud Data

Distance Threshold (m)	Number of Plane Cluster	Details
1.00	2	Too coarse, unable to distinguish wall object
0.50	4	Too coarse, unable to distinguish wall object
0.25	**7**	**Suitable for distinguishing wall object**
0.10	16	Able to detect wall object
0.01	184	Unable to distinguish object shape as it is too small

Determining the normal at a specific point on the surface is approximated by estimating the normal of a plane tangent to the surface. This estimation is typically done using the surrounding point neighborhood, known as the k-neighborhood. The correct scale factor (k or radius) for determining the nearest neighbors of a point is crucial for accurate normal estimation. In *point cloud library*, selecting the appropriate k or radius (r) values is critical for identifying the nearest neighbors effectively.

The scale for determining a point's neighborhood should be selected based on the level of detail required by the application. Table 2 presents various search radius tested on a point cloud of approximately 20,000 points, representing the target object of a wall. We found that a radius of 0.30 meters is the most suitable for our data, as it perfectly distinguishes the orientation of the object.

Tabel 2 Search Radius for Surface Normal Estimation on 20k Point Cloud Data

Search Radius (m)	Details Plane Cluster
3.00	Unable to detect normal on any plane
1.00	Works best with large planes
0.50	No improvement from previous step
0.30	**Able to capture planes representing walls of any size**
0.20	Unable to compile results, terminated
0.03	Unable to compile results, terminated

In this study, a wall object is identified by high coefficients of the normal vector in the x and y directions, indicating that the segment is perpendicular to the x-y plane and represents a wall configuration (Figure 6). Conversely, if the object has low coefficients in both the x and y directions, it can be concluded that the object is parallel to the x-y plane, meaning it does not represent a wall.

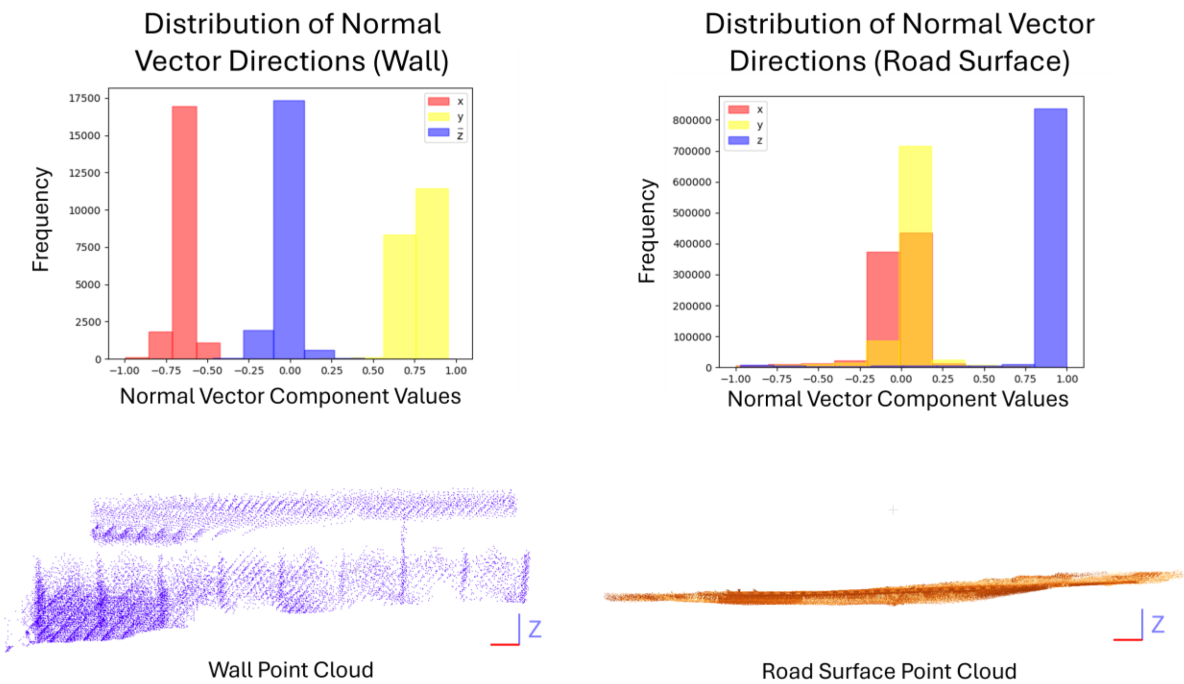

Figure 6 Histogram of surface normal for wall *(Left)* and road surface *(Right)*.

3.5 Distance Calculation

The distance will be calculated by determining the distance between the border line and the wall. This study utilized the *pcl_sample_consensus* library, which includes Sample Consensus (SAC) methods such as RANSAC and models like planes and cylinders. The use of SAC methods like RANSAC helps in robustly fitting models to the point cloud data, even in the presence of noise and outliers. The library also provides functions for computing the distance from a point to a plane. To perform the calculation, the centroid of the segmented road line is used as the reference point. This centroid represents the central position of the road line and serves as a critical point for accurate distance measurement. The detected wall is treated as a plane, defined by equation 2 (Figure 7).

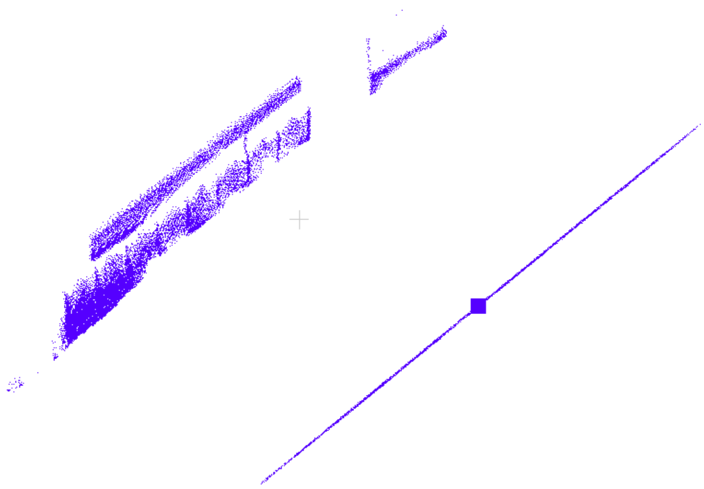

Figure 7 Point to plane distance

Given that the edge line of road is used as the reference, it is essential to determine which side the wall is located on. To achieve this, the direction of the vehicle's trajectory during the data collection process is utilized. The trajectory provides context about the vehicle's position relative to the road's edge line and helps in identifying whether the wall or object is located on the same side as the vehicle or on the opposite side. If the wall is located on the opposite side of the road lane from the vehicle's trajectory, the detected distance must be adjusted to account for the lane's width. This adjustment involves subtracting the width of the road lane, which, for a two-lane road, is typically assumed to be 6 meters. This step is crucial to ensure that the calculated distances accurately reflect the actual spatial relationships between the road and roadside objects.

3.6 Validation

To assess the accuracy and effectiveness of the proposed algorithm, we conducted a comparison between the algorithm's detection results and manually detected distances. For the manual detection process, we utilized CloudCompare, an open-source 3D point cloud and mesh processing software (CloudCompare, 2024). CloudCompare provides tools for precise measurement and validation of distances within point cloud data, but it requires manual intervention to identify and specify objects (Figure 8). This approach allowed us to comprehensively evaluate the algorithm's performance and ensure its reliability.

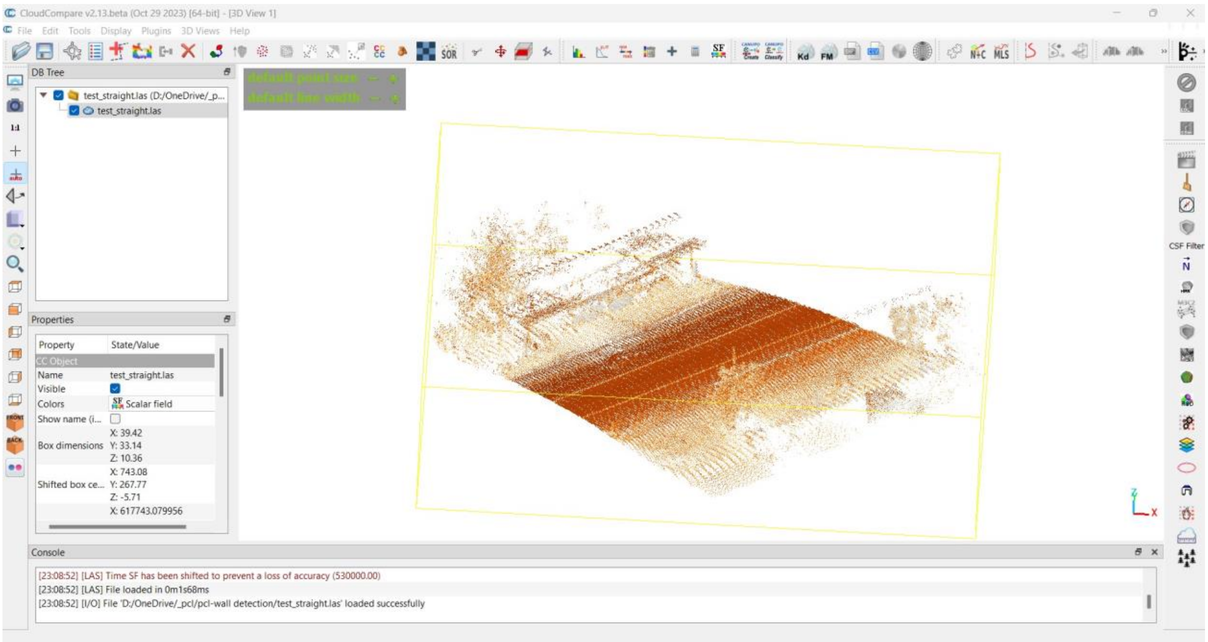

Figure 8 CloudCompare Software

Mean Absolute Error (MAE) is selected as the measurement metric for this study, as it provides a clear and straightforward assessment of the algorithm's prediction accuracy. MAE calculates the average absolute difference between the distances detected by the algorithm and the ground truth values measured manually using CloudCompare. By focusing on absolute differences, MAE ensures that the magnitude of errors is accounted for without considering their direction whether the detected distance is overestimated or underestimated. The equation for calculating MAE for n instances is as follows:

$$MAE = \frac{1}{n}\sum_{i=1}^{n}|distance_i - groundtruth_i|$$

In this equation, $distance_i$ represents the distance calculated by the algorithm for the i-th instance, and $groundtruth_i$ represents the corresponding ground truth distance measured using CloudCompare. We used MAE for this dataset because the presence of outliers is not particularly significant. The setting of the wall is random and does not correlate with specific road classes, meaning that outliers can appear anywhere without a specific pattern. Therefore, MAE, which provides a straightforward average error without disproportionately penalizing larger deviations, is a more appropriate metric for evaluating the accuracy of our distance calculations.

To conduct a thorough analysis, the point cloud data obtained from mobile laser scanning was divided into subsegments, each with a length of approximately 10 meters. This segmentation approach facilitates a more manageable and detailed examination of the data, ensuring that each segment can be analyzed individually for specific characteristics and anomalies. We specifically tested only those subsegments where walls were identified. This targeted approach ensures that the analysis is relevant and focused on the areas of interest, providing insights into the algorithm's performance in detecting and measuring walls accurately. To ensure a fair comparison of the accuracy of different observations, especially considering the varying lengths of the segments, we normalized the error by computing the Mean Absolute Error (MAE) per kilometer.

4. RESULTS

This study proposes an algorithm for automatically calculating lateral distance using point cloud data obtained from mobile laser scanning. The point cloud data were preprocessed to remove noise and separate ground from non-ground points, enhancing the efficiency of the algorithm. The road edge line and wall were detected separately, and the distance between these two objects was then computed. CloudCompare software was used for manual validation of the detected results. The generalizability of the algorithm was tested using three distinct scenarios, each representing different road characteristics: a road along the river, a road in a residential area, and a high-volume road. These scenarios were chosen because they each present unique features and challenges, offering a diverse basis for evaluating the algorithm's performance.

For this study, we utilized 10 kilometers of point cloud data collected through mobile laser scanning. The road along the river scenario offers insights into how proximity to natural features affects lateral distance calculations. The residential area scenario highlights the complexities introduced by varying building densities, pedestrian pathways, and local signs. Finally, the high-volume road scenario showcases the algorithm's capability to handle dense traffic conditions and multiple lanes.

Table 3 presents a comprehensive performance analysis of the algorithm across different road environments, and Table 4 displays the measured and calculated lateral distances used for validation, with panoramic images included for reference. Each row represents a different test scenario, illustrating the algorithm's performance in various contexts.

Table 3 Performance analysis of the algorithm

Class	Road Name	Total length (km)	MAE (m)	MAE per km (m/km)	Average lateral distance (m)
Residential	CNT1021	2.91	1.635	0.562	4.911
Road along river	AYA2045	1.95	1.301	0.667	10.787
High Traffic Volume	AYA5042	5.12	1.758	0.343	5.406

Among the three categories analyzed, roads in high-traffic volume areas exhibit the lowest Mean Absolute Error (MAE) per kilometer of 0.343, demonstrating the effectiveness of our method in these environments. In contrast, roads along the river and roads in residential areas have higher MAE per kilometer values of 0.667 and 0.562, respectively. During manual detection, we observed that high-traffic volume areas typically have clearer roadsides to accommodate the heavy traffic. Conversely, our algorithm performed well on straight-road segments but showed weaknesses on curved segments. Some subsegments had road surfaces covered by vegetation or were under maintenance, which impeded our model's ability to detect road lines accurately. Roads with multiple lanes also require human interpretation, as our current algorithm lacks the capability to precisely detect outer lines. In terms of wall detection, large flat planes yielded higher accuracy. Walls that were covered by vegetation or were not continuous, such as fences, often resulted in errors. Awnings and roofs, which are commonly found along roads in residential areas, led to shorter lateral distances due to plane fitting during wall detection. Additionally, pruned shrubs often created planar surfaces that the algorithm mistakenly detected as walls.

Another objective of this study is to report the average lateral distance across different road classes. The analysis revealed that roads along the river have the widest average lateral distance at 10.787 meters, while roads in residential areas have the shortest average lateral distance at 4.911 meters. This finding is consistent with expectations for residential areas, where space is often maximized, and infrastructure is densely packed. Additionally, temporary roadside structures, such as curbside stores, frequently violate legal limitations and can skew measurements. In contrast, along river roads, natural barriers and the need to mitigate risks like landslides typically result in constructions being placed further from the riverbank, which increases the average lateral distance. However, temporary structures can still be detected along these roads, though they generally do not significantly impact the overall average distance. This variation in lateral distances highlights the influence of environmental and infrastructural factors on road design and safety considerations.

Table 4 Measured and calculated lateral distances with panoramic images for road in residential area (Top), road along river (Middle), and road with high traffic volume (Bottom)

Measured lateral distances	**Panoramic image**
Class: Residential (Calculated = 13.71 m / Measure = 13.79 m) 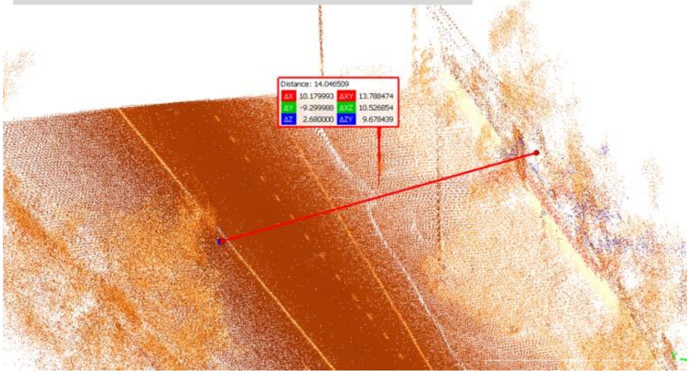	
Class: Road along river (Calculated = 8.56 m / Measure = 8.50 m) 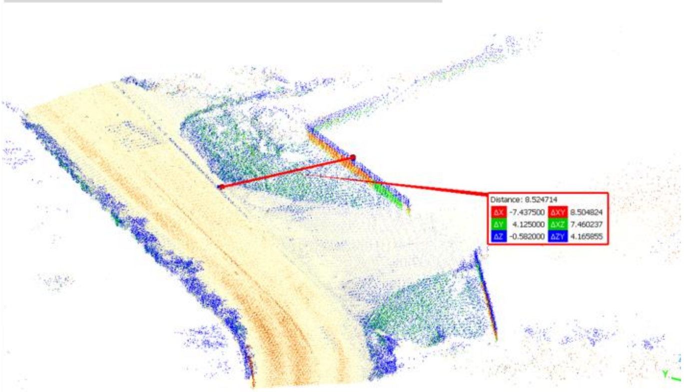	
Class: High Traffic Volume (Calculated = 14.62 m / Measure = 14.70 m) 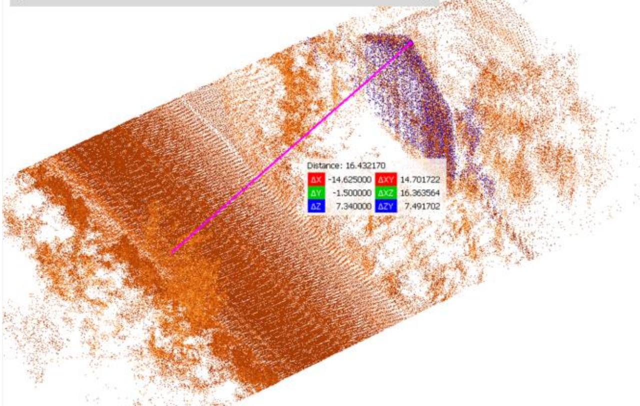	

5. CONCLUSIONS

This study introduces an automated methodology for calculating lateral offset distance using point cloud data. Approximately 10 kilometers of point cloud data were collected from rural roadways in Thailand and used as a dataset for developing a detection algorithm. To conduct a comprehensive analysis of different road types, three road classifications were selected. Our developed algorithms achieved an MAE per kilometer of 0.343 meters for roads with high traffic volumes, as these roads typically have clear roadsides that align with their intended function. We also found that roads in residential areas have the shortest average lateral distance of 4.911 meters. The calculated lateral distance provide valuable data that can be directly used by road authorities for safety assessments and infrastructure planning.

This study does present some limitations. The total dataset covers only approximately 10 kilometers of roadways. While this provides a starting point, it may not be sufficient to generalize the findings across different road types and conditions. Additionally, the study only includes three distinct types of roads. Expanding the dataset to include a broader variety of road types, such as urban roads, highways, and rural roads with different characteristics, would allow for a more comprehensive evaluation. Moreover, it would be beneficial to assess how the algorithm performs across different segments within each road type, particularly given the challenges faced in certain environments. The proposed algorithm also showed limitations in detecting curved lines or fences, indicating areas where further refinement and improvement are needed. These factors suggest that while the study provides valuable insights, additional research with a more diverse dataset and enhanced algorithm capabilities is necessary to fully validate and extend the findings.

Infrastructure along rural roads in Thailand, both temporary and permanent, is often random and challenging to detect through pattern recognition. To improve the algorithm, it is recommended to utilize deep learning techniques for object detection to better obtain semantic descriptions and make accurate classifications. Additionally, as road markings are sometimes missing due to obstructions or maintenance, implementing road marking detection will provide a more accurate and comprehensive assessment of all components on the road surface, reducing many of the assumptions made in this study. Moreover, integrating image data with point cloud data is another approach that can significantly enhance point cloud segmentation and classification tasks by providing color information. This process will improve the accuracy of detecting and classifying road features, leading to more reliable infrastructure assessments and development plans. Combining these techniques will help overcome the limitations observed in rural road infrastructure detection and contribute to more effective road safety and maintenance strategies.

6. ACKNOWLEDGMENTS

Authors would like to thank to Department of Rural Roads of Thailand, Ministry of Transportation, for the use of their data.

7. REFERENCE

Ai, C., and Tsai, Y. J. (2012). Critical Assessment of Automatic Traffic Sign Detection Using Three-Dimensional LiDAR Point Cloud Data. Transportation Research Board 91st Annual Meeting. Volume: 12-3214.

American Association of State Highway and Transportation Officials. (2018). A Policy on Geometric Design of Highways and Streets, 2018. Green book, American Association of State Highway and Transportation Officials.

Balado, J., Martínez-Sánchez, J., Arias, P., & Novo, A. (2019). Road Environment Semantic Segmentation with Deep Learning from MLS Point Cloud Data. Sensors, 19(16). doi:10.3390/s19163466

Bamrungwong, C., P. Soparat, K. Saiprasertkit, and N. Jantarathaneewat. (2017). A Study of Applying Mobile Mapping Result for Road Safety Audit on Rural Roads in Thailand. Transportation Research Circular, , No. E-C220.

CloudCompare. (2024). CloudCompare: 3D point cloud and mesh processing software Open 2 Source Project. https://www.cloudcompare.org/. Accessed 2024.

Department of Rural Roads of Thailand (DRR). (2024). The Accident Report Management System (ARMS). https://arms.drr.go.th/. Accessed 2024.

FHWA Highway Safety Programs (2023). Clear Zones. https://highways.dot.gov/safety/rwd/provide-safe-recovery/clear-zones/clear-zones. Accessed 2023.

Fischler, M. A. and R. C. Bolles. (1981). Random sample consensus: a paradigm for model fitting with applications to image analysis and automated cartography. Vol. 24, No. 6, p.381–395.

Gargoum, S. A., L. Karsten, K. El-Basyouny, and J. C. Koch. (2018). Automated assessment of vertical clearance on highways scanned using mobile LiDAR technology. Automation in Construction, Vol. 95, pp. 260–274.

González-Gómez, K., L. Iglesias, R. Rodríguez-Solano, and M. Castro. (2019). Framework for 3D point cloud modelling aimed at road sight distance estimations. Remote Sensing, Vol. 11, No. 23, p. 2730.

Gouda, M., Shalkamy, A., Li, X., and El-Basyouny, K. (2022). Fully Automated Algorithm for Light Pole Detection and Mapping in Rural Highway Environment Using Mobile Light Detection and Ranging Point Clouds. Transportation Research Record, 2676(7), 617-629. https://doi.org/10.1177/03611981221082531

Hou, Q., & Ai, C. (2020). A network-level sidewalk inventory method using mobile LiDAR and deep learning. Transportation Research Part C: Emerging Technologies, 119, 102772. doi:10.1016/j.trc.2020.102772

Insurance Institute for Highway Safety (IIHS). (2024). Fatality Facts 2022: Collisions with fixed objects and animals. https://www.iihs.org/topics/fatality-statistics/detail/collisions-with-fixed-objects-and-animals. Accessed 2024.

iRAP. (2022). Forgiving Roads Concept. https://toolkit.irap.org/safer-road-treatments/forgiving-roads-concept/. Accessed 2024.

Kharroubi, A. (2023). Introduction to 3D Point Cloud. 3D Point Cloud Masterclass. Udemy.

Lee, J. and F. Mannering. (2002) Impact of roadside features on the frequency and severity of run-off-roadway accidents: an empirical analysis. Accident Analysis Prevention, Vol. 34, No. 2, pp. 149–161.

Lorenz Partners. (2019). Basic Conditions for Building Construction in Thailand. https://www.lorenz-partners.com/wp-content/uploads/2019/01/NL221E-Basic-Conditions-for-Building-Construction-in-Thailand-Jan19. pdf, accessed 2024.

Ma, L., Ying L., Jonathan L., Cheng W., Ruisheng W., and Michael A. C. (2018). Mobile Laser Scanned Point-Clouds for Road Object Detection and Extraction: A Review.

Remote Sensing 10, no. 10: 1531. https://doi.org/10.3390/rs10101531

Mohamed, M., Morsy, S., and El-Shazly, A. (2022). Improvement of 3D LiDAR point cloud classification of urban road environment based on random forest classifier. Geocarto International, 37(27), 15604–15626. https://doi.org/10.1080/10106049.2022.2102218

Peng, C. L., Z. and L. Wang. (2020). Point cloud segmentation (clustering). https://yzrobot.github.io/mobile_robotics/P20-UN56-clustering.pdf. Accessed 2024.

Point Cloud Library. (2020). Downsampling a PointCloud using a VoxelGrid filter. https://pcl.readthedocs.io/projects/tutorials/en/latest/voxel_grid.html. Accessed 2024.

Point Cloud Slam Image Web3. (2024). Implementation of DBSCAN clustering algorithm based on PCL. https://medium.com/point-cloud-python-matlab-plus/implementation-of-dbscan-clustering-algorithm. Accessed 2024.

Qi, C. R., Su, H., Mo, K., & Guibas, L. J. (2016). PointNet: Deep Learning on Point Sets for 3D Classification and Segmentation. CoRR, abs/1612.00593. http://arxiv.org/abs/1612.00593

Qi, C. R., Yi, L., Su, H., & Guibas, L. J. (2017). PointNet++: Deep Hierarchical Feature Learning on Point Sets in a Metric Space. CoRR, abs/1706.02413. http://arxiv.org/abs/1706.02413

Road Safety Thailand Road Safety Policy Foundation. (2018). KEY FACTS ON ROAD SAFETY SITUATIONS IN THAILAND 2012-2013. https://www.roadsafetythai.org/edoc/doc_20181208173742.pdf. Accessed 2024.

Rusu, R. B. and S. Cousins. (2011). 3D is here: Point Cloud Library (PCL). In IEEE International Conference on Robotics and Automation (ICRA), Shanghai, China, 2011.

Se, C., T. Champahom, S. Jomnonkwao, and V. Ratanavaraha (2020). Risk factors affecting driver severity of single-vehicle run off road crash for Thailand highway. Engineering Journal,Vol. 24, No. 5, pp. 207–216.

Sirokujira. (2018). python-pcl. https://github.com/Sirokujira/python-pcl?tab=readme-ov-file#readme. Accessed 2023.

Somchainuck, O., P. Taneerananon, and S. Jaritngam. (2013). An in-depth investigation of road side crashes on Thai National Highways. Engineering Journal, Vol. 17, No. 2, pp.63–74.

Wang, D., Wang, J., Scaioni, M., & Si, Q. (2019). Coarse-to-Fine Classification of Road Infrastructure Elements from Mobile Point Clouds Using Symmetric Ensemble Point Network and Euclidean Cluster Extraction. Sensors (Basel, Switzerland), 20(1), 225. https://doi.org/10.3390/s20010225

Wang, W. and F. Wang. (2018). lane-detection. Retrieved from: https://github.com/willshw/37 lane-detection. Accessed 2023.

Yin, S., and Zhu, L. (2022). Country Road Boundaries Detection for Autonomous Driving Based on LiDAR Point Cloud. 2022 IEEE 5th International Conference on Electronics Technology (ICET), Chengdu, China, 2022, pp. 1117-1120, doi: 10.1109/ICET55676.2022.9824682.

Zhang W, Q. J. (2016). An Easy-to-Use Airborne LiDAR Data Filtering Method Based on Cloth Simulation. Remote Sensing, 8(6):501.

Zhong, M., Verma, B., & Affirm, J. (2019). Point Cloud Classification for Detecting Roadside Safety Attributes and Distances. 2019 IEEE Symposium Series on Computational Intelligence (SSCI), 1078–1084. doi:10.1109/SSCI44817.2019.9002813

Identification of Maintenance Prioritization across Multiple Highway Categories

Pornchita Arundachachai[1, *], Thitipong Chaiwannakupt[2] and Kanisa Rungjang[2]

[1] Department of Highways, Ministry of Transport, Bangkok, Thailand, arundachachai.p@gmail.com
[2] Department of Civil Engineering, Kasetsart University, Bangkok, Thailand, thitipong.chaiwa@ku.th
[2] Department of Civil Engineering, Kasetsart University, Bangkok, Thailand, fengksr@ku.ac.th

ABSTRACT

Road have deteriorated over time due to various factors demanding repair and rehabilitation to provide desirable service level for road users. Prioritizing road maintenance is done to ensure that a critical road is selected with higher priority considering limited budget. Therefore, it is necessary for decision makers to assess road condition and prioritize maintenance based on a systematic evaluation of road condition using specific criteria. This study employs Fuzzy Analytic Hierarchy Process (FAHP) to determine the weights of influencing factors and Technique for Order Preference by Similarity to Ideal Solution (TOPSIS) to prioritize highway categories for maintenance. The results reveal that pavement condition is the most influential factor, followed by traffic characteristic, life cycle and maintenance, and context of land use. Furthermore, the priorities for highway maintenance among different experts' group is shown to be varying. Those responsible for Location and Design prioritize Rural Roads, while Construction and Maintenance professionals prioritize National Highways. Planning and Monitoring professionals, on the other hand, prioritize Motorways. The differing perspectives on prioritization demonstrate the importance and unique maintenance strategies of each road type. By understanding and adopting these findings, time management, financial allocation, and personnel mobilization can be optimized, leading to more effective and efficient highway maintenance practice.

Keywords: Highway Maintenance, Prioritization, FAHP, TOPSIS

1. INTRODUCTION

Roads deteriorate over time due to various factors such as traffic loading, weather, temperature, and construction quality. Maintenance is necessary to ensure their functionality and safety for road users. Either routine or periodic maintenance can be conducted to preserve their serviceability and extend their service life, the proper decision making of time management and resource allocation should be accounted. (Kumar & Suman, 2022) The timing of these interventions should consider the current road condition and its expected service life. Premature rehabilitation efforts can result in unnecessary and wasteful of resources. However, delaying rehabilitation beyond critical point can lead to a significant deterioration where a more extensive and expensive reconstruction is required. (Nautiyal & Sharma, 2022) The ideal timing of rehabilitation falls within a window between the initial decline in service level and the critical point of deterioration of the roads. Intervention at this stage can significantly extend their service life as well as postpone or avoid the need of reconstruction. (Kresnanto, 2022) It is important to prioritize the maintenance and rehabilitation of roads based on specific criteria, especially for highway maintenance, where budgetary constraints limit the resources available for repairs across the entire network. (Ahmed et al., 2017) Furthermore, in the absence of historical data on road condition, a systematic assessment become necessary for decision-maker to determine and prioritize roads in need of immediate repair. (Kresnanto, 2022)

To address this challenge, several studies examined different factors that influenced how decision makers prioritize highway maintenance. These factors are broadly categorized into four groups including pavement condition, traffic characteristic, life cycle and maintenance, and context of land use. The influence of these factors can differ depending on the categories of highway and their characteristic. In Thailand, highways are categorized into four groups including Motorway, National Highway, Rural Road, and Local Road. (Office of the Council of State, 1992)

This research aims to address this challenge by employing Fuzzy Analytic Hierarchy Process (FAHP) to weight the relative important of influencing factors and Technique for Order Preference by Similarity to Ideal Solution (TOPSIS) to determine the priority of highway maintenance in Thailand.

2. INFLUENCING FACTORS SELECTION

The complexity of prioritizing highway maintenance and rehabilitation needs a systematic assessment to support decision making considering the budget constraints. There are various factors influencing the decision-making process. It is categorized into four main groups including pavement condition, traffic characteristic, life cycle and maintenance, and context of land use. Each categories encompasses specific indicator, i.e. Pavement Condition

Pavement condition, encompassing, surface condition and age, is a primary factor in prioritizing highway maintenance. Pavement Condition Index (PCI) was utilized as a key indicator in assessing and quantifying pavement condition. In addition, other indicators such distress, characteristic deflection, and International Roughness Index (IRI) were incorporated alongside PCI to gain a better comprehension on the function and structure of pavement, i.e. Table 1.

2.1 Traffic Characteristic

Traffic characteristic significantly impact on the rate and severity of pavement deterioration. Traffic volume is a major indicator in this category that accelerates the deterioration. Several studies expanded the evaluation by differentiating the characteristic and level of traffic volume, such as the traffic volume of truck, car, bus and motorcycle, and light to very heavy traffic volume, i.e. Table 1.

2.2 Life Cycle and Maintenance

Life cycle and maintenance are crucial to maintenance aspect, encompassing the historical data of the specific highway from construction to rehabilitation. Studies showed that the maintenance strategies can be optimized in term of pavement life and resource allocation, considering Life cycle and maintenance. These involve its remaining structural life as well as maintenance expenditure and cost-benefit, i.e. Table 1.

2.3 Context of Land Use

Context of land use is required to gain a better understanding of the importance of specific highway. Several studies focus on the land use type, such as industrial, agriculture and residential area, and some incorporated the economic aspect to get more specific maintenance strategies for each region. Additionally, the surrounding environment of highway was incorporated alongside land use type to obtain more comprehensive evaluation, i.e. Table 1.

Table 1 Influencing factors on highway maintenance prioritization.

Author (s)	Pavement Condition	Traffic Characteristic	Life Cycle and Maintenance	Context of Land Use
(Moazami et al., 2011)	Pavement Age			National roadways, regional roadways
(Babashamsi et al., 2016)	PCI, Operation condition index	Traffic congestion	Operation cost	
(Porras-Alvarado et al., 2017)	Failure, Rutting, Fatigue cracking, Longitudinal cracking, Ride score, Change in ride, Score since last year, Change in distress score since last year	Truck ADT, Total ADT	Remaining structural life (%), Routine maintenance expenditure, Preventative M&R expenditures, Years since last resurfacing, Years since last structural rehabilitation	
(Hendhratmoyo et al., 2017)	Area of Cracks, Crack Width, Potholes, Depth of Wheel Rutting	Traffic Volume		
(Siswanto et al., 2019)	Deformation, Cracking, Rutting	Light truck, Heavy truck, Car, Bus, Motorcycle	Cost, Benefit	Agriculture, School & residential, Tourism & Trading
(Chaipetch, 2022)	IRI	Traffic Volume, Volume of Heavy Truck	Economic	Tourist Spot, Business Center, Government Offices, Hospitals, Industrial Areas
(Nautiyal & Sharma, 2022)	Road condition	Public transportation routes, Number of public facilities,	Primary commodities, Economic feasibility,	Population, People participation, Road hierarchy

Author (s)	Pavement Condition	Traffic Characteristic	Life Cycle and Maintenance	Context of Land Use
		Service rates, Traffic volumes	Accessibility, Maintenance type	
(Chundi et al., 2021)	IRI, Deflection, Rutting, Cracking, Raveling			
(Kresnanto, 2022)	Road condition (Heavy damage, medium damage, Light damage)	Traffic Volume (Motorcycle, Bus, Car, Med-Heavy Truck, Light truck)	Cost Estimation, Benefit/Eligibility, Damage Prevention, Maintenance, New Construction	Trading Area, Social-culture, Education, Agriculture
(Kumar & Suman, 2022)	Pavement Condition, Pavement Age	Commercial vehicle repetitions		Air temperature, Wind Speed, Precipitation, Relative Humidity
(Fawzy et al., 2023)	PQI	light traffic, medium traffic, heavy traffic, very heavy traffic		
(Smrudu et al., 2023)	PCI, Characteristic defection, IRI	Commercial Vehicles Per Day (CVPD)		

3. Highways in Thailand

The prioritization of highway maintenance is a crucial aspect in infrastructure management. Considering influencing factor, there might be a variation in the result from decision-making process depending on the context and location of specific highway. This study focuses on prioritize the maintenance for Highway in Thailand including Motorway, National Highway, Rural Roads, and Local Roads. (Office of the Council of State, 1992)

The numbering system is invented to identify the location and hierarchy of each road, and is applied to Motorways and National Highways. This system uses four-digit numbers to categorize roads into four levels, including primary highways (first digit), regional highways (second digit), secondary highways (third digit), and local highways (fourth digit). (Department of Highways, 2017)

3.1 Motorways

Motorways, including expressways, are highways arranged or built for high-speed traffic, with limited access point. The authority of construction, maintenance and improvement is under the Department of Highways. Motorways are designated with a leading "5-9".

3.2 National Highways

National Highways are main highways in which its network connect regions, cities, districts, and other significant places. The authority of construction, maintenance and improvement is under DOH. National Highways are designated with a leading "1-4", connecting Bangkok to main region of Thailand including the North, Northeast, Central and South. Additionally, there are another 12 routes including Asian Highway designated with a leading (AH 1, AH 2, AH 3, AH 12, AH 13, AH 15, AH 16, AH 18 and AH 19), and ASEAN Highway Network designated with a leading (AH 112, AH 121 and AH 123)

3.3 Rural Roads

Rural Roads connect rural area to National Highways and other major roads. The authority of construction, maintenance and improvement is under the Department of Rural Roads (DRR).

3.4 Local Roads

Local Roads connect communities, designed for local traffic as well as providing access to properties. The authority of construction, maintenance and improvement is under local administrative organization

4. MATERIAL AND METHODS

4.1 Research Framework

The framework of this study is built upon the existing literature on highway maintenance prioritization. The data used in this analysis was gathered through pairwise questionaries and interviews with experts, who work in road construction-related organizations such as DOH, DRR, Department of Public Works and Town & Country Planning (DPT), and other private company. The reliability and creditability of these data is validated with the consistency ratio (C.R.) definition. The criteria, namely, influencing factors are then analyzed by FAHP to determine the weight of each criterion. Furthermore, the highway categories will be prioritized employing TOPSIS method in accordance to the weight of influencing factor obtained from FAHP, refer to Figure 1.

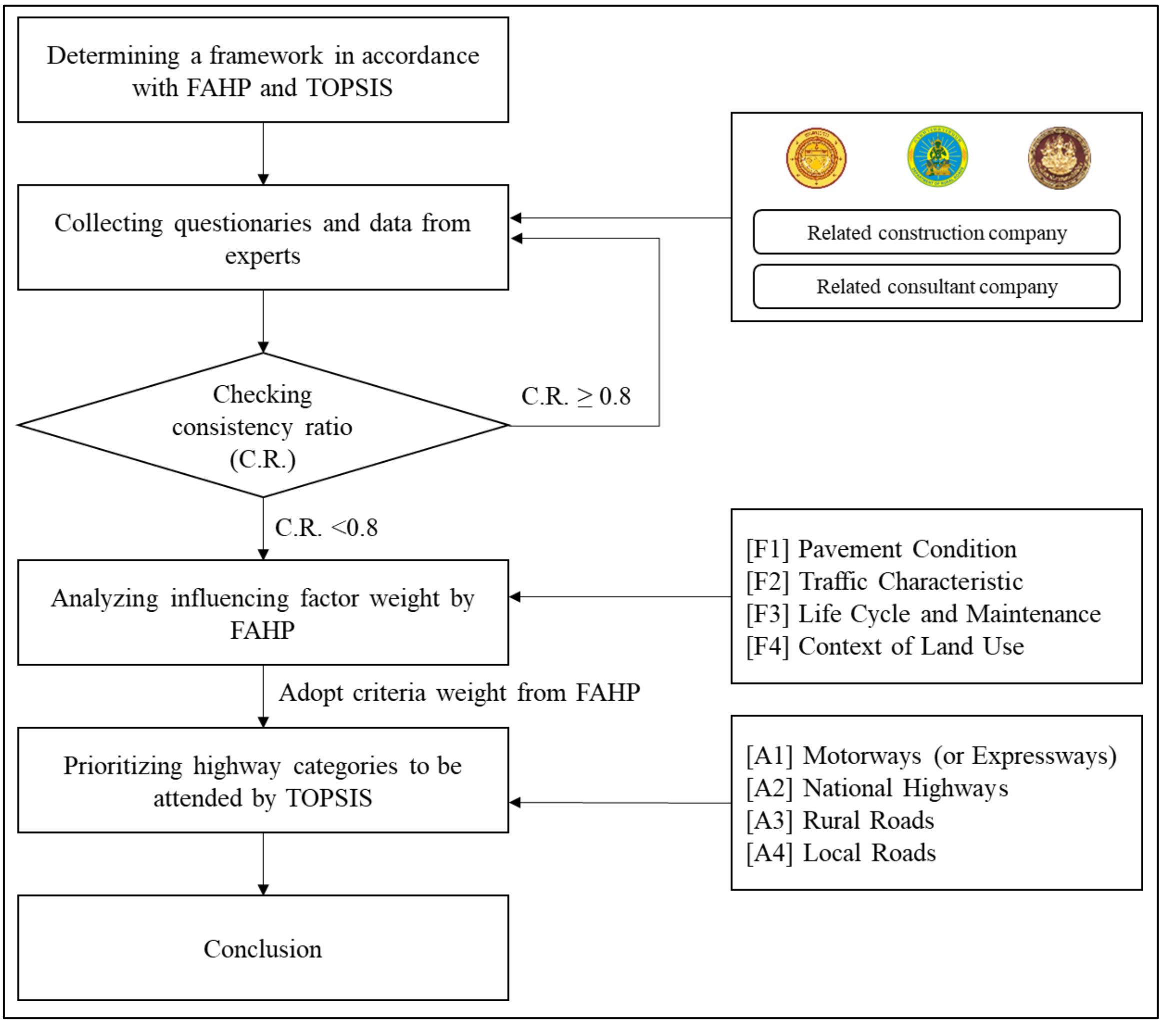

Figure 1 FAHP and TOPSIS Framework.

4.2 AHP

AHP is a decision-making method that considers multi criteria and alternatives, widely used in dealing with complex decisions, i.e. Figure 2. This method simplifies the complex problems into a hierarchy composed of three levels. The first level is obtained by defining a clear objective for the decision. To support this objective, criteria (level 2) are identified to evaluate the potential options/alternative (level 3). In this study, the criterions are represented by the influencing factors, and the alternatives are highway categorizes in Thailand. The hierarchy for AHP, therefore, is constructed, refer to Figure 3. The key principle of AHP involves pairwise comparison of elements in each level which is designed to determine the relative importance of each criterion. To quantify the relative importance of factors in comparison with the preceding level, matrices of each hierarchical level are constructed. The value that represents factor importance ranges from 1 (Equal importance) to 9 (extremely strong) with incremental of 2. The inconsistency due to human judgement is measured and addressed through the consistency ratio (CR). A CR for matrix 4x4 is acceptable at 0.08 or below. (Saaty & Vargas, 2001, Babashamsi et al., 2016)

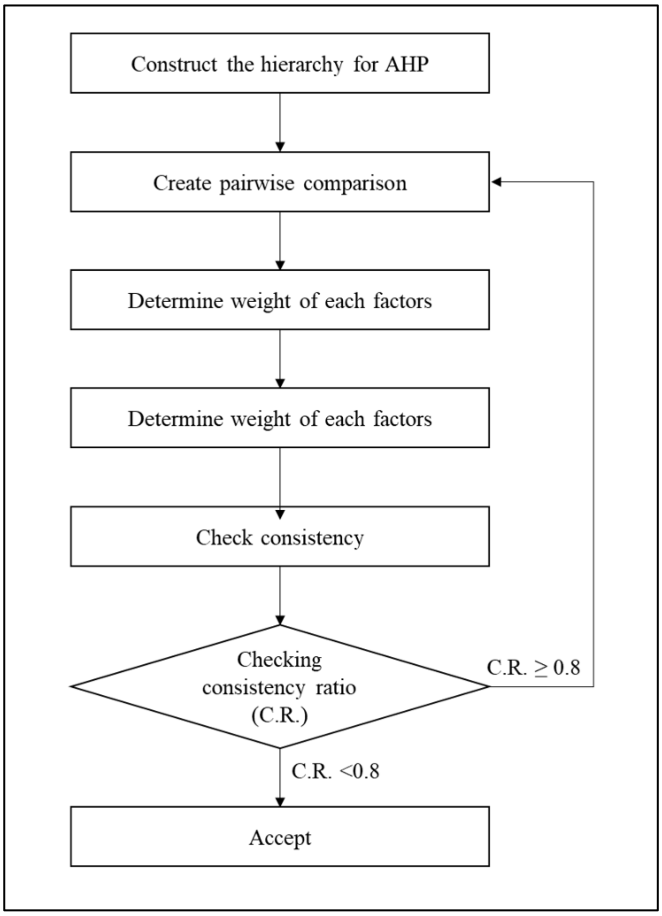

Figure 2 Analytic hierarchy process of Highway Maintenance Prioritization in Thailand

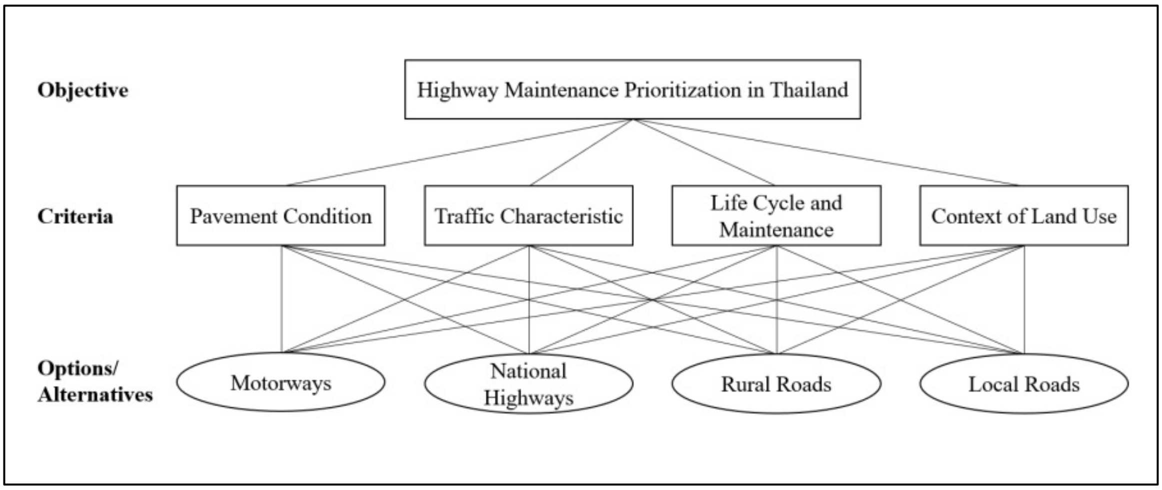

Figure 3 Analytic hierarchy of Highway Maintenance Prioritization in Thailand

4.3 Fuzzy AHP

FAHP, like AHP, uses crisp numerical values to represent the weight of each criterion. However, it is difficult to determine the exact value due to the vagueness and uncertainty in human judgment. To express the preference of decision makers, fuzzy numbers is employed instead of crisp numbers in term of linguistic such as "equally important," "moderately important," "strongly important", i.e. Table 2. Triangular fuzzy numbers (TFNs) is commonly used in FAHP, identified from three real numbers in form of (m1, m2, m3) where m1 is the lowest possible value, m2 is the most promising value, and m3 is the highest possible value. Figure 4 represent the construction of triangular fuzzy number. (Angelia & Mazni, 2019; Ouma et al., 2015)

Table 2 Fuzzy linguistic terms and Triangular fuzzy scale.

Importance intensity	Linguistic terms for alternatives	Triangular fuzzy scale
1	Equal importance	(1,1,1)
2	Weak or slight	(1,2,3)
3	Moderate importance	(2,3,4)
4	Moderate plus	(3,4,5)
5	Strong importance	(4,5,6)
6	Strong plus	(5,6,7)
7	Very strong importance	(6,7,8)
8	Very strong plus	(7,8,9)
9	Extremely strong	(9,9,9)

(Saaty & Vargas, 2001)

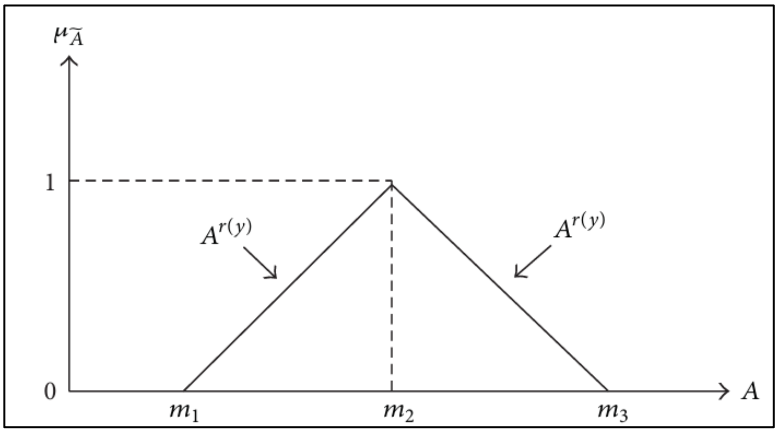

Figure 4 Construction of triangular fuzzy number.
(Ouma et al., 2015)

4.4 TOPSIS

TOPSIS is multi-criteria decision analysis method, traditionally ranks a set of alternatives by evaluating the distance to both the Positive Ideal Solution (PIS, A^+) and Negative Ideal Solution (NIS, A^-), refer to Figure 5. Hypothetically, PSI is a solution that maximize all the criteria, while NIS minimizes all the criteria. The selected alternative should be closet to PIS and furthest from NIS. (Ayalew et al., 2022; Li et al., 2023; Omari et al., 2021)

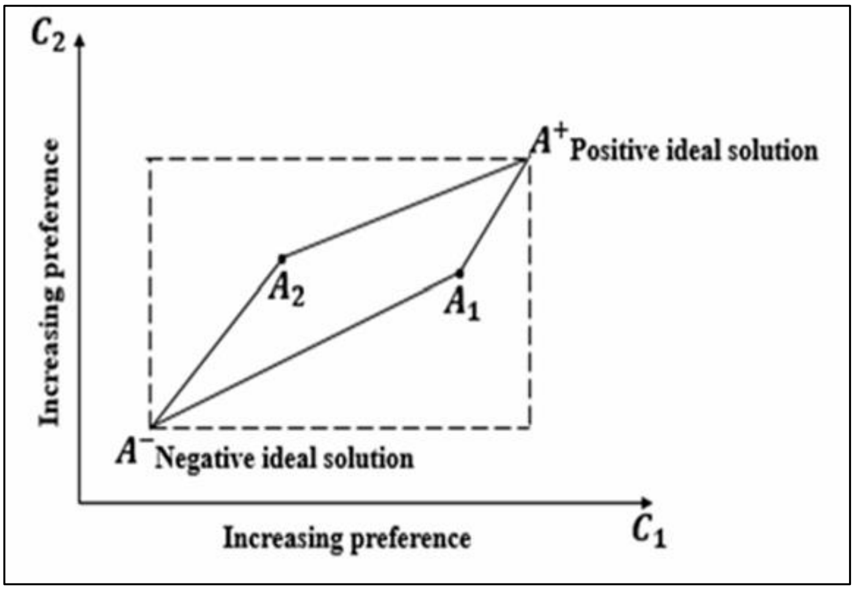

Figure 5 TOPSIS Concept.
(Omari et al., 2021)

5. RESULTS

This research involved the participation of 58 experts with an average of 10 years' experience in road construction and maintenance project, they were invited to contribute their knowledge and experience. The questionnaires were distributed among these experts to gather preliminary data and opinions regarding four influencing factors which are Pavement Condition, Traffic Characteristic, Life Cycle and Maintenance, and Context of Land Use.

To facilitate a more comprehensive analysis, the experts were further categorized into three distinct groups based on their responsibility of work, which are Location and Design, Construction and Maintenance, and Planning and Monitoring. This categorization aimed to ensure a well-rounded understanding of the subject matter and enhance the depth of the subsequent analysis.

5.1 Results of AHP Analysis on Influencing factors on highway maintenance prioritization

The weights of influencing factors on highway maintenance prioritization analyzing from the experts' opinion and experiences through AHP method are Pavement Condition (0.357), Traffic Characteristic (0.243), Life Cycle and Maintenance (0.230) and Context of Land Use (0.170) accordingly., i.e. Table 3.

Table 3 Influencing factors weights analysis through AHP.

Experts	**[F1]**	**[F2]**	**[F3]**	**[F4]**
1	0.283	0.127	0.538	0.052
2	0.622	0.170	0.156	0.053
3	0.541	0.308	0.110	0.040
…	…	…	…	…
58	0.250	0.250	0.250	0.250
Geometric Mean	0.357	0.243	0.230	0.170

5.2 Results of FAHP Analysis on Influencing factors on highway maintenance prioritization

The decision of influencing factors through AHP method are based on experts' opinion and experiences, therefore, applying Fuzzy theory will reduce the fuzziness of the decision making during the interview. The results analyzed through Fuzzy AHP are Pavement Condition (0.480), Traffic Characteristic (0.241), Life Cycle and Maintenance (0.166) and Context of Land Use (0.113) accordingly i.e. Table 4. Comparing to the results of AHP, the weights of Pavement Condition are higher, Traffic Characteristic remains the same, Life Cycle and Maintenance and Context of Land Use, refer to Figure 6.

Table 4 Influencing factors weights analysis through FAHP.

Experts	[F1]	[F2]	[F3]	[F4]
1	0.239	0.000	0.761	0.000
2	1.000	0.000	0.000	0.000
3	0.760	0.240	0.000	0.000
…	…	…	…	…
58	0.250	0.250	0.250	0.250
Geometric Mean	0.480	0.241	0.166	0.113

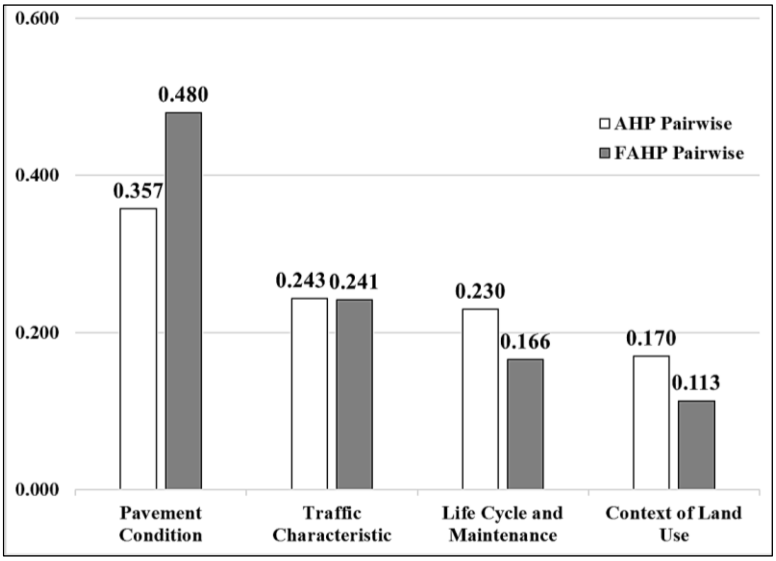

Figure 6 The comparison of factor weights between AHP and FAHP analysis.

5.3 Results of TOPSIS Analysis on highway maintenance' most priority road types

Regarding the prioritization of highway maintenance' road types, the influencing factors from FAHP method are used as the criteria weight for TOPSIS analysis. The results of prioritization for relative closeness are National Highways (0.701), Motorways (0.663), Rural Roads (0.523) and Local Roads (0.431), i.e. Table 5 and Figure 7..

The normalized results from TOPSIS method reveal the following priorities for road maintenance which are National Highways (Highest priority with a normalized score of 30.24%), Motorways (Second-highest priority with a normalized score of 28.60%), Rural Roads (Third priority with a normalized score of 22.55%) and Local Roads (Lowest priority with a normalized score of 18.61%), refer to Figure 8.

Table 5 Influencing factors weights analysis through FAHP.

Experts	[A1]	[A2]	[A3]	[A4]
1	0.312	0.230	0.574	0.688
2	0.000	1.000	0.000	0.500
3	0.932	0.751	0.932	0.068
…	…	…	…	…
58	0.000	0.000	1.000	0.000
Geometric Mean	0.663	0.701	0.523	0.431

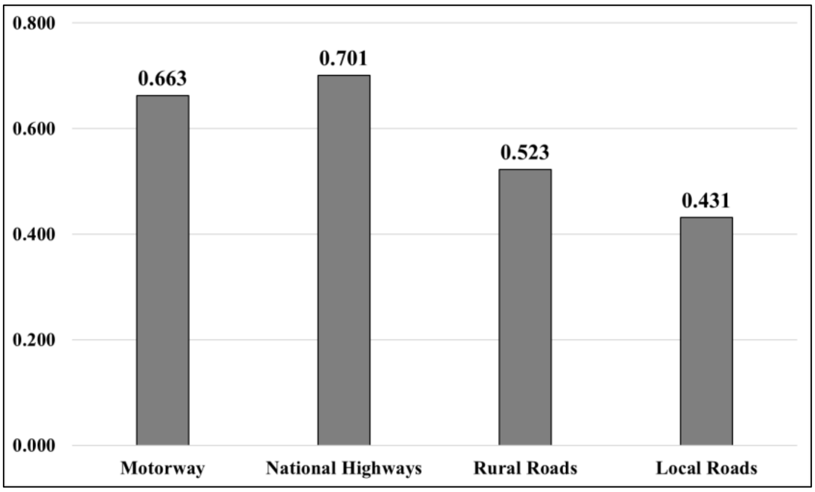

Figure 7 The relative closeness of each highway category using TOPSIS.

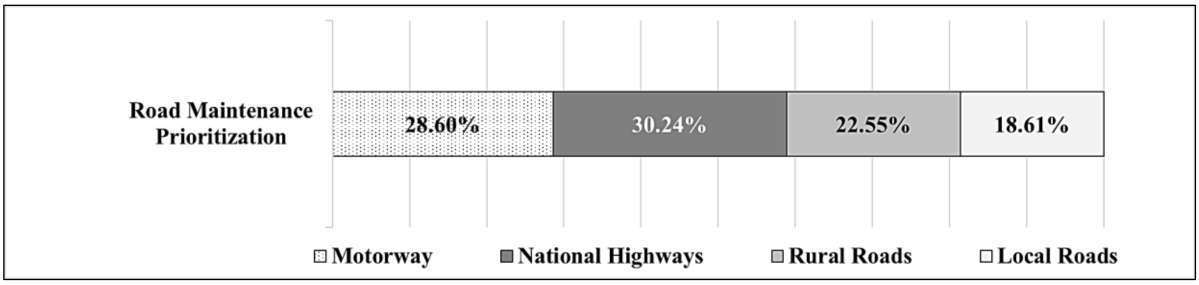

Figure 8 The normalized score of each highway category.

5.4 FAHP Result categorized by groups

The results of influencing factors among the 3 groups of experts vary depending on the experiences according to their responsibilities of work, i.e. Table 6 and Figure 9.

For a group responsible for Location and Design, the most influencing factor is Pavement Condition (0.492), followed by Traffic Characteristic (0.297), Life Cycle and Maintenance (0.142), and Context of Land Use (0.069) accordingly.

For a group responsible for Construction and Maintenance, the most influencing factor is Pavement Condition (0.447), followed by Traffic Characteristic (0.275), Life Cycle and Maintenance (0.139), and Context of Land Use (0.139) accordingly.

For a group responsible for Planning and Monitoring, the most influencing factor is Pavement Condition (0.534), followed by Life Cycle and Maintenance (0.228), Traffic Characteristic (0.149). and Context of Land Use (0.089) accordingly.

Table 6 Influencing factors weights categorized by responsibilities of work.

Responsibility of Work	[F1]	[F2]	[F3]	[F4]
Location and Design	0.492	0.297	0.142	0.069
Construction and Maintenance	0.447	0.275	0.139	0.139
Planning and Monitoring	0.534	0.149	0.228	0.089

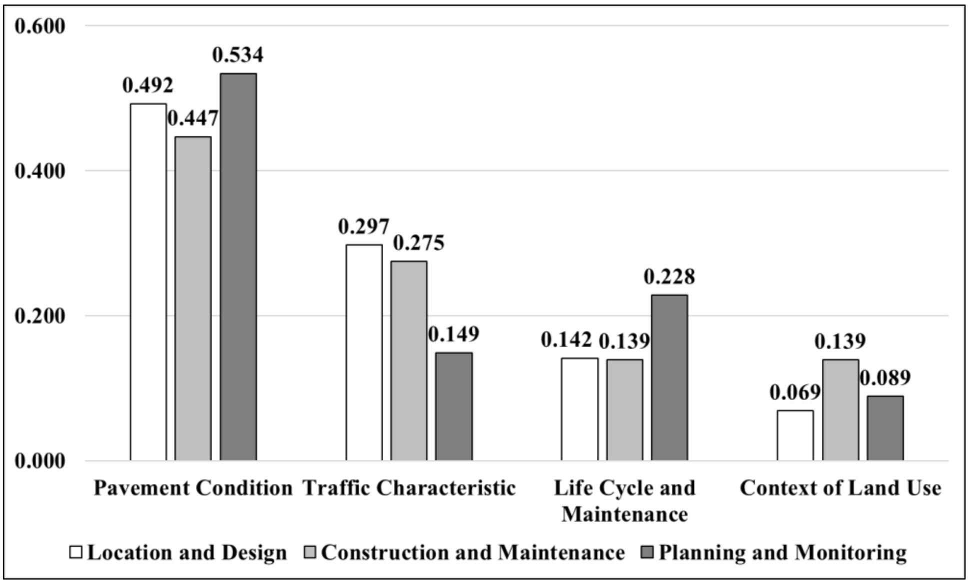

Figure 9 Influencing factors weights categorized by responsibilities of work.

5.5 TOPSIS Result categorized by groups

The results of the most highway category to be attended maintenance among the 3 groups of experts are as follows, i.e. Table 7 and Figure 10

For a group responsible for Location and Design, the most highway category to be attended maintenance is Rural Roads (0.666), followed by Motorway (0.648), National Highways (0.634) and Local Roads (0.236) accordingly. The normalized results reveal the priorities for road maintenance as follows, Rural Roads (30.51%), Motorways (29.68%), National Highways (29.02%) and Local Roads 10.78%), refer to Figure 11.

For a group responsible for Construction and Maintenance, the most highway category to be attended maintenance is National Highways (0.727), followed by Motorway (0.637), Rural Roads (0.496) and Local Roads (0.419) accordingly. The normalized results reveal the priorities for road maintenance as follows, National Highways (33.27%), Motorways (29.15%), Rural Roads (22.69%) and Local Roads (19.18%), refer to Figure 12.

For a group responsible for Planning and Monitoring, the most highway category to be attended maintenance is Motorway (0.720), followed by National Highways (0.688), Local Roads (0.558), and Rural Roads (0.497) accordingly. The normalized results reveal the priorities for road maintenance as follows, Motorways (32.94%), National Highways (31.49%), Local Roads (25.55%) and Rural Roads (22.77%), refer to Figure 13.

Table 7 The highway category to be attended maintenance categorized by responsibilities of work.

Responsibility of Work	[A1]	[A2]	[A3]	[A4]
Location and Design	0.648	0.634	0.666	0.236
Construction and Maintenance	0.637	0.727	0.496	0.419
Planning and Monitoring	0.720	0.688	0.497	0.558

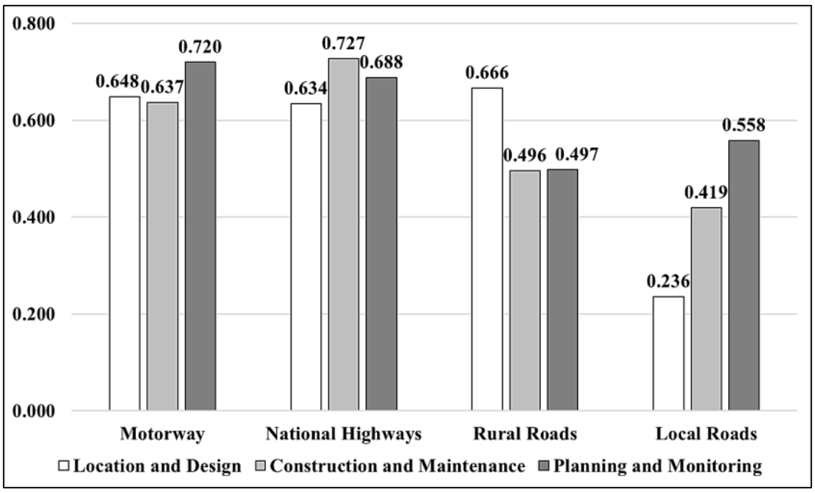

Figure 10 The relative closeness of highway category categorized by responsibilities of work.

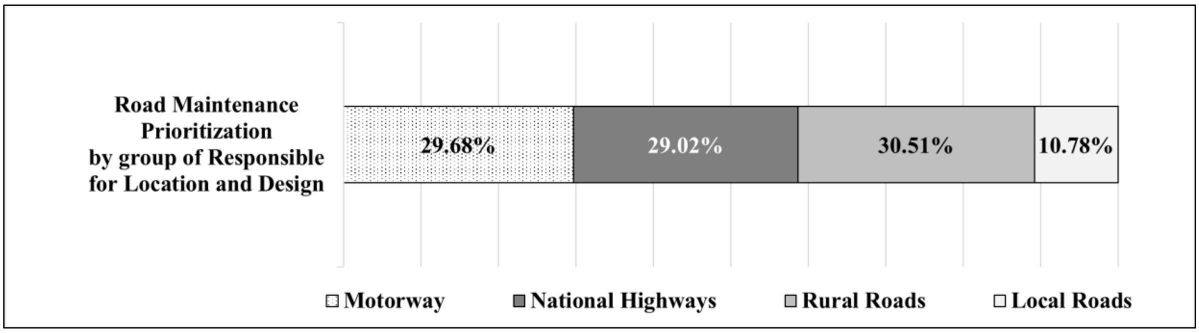

Figure 11 The normalized score of highways prioritization of Location and Design group.

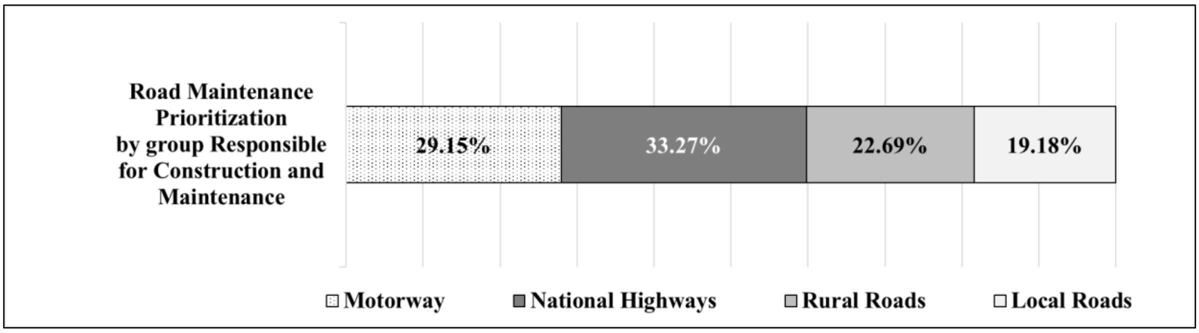

Figure 12 The normalized score of highways prioritization of Construction and Maintenance group.

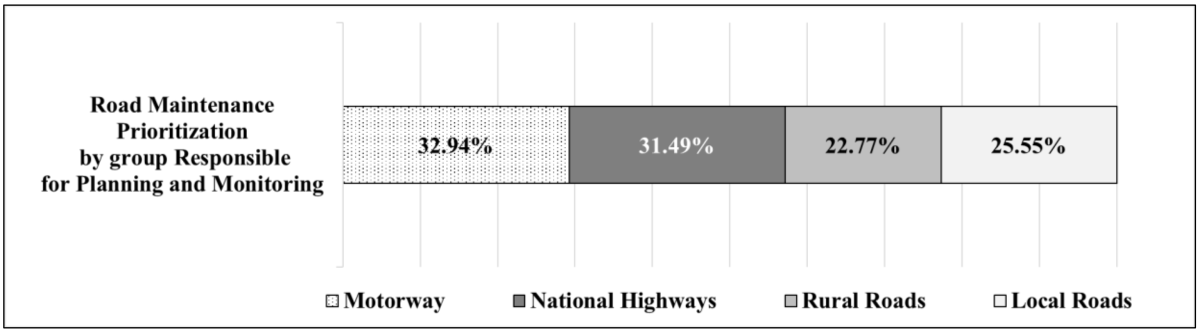

Figure 13 The normalized score of highways prioritization of Planning and Monitoring group.

6. CONCLUSIONS

This study employed FAHP to weight the relative important of influencing factors and Technique for Order Preference by Similarity to Ideal Solution (TOPSIS) to determine the priority of highway maintenance in Thailand. The analysis is performed based on the data gathered from 58 experts working in road construction-related organization, including DOH, DRR, DPT, and other relevant organization.

The results from both AHP and FAHP analyses reveal a consistent pattern of relative importance among influencing factors. The most influential factor is pavement condition, followed by traffic characteristic which remained consistent in both analyses. This is followed by Life Cycle and Maintenance and Context of Land Use. And according to these significant influencing factors. Regarding the prioritization of highway maintenance, the most priority road to be focused on maintenance is National Highways followed by Motorways, Rural Roads and Local Roads accordingly.

The data obtained from the experts can be categorized by their responsibility while they are working at the road construction project. Consisting of three groups, Personnel who are responsible for Location and Design, Construction and Maintenance, and Planning and Monitoring. The result illustrates that each group of experts have completely different in prioritizing the highway maintenance choice. Location and Design group prioritize maintenance of Rural Roads the most. Construction and Maintenance group prefer maintenance on National Highway as their top priority while Planning and Monitoring group would like to make the most focus on Motorway. The differing perspectives on prioritization demonstrate the importance and unique maintenance strategies of each road type.

Furthermore, the normalized data extracted from TOPSIS method provides a standardized and comparable scale for prioritizing road maintenance and can be used as a valuable tool for evidence-based decision-making and prioritization in road maintenance. In the context of resource management, normalized data can be directly translated into a percentage-based allocation of resources.

For Time management aspect, the normalized scores can guide the scheduling of maintenance activities, allocating more time to higher-priority roads, e.g. if National Highways have a score of 30.24%, roughly 30% of the total maintenance time should be dedicated to them. This ensures that critical roads receive adequate attention while optimizing the use of available time.

For Financial allocation aspect, the normalized scores can be used to determine the budget allocation for each road type. This ensures that funding is distributed proportionally to the importance and maintenance needs of each category, preventing overspending on less critical roads and ensuring sufficient funds for essential repairs and upkeep.

For Personnel mobilization aspect, the normalized scores can also guide workforce allocation. A higher score for a road type indicates the need for a larger team or more specialist to perform maintenance issues. This proportion-based approach can optimize workforce deployment and ensure that maintenance is available where it's most needed.

It facilitates a transparent and objective process for allocating resources, ensuring that maintenance efforts are aligned with the overall goals of the transportation network. By considering significant influencing factors and their relative importance, this approach can lead to more efficient resource utilization, improved road conditions, and enhanced safety for all road users.

7. ACKNOWLEDGMENTS

The author gratefully acknowledges DOH, DRR, DPT and other relevant organizations for providing the data for this study, and Department of Civil Engineering, Faculty of Engineering, Kasetsart University for the assistance on the data processing.

8. REFERENCES

Ahmed, S., Vedagiri, P., & Krishna Rao, K. V. (2017). Prioritization of pavement maintenance sections using objective based Analytic Hierarchy Process. *International Journal of Pavement Research and Technology*, *10*(2), 158–170. https://doi.org/10.1016/j.ijprt.2017.01.001

Angelia, N., & Mazni, D. (2019). *Determining the priority criteria and ranking of provincial bridge maintenance in West Sumatra using a combination of the Fuzzy Analytical Hierarchy Process and VIKOR-Modification methods*. *602*(1), 012105.

Ayalew, G. G., Meharie, M. G., & Worku, B. (2022). A road maintenance management strategy evaluation and selection model by integrating Fuzzy AHP and Fuzzy TOPSIS methods: The case of Ethiopian Roads Authority. *Cogent Engineering*, *9*(1), 2146628.

Babashamsi, P., Golzadfar, A., Yusoff, N. I. M., Ceylan, H., & Nor, N. G. M. (2016). Integrated fuzzy analytic hierarchy process and VIKOR method in the prioritization of pavement maintenance activities. *International Journal of Pavement Research and Technology*, *9*(2), 112–120. https://doi.org/10.1016/j.ijprt.2016.03.002

Chaipetch, P. (2022). ANALYTICAL OF MULTI-CRITERIA APPROACH FOR IDENTIFYING THE WEIGHT AND FACTOR OF RURAL ROAD MAINTENANCE PRIORITIZATION. *International Journal of GEOMATE*, *22*. https://doi.org/10.21660/2022.91.gxi334

Chundi, V., Raju, S., Waim, A. R., & Swain, S. S. (2021). Priority ranking of road pavements for maintenance using analytical hierarchy process and VIKOR method. *Innovative Infrastructure Solutions*, *7*(1), 28. https://doi.org/10.1007/s41062-021-00633-7

Department of Highways. (2017). *Highway Numbering System*. Department of Highways.

Fawzy, M. M., Elsharkawy, A. S., Hassan, A. A., & Khalifa, Y. A. (2023). Prioritization of Egyptian Road Maintenance Using Analytic Hierarchy Process. *International Journal of Pavement Research and Technology*. https://doi.org/10.1007/s42947-023-00351-6

Hendhratmoyo, A., Syafi'i, & Pramesti, F. P. (2017). The Evaluation of Screening Process and Local Bureaucracy in Determining the Priority of Urban Roads Maintenance and Rehabilitation. *Journal of Physics: Conference Series*, *909*(1), 012072. https://doi.org/10.1088/1742-6596/909/1/012072

Kresnanto, N. C. (2022). Prioritizing District Road Maintenance Using AHP Method. In H. A. Lie, M. Sutrisna, J. Prasetijo, B. H. W. Hadikusumo, & L. S. Putranto (Eds.), *Proceedings of the Second International Conference of Construction, Infrastructure, and Materials* (pp. 363–371). Springer Nature Singapore.

Kumar, R., & Suman, S. K. (2022). Prioritization of Flexible Pavement Sections for Maintenance Using Multi-criteria FAHP Integrated with Multi-attribute Utility Theory. *Process Integration and Optimization for Sustainability*, *6*(3), 633–656. https://doi.org/10.1007/s41660-022-00235-5

Li, Y., Zhang, J., He, Y., & Li, Z. (2023). Suitability evaluation method for preventive maintenance of asphalt pavement based on interval-entropy weight-TOPSIS. *Construction and Building Materials*, *409*, 134098.

Moazami, D., Behbahani, H., & Muniandy, R. (2011). Pavement rehabilitation and maintenance prioritization of urban roads using fuzzy logic. *Expert Systems with Applications*, *38*(10), 12869–12879.

Nautiyal, A., & Sharma, S. (2022). Methods and factors of prioritizing roads for maintenance: A review for sustainable flexible pavement maintenance program. *Innovative Infrastructure Solutions*, *7*(3), 190. https://doi.org/10.1007/s41062-022-00771-6

Office of the Council of State. (1992). *Act of Highway*. Office of the Council of State.

Omari, K., Harchi, S., Ouchaouka, L., Rachik, Z., Moussetad, M., & Labriji, L. (2021). Application the fuzzy topsis and fuzzy electre in the serious games evaluation tool. *Journal of Theoretical and Applied Information Technology*, *Vol.99*, 1931–1942.

Ouma, Y. O., Opudo, J., & Nyambenya, S. (2015). Comparison of fuzzy AHP and fuzzy TOPSIS for road pavement maintenance prioritization: Methodological exposition and case study. *Advances in Civil Engineering*, *2015*(1), 140189.

Porras-Alvarado, J. D., Murphy, M. R., Wu, H., Han, Z., Zhang, Z., & Arellano, M. (2017). Analytical Hierarchy Process to Improve Project Prioritization in the Austin District, Texas. *Transportation Research Record*, *2613*(1), 29–36. https://doi.org/10.3141/2613-04

Saaty, T. L., & Vargas, L. G. (2001). Models, Methods, Concepts & Applications of the AHP. *Boston, Dordrecht and London*.

Siswanto, H., Supriyanto, B., Pranoto, P., Prihatditya, R. P., & Friansa, M. A. (2019). *District road maintenance priority using analytical hierarchy process*. *2114*(1).

Smrudu, T. K., Sanjay Kumar, V. S., & Akkara, J. (2023). Pavement Condition Assessment Using Fuzzy Analytic Hierarchy Process. *International Journal of Pavement Research and Technology*. https://doi.org/10.1007/s42947-023-00335-6

Evaluating the effectiveness of traffic calming measures in Silver Zones

Jamie Cheong[1*], Puay Ping Koh[2], Andrew Tan[3], Chandrasekar[4]

[1]Traffic & Road Operations, Road Safety Engineering Division, Jamie_cheong@lta.gov.sg
[2]Road & Traffic Specialists, Traffic Safety Engineering, Koh_puay_ping@lta.gov.sg
[3]Traffic & Road Operations, Road Safety Engineering Division, Andrew_cs_tan@lta.gov.sg
[4] Chief Engineer, Road & Traffic, Chandrasekar@lta.gov.sg

ABSTRACT

Traffic Accident data for the period 2010 to 2012 showed pedestrian fatalities accounting for almost half of all traffic fatalities, with 78 elderly losing their lives. With Singapore's aging population projected to increase yearly, the elderly overrepresenting issue in traffic accidents will amplify multifold.

This paper will share Singapore's experience in creating a safer road environment for pedestrians, through the implementation of Silver Zones since 2014. Silver Zones utilize the concept of changing the character of the streets to positively influence motorists' behaviour to significantly alter the vehicle's operating speed at selected locations and be aware of their surroundings. A wide variety of traffic calming measures accompanied by road markings, traffic signs and lowered speed limit are implemented. These measures creates either horizontal or vertical deflections and visual cue to slow motorists, creating a safer environment for the elderly pedestrians to cross the road safely to reach their amenities.

Before and after studies measuring the motorists' spot speeds and accident records within the Silver Zones were analysed to gauge the overall effectiveness of the new scheme. The study examined a total of 11 types of traffic calming measures implemented within 22 Silver Zones with speed data collected for the before-after study. 2-sample t-tests were used to determine the significance of the data. Out of 22 Silver zones, 20 sites showed significant decrease in speeds between 3 and 37% with a corresponding of about 80% reduction in overall traffic accidents.

Keywords: Traffic calming, elderly pedestrians, pedestrian crossing, evaluation study

1.0 INTRODUCTION

Elderly pedestrian (aged 60 years and above) fatalities have always been Singapore's top key concerns over the past decades. Between 2010-2023, the elderly took up an average of 59% of the pedestrian fatalities. As the population aged with increasing percentage of elderly (24% in 2023, 14% in 2010), the involvement of elderly in road traffic accidents has grown and continued to be a concern.

As part of LTA's continual efforts to enhance safety for vulnerable road users, Silver

Zones were introduced since 2014, to help pedestrians especially the elderly to cross the roads safely in their neighbourhoods. It was a state-of-the-art area-based safety treatment to introduce a series of measures to influence motorists' behaviour, primarily to slow down and be more aware of pedestrians' presence. Many research studies have shown that slower vehicle speeds can greatly increase the chances of pedestrians' survival upon hit by vehicle (WHO, 2018). When travelling at lower speeds, motorists have more time to react and avoid potential collisions with others, making the roads safer for everyone.

The suite of measures adopted in Silver Zones warranted an evaluation study on the safety effectiveness and the acceptance by the residents. This allows improvements to be made to further enhance safety and for possibly applications to other locations.

In this paper, both quantitative and qualitative analyses were conducted to have a holistic understanding of the effectiveness of the measures. Road traffic accident data and speed surveys before and after the implementation of the measures were collected and perception surveys were conducted. The three-pronged analyses shed useful insights on the Silver Zones effectiveness.

2.0 LITERATURE REVIEW

The occurrence of a road traffic accident is a result of several contributing factors. In many cases, high or aggressive speeds were involved. Research have also established that higher speeds lead to higher probability of collisions and more severe injuries (OECD, 2018; Doecke, et.al, 2020). As such, it is prudent to introduce speed calming measures (both physically and legally), to alter the motorists' behaviour, thereby enhancing safety for all road users. Many countries have been starting to introduce lower speed limits and many found benefits in doing so (Lawrence et.al, 2020). For example, the European Member States in the European Commission are strongly encouraged to apply maximum default speeds of 30kph in residential areas and areas with high number of cyclists and pedestrians (ARUP, 2022). Helsinki first introduced large-scale 30kph roads in the city centre and some residential areas in 2004, then modified effectively in all the streets. In places where speed limit was reduced from 40kph to 30kph, pedestrian injuries were found to decrease by 19% and vehicle damages by 34% (EDJNet, 2024). In places where monitoring cameras were installed, mean vehicle speeds lowered to 23.5kph and the number of accidents decreased from 2.2 per year to 1.1 per year. Other examples of European cities which have adopted the 30kph successfully include Brussels, Zurich, Glasgow, Germany, Italy and Budapest and others like Melbourne, Toronto, New York and Ho Minh City. Some introduced speed restrictions in stages (often in residential areas or inner cities, smaller streets without public transport, then bigger roads) while others applied to the whole city except the multi-lane roads or roads connecting to other neighbouring cities. Many are monitoring and measuring the effectiveness.

Many countries have done evaluation studies on different traffic calming measures. Among which, speed tables and speed humps are known to have best effectiveness (Barbosa, et. al., 2000, FHWA, 2024), chicanes could reduce average motorist speeds by 19.3kph (12mph) (Sayer, et.al, 1998) and (virtual) lane markings could reduce speeds by about 10% (Koh, et.al, 2009). Gateway treatment with signages could be more effective if other determinants such as good visibility of the built-up area and the road downstream are also present (Kacprzak and Solowczuk, 2019).

Evaluation studies of traffic calming effects on road safety include a great variety of methodologies, for example accident reduction analysis, meta-analysis, speed analysis and perception interpretation. For accident analysis, it depends greatly on data availability and it is essential to take into the account of the regression-to-the-mean effect and also the potentially important confounding factors like change in traffic volume, and modifications of land use (Grana, et. al. 2010) in influencing the accident data.

There are several methods in measuring speeds. These include using handheld radar /laser gun, detector loops, and measuring travel time over a distance using stopwatch or video recording/analytics (Herath, et.al. 2021, Minnema, 2006). There are several considering factors (e.g. available resources, accuracy, portability) to select the appropriate type of measurement. Speed data collection should be unobtrusive and not influenced by external factors such as congestion and behaviour of vehicle/user in front. Typically speed test runs have been used to complement spot speed data to validate the 85th percentile speeds for the whole area (Forbes, et. al, 2012).

Understanding the needs of the users form a crucial part of the evaluation. This is the channel to assess users' acceptance and review possible improvements to the measures. It is commonly gathered by the use of surveys and interviews.

When all local data is difficult to collect, another method is to conduct meta-analysis (i.e. a statistical combination of results from two or more separate studies). This approach enables enhanced precision, the ability to address inquiries not posed by individual studies, and the opportunity to resolve controversies arising from conflicting claims.

3.0 METHODOLOGY

3.1 Silver Zones

Silver Zones were selected in housing estates with higher population of elderly (more than or equal to 60 years old), amenities frequented by elderly and with relatively higher accident rates involving elderly.

Local or primary access (roads with speed limit of 50kph) roads near to elderly frequented areas (neighbourhood centres, eateries, medical facilities, etc) were chosen. Typically, dual-1 or 2 roads (between 1-3km length) are chosen (see Figure 1). Ring/loop roads seem to be more suited for Silver Zone retrofitting as these roads primarily serve the restricted residents and not bypass roads which generate higher traffic flow. In addition, the connecting roads into Silver Zone may be treated with traffic calming measures to complement the lowered speed limit.

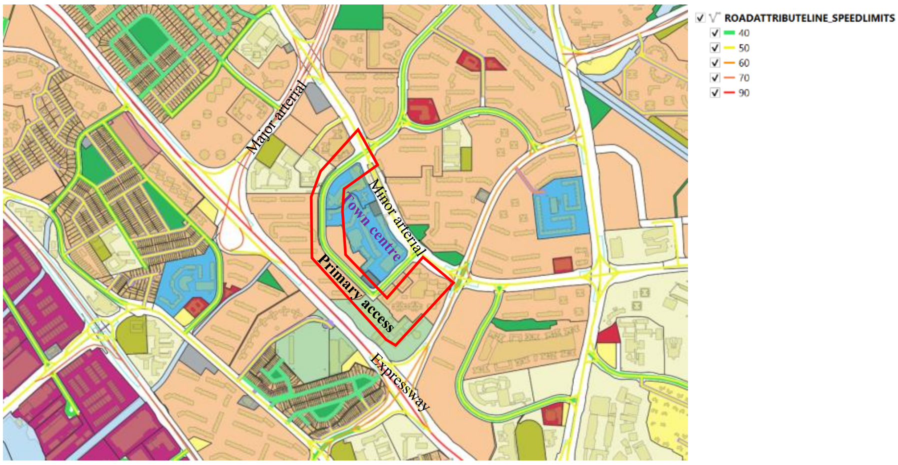

Figure 1: Selection of Silver Zone stretch from the different road classification

This paper examines the local effectiveness of various countermeasures (targeting at reducing vehicular speeds) implemented in Silver Zones, including existing measures such as humps, centre dividers, and newly introduced measures such as chicanes, eye-lands, pinch points, small roundabouts, etc (see Figures 2-4).

Figure 2: Gateway Treatment

Figure 3: Junction treatment a) Raised Junction b) Y-Junction c) Roundabout

Figure 4: Mid-block treatments a) Chicane b) Eye-Land c) Pinch Point

A Silver Zone is typically demarcated with a pair of gateway and speed limit signs, yellow rumble strips and speed limit road markings. The key aim of Silver Zone is to introduce a series of speed calming measures and lowering the speed limit to slow down motorists, for pedestrians especially elderly to cross the roads safely. Today, there is a total of 40 Silver Zones built throughout the island. Figure 5 shows the first 22 Silver Zones implemented.

3.2 Traffic accident data

The number of traffic accidents that occurred along the Silver Zones have been examined for a period of 5 years "before" and "after" implementation of Silver Zone schemes. There was a total of 16 zones with at least 5 years of "after" accident record, 3 with at least 3 years and 21 with less than 3 years. These are reported traffic accident cases that are fatal, with serious injuries (minimum 7 days in severe bodily pain) or slight injuries (at least 1 party was conveyed to hospital). The limitations of traffic accident analysis include accumulating a good number of years for meaningful analysis. Hence, several recently implemented Silver Zones cannot be analysed. Within each sample site, the decrease in accident numbers may not be significant if the total number of accidents over 5 years is low.

Figure 5: 22 Silver Zone locations

3.3 Speed profile

The data collection process utilized an unobtrusive technique (using handheld radar gun and not noticeable to motorists) to capture typical traffic behaviour without affecting it. Speeds were collected only on weekdays and non-rainy days, for both before and after implementation (at least 7 months post implementation to take novelty effects into consideration) periods. Vehicle classification was also collected along with the speed so that speed profiles for different types of vehicles can be studied. Care was taken to collect free-flow speeds of different Silver Zone countermeasures: off-peak (1000hr to 1200hr, 1400hr to 1600hr & 2000hr to 2200hr), and at sufficient distance away from the intersections and accesses where vehicles are accelerating/ decelerating (except for traffic calming measures at intersections). 2-sample t-tests were then used to determine if the "before" and "after" speeds at each approach showed statistical differences.

There was a total of 11 types of measures implemented in Silver Zones. They are categorized based on specific sites where they are being implemented at, such as i) the start of the Silver Zone, ii) at the junctions, and iii) in the mid-block sections (see Table 1). These measures were designed to suit the local context (e.g. side table availability, curvature of the road, type of vehicles plying), with the aim to maintain motorists' speeds constantly low throughout the identified zone. Some measures cater for pedestrians to cross safely and comfortably in two-stages.

3.4 Public perception

User feedback was gathered after Silver Zones have been implemented, using various platforms such as face-to-face surveys, posters with QR code at void decks and various resident engagement sessions. Efforts were made to have representation from both pedestrian and motorist groups, in an unbiased manner. At least 70 surveys were collected at each location. The survey questionnaire was designed to understand user's awareness, safety rating and acceptance of the overall and individual countermeasures of the Silver Zone scheme. As the application of Silver Zone measures varied across different site contexts and local residents' behaviour, perception survey served as a complimentary tool to evaluate Silver Zones' effectiveness.

Table 1: Type of measures and their classifications

Location	Physical/virtual	Measure	Provision for crossing facilities
At the start of zone	Physical/virtual	Gateways	No
At the junctions	Physical/virtual	Roundabouts	No
	Physical	Raised Junctions	Yes
	Physical/virtual	Y-Junctions	No
In the mid-block sections	Physical	Eye-Lands	Yes
	Physical/virtual	Pinch Points	Yes
	Physical	Chicanes	No
	Physical	Bus-Friendly Humps	No
	Physical	Centre Dividers	Either
	Virtual	Chevron Markings	No
	Virtual	Traffic Calming Markings	No

4.0 RESULTS

4.1 Accident analysis

Traffic accident records were examined within the completed Silver Zones, 5 years "before" and 5 years "after" the implementation. 5 years of records were chosen as it is of considerable length to smooth out any abnormal high annual crash frequency. Major activities (e.g. Rail construction within the vicinity, major road diversion that occurred more than 6 months) that will affect the accident occurrences within the 10-year period in the selected Silver Zone locations were noted and these locations were excluded from the study.

Table 2 shows the summarized road traffic accidents at the selected 14 locations. There was a total of 62 elderly pedestrian accidents that have occurred before Silver Zones were implemented and 10 accidents after. This is equivalent to a reduction from 12.4 accidents per year to 2 per year. The Underlying True Accident Rate (UTAR) method (by Nicholson, 1987) was used to determine if the overall reduction in accidents is significant [(62-4.4*5=40) >10]. Hence, null hypothesis of "after" accident rate is equal to 12.4/year is rejected, i.e. the reduction in accident frequency due to the improvements is statistically significant at 95% confidence level.

Table 2: Accident records at the 14 Silver Zones

Locations	*Before accidents	After accidents
1	4	0
2	1	1
3	4	0
4	5	0
5	6	2
6	11	4
7	4	1
8	2	0
9	5	0
10	3	0
11	5	2
12	4	0
13	3	0
14	5	0
Total	**62**	**10**

**Before accidents for each sample site are too low for meaningful interpretation of the UTAR method*

4.2 Speed study

Two types of speed studies were conducted: **segment-based** and **type-based**. Segment-based study incorporated a few speed check points within the whole stretch(es) of each Silver Zone whereas type-based study comprised the analysis of motorists' speed performance at each type of countermeasure.

Segment-based study

Around 3 to 6 spot speeds were selected for each zone for segment-based study. 20 out of 22 Silver Zone locations saw a decrease in overall operating speeds of vehicles plying within the Silver Zones (See Table 3). The decrease in speeds ranged from 1 to 20kph (3-37%). All the "after" speed for dual-1 locations decreased to below 40kph (posted speed limits for Silver Zones), whereas only 5 out of 9 dual-2 locations decreased to less than or equal to 40kph. The remaining 4 dual-2 locations have mixed results with 2 out of 4 with reduction in speed, 1 remained at same speed and 1 slight increase. A possible reason for the slight increase was the already low "before" speed. This shows that Silver Zone schemes were more effective in managing motorists' speeds (to below 40kph) along dual-1 roads.

Table 3: "Before" and "After" speeds at 22 Silver Zones

Silver Zones	No. of Lanes	85th Percentile Before Speed	85th Percentile After Speed	Speed Reduction (km/h)	Speed Reduction (%)
Chai Chee Road	D1	41.0	28.0	-13.0	**-32%**
Bukit Merah View	D1	31.0	29.0	-2.0	**-6%**
Commonwealth Drive	D1	41.0	29.0	-12.0	**-29%**
Hougang St 21	D1	42.0	29.0	-13.0	**-31%**
Teck Whye Lane	D1	43.0	30.0	-13.0	**-30%**
Whampoa Drive	D1	44.0	33.0	-11.0	**-25%**
Jurong West Street 52	D1	41.0	34.0	-7.0	**-17%**
Woodlands Ring Road	D1	44.0	34.0	-10.0	**-23%**
Marine Crescent and Marine Terrace	D1	40.0	35.5	-4.5	**-11%**
Tampines Street 11	D1	47.0	37.0	-10.0	**-21%**
Woodlands Drive 14	D1	41.0	38.0	-3.0	**-7%**
Lengkok Bahru, Redhill Rd and Jln Tiong	D1	42.0	39.0	-3.0	**-7%**
Telok Blangah Crescent	1 lane 1 way	35.0	34.0	-1.0	**-3%**
Bukit Panjang Ring Road	D2	54.0	34.0	-20.0	**-37%**
Lorong 8/8A Toa Payoh	D2	50.0	35.0	-15.0	**-30%**
Hougang Avenue 5	D2	44.0	36.0	-8.0	**-18%**
Yishun Ring Road	D2	49.0	40.0	-9.0	**-18%**
Potong Pasir Ave 1 and Ave 2	D2	43.0	40.0	-3.0	-7%
Clementi Ave 3	D2	41.0	41.0	0.0	0%
Bedok North St 3, Ave 1 and Ave 2	D2	39.0	42.0	3.0	8%
Bedok North St 1	D2	53.0	42.0	-11.0	**-21%**
Woodlands Ave 1	D2	53.0	48.0	-5.0	**-9%**

The combined "before" and "after" speeds of the locations were compared between day (7am-7pm, following the national street lighting operating hours) and night. Figure 6 shows that the distributions are similar between the day and night data and statistical tests (2-sample t-tests) showed that it is 95% confidence to accept the null hypothesis that there is no difference in mean day and night speeds, for both "before" and "after" data sets.

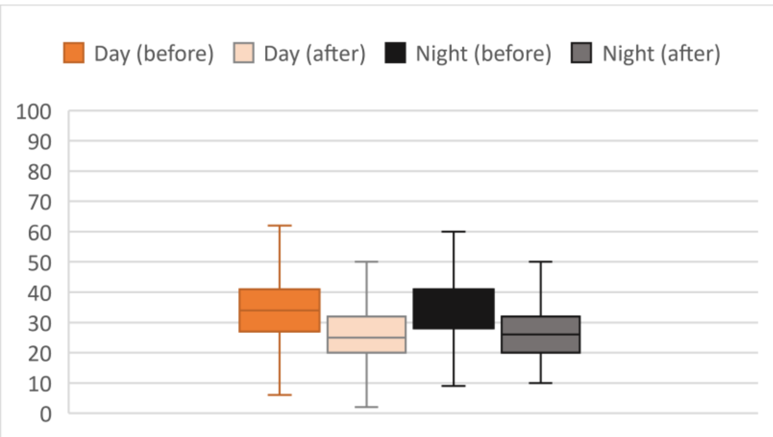

Figure 6: Speed distributions of day and night "before-after" data

Feature-based study

Point speed data were collected at each selected Silver Zone countermeasure and classified by the following vehicle types: Motorcycle (MC), Car, Light Goods Vehicle (LGV), Heavy Goods Vehicle (HGV) and Bus. Only sample size with at least 30 in each vehicle type during each collection period were used in the analyses. "Approach" indicated the segment (by direction of traffic) where speed data is collected, "Lanes" indicated if it is D1: Dual 1 divided road, D2: Dual-2 divided road or 1-way and "Additional features" documented features like bends, signalized crossing, humps, merging lane, etc. Statistical tests (2 sample t-tests) were performed to find if the "after" speeds were statistically lower than the "before" situation at 95% confidence level. For each countermeasure, the "before" and "after" speeds will be compared (See Table 4 for an example).

Table 4: 'Before" and "After" speeds of vehicles at each countermeasure (example)

Location	Approach	Lanes	Additional features	MC*	Car	LGV	Bus
Bukit Merah View	B7	D1	Bend Upstream	21.4[1]	19.2	19.5	-
				22.6[2]	21.0	19.4	-
				(1.1)[3]	(1.7)	(0.1)	-
				5%[4]	9%	1%	-

**MC: Motorcycles; LGV: Light Goods Vehicles (lorry, truck, pickup, etc); [1]"Before" speed; [2]"After" speed; [3]speed difference between "Before" & "After" speeds (-ve: decrease); [4]Percentage decrease in speed; Statistical tests performed at 95% confidence level- Black font: no significant difference; Green font: significant decrease; Red font: significant increase*

i) <u>At the start of the Silver Zone: Gateway</u>

Gateway treatments are applied at the start of a designated zone. It is relatively easy to identify, with the use of conspicuous signages and markings (Gateway's standard features: a pair of "Silver Zone" signs and speed limit signs, speed limit markings, & 3 yellow rumble strips).

The "before-after" speed counts at 19 gateway treatments were taken at sites with standalone gateway and gateway with additional features. The latter showed significant reduction in speeds (between 2-21kph), lowering the entry speed to at least 31.6kph (lowest to 18.1kph). In general, gateway treatments seemed to be effective in reducing speeds at sites with other speed reducing features like lane narrowing, signal control or vertical displacement. Those standalone gateway treatments have mixed results. At sites with Dual-2 road (Dual-2 means a road with 2 lanes each direction) and/or with existing centre divider, decreases in speeds were not so apparent.

ii) <u>At the junction: Roundabout</u>

Roundabout is a traffic circle by converting the regular X or T-junctions into all give-way entering approaches. Due to this traffic flow dynamics at a roundabout where motorists are expected to yield, deliberate design considerations were implemented to encourage motorists to reduce speed. These measures included creating horizontal deflection before the roundabout or expanding the central kerb where space permits. It reduces the number of conflict points as motorists would only have to look out for vehicles from one direction at a time.

The speed before entering the roundabouts at 4 sites showed significant decreases (by 8-19kph), lowering the speed to at least 30.3kph, with the exception at 1 site, which is likely due to the already low "before" speed where the roundabout is located at a bend. At another site, the speeds consistently decreased to 22-24kph when measured within the roundabout. Overall, roundabouts did successfully influence motorists to slow down.

iii) <u>At the junction: Raised Junction</u>

This is a feature where the entire junction is being raised like a table, so that motorists slow down before driving up the hump, entering the junction. [1]Barrier-free crossings may be installed at junctions with frequent crossing activities. This design elevates pedestrians while crossing, enhancing visibility for motorists.

A total of 3 sites were examined for this type of treatment. The first 2 sites were observed to have significant speed decreases (by 5-20kph) in all types of vehicles, lowering the speed to at least 28.5kph. The third site did not show a significant speed decrease likely because it is located around a bend with already lower 'before' speed (less than 30kph).

The raised junction is demarcated by yellow checkered strips at the ramp up/down. An additional set of yellow checkered strips on the raised top near the end of the raised junction was included as a feature to alert motorists to slow down before the ramp down ahead. One possible enhancement to further alert the motorists of the upcoming ramp down and to reduce speed is to explore improving the conspicuity of the raised junction.

iv) <u>At the junction: Y-Junction</u>

Y-Junctions are reformed T-junctions by physically bulbing out introducing horizontal deflection via realigning the road kerbs towards the road. Motorists entering the Y-Junction will be 'forced' to slow down to negotiate the gradual bends. Care must be taken to ensure that the curved portions meet the minimum turning radius of the intended vehicles for safe maneuvers at the constricted parts.

2 out of 3 sites showed positive and significant speed reduction (between 4-11kph), especially among the Cars with lowered speed to at least 29.5kph. Another site showed an increase especially to the motorcyclists' speed, possibly due to the alteration in kerb radius along the connecting road to the Y-Junction, to allow bigger vehicles to make left-turns.

v) <u>In the mid-block section: Eye-Land</u>

An Eye-Land is curving the road outward to form an 'eye' shape, and typically consists of a barrier-free crossing in the middle and a set of raised humps at the beginning of the Eye-Land (both ends). The Eye-Land also serves as a refuge for pedestrians to cross in two-stages.

Majority of the paired groups at the 5 sites showed significantly lower speeds (by 3-16 kph) after Eye-Lands have been installed, together with raised crossings or humps. Along dual-2 roads, the percentage of speed reductions can even increase to more than 20%.

[1] The kerb at such crossing is lowered to improve accessibility. The motorists have the right-of-way at these crossings.

vi) In the mid-block section: Pinch Point

Pinch Points are slightly narrowed roads using (wider) centre dividers or extending the side table towards the road carriageway. It utilises the funneling effect to calm traffic. Similar to Eye-Land, barrier-free crossing could be installed in the middle.

The effectiveness of Pinch Points was less apparent (mixture of speed decreases and increases) across the sites. There were significant decreases in speeds (2-10 kph) at some sites while half of the sites even showed significant increases in speeds. In sites where speeds have increased, this is likely attributed to either shorter receiving channel (less alert to motorists) or diminishing funneling effect (gradual pinching) due to the extended tapering along the center. A further analysis of the sites with significant speed decreases showed that these sites either tend to be coupled with other traffic calming features upstream the pinch points or the lane widths were reduced relatively narrower (to 3.1m). Hence, application of Pinch Points is recommended to be combined with other features, for better speed control.

vii) In the mid-block section: Hump

Humps are the most common traffic calming measure found on the road. There are many types of humps, including the round top humps, bus-friendly humps (longer in length), raised zebra crossings, etc.

The humps implemented along dual-1 road showed a significant speed reduction between 3-14kph. Bus-friendly humps installed along dual-2 road seemed to be more effective due to greater "before" speed (between 5-19kph).

viii) In the mid-block section: Centre divider

Centre dividers are concrete kerbs installed to separate the road between the two approaches. They narrow the road width physically to 3.5m for single lane and 3.3m and 3.5m for 2 lanes and act as a traffic calming measure. Sometimes centre divider (if wide enough) also provides as a refuge for pedestrians to cross the road in two-stages. Besides calming traffic, it deters overtaking activities especially at bends where motorists should focus on negotiating the turn.

Most of the sites installed with new centre dividers showed positive speed reductions (2-19kph). Sites where centre dividers are installed at mid-block signalized crossing showed greater speed reductions of (11-19kph) compared to those with existing raised zebra crossings (2-7kph). However, this could be due to the lower "before" speed at raised zebra crossing where the raised hump acts as an additional traffic calming measure. 1 site with widening to existing centre divider showed marginal speed reduction (3-4kph) possibly due to a smaller reduction in lane width as compared to where new centre dividers were introduced. Besides eliminating overtaking movements at bends, the centre divider further reduces low turning speed (2-6kph).

ix) In the mid-block section: Chicane

Chicane consists of a series of alternating turns in opposite directions, designed to slow vehicle downs by intentionally introducing an element of change to road alignment. Low height kerbs are used to still allow emergency vehicles to ply through.

Out of the 5 Silver Zones implemented with chicanes, 23 out of 27 groups of speed comparisons showed significant reduction in speeds (between 2-22kph). Speed reduction was more effective on Cars, LGV and Buses, compared to the motorcycles as it was observed that the "after" speeds of motorcycles were higher. This could be a design limitation as the road curvature has to suit the maneuvering of larger vehicles which are also plying along the road and in turn, reduces horizontal deflection effect to the motorcyclists.

x) In the mid-block section: Lane narrowing

Chevron markings are used to virtually narrow the road lane. They can be drawn at the roadside or in the middle of the two-way road as virtual centre divider.

As was expected, most of the sites showed lower reduced speeds (by 3-12 kph), when compared to physical kerbs. As such, virtual lane narrowing is used only when physical kerbs cannot be constructed.

xi) In the mid-block section: Traffic Calming Markings (TrCM)

TrCM is a set of "dragon-like teeth" triangles painted at the edges of the road lane to virtually narrow the lane, encouraging motorists to slow down. There is no physical bump.

Both sites implemented with TrCM are dual-2 roads in residential area. For 1 of the sites, TrCM was painted about 100m upstream of a signalized control, whereas for the other site, the signalized control was further downstream (about 250m). The proximity of the signal control downstream could have some influences on the effectiveness of the TrCM. The speed reduction at the former site saw significant decreases in speed between 8-14kph. It would be interesting to monitor longer term effect, to see its effectiveness after motorists get used to the markings.

4.3 Perception survey

Perception survey were used to complement results from the revealed motorists' behaviour (i.e. speeds) and long-term safety performance (accidents). Out of the 903 surveyed respondents, 73.7% were aware of the Silver Zone scheme in their residential area.

The results from the surveyed locations showed that the respondents felt that Silver Zones have brought an overall improvement to road safety in the vicinity in the score between 3.4-4.8 out of 5 (Agree). In general, pedestrians rated higher (i.e. felt safer) than motorists.

Feedback was also gathered for the various types of Silver Zones countermeasures to assess user acceptance. In Silver Zones, pedestrians were typically being channeled in Silver Zones to use different types of crossings: signalized pedestrian crossing, raised zebra crossings, and also informal barrier-free crossings. Majority of the residents (72.6%-83.3%) in locations with newly introduced signalized pedestrian crossings generally found that the signalized pedestrian crossings have made it safer to cross the roads. Raised zebra crossings were also welcomed by 75.3%-82.5% of the residents. Though majority liked the idea of more barrier-free routes facilitated by the kerb cut ramps and cut through kerbs (in the centre medians), a low percentage of users (29-53%) thought that they are safe. The respondents also reported that the additional safety features such as the 'Look' markings (80-92.2%) and bollards (54-88%) implemented at the crossings, were useful to make pedestrians more aware of the motorists and motorists more aware of the pedestrians, respectively. However, in a separate study on these additional features at the crossings, road users indicated that they often mixed up these informal crossings with the formal crossings and were unsure which party has the right-of-way. These additional enhancements were subsequently removed in view of the confusion which may lead to safety issues.

The majority were in favour of the lowered 40kph speed limit (81.2-94%) and some were receptive to even lower to 30kph (58.6-70.2%). Figure 7 depicted the percentage of the respondents' agreement that the various Silver Zone countermeasures have helped to reduce motorists' speeds. The different bars represented different sites where perception survey data was collected for each countermeasure. While the motorists' speed reduction of Pinch Points was not consistently obvious across the sites (from the previous section on speed study), the majority of the users (both pedestrians and motorists) thought that Pinch Points have been effective in reducing speeds.

Figure 7: Respondents' agreement in % on the effectiveness of each traffic calming measures implemented at various selected sites

5.0 DISCUSSIONS & CONCLUSIONS

The implementation of Silver Zones schemes has lowered the motorists' travelling speeds along these selected housing estates, contributing to the reduced number and severity of accidents involving pedestrians. This is supported by the five year "after" accident data which showed an overall of about 80% decrease in the number of elderly pedestrian injury accidents at the Silver Zone locations.

The choice of which measures to implement depends largely on the layout of the site and specific factors such as pedestrian crossing needs. Nonetheless, the paper has demonstrated that all the countermeasures were generally effective in slowing motorists down, though some were more effective than others. Enhancements to the specific countermeasure can be reviewed by taking into account users' travel experience through perception surveys or more in-depth focus group discussions, to further enhance the experience in Silver Zones. An instance of improvement arising from the perception survey is to review the standalone barrier-free crossings that were implemented at mid-blocks where there were prevalent activities but not warranted for controlled crossing and enhance them with additional traffic calming measures for safer crossing experience.

Channelisations such as railings and aesthetic landscape plantings are often introduced together with the measures to guide pedestrians to safer crossing points. However, conscious efforts must be made to ensure that the diverted paths should not be overly long that make it inconvenient for elderly to travel. Complemented with the comprehensive community engagement and publicity efforts on the benefits of such measures, the Silver Zone scheme has achieved its aim to co-create a safer environment for the community, with large acceptance from the residents.

When implementing the countermeasures in particular, Pinch Points and Eye-Lands, traffic volume was also analyzed to ensure that traffic flows were not impeded particularly when the number of lanes were reduced from 2 to 1 lane. In areas where a center divider is added to single-lane roads, they are designed at low heights and with mountable loads to allow emergency vehicles to pass through in the event of emergencies.

Improvement can also be made to current methodology. For example, the use of video analytics can replace the manual radar speed gun method, providing higher efficiency and accuracy. If automated counts were conducted in future, the 24h data could be used to account for variation in traffic patterns and allow determination of different speed limit for different times of the day (e.g. lower speed limit during high elderly activity period), if needed. However, care has to be taken to account for any factor adjustment between spot speed and derived speed (distance over time).

As more Silver Zones are being implemented island wide, it is prudent to continue monitoring the safety performance and deep dive into the specific design through user behaviour studies. This would provide additional insights into user experience and allow for adjustments to be made to the schemes.

6.0 ACKNOWLEDGMENT

We would like to thank Traffic Police, Singapore Police Force for providing the road traffic accident data for the analysis.

7.0 REFERENCES

ARUP (2022). Speed limit review international research. Transport Infrastructure Ireland.

Barbosa, H.M., Tight, M.R. and May, A.D. (2000). "A model of speed profiles for traffic calmed roads", Transportation Research Part A, 34, pp. 103-123.

CNA (2024). Road traffic deaths rise in 2023; more fatal accidents involving speeding, red-light running, drink driving. Channel News Asia, https://www.channelnewsasia.com/singapore/traffic-police-fatal-accidents-2023-speeding-red-light-drink-driving-4135916

Doecke, S., Baldock, M.R. Kloeden, C.N. and Dutschke, J.K. (2020). Impact speed and the risk of serious injury in vehicle crashes. Accident Analysis and Prevention, Vol144, September 2020.

EDJNet (2024). None of the European cities that lowered the speed limit to 30km/h regrets it. European Data Journalism Network. Retrieved 17 May 2024 from https://www.europeandatajournalism.eu/cp_data_news/none-of-the-european-cities-that-lowered-the-speed-limit-to-30-km-h-regrets-it/

FHWA (2024). Traffic calming e-primer. Module 4: Effects of traffic calming measures on motor vehicle speed and volume. Available on 28 July 2024 from https://highways.dot.gov/safety/speed-management/traffic-calming-eprimer

Forbes, G, J. Gardner, T. McGee, H. and Srininvasan, R. (2012). "Methods and practices for setting speed limits: an informational report", Federal Highway Administration, FHWA-SA-12-004, April 2012.

Grana, A., Giuffre, T. and Guerrieri, M. (2010). Exploring effects of area-wide traffic calming measures on urban road sustainable safety. Journal of Sustainable Development, November 2010.

Herath, O.K. Amarajeewa, P., Ayesha, B. and Thillaiampalam, S. (2021). A comparison of speed data by different speed detection techniques. Proceedings of the Eastern Asia Society for Transportation Studies, Vol13.

Kacprzak, D. and Solowczuk, A. (2019). Effectiveness of road chicanes in access zones to a village at 70km/h speed limit. IOP Conference Series: Materials Science and Engineering, 471.

Lawrence, B., Thompson, L., Newstead, S. Oxley, J. and Fildes, B. (2020). Final report of the 30km/h speed limit trial evaluation in the city of Yarra. Accident Research Centre, Monash University, Report 340.

Minnema, R. (2006). The evaluation of the effectiveness of traffic calming devices in reducing speeds on "local" urban roads in New Zealand. University of Cantebury, Research report.

Nicholas, A.J. (1987). The estimation of accident rates and countermeasure effectiveness. Traffic Engineering & Control, Vol 28 (10), pp. 518-523.

OECD (2018). Speed and crash risk. International Traffic Safety Data and Analysis Group, Research Report.

Sayer, I.A., Parry, D.I. and Barker, J.K. (1998). Traffic calming- an assessment of selected on-road chicane schemes. Transport Research Laboratory, TRL Report 313.

WHO (2018). "Global Status Report on Road Safety". Internet. Available from https://www.who.int/violence_injury_prevention/road_safety_status/2018/en/

Evaluation of Pedestrian Level of Service on Foot Over-Bridges' Staircases in Dhaka City

Md. Rakibul Haque[1], Md. Mahbubur Rahman[2], Md. Mamun Kaysar[2], Joy Prakash Chowdhury[2], Md Waliur Rahman[2], Md Nurul Alam[3] and Nazmus Sakib[4*]

[1] SMCC-ITD JV, Bangladesh, Email: rakibulhaque@iut-dhaka.edu
[2] Roads and Highways Department, Bangladesh
[3] Asian Disaster Preparedness Center, Thailand
[4] Department of Civil and Environmental Engineering, Islamic University of Technology, Bangladesh, Email: sakib@iut-dhaka.edu

ABSTRACT

The pedestrian movement plays a vital role in urban infrastructure, especially in densely populated cities like Dhaka. Foot over-bridges (FOBs) are essential pedestrian facilities that provide a safe way for people to cross the roads. However, there are concerns about the effectiveness of FOBs staircases in ensuring smooth pedestrian flow. This study aims to evaluate the effectiveness of pedestrian flow on FOBs staircases in Dhaka City. To analyze pedestrian flow characteristics, the research utilizes methodologies outlined in the Indian Highway Capacity Manual (Indo-HCM). Data collection involves observational studies conducted during peak and off-peak hours at selected FOBs in different locations across Dhaka City. Parameters such as pedestrian density, speed, and flow rate are measured to assess the Pedestrian Level of Service (LOS) performance of FOBs staircases. Findings indicate that many FOBs staircases in Dhaka City experience congestion during peak hours, resulting in inefficient pedestrian flow. Factors contributing to this congestion include narrow staircase width, inadequate design, and insufficient capacity to handle the high demand of pedestrians during peak times.

Keywords: Foot over-bridges, Stairway, Pedestrian flow, PLOS

1. INTRODUCTION

Foot over-bridges, or pedestrian overpasses, are indispensable in Dhaka city, where rapid urbanization and a population exceeding 21 million have precipitated heavy traffic and perilous pedestrian conditions. The inadequacy of proper pedestrian facilities has culminated in numerous accidents and fatalities, as people often cross roads haphazardly. Foot over-bridges provide a safe and efficient solution, enabling pedestrians to traverse busy roads without competing with vehicular traffic, thereby ameliorating traffic flow and alleviating congestion. Consequently, foot over-bridges are a crucial infrastructural development for enhancing pedestrian safety and convenience in Dhaka city.

Despite the critical role of pedestrian infrastructure, limited research specifically addresses pedestrian flow rates for determining Pedestrian Level of Service (PLOS) in Bangladesh. However, several studies have examined this topic in various contexts, offering insights that may be applicable. Rahman et al. (2013) analyzed pedestrian flow characteristics in Dhaka, revealing an average walking speed of 1.23 meters per second and flow rates ranging from 1.54 to 1.75 persons per second, though Level of Service (LOS) was not explicitly assessed. Hasan et al. (2019) found that in a busy commercial street in Dhaka, a flow rate of 2.0 persons per second corresponded to LOS E, while a rate of 1.0 persons per second corresponded to LOS C. Additionally, Nazir et al. (2012) identified factors such as pedestrian behavior, FOB design, and safety perception as influential to flow rates.

This research aims to fill the gap in the literature by focusing on pedestrian flow rates at foot over-bridges in Dhaka city to determine the LOS. By analyzing pedestrian movement patterns and their interaction with FOB design and environmental factors, this study seeks to establish a comprehensive understanding of pedestrian dynamics in urban Bangladesh, ultimately contributing to improved safety and efficiency in pedestrian infrastructure planning.

2. METHODOLOGY

The categorization of foot over-bridges into PLOS categories A to F can be achieved by evaluating factors such as flow rate, using the Indo-HCM Pedestrian Level of Service (PLOS) criteria tables designed for foot over-bridges, encompassing both (Entrance and Exit) stairway components. This method allows an independent assessment to determine the appropriate PLOS category for each foot over-bridge stairway.

2.1 Data collection

During the field data collection in Dhaka, quantitative data was collected from three-foot over-bridges (Figure 1). This involved observing the flow rates and counts of pedestrians in both directions on the stairways of the foot over-bridges. The characteristics of the stairways were measured to calculate the quantitative pedestrian Level of Service scores. The data collection took place from (7:30 to 10:30) 3 hours in the morning, (13:00 to 15:00) 2 hours in the afternoon, and (17:00 to 20:00) 3 hours in the evening, Ali et al. (2023)

Periods	Morning	Afternoon	Evening
Peak	7:30-9:00	13:00-14:30	17:00-19:00
Off-Peak	9:00-10:30	14:30-15:00	19:00-20:00

Data collection day:
Case-1: Mirpur-2 (Bus Stand) Foot over-bridge; Thursday, Friday and Sunday
Case-2: Shewrapara Foot over-bridge; Thursday, Saturday and Sunday
Case-3: Kazipara Foot over-bridge; Monday, Tuesday and Wednesday

Case-1 were chosen because as it is near a shopping center, stadium, and educational institute. Case-2 was selected due to its proximity to an institute, residential area, metro station, and supermarket. Case-3 was chosen for its proximity mosque, residential area, marketplace, and metro station. Overall, all three sites are near major pedestrian traffic trip generators.

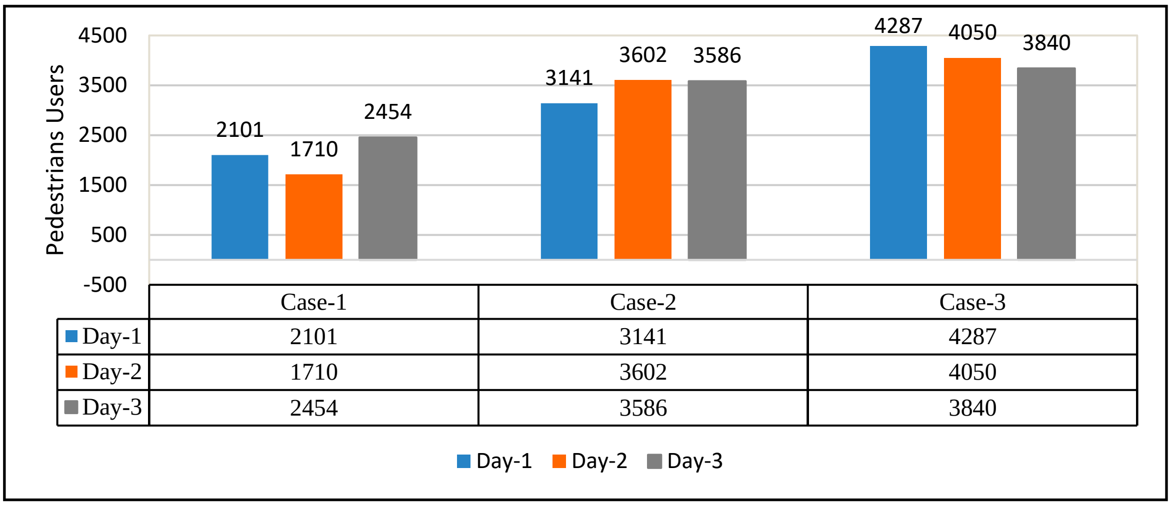

The rate of pedestrian users for each case:

- Case-1: Mirpur-2 (Bus Stand) Foot over-bridge. Total pedestrians observed 6265.00.
- Case-2: Shewrapara Foot over-bridge. Total pedestrians observed 10329.00.
- Case-3: Kazipara Foot over-bridge. Total pedestrians observed 12177.00.

The following data was collected through video recording and field analysis at each site.

1. Pedestrian volume: This refers to the number of pedestrians using the foot over-bridge. It can be measured using manual or automated counting methods. A higher pedestrian volume can lead to overcrowding and reduce PLOS.

2. Pedestrian speed: This refers to the average speed at which pedestrians move across the foot over-bridge. It can be measured using manual or automated methods, such as video recording or radar. Slow pedestrian speed can indicate congestion or other obstacles, which can reduce PLOS.

3. Pedestrian density: This refers to the number of pedestrians per unit area on the foot over-bridge. It can be measured using manual or automated counting methods. High pedestrian density can lead to overcrowding and reduce PLOS.

4. Width of foot over-bridge: This refers to the width of the foot over-bridge. It can be measured using tape measures or other measuring tools. A wider foot over-bridge can accommodate more pedestrians and improve PLOS.

Pedestrian traffic is measured manually by recording video and replaying it to count individuals one by one. This method ensures accuracy in capturing pedestrian flow, providing detailed data for analysis. It involves a systematic approach to observe and document the number of pedestrians in a specific area

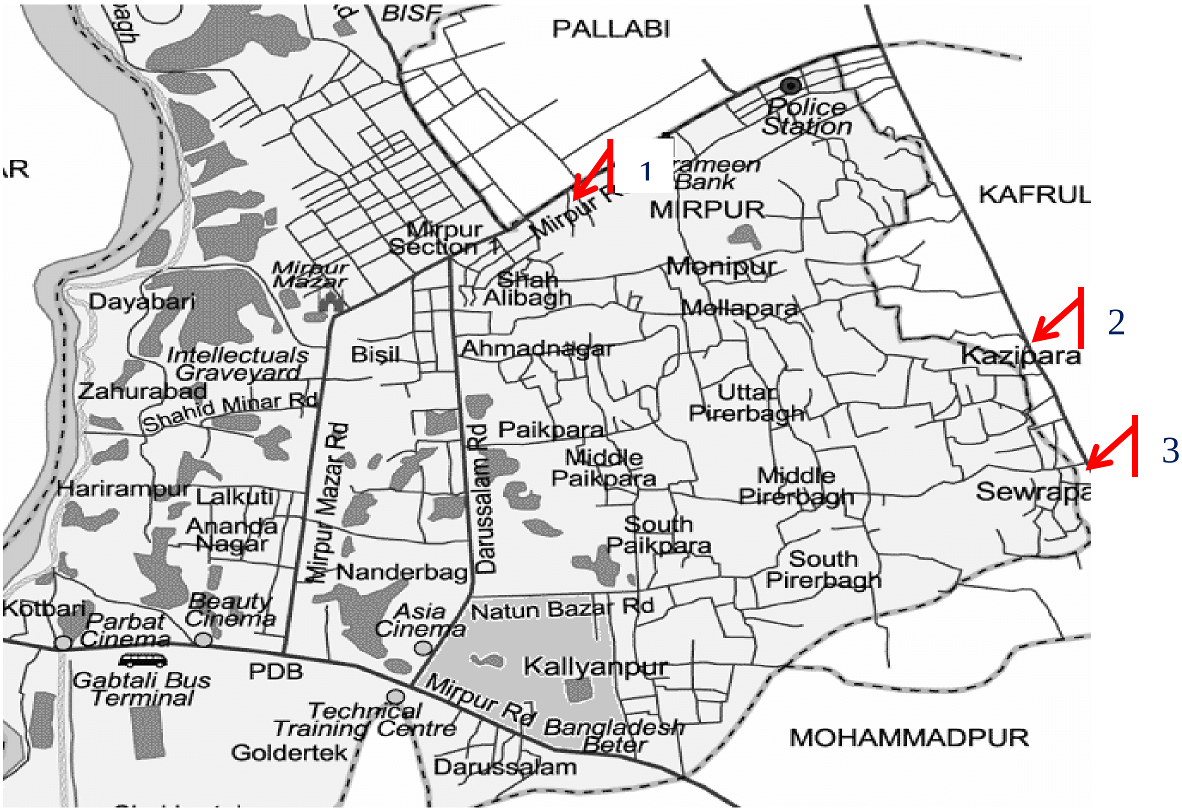

Figure 1 Location of studied Foot Over Bridges in Dhaka.

2.2 Application of PLOS Concept

The concept of PLOS, as dictated in Indo-HCM was applied using the collected data and several calculated data. Following steps were taken during measurement of PLOS:

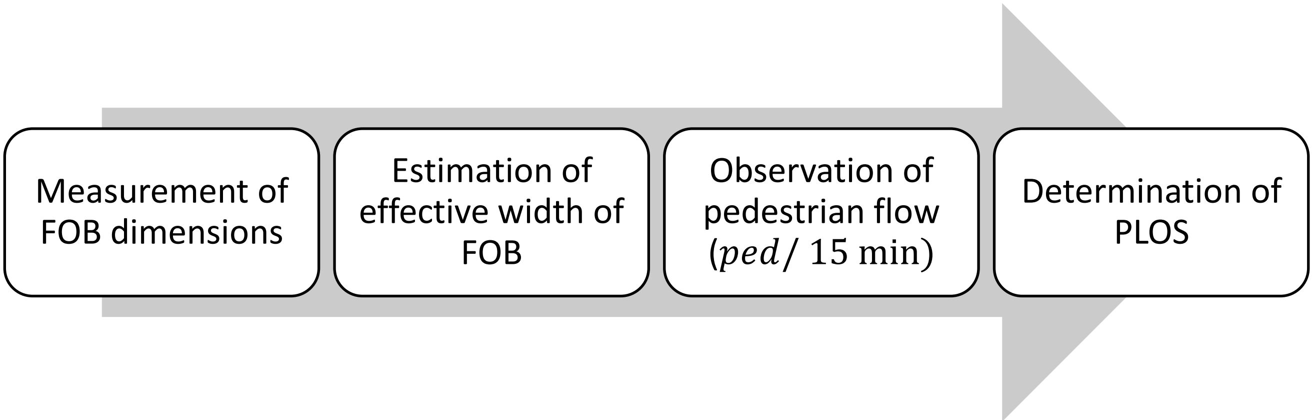

Figure 2 PLOS Determination Flowchart

As outlined by Indo-HCM, the following values of Pedestrian flow rate can be used to evaluate PLOS of stairways.

The effective width of the walkway, W_e, is calculated as:

$W_e = W_t - W_o$

- W_t Total walkway width at an assumed point along the pathway

- W_o Sum of fixed object effective widths and linear feature shy distances at a given point along the facility

Pedestrian flow:

$$Vp = \frac{\mathrm{V15}}{\mathrm{15XWe}}$$

- Where Vp is the pedestrian flow per unit of width (pedestrians per minute per meter)
- W_{15} is the peak flow of pedestrians within a 15-minute interval
- W_e Effective width of the walkway

Table 1 Pedestrian Level of Service for stairways as per Indo-HCM, using flow rate.

LOS	$\boldsymbol{Flow}\ (\boldsymbol{ped/min/m})$
A	≤ 10
B	> 10-22
C	> 22-46
D	> 46-55
E	> 55-70
F	Variable

3. RESULTS

The analysis focused on the peak and off-peak values derived from a three-day count of pedestrian foot over-bridge usage. They can be summarized in the following Figures 3 and Figures 4.

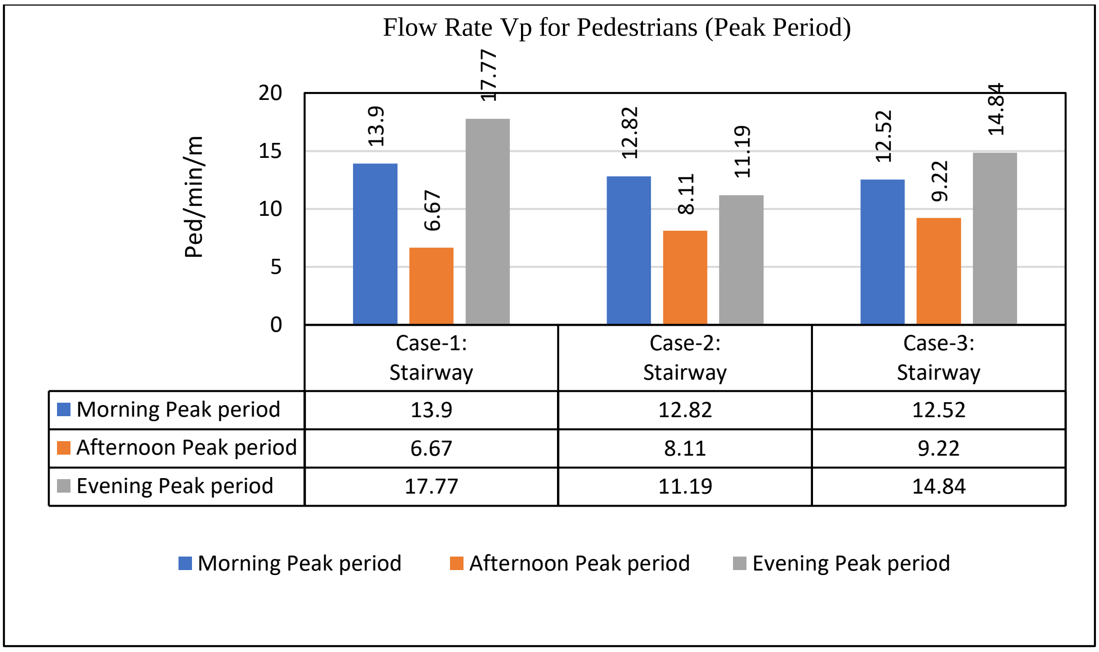

Figure 3 Flow Rate V_P for Pedestrians (Peak Period)

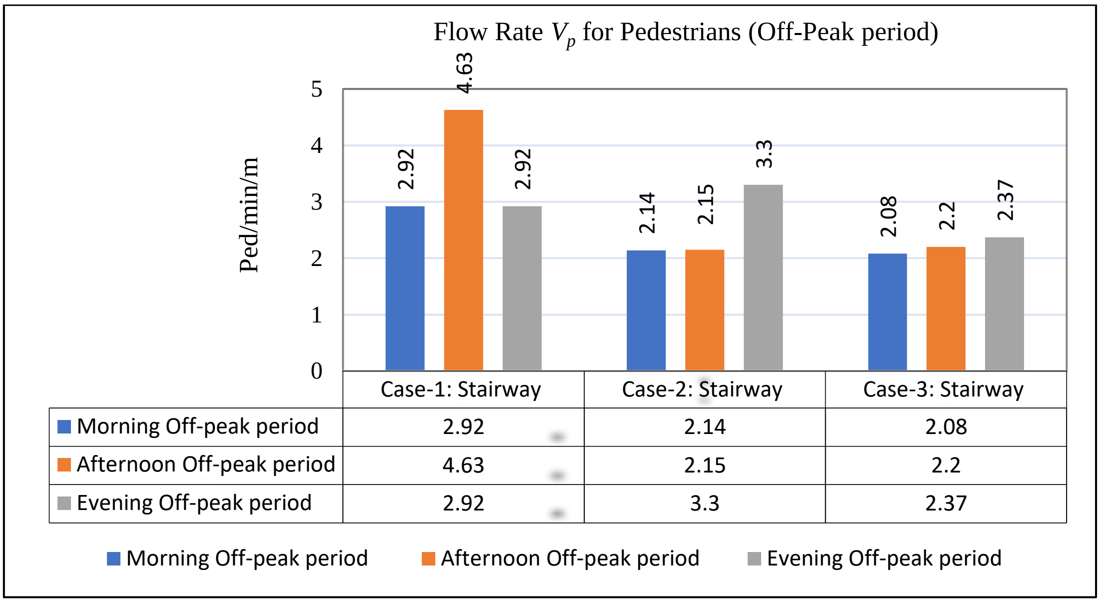

Figure 4 Flow Rate V_P for Pedestrians (Off-Peak Period)

Using the information obtained in the pedestrian flow analysis along with methodology described in Figure 2, we have calculated the Level of service at each location at different peak and off peak periods. The results can be seen in Table 2.

Table 2 Level of Service Flow Rate (V_P) for Pedestrians in selected foot over-bridges.

Pedestrian Level of Service based on Flow Rate V_p									
Stairway	**Peak Period / Off-Peak period**	**Case-1**			**Case-2**			**Case-3**	
Morning.	Peak	13.9	B		12.82	B		12.52	B
	Off Peak	2.92	A		2.14	A		2.08	A
Afternoon.	Peak	6.67	A		8.11	A		9.22	A
	Off Peak	3.63	A		2.15	A		2.20	A
Evening.	Peak	17.77	B		11.19	B		14.84	B
	Off Peak	2.92	A		3.30	A		2.37	A

4. DISCUSSION

The analysis of pedestrian flow on foot over-bridge (FOB) staircases in Dhaka City has revealed critical insights into the performance and limitations of these urban infrastructures. The study focused on three locations: Mirpur-2 (Bus Stand), Shewrapara, and Kazipara, examining pedestrian volume, speed, density, and the width of FOBs during peak and off-peak hours. The findings highlighted significant issues, particularly during peak periods, and suggested several areas for improvement.

Mirpur-2 is a significant bus stand area, resulting in a high volume of pedestrian traffic due to the convergence of bus passengers and local pedestrians. During peak periods, this location exhibited substantial congestion, with a PLOS categorized as B.

- Morning Peak (13.9 ped/15 min): The high volume during the morning peak period leads to congestion, as the narrow staircases cannot accommodate the flow efficiently.
- Evening Peak (17.77 ped/15 min): This period experiences the highest congestion, resulting in significant delays and reduced flow efficiency.

The narrow width of the FOB staircases at this site is a critical issue, exacerbating the bottleneck effect and reducing pedestrian flow efficiency. Additionally, the design of the staircases, which lack sufficient entry and exit points, further compounds the congestion problem. To improve PLOS at Mirpur-2, widening the staircases and redesigning them to include multiple entry and exit points would be beneficial.

The Shewrapara site, situated in a busy commercial area, experiences significant pedestrian traffic, particularly during business hours. The peak period PLOS at Shewrapara was similarly categorized as B, indicating congestion issues.

- Morning Peak (12.82 ped/15 min): High pedestrian density during business hours leads to congestion.
- Afternoon Peak (8.11 ped/15 min): Although lower than the morning peak, this still results in congestion due to commercial activity.
- Evening Peak (11.19 ped/15 min): Similar to the morning, evening congestion is influenced by people returning home from work and shopping.

The primary factors contributing to reduced PLOS at this location include the narrow staircases and the high density of pedestrians during peak times. Unlike Mirpur-2, Shewrapara site's congestion is also influenced by the commercial activities in the area, which attract a large number of pedestrians. To enhance PLOS at Shewrapara, expanding the width of the staircases is essential.

Kazipara, another busy area with substantial pedestrian traffic, showed a peak period PLOS of B, indicating similar congestion issues to the other sites.

- Morning Peak (12.52 ped/15 min): The narrow staircases struggle to handle the morning rush, leading to delays.
- Afternoon Peak (9.22 ped/15 min): While lower, the volume still causes congestion due to the existing infrastructure's limitations.
- Evening Peak (14.84 ped/15 min): High evening volumes result in significant congestion and reduced pedestrian flow.

The narrow width of the staircases and the high pedestrian volume during peak hours are significant contributors to the reduced PLOS. Additionally, the design of the FOBs at Kazipara does not adequately accommodate the high demand, leading to inefficiencies in pedestrian movement. To improve PLOS at Kazipara, widening the staircases and redesigning them to include multiple entry and exit points are necessary steps.

5. Conclusion

The evaluation of the Level of Service (LOS) for pedestrian foot over-bridge facilities spanning from Agargon Begum Rokeya Avenue to Mirpur-10 to Mirpur-1 Road in Dhaka indicates that these structures provide satisfactory service. Based on the Pedestrian Level of Service (PLOS) categories A and B, it is evident that the foot over-bridges effectively meet the needs of pedestrians, offering ample capacity without significant congestion or delays. This assessment underscores the success of the infrastructure in facilitating safe and efficient pedestrian movement across these busy thoroughfares. The classification into categories A and B signifies that pedestrians can traverse the foot over-bridges comfortably, with minimal interruptions and adequate space for all users.

This study also underscores the critical role of foot over-bridges (FOBs) in urban mobility within Dhaka City, highlighting challenges related to pedestrian flow dynamics, particularly during peak hours. The findings reveal that current FOB staircases often face congestion due to design limitations and high pedestrian demand. To optimize effectiveness, recommendations include widening staircases, redesigning layouts for better flow management, and promoting pedestrian awareness

6. References

Hasan, T., Siddique, A., Hadiuzzaman, M., & Musabbir, S. R. (2015). Determining the most suitable pedestrian level of service method for Dhaka city, Bangladesh, through a synthesis of measurements. *Transportation Research Record, 2519*(1), 104-115

HCM 2000, Highway Capacity Manual Transportation Research Board, National Research Council, Washington, D.C

Indian highway capacity manual (Indo-HCM) (2017), Council of Scientific and Industrial Research, New Delhi, India

Nazir, M. I., Adhikary, S. K., Hossain, Q. S., & Ali, S. A. (2012). Pedestrian flow characteristics in Khulna metropolitan city, Bangladesh. *Journal of Engineering Science*, 3(1), 25-31.

Rahman, K., Ghani, N. A., Kamil, A. A., & Mustafa, A. (2013). Weighted regression method for the study of pedestrian flow characteristics in Dhaka, Bangladesh. *Modern Applied Science*, *7*(4), 17.

Reclaimed Walkway Utilization at Skytrain Station in Suburban Area : Khu Khot Station, Pathum Thani, Thailand's Experience

Prach Thatsaneeyaporn[1,*], Theerawongdech Chanpeng[1], Pornchai Silarom[1], Tanach Sripat-In[1]

[1] Bangkok Highway District, Department of Highways, Bangkok, Thailand, doh1111@doh.go.th

ABSTRACT

In year 2020, the extension of sky train mass rapid transit was finished and opened to pubic. The end station in the north of Bangkok named Khu Khot station (N24) located in Lamlukka District, Pathum Thani Province. There is big benefit of travelling time saving and most convenient to whom travel in-out CBD of Bangkok from Lamlukka. Many people use park and ride by both private cars and motorcycles. Due to limited parking lot, illegal parking of motorcycles on footpath was serious problem and obstructed the utilization for pedestrian, wheelchair, and bicycles. Due to limitation of legal enforcement, some additional urgent measures should be considered to relieve the number of illegal cases. The special design of bollard with conventional guardrail and on ground marking brought to pilot action by Lamlukka Highway Depot, Bangkok Highway District, Department of Highways (DOH). The specific bollards comprised of two steel columns. The size of each column is 90 centimeters tall with 30 centimeters bending of 120 degrees angle. They obstructed handlebars of motorcycles, but bicycles, wheelchair, and stroller can pass through. The number of motorcycle's parking cases were reduced, the left can be enforced and completely reclaim footpath as function. The special designed bollard with conventional railing and on ground marking were the first step measure to reclaim footpath effectively. Long term measures shall be implemented for sustainable social equity and accessibility.

Keywords: Motorcycle, Walkway, Footpath, Pedestrian

1. INTRODUCTION

Year 2020, the extension of sky train mass rapid transit was finished and opened to pubic. The end station in the north of Bangkok named Khu Khot station (N24) located in Lamlukka District, Pathum Thani Province. There is big benefit of travelling time saving and most convenient to whom travel in-out CBD of Bangkok from Lamlukka. Regardless public transport to Khu Khot station, many people use park and ride by both private cars and motorcycles.

In Thailand, there are 22 million of motorcycles and increase approximately 1.95% each year which is the main transportation mode for Thai's salary man. Pathum Thani province, located in the north of Bangkok, there are 953,660 rai with 1,201,532 people or 787.45 people per square kilometers (year 2022). There are 78,775 numbers of registered motorcycle (year 2024).

Parking area is provided but not enough to all demand of motorcycles. Then some of motorcycles used footpath area to park and increase the coverage area, as shown in Figure 1.

The illegal numbers were too much and over than legal enforcement capability. Pedestrian, bicycles, and wheelchairs were affected, could not utilize walkway, elevator, and any other public area as their own right. The social problem was expanded and built up in social media. Lamlukka Highway Depot, Bangkok Highway District, Department of Highways (DOH), the authority responsible for this road section including footpath, need to solve this matter to reclaim public footpath.

Figure 1 The Parking on walkway.
(https://www.google.com/maps/, 2022)

2. HOW TO RECLAIM

1) From DOH's road inventory information, this highway is number 3312 at kilometer 4+800 approximately, with AADT 58,581 and %truck = 9.6%. This highway is 6 lanes – two direction, high volume traffic and very congested in peak hour working day. Sidewalk or footpath is 3 meters width. This area represents important node of transportation mode changing from private to public and vice versa. By the important of footpath's function to serve road users, there is high priority for DOH to restore sidewalk area.

2) Seek for participation from related authorities to settle the measures for step by step.

The meeting was held in March 2023, as shown in Figure 2.

3) DOH setup the equipment/materials to block motorcycles, but can allow bicycles, pedestrian and wheelchair. All other experiences in social media or any case study were studied. Then built up and install the specific equipment.

4) Monitor the number of illegal parking, evaluate, improve the design and apply to other walkway with the same condition.

Figure 2 Meeting with related authorities.

3. IMPLEMENTATION

After totally agree with related authorities, in May 2024, DOH installed conventional guardrail along the roadside to make longitudinal boundary, as shown in Figure 3. Then the specific design of bollards was produced and installed. The bollards comprised of two steel columns, to obstruct handlebars of motorcycles, but bicycles can use. The size of each column is 90 centimeters tall with 30 centimeters bending of 120 degrees angle. The shape of bollards is shown in Figure 4, which wheelchair and stroller can pass. Figure 5 demonstrate the installation and testing with wheelchair and baby stroller.

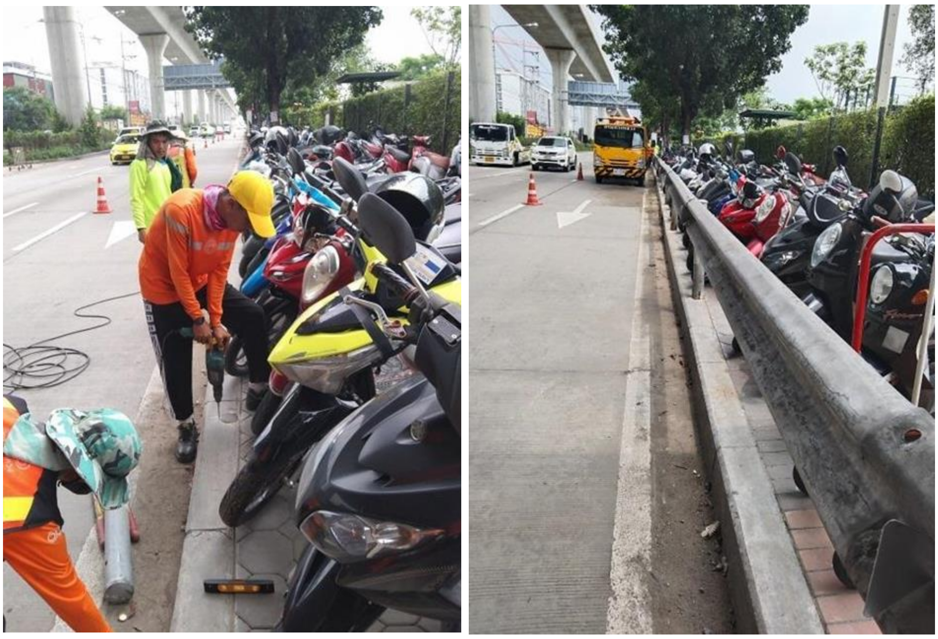

Figure 3 Install guardrail along the roadside to make longitudinal boundary.

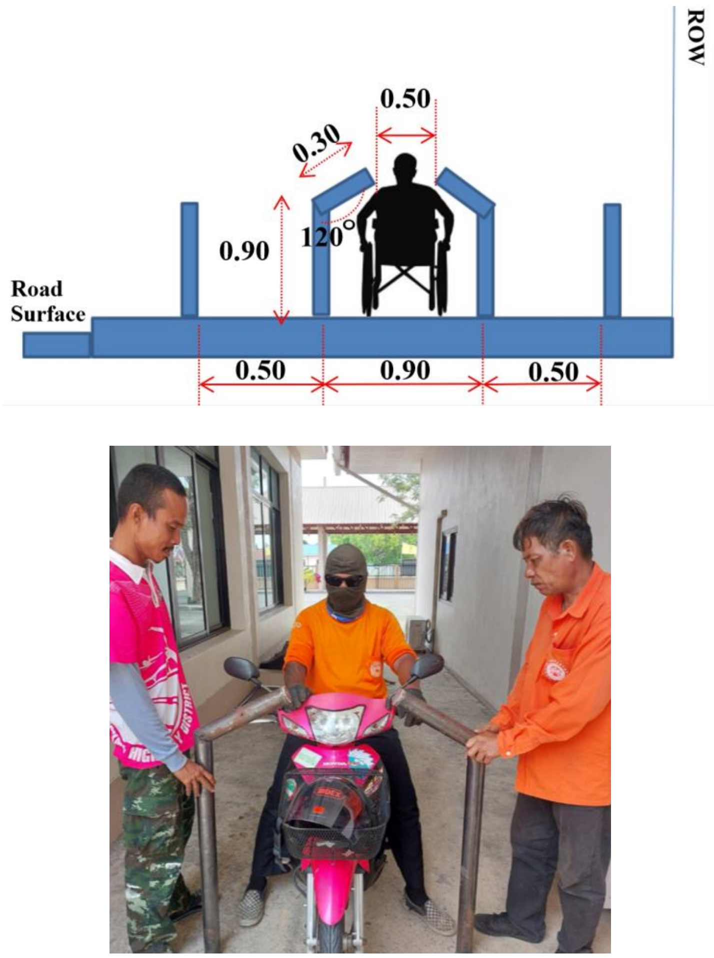

Figure 4 Trial and Error for specific designed bollard.

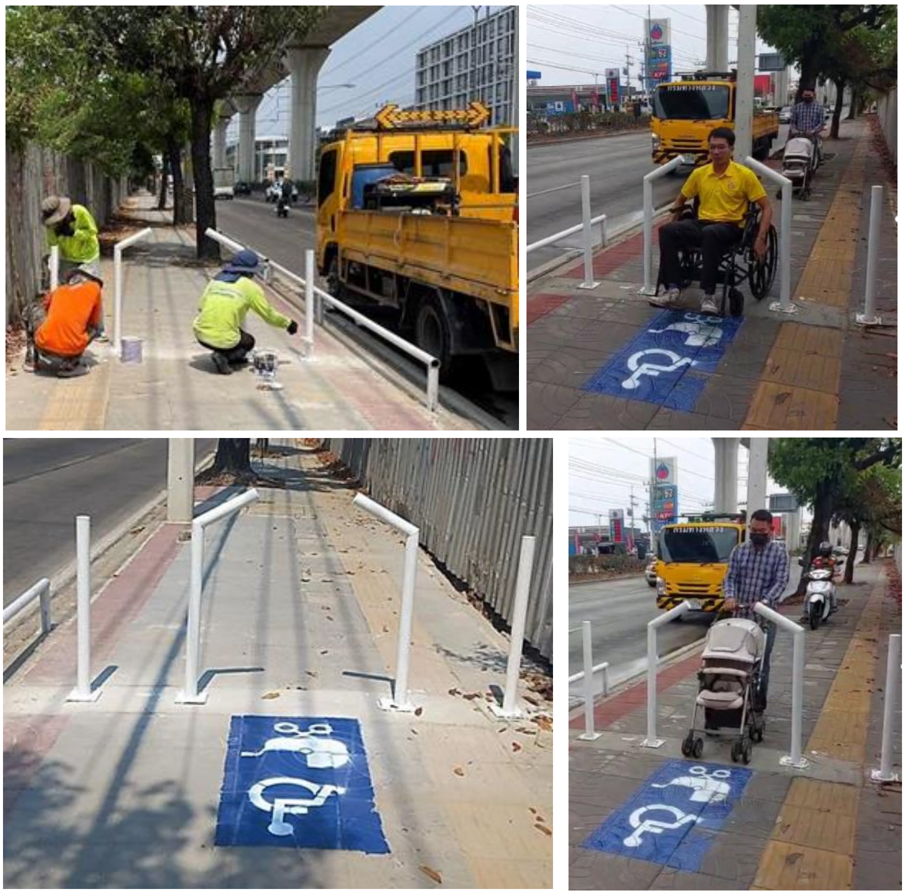

Figure 5 Installation and testing for wheelchair and baby stroller.

4. RESULTS

As the objectives to protect walkway area, the install's equipment is working properly. No motorcycles are parked. As shown in Figure 6, three meters width of walkway is reclaimed to pedestrian, wheelchair, and bicycles. Even though there is some illegal parking, the enforcement can be operated effectively. The improved design may implement in next step or in other same illegal case.

Figure 6 Footpath for fully utilization.

(https://www.google.com/maps/, 2024)

5. CONCLUSIONS

The development of mass rapid transit in some specific suburban area induced illegal parking behavior of existing local transportation mode such as motorcycles. It had affected the walkway utilization. Pedestrian and bicycles, especially wheelchair, could not access.

Due to limitation of legal enforcement, some additional urgent measures should be considered to relieve the number of illegal cases. The special design of bollard with conventional guardrail and on ground marking brought to pilot action by Lamlukka Highway Depot, Bangkok Highway District, Department of Highways (DOH). The number of motorcycle's parking cases were reduced, the left can be enforced and completely reclaim footpath as function.

The special designed bollard with conventional railing and on ground marking were the first step measure to reclaim footpath effectively. Long term measures shall be implemented for sustainable social equity and accessibility.

6. REFERENCES

Department of Land Transport. (2023). Transport Statistics Report 2023. https://web.dlt.go.th/statistics/

Department of Land Transport. (2024). https://web.dlt.go.th/statistics/

National Statistical Office. (2023). Pathum Thani Provincial Statistical Report: 2023.

iCHE
BANGKOK 2024

iCHE
BANGKOK 2024